UNIVERSITY OF CALIFORNIA

Santa Barbara

Ecosystem productivity and water temperature in coastal California streams

A dissertation submitted in partial satisfaction of the

requirements for the degree Doctor of Philosophy

in Geography

by

Heather Nicole-Berry Frazier

Committee in charge:

Professor John Melack, Co-Chair

Professor Hugo Loaiciga, Co-Chair

Professor Scott Cooper

January 2018

The dissertation of Heather Nicole-Berry Frazier is approved.

_____

Scott Cooper

_____

Hugo A. Loaiciga, Committee Co-Chair

_____

John Melack, Committee Co-Chair

December 2017

Ecosystem productivity and water temperature in coastal California streams

by

Heather Nicole-Berry Frazier

ACKNOWLEDGEMENTS

This dissertation was made possible due to financial support from a National Science Foundation Graduate Research Fellowship (DGE 1144085), a UC Regents Special Fellowship, and a grant from the UCSB Associated Students Coastal Fund (WIN13-17). The research was supported by the Santa Barbara Coastal Long Term Ecological Research program, funded by the U.S. National Science Foundation (OCE 9982105, 0620276, and 1232779). Additional support was provided by the UCSB Geography Department and the Marine Science Institute at UCSB. I would also like to thank several others who made this work possible: Matt Meyerhoff for providing laboratory and field support; The Land Trust for Santa Barbara and John Warner for providing access to the Arroyo Hondo Preserve; Professor Ed Keller for providing access to Rattlesnake Creek; Professor Josh Schimel for providing access to Sycamore Creek; Professor Dar Roberts and the VIPER lab for providing the AVIRIS classification maps; and staff from the County of Santa Barbara Public Works and Public Health Departments for providing access to County data. I would also like to thank Professor Sally McIntyre, Steve Sadro, Blair Goodridge, and Mike Alonzo for providing additional ideas and discussion related to this work.

I am grateful for the seemingly endless patience and good humor I received from everyone who helped me collect data in the field, including Michael Ackel, Javier Aguilar, Miguel Arteaga, Dylan Berry, Theresa Berry, Taylor Berryman, Matthew Chan, Helen Chen, Julian Consoli, Nathan Dias, Michael Habitz, Sean Harwood, Anna Hou, Fernando Idiarte, Tim Kershaw, Trace Martin, Sarah Shivers, Neha Subramanyam, Cary Snyder, Caitlyn Teague, Patrick Turner, Cody Wilgus, Danielle Yaconelli, and Erik Young. In

particular, I would like to thank Kaitlyn Smith, Ryan Fallgatter, and Kimberly Yom for being consistent and enthusiastic assistants; I enjoyed working with each of you and learning more about you with each field excursion.

The guidance and feedback of my committee was an integral part of this document and my personal academic formation. I would like to thank Professor Scott Cooper for always asking questions and providing extraordinarily detailed feedback; you have a wealth of knowledge and I appreciate that you shared some of it with me. I want to thank Professor Hugo Loaiciga for teaching me hydrology; your classes were some of my favorite as an undergraduate, a graduate, and a teaching assistant and learning from you was the foundation of my decision to pursue a graduate degree. I would especially like to thank Professor John Melack for being a patient and understanding mentor; your scientific guidance was critical to this work, but your willingness to see the big picture in life was invaluable to me.

I would like to thank the UCSB Department of Geography for providing direct and indirect support to me throughout my time as a graduate student. I would especially like to thank the Geography staff members, who were always a joy to work with, providing cheerful support to me and my fellow students. In particular, I want to thank Mo Lovegreen, who is an amazing advocate for students and a force for good. Your ability to multi-task and still engage on a personal level astounds me. A special thank you is also reserved for the late Jose Saleta, who was a source of inspiration, always willing to listen, to offer advice, and to provide academic and emotional support. Jose, you were a unique soul and someone I aspire to be like. I also need to thank my fellow Geography students, especially the cohort of 2010. I feel fortunate to have such a wonderful network of smart and social people in my life. I

also want to thank my fellow Outreach Committee members for enriching my time in the Geography Department and for giving me the opportunity to share my passion for water and the environment with a broader community, both on and off campus.

There are moments in the pursuit of a graduate degree that are isolating and lonely, but I have been blessed with family and friends to help me through it. I do not wish to fill dozens of pages with names, but I hope all my friends, from home, from UCSB, from soccer, and from all the other realms of life, know that you kept my life interesting and my outlook positive at times when I could not manage those things for myself. Thank you, SBX and CBTL for being my home away from home. I would like to thank, in particular, my long-time friend, Kelsey Tinkham, for always being there; I'm glad to have another "sister" with whom to share life's joys and challenges. I have also been quite blessed to have a wonderful extended family. Every person in the extended Riebli, Berry, Cowan, and Frazier families has improved my life by offering support, love, and laughter without question and without the need for something in return. To Chuck, Margaret, Maegan, Angie, Danielle, and Momi, thank you for welcoming me into your family. To my sisters, thank you for being my first friends and a constant source of love and entertainment. To my parents, my first teachers, thank you for encouraging me while allowing me space to make my own decisions. Mom, as I am sure you know, I could not have finished writing this dissertation without your help. Thank you for watching Charlie and giving me the opportunity to work at such a critical time. Your generosity is humbling and I hope I can be more like you. To Charlie, thank you for bringing new joy into my life and giving me new challenges.

Finally, to my dear husband, Charles, thank you for being by my side through all of this. I am so grateful to have you with me, nudging me forward and reminding me who I am and

what I truly care about, every single day. You really are my other half, my twin, bringing me balance and peace. Thank you for getting me through this and giving me so much to look forward to in our life together. I love you.

Heather Nicole-Berry Frazier

December 2017

EDUCATION

- Doctor of Philosophy in Geography, University of California, Santa Barbara, CA
  December 2017
- Bachelor of Science in Hydrologic Sciences, emphasis in Geography, minor in Geologic Sciences, University of California, Santa Barbara, CA
  June 2009

AWARDS

- Jack and Laura Dangermond Geography Travel Award 2016
- Academic Senate Doctoral Student Travel Grant 2015
- David S. Simonett Memorial Award 2013
- National Science Foundation Graduate Research Fellowship 2011
- Regents Special Fellowship 2010
- Outstanding Academic Achievement, Distinction in the Major 2009
- Environmental Studies Outstanding Senior Award 2009
- Academic Excellence Award 2009
- Regents Scholarship 2005

TEACHING EXPERIENCE

- Teaching Assistant, Geog 162: Water Quality 2016
- Teaching Assistant, Geog 116: Groundwater Hydrology 2016
- Teaching Associate, Geog 3B: Physical Geography 2015
- Teaching Assistant, Env S 2: Intro to Environmental Science 2013
- Teaching Assistant, Geog 8W: Global Warming 2012
- Teaching Assistant, Geog 135: Mock Environmental Summit 2011

PUBLICATIONS

- "To drink or not to drink: Assessing the feasibility of developing direct potable reuse in the south coast region of southern California," Unpublished thesis submitted in partial fulfillment of the requirements for the Bachelor of Science degree in Hydrologic Sciences, University of California, Santa Barbara, 2009.

PRESENTATIONS

- "Ecosystem metabolism response to urban development in coastal California streams." Oral Presentation: Society for Freshwater Science Annual Meeting, Sacramento, CA, May 25, 2016.
- "Stream ecosystem metabolism in urban California coastal streams." Poster Presentation: Society for Freshwater Science Annual Meeting, Milwaukee, WI, May 20, 2015.

SERVICE

- Geography Outreach Committee Member and Volunteer 2010 – 2016
- Graduate Students for Diversity in Science Outreach Volunteer 2011 – 2015

ABSTRACT

Ecosystem productivity and water temperature in coastal California streams

by

Heather Nicole-Berry Frazier

Land use change is a key driver of change in stream ecosystems worldwide and poses a significant risk to streams in areas with high biodiversity and large human populations, such as regions with Mediterranean climates. Two important characteristics of stream ecosystems, whole ecosystem metabolism and water temperature, are sensitive to the changes caused by urban and agricultural development.

In the first section of this dissertation, the effects of urbanization on stream metabolism (gross primary productivity (GPP), community respiration (CR), net ecosystem productivity (NEP), and the ratio of GPP to CR (P/R)) in Santa Barbara, California were assessed by comparing stream metabolism, measured using a single-station diel oxygen change method, across 6 streams with varying catchment urban development between March and July 2014. Environmental variables at each site were measured, including water temperature; light; algal biomass; nutrients (N, P); dissolved and particulate organic carbon; specific conductance; total suspended solids; canopy openness; water width, depth, and velocity; discharge; slope; and elevation. Nitrate concentration was identified as an important driver of GPP, NEP, and P/R, and both GPP and nitrate levels were found to be higher at

developed than undeveloped sites. However, elevation was found to be a potential confounding factor in the study, especially for CR, which was significantly higher at higher elevation sites. GPP, NEP, and P/R were related to multiple urban metrics and leaking septic fields were identified as a potential nitrate source driving GPP and P/R.

In the second section of this dissertation, the thermal environment of Santa Barbara streams was characterized using water temperature data collected between 2001 and 2015 in 21 stream locations. Temperatures exceeding the upper tolerance limits (25°C) for the endangered, native southern California steelhead trout (*Oncorhynchus mykiss*) were identified and the effects of agricultural, urban, and undeveloped land use on water temperatures were assessed. Sub-lethal temperatures for southern California steelhead trout were found at most sites, but a subset of sites in key watersheds for steelhead conservation efforts sometimes exceeded lethal limits. The warmest sites lacked riparian vegetation, the coolest sites were at high elevations, and the sites with small annual temperature ranges were located where significant groundwater influence was expected. Mean and maximum daily temperatures, in the spring and summer, were positively related to percent impervious surface cover, with evidence that the relationship was driven by warm temperatures at channelized sites. Excluding the channelized sites, minimum daily temperatures in the spring and summer were positively related to percent impervious cover, with or without the inclusion of high elevation sites, possibly indicating warmer groundwater inputs to streams in the urban areas of Santa Barbara.

TABLE OF CONTENTS

LIST OF ABBREVIATIONS

AB – Arroyo Burro Creek; metabolism site

AB00 – Arroyo Burro Creek; temperature site

AB21 – Arroyo Burro Creek at Calle de los Amigos; temperature site

AB25 – Arroyo Burro Creek at the Las Positas Drain; temperature site

Ag – designates a site categorized as agricultural in the temperature analysis

ANOVA – analysis of variance

AOI – area of influence

AT – Atascadero Creek; metabolism site

AT07 – Atascadero Creek; temperature site

AVIRIS – Airborne Visible-Infrared Imaging Spectrometer

BC02 – Bell Canyon Creek; temperature site

BOM – benthic organic matter

CBOM – coarse benthic organic matter

CP00 – Carpinteria Creek; temperature site

CR – community respiration

CV – coefficient of variation

DO – dissolved oxygen

DOC – dissolved organic carbon

DOY – day of year

Dv – designates a site categorized as developed in the temperature analysis

DV01 – Devereux Creek; temperature site

EL00 – El Capitan Creek; temperature site

FBOM – fine benthic organic matter

FK00 – Franklin Creek; temperature site

GB04 – Gobernador Creek; temperature site

GPP – gross primary productivity

GV01 – Gaviota Creek; temperature site

HO – Arroyo Hondo Creek; metabolism site

HO00 – Arroyo Hondo Creek; temperature site

MC00 – Mission Creek at Montecito Road; temperature site

MC07 – Mission Creek at Mission Road; temperature site

MESMA – Multiple end-member spectral mixing analysis

NAg = designates a site categorized as non-agricultural in the temperature analysis

NEP – net ecosystem productivity

NUrb – designates a site categorized as non-urban in the temperature analysis

ON02 – San Onofre Creek; temperature site

P - productivity

PAR – photosynthetically available radiation

PCA – principal component analysis

PH – Phelps Creek, metabolism site

POC – particulate organic carbon

pPAR – peak daily photosynthetically available radiation

P/R – the ratio of GPP to CR

R - respiration

RG01 – Refugio Creek; temperature site

RG09 – Refugio Creek at Circle Bar-B Ranch; temperature site

RN01 – Rincon Creek; temperature site

RS – Rattlesnake Creek; metabolism site

RS02 – Rattlesnake Creek; temperature site

SBC-LTER – Santa Barbara Coastal Long Term Ecological Research Project

SD – standard deviation

SE – standard error

SR04 – San Roque Creek; temperature site

SY – Sycamore Creek; metabolism site

TE03 – Tecolotito Creek; temperature site

TOD – time of day

tPAR – total daily photosynthetically available radiation

TSS – total suspended solids

UDv – designates a site categorized as undeveloped in the temperature analysis

Urb – designates a site categorized as urban in the temperature analysis

UTC – Coordinated Universal Time

LIST OF FIGURES

LIST OF TABLES

1. Introduction

Land use changes driven by human activity, including agricultural development, deforestation, and urbanization, cause significant changes in aquatic ecosystems at a global scale (Foley et al., 2005). Agricultural areas cover about 40% of the total land surface of the Earth (Foley et al., 2005), having significant impacts on freshwater ecosystems. Currently, about 50% of the world's human population lives in urban areas with this proportion expected to increase to 66% by 2050 (United Nations, 2015). Although urban development often represents only a small portion of overall watershed land use, it can have large local and downstream influences on stream characteristics (Paul and Meyer, 2001).

Land use changes alter the physical, chemical, and biological characteristics of stream ecosystems. For example, agricultural and urban land uses alter the chemical composition of streams. From the 1960s to the late 1990s, global fertilizer use, mostly associated with agricultural activities, increased 700%, contributing significant nutrient pollution to downstream aquatic ecosystems, sometimes leading to increased algal biomass and hypoxic conditions (Foley et al., 2005; Matson 1997; Allan, 2004). Runoff from agricultural land also can lead to elevated levels of suspended sediments, insecticides, and herbicides (Allan, 2004). Urban landscapes are also associated with increased levels of nutrients and toxic compounds, such as metals, pesticides, and organic contaminants (Lee and Bang, 2000; Paul and Meyer, 2001; Walsh et al., 2005). Both agricultural and urban land uses can be associated with the loss of riparian vegetation, which may increase water temperatures, alter light availability, and change the supply of allochthonous organic matter (Allan, 2004; Walsh et al., 2005; Cooper et al., 2013).

Land use also can significantly affect hydrology and the resulting stream flow. In agricultural areas, local and regional water budgets can be changed due to water extraction from groundwater or rivers, due to damming, or due to altered evapotranspiration rates caused by vegetation changes (Allan, 2004; Barnett et al., 2008). In urban areas, increased surface imperviousness and resulting decreases in infiltration often leads to earlier, higher peak flows during storms (Paul and Meyer, 2001; Walsh et al., 2005) and increased channel erosion, altering channel geomorphology and habitat for stream organisms (Walsh et al., 2005). Many of the physical, hydrological, and geomorphological changes associated with human land uses lead to reduced habitat complexity (Allan, 2004; Walsh et al., 2005; Cooper et al., 2013).

Urban and agricultural development also alters stream biological characteristics. In urban and agricultural streams, increased nutrients and light have been associated with increased algal biomass (Allan, 2004; Walsh et al., 2005), although metal toxicity, herbicides, and bed disturbance can lead to inconsistent responses of algal biomass to urban development (Paul and Meyer, 2001; Walsh et al., 2005). Urban streams can have higher bacterial densities than undeveloped streams and antibiotic resistance has been demonstrated in some bacterial communities from urban streams (Paul and Meyer 2001; Cooper et al., 2013). Increased abundance of macroinvertebrate grazers has been found in agricultural streams, although changes in sedimentation and storm flows can eliminate some taxa (Allan, 2004). Increased urbanization is often associated with decreased macroinvertebrate diversity and abundance, along with decreases in the relative abundance of sensitive orders and relative increases in tolerant orders (Paul and Meyer, 2001; Walsh et al., 2005; Cooper et al.,

2013). Increasing urban and agricultural development is generally associated with decreases in fish diversity and biotic indices (Paul and Meyer, 2001; Allan, 2004).

One characteristic of streams that has received inadequate attention related to land use is water temperature. Temperature strongly influences many biological reactions and processes. For example, the solubility of oxygen decreases with increasing temperature (Benson and Krause, 1980), so warm temperatures can determine the distributions of aquatic organisms by affecting oxygen availability (e.g., Matthews and Berg, 1997). The toxicity of certain chemicals for aquatic organisms also can be temperature-dependent (Cairns et al., 1975). Temperature also influences rates of cellular, individual, and ecosystem metabolism (Gillooly et al., 2001; Allen et al., 2005; Demars et al., 2011). At the community and ecosystem level, temperature alters fungal diversity and leaf decomposition (Fernandes et al., 2012), and also affects the distributions, abundances, community composition, and life cycles of macroinvertebrates (Hawkins et al., 1997; Li et al., 2011). Temperature and nutrient availability also affects macroinvertebrate growth and leaf litter consumption rates (Kendrick and Benstead, 2013). Over a broad temperature range (4.5°C to 93°C), ecosystem food-chain length decreases with increasing temperatures in spring ecosystems (Glazier, 2012), and increased temperature variability can lead to reduced food chain length in temperate streams (Hette-Tronquart et al., 2013). Water temperature affects all fish life stages, directly influencing individual growth, development, behavior (e.g., swimming performance), and survival, and affecting the susceptibility of fish to diseases and the impacts of fish on prey communities (Myrick and Cech, 2000; Carter, 2005; Kishi et al., 2005). Temperature also affects habitat suitability for fish, as well as competitive

interactions between fish species along longitudinal gradients (Baltz et al., 1987; Taniguchi et al., 1998).

The factors influencing stream temperature are well-known. Important heat fluxes in the energy budget of streams include heat fluxes due to net solar radiation, evaporation and condensation, bed conduction, sensible heat transfer between air and water, friction, and advection from groundwater, tributaries, upstream flows, precipitation, or effluent discharges (Webb, 1996). These heat fluxes are responsive to a variety of factors, such as surface discharge, interaction with groundwater, bed albedo, the presence and extent of riparian vegetation, channel morphology, and ambient air temperature (Webb et al., 2008; Bray et al., 2017), many of which are altered by land use change. The relative importance of each of these stream characteristics for stream heat budgets and temperature have been explored through both data collection and modeling (see reviews in Webb, 1996, and Webb et al., 2008).

Temperature is a dynamic variable, responding simultaneously to a number of environmental drivers over short temporal and spatial scales. However, despite its dynamic nature, many ecological studies have relied upon small numbers of measurements through space and time that are inadequate for capturing the magnitude, frequency, and extent of thermal conditions in flowing waters. The increasing availability of accurate and affordable sensors for making frequent temperature measurements has allowed the incorporation of dynamic temperature regimes into ecological studies (Webb et al., 2008). However, the inadequacy of historical data collection has limited the availability of long-term temperature datasets (Webb, 1996; Arismendi et al., 2012), which hinders the accurate characterization of stream temperatures over long time scales, limiting our knowledge of how thermal

regimes respond to changes in weather, climate, or land use. Research devoted to characterizing and understanding the thermal regime of stream ecosystems has been stimulated by studies and projections of the direct and interactive effects of climate and land use changes on aquatic ecosystems (Vitousek et al., 1997; Cooper et al., 2013).

Much of the literature on temperature responses to land use change has focused on the influence of clear-cut logging practices on fish thermal habitat (Webb et al., 2008; Moore et al., 2005), with much less work examining the effects of urban and agricultural development on stream temperatures (e.g., Pluhowski et al., 1970; Rice et al., 2011; Goss et al., 2014; Macedo et al., 2013). Further, most work on the effects of urban and agricultural land use patterns on stream thermal regimes has been concentrated in the eastern U.S.A., with limited information on Mediterranean ecosystems, which have much different climatic, edaphic, hydrological, topographic, and vegetation characteristics. Thus, there remains a need to characterize the influence of land use on the thermal regimes of streams in Mediterranean climates (Mediterranean streams).

Owing to the natural variability and high biodiversity of streams in Mediterranean climates (Bonada and Resh, 2013), as well as large and increasing human populations in their drainage basins, large impacts of land use and climate change on Mediterranean streams are expected (Felipe et al., 2013, Cooper et al., 2013). However, our knowledge of the impacts of urban and agricultural development on Mediterranean stream ecosystems is incomplete and many existing studies fail to describe the mechanisms generating stream ecosystem changes (Young et al., 2008), confounding the identification of appropriate management targets and practices.

There is a need, then, to identify response variables that effectively and sensitively reflect the effects of land use changes on stream ecosystems. One ecosystem measure that provides a synthetic index of, and links among, multiple human influences on streams is stream metabolism (see Bernot et al., 2010 for a conceptual model). Stream metabolism integrates information on the creation and use of energy or organic matter by stream ecosystems by assessing rates of primary production and respiration. Gross primary productivity (GPP) is the rate of autotrophic organic matter production before losses due to community respiration (CR), which represents organic matter consumption by all organisms in the ecosystem. GPP and CR represent basic ecosystem processes that are influenced by the physical, chemical, and biological characteristics of the ecosystem with their difference or ratio (NEP or P/R) indicating whether the ecosystem is a net producer (NEP>0; P/R > 1) or consumer (NEP<0; P/R < 1) of organic matter (but see Rosenfeld and Mackay, 1987). P/R gives an indication of the proportion of organic matter consumed by the organisms within a system that is produced within the ecosystem due to autotrophic processes (autochthonous organic matter) as opposed to coming from upstream or upland inputs (allochthonous organic matter). The concept of P/R is often referenced in the River Continuum Concept (Vannote et al., 1980), which outlines a framework for predicting the biological and chemical characteristics of stream ecosystems (e.g., macroinvertebrate assemblage structure, organic matter availability) from their physical characteristics (e.g., width, depth, and discharge), which in turn are tied to their longitudinal position in a stream network (Tank et al., 2010). Similarly, NEP also assesses whether a stream is heterotrophic or autotrophic and quantifies the magnitude of the rate of organic matter loss or accumulation in streams, which is useful in estimating stream carbon budgets and the

transfer of carbon from upland areas to downstream aquatic ecosystems such as lakes or oceans. Most previous studies have reported that streams have negative NEPs, acting as a sink, rather than source, for organic carbon (e.g., Mulholland et al., 2001; Bernot et al., 2010). Thus, stream metabolism provides a measure of the organic carbon supply to higher trophic levels and the demand for that energy by all organisms in the system.

The primary drivers of GPP are light and nutrients, whereas CR is sensitive to organic matter inputs, hydrological conditions, temperature, and also nutrients (Mulholland et al., 2001, Bernot et al., 2010), making stream metabolism responsive to a number of chemical, biological, and physical drivers that are commonly altered by land use changes. Urban areas often have disturbed riparian areas and elevated nutrients, reduced organic matter retention, and increased temperatures (Walsh et al., 2005), each of which may alter the balance between organic matter creation and consumption in the ecosystem. Stream metabolism integrates local and upstream conditions that influence its proximal drivers, measures how an ecosystem creates and uses organic matter, and reveals the relative contributions of allochthonous and autochthonous inputs to stream food webs, providing a responsive indicator of disturbance (Williamson et al., 2008; Young et al., 2008).

Previous studies of urbanization on stream metabolism, however, have produced mixed results. Some studies were inconclusive or found no relationship between GPP, CR, or NEP and indicators of urbanization (Meyer et al., 2005; von Schiller et al., 2008), others found that GPP, CR, or GPP/CR was negatively related to indicators of urban development (Bott et al. 2006, Izagirre et al. 2008), and still others found positive relationships between production or autotrophy and the degree of urban development (Bernot et al. 2010; Iwata et al. 2007; Clapcott et al. 2010).

The research described in this thesis, then, addresses the influences of land use change on stream metabolism and water temperature in Mediterranean streams. The general question guiding my research can be stated as follows: what are the effects of land use changes on stream metabolism and water temperature in southern California? Towards this end, I compared metabolism and temperature at sites draining basins with different land uses in southern Santa Barbara County, USA. The first section of this dissertation examines stream metabolism in watersheds across a gradient of urban development, focusing on human-induced changes, such as increased nutrient concentrations and reduced canopy cover, which drive increases in productivity and stream autotrophy. The second section of this dissertation addresses the effects of increased land use disturbance in watersheds on patterns in stream water temperature.

1.3. References

Allan, J.D. 2004. Landscapes and riverscapes: The influence of land use on stream ecosystems. Annual Review of Ecology, Evolution, and Systematics 35: 257-284.

Allen, A.P., J.F. Gillooly, and J.H. Brown. 2005. Linking the global carbon cycle to individual metabolism. Functional Ecology 19: 202-213.

Arismendi, I., S.L. Johnson, J.B. Dunham, and R. Haggerty. 2012. The paradox of cooling streams in a warming world: Regional climate trends do not parallel variable local trends in stream temperature in the Pacific continental United States. Geophysical Research Letters 39: L10401. doi: 10.1029/2012GL051448

Baltz, D.M., B. Condracek, L.R. Brown, and P. Moyle. 1987. Influence of temperature on microhabitat choice by fishes in a California stream. Transactions of the American Fisheries Society 116(1):12-20. http://dx.doi.org/10.1577/1548-8659(1987)116<12:IOTOMC>2.0.CO;2

Barnett, T.P., D.W. Pierce, H.G. Hidalgo, C. Bonfils, B.D. Santer, T. Das, G. Bala, A.W. Wood, T. Nozawa, A.A. Mirin, D.R. Cayan, and M.D. Dettinger. 2008. Human-induced changes in the hydrology of the western United States. Science 319: 1080-1083.

Benson, B.B. and D. Krause. 1980. The concentration and isotopic fractionation of gases dissolved in freshwater in equilibrium with the atmosphere. 1. Oxygen. Limnology and Oceanography 25: 662-671.

Bernot, M.J., D.J. Sobota, O. Hall Jr., P.J. Mulholland, W.K. Dodds, J.R. Webster, J.L. Tank, L.R. Ashkenas, L.W. Cooper, C.N. Dahm, S.V. Gregory, N.B. Grimm, S.K. Hamilton, S.L. Johnson, W.H. McDowell, J.L. Meyer, B. Peterson, G.C. Poole, H.M. Valett, C. Arango, J.J. Beaulieu, A.J. Burgin, C. Crenshaw, A.M. Helton, L. Johnson, J. Merriam, B.R. Niederleehner, J.M. O'Brien, J.D. Potter, R.W. Sheibley, S.M. Thomas, and K. Wilson. 2010. Inter-regional comparison of land-use effects on stream metabolism. Freshwater Biology 55:1874-1890.

Bonada, N. and V.H. Resh. 2013. Streams in mediterranean climate regions: lessons learned from the last decade. Hydrobiologia 719: 1-29.

Bott, T.L., D.S. Montgomery, J.D. Newbold, D.B. Arscott, C.L. Dow, A.K. Aufdenkampe, J.K. Jackson, and L.A. Kaplan. 2006. Ecosystem metabolism in streams of the Catskill Mountains (Deleware and Hudson River watersheds) and Lower Hudson Valley. Journal of the North American Benthological Society 25:1018-1044.

Bray, E.N., J. Dozier, and T. Dunne. 2017. Mechanics of the energy balance in large lowland rivers, and why the bed matters. Geophysical Research Letters 44: 8910-8918, doi:10.1002/2017GL075317.

Cairns, J., A.G. Heath, and B.C. Parker. 1975. The effects of temperature upon the toxicity of chemicals to aquatic organisms. Hydrobiologia 47: 135-171.

Carter, K. 2005. The Effects of Temperature on Steelhead Trout, Coho Salmon, and Chinook Salmon Biology and Function by Life Stages: Implications for Klamath Basin TMDLs. California Regional Water Quality Control Board, North Coast Region. 26p.

Clapcott J.E., R.G. Young, E.O. Goodwin, and J.R. Leathwick. 2010. Exploring the response of functional indicators of stream health to land-use gradients. Freshwater Biology 55: 2181-2199.

Cooper, S.D., P.S. Lake, S. Sabater, J.M. Melack, and J.L. Sabo. 2013. The effects of land use changes on streams and rivers in Mediterranean climates. Hydrobiologia 719:383-425.

Demars, B.O.L., J.R. Manson, J.S. Olafsson, G.M. Gislason, R.Gudmundsdottir, G. Woodward, J. Reiss, D.E. Pichler, J.J. Rasmussen, and N. Friberg. 2011. Temperature and the metabolic balance of streams. Freshwater Biology 56: 1106-1121.

Felipe, A.F., J.E. Lawrence, and N. Bonada. 2013. Vulnerability of stream biota to climate change in mediterranean climate regions: a synthesis of ecological responses and conservation challenges. Hydrobiologia 719: 331-352.

Fernandes, I., C. Pascoal, H.Guimaraes, R. Pinto, I. Sousa, and F. Cassio. 2012. Higher temperature reduces the effects of litter quality on decomposition by aquatic fungi. Freshwater Biology 57: 2306-2317. Doi:10.1111/fwb.12004

Foley, J.A., R. DeFries, G.P. Asner, C. Barford, G. Bonan, S.R. Carpenter, F.S. Chapin, M.T. Coe, G.C. Daily, H.K. Gibbs, J.H. Helkowski, T. Holloway, E.A. Howard, C.J. Kucharik, C. Monfreda, J.A. Patz, I.C. Prentice, N. Ramankutty, and P.K. Snyder. 2005. Global Consequences of Land Use. Science 309: 570-574.

Gillooly, J.F., J.H. Brown, G.B. West, V.M. Savage, and E.L. Chamov. 2001. Effects of size and temperature on metabolic rate. Science 293:2248-2251.

Glazier, D.S. 2012. Temperature affects food-chain length and macroinvertebrate species richness in spring ecosystems. Freshwater Science 31(2): 575-585. Doi: http://dx.doi.org/10.1899/11.058.1

Goss, C.W., P.C. Goebel, S. Mazeika, and P. Sullivan. 2014. Shifts in attributes along agriculture-forest transitions of two streams in central Ohio, USA. Agriculture, Ecosystems, and Environment 197: 106-117.

Hawkins, C.P., J.N. Hogue, L.M. Decker, and J.W. Feminella. 1997. Channel morphology, water temperature, and assemblage structure of stream insects. Journal of the North American Benthological Society 16:728-749.

Hette-Tronquart, N., J.Roussel, B. Dumont, V. Archaimbault, D. Pont, T. Oberdorff, J. Belliard. 2013. Variability of water temperature may influence food-chain length in temperate streams. Hydrobiologia DOI: 10.1007/s10750-013-1613-7

Iwata, T., T. Takahashi, F. Kazama, Y. Hiraga, N. Fukuda, M. Honda, Y. Kimura, K. Kota, D. Kubota, S. Nakagawa, T. Nakamura, M. Shimura, S. Yanagida, L. Xeu, E. Fukasawa, Y. Hirasuka, T. Ikebe, N. Ikeno, A. Kohno, K. Kubota, K. Kuwata, T. Misonou, Y. Osada, Y. Sato, R. Shimizu, and K. Shindo. 2007. Metabolic balance of streams draining urban and agricultural watersheds in central Japan. Limnology 8: 243-250.

Izagirre, O., U. Agirre, M. Bermejo, J. Pozo, and A. Elosegi. 2008. Environmental controls of whole-stream metabolism identified from continuous monitoring of Basque streams. Journal of the North American Benthological Society 27: 252-268.

Kendrick, M.R. and J.P. Benstead. 2013. Temperature and nutrient availability interact to mediate growth and body stoichiometry in a detritivorous stream insect. Freshwater Biology 58: 1820-1830. Doi:10.1111/fwb.12170

Kishi, D., M. Murakami, S. Nakano, and K. Maekawa. 2005. Water temperature determines strength of top-down control in a stream food web. Freshwater Biology 50: 1315-1322. Doi: 10.1111/j.1365-2427.2005.01404.x

Lee, J.H., and K.W. Bang. 2000. Characterisation of urban stormwater runoff. Water Research 34: 1773-1780.

Li, J.L., S.L. Johnson, and J.B. Sobota. 2011. Three responses to small changes in stream temperature by autumn-emerging aquatic insects. Journal of the North American Benthological Society 30: 474-484. Doi: http://dx.doi.org/10.1899/10-024.1

Macedo, M.N., M.T. Coe, R. DeFries, M. Uriarte, P.M. Brando, C. Neill, and W.S. Walker. 2013. Land use driven stream warming in southeastern Amazonia. Philosophical Transactions of the Royal Society B 368: 20120153. http://dx.doi.org/10.1098/rstb.2012.0153

Matson, P.A., W.J. Parton, A.G. Power, and M.J. Swift. 1997. Agricultural intensification and ecosystem properties. Science 277: 504-509.

Matthews, K.R. and N.H. Berg. 1997. Rainbow trout responses to water temperature and dissolved oxygen stress in two southern California stream pools. Journal of Fish Biology 50: 50-67.

Moore, R.D., D.L. Spittlehouse, and A. Story. 2005. Riparian microclimate and stream temperature response to forest harvesting: a review. Journal of the American Water Resources Association 41: 813-834.

Meyer, J.L., M.J. Paul, and W.K. Taulbee. 2005. Stream ecosystem function in urbanizing landscapes. Journal of the North American Benthological Society 24: 602-612.

Mulholland, P.J., C.S Fellows, J.L. Tank, N.B. Grimm, J.R. Webster, S.K. Hamilton, E. Marti, L. Ashkenas, W.B. Bowden, W.K. Dodds, W.H. McDowell, M.J. Paul, and B.J. Peterson. 2001. Inter-biome comparison of factors controlling stream metabolism. Freshwater Biology 46: 1503-1517.

Myrick, C.A. and J.J. Cech. 2000. Swimming performances of four California stream fishes: temperature effects. Environmental Biology of Fishes 58: 289-295.

Paul, M.J., and J.L. Meyer. 2001. Streams in the urban landscape. Annual Review of Ecology and Systematics 32: 333-365.

Pluhowski, E.J. 1970. Urbanization and its effect on the temperature of streams in Long Island, New York. USGS Professional Paper 627-D.

Rice, J.S., W.P. Anderson, Jr., and C.S. Thaxton. 2011. Urbanization influences on stream temperature behavior within low-discharge headwater streams. Hydrological Research Letters 5: 27-31. doi: 10.3178/HRL.5.27

Rosenfeld, J.S., and R.J. Mackay. 1987. Assessing the food base of stream ecosystems: Alternatives to the P/R ratio. Oikos, 50: 141-147.

Taniguchi, Y, F.J. Rahel, D.C. Novinger, and K.G. Gerow. 1998. Temperature mediation of competitive interactions among three fish species that replace each other along longitudinal stream gradients. Canadian Journal of Fisheries and Aquatic Sciences 55: 1894-1901.

Tank, J.L., E.J. Rosi-Marshall, N.A. Griffiths, S.A. Entrekin, and M.L. Stephen. 2010. A review of allochthonous organic matter dynamics and metabolism in streams. Journal of the North American Benthological Society, 29: 118-146.

United Nations, Department of Economic and Social Affairs, Population division. 2015. World Urbanization Prospects: The 2014 Revision, (ST/ESA/SER.A/366). Accessed on November 4, 2015 at http://www.un.org/en/development/desa/population/theme/urbanization/index.shtml

Vannote, R.L., G.W. Minshall, K.W. Cummins, J.R. Sedell, and C.E. Cushing. 1980. The river continuum concept. Canadian Journal of Fisheries and Aquatic Sciences 37: 130-137.

Vitousek, P.M., H.A. Mooney, J. Lubchenco, and J.M. Melillo. 1997. Human domination of earth's ecosystems. Science 277: 494-499.

von Schiller, D., E. Marti, J.L. Riera, M. Ribot, J.C. Marks, and F. Sabater. 2008. Influence of land use on stream ecosystem function in a Mediterranean catchment. Freshwater Biology 53: 2600-2612.

Walsh, C.J., A.H. Roy, J.W. Feminella, P.D. Cottingham, P.M. Groffman, and R.P. Morgan II. 2005. The urban stream syndrome: current knowledge and the search for a cure. Journal of the North American Benthological Society 24: 706-723.

Webb, B.W. 1996. Trends in stream and river temperature. Hydrological Processes 10: 205-226.

Webb, B.W., D.M. Hannah, R.D. Moore, L.E. Brown, and F. Nobilis. 2008. Recent Advances in stream and river temperature research. Hydrological Processes 22: 902-918. Doi: 10.1002/hyp.6994

Young , R.G., C.D. Matthaei, and C.R. Townsend. 2008. Organic matter breakdown and ecosystem metabolism: Functional indicators for assessing river ecosystem health. Journal of the North American Benthological Society 27(3): 605-625.

Williamson, C.E., W. Dodds, T.K. Kratz, and M.A. Palmer. 2008. Lakes and streams as sentinels of environmental change in terrestrial and atmospheric processes. Frontiers in Ecology and Environment, 6(5): 247-254.

2. Study Area

The study area is located in the south-facing coastal area of Santa Barbara County, California (Figure 2). The region is tectonically active, lying at the boundary of the North American and Pacific tectonic plates. The Santa Barbara coastline features many steep streams draining watersheds in the Santa Ynez mountain range, with ridgeline elevations ranging from 678 m at San Marcos Pass to 1435 m at Divide Peak, and discharging to the Pacific Ocean in the Santa Barbara Channel. The Santa Ynez Mountains are part of the western Transverse Ranges and primarily consist of sedimentary rocks of marine and non-marine origin (Minor et al., 2009).

The Santa Ynez Mountains also form the northern boundary of the study area for the Santa Barbara Coastal Long Term Ecological Research Project (SBC LTER). The SBC LTER program studies the chemical, biological, and physical relationships between the terrestrial environment of the Santa Barbara south coast and the marine ecosystems in the Santa Barbara Channel.

Similar to other regions with Mediterranean climates containing many endemic plant and animal species (Myers et al., 2000), the Santa Barbara coast is part of the California Floristic Province, which has been recognized as a global hotspot of biodiversity (Cincotta et al., 2000; Myers et al., 2000). High levels of plant biodiversity have been attributed to a variety of geographic and topographic factors that lead to evolutionary divergence while also preventing extinctions (Baldwin, 2014). Additionally, the adjacent Santa Barbara Channel is located in a transition zone between cold and warm waters, leading to high biodiversity in the near-shore waters (Myers et al., 2017).

2.1. Climate

The study region is characterized by a Mediterranean climate with wet winters and an extended summer dry season, but exhibiting high inter-annual variation in rainfall. On average, about 75% of rainfall and runoff occurs between December and March in the Santa Barbara area (Figure 1a, Beighley et al., 2005). During the years covered by this study (2001-2015), annual rainfall totals in downtown Santa Barbara were both exceptionally low (16.3 cm in 2007, lowest total in 118 year record) and high (93.8 cm in 2005, 95th percentile) when compared to the long-term record (1900 to 2017, Figure 1b), which had a long-term annual mean of 46.7 cm (County of Santa Barbara, 2017a). The east-west orientation of the Santa Ynez Mountains, paired with southerly winds during winter storms, leads to orographically enhanced rainfall (Myers et al. 2017). For the period from 2001-2017, average annual rainfall totals at San Marcos Pass (77.7 cm, elevation 681 m) were 178% of those recorded on the coastal plain in downtown Santa Barbara (43.6 cm, elevation 40 m) (County of Santa Barbara, 2017b).

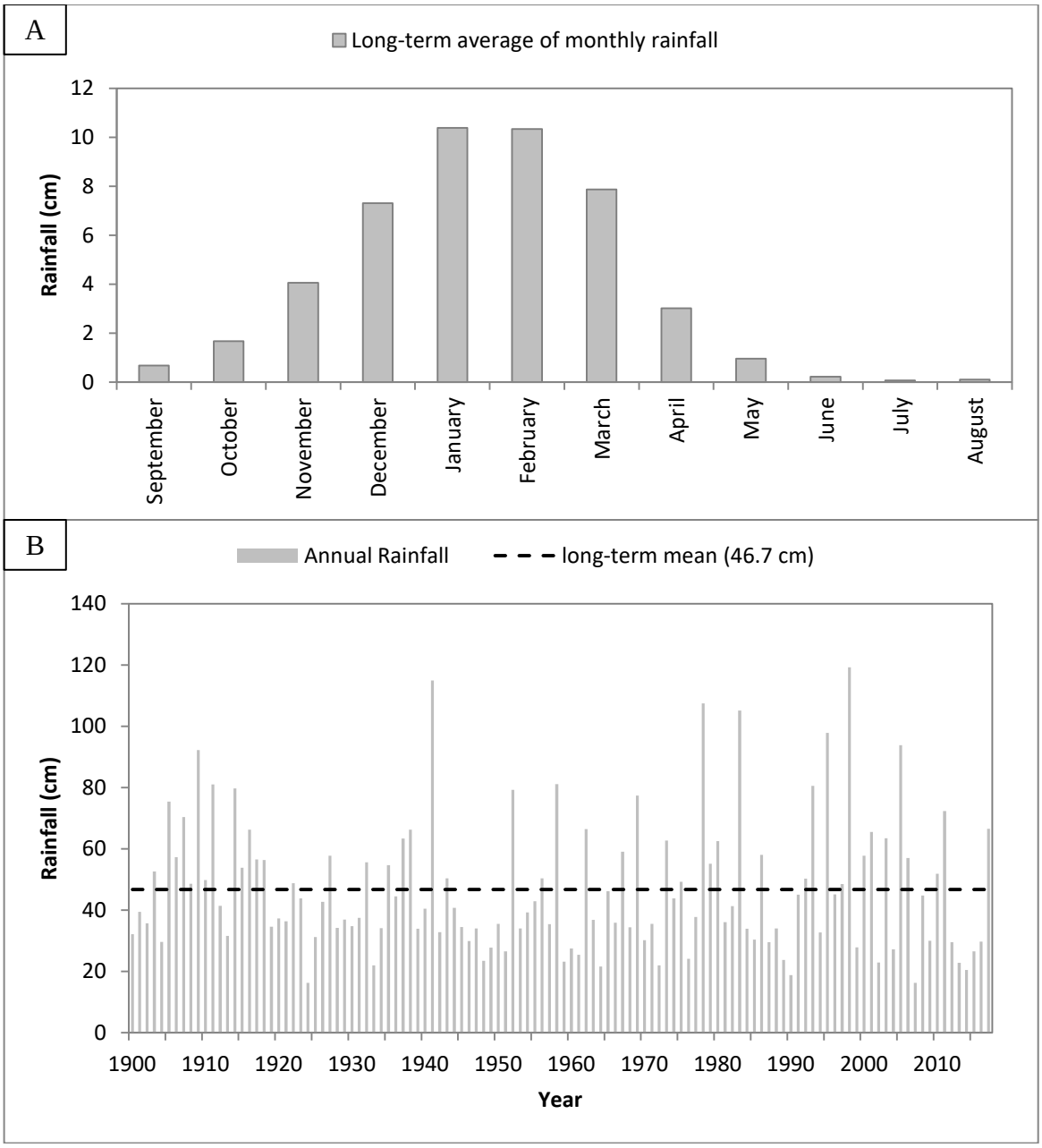

Figure 1: Rainfall data from 1900 to 2017 at County of Santa Barbra Station 234, located in downtown Santa Barbara, showing (A) long-term average rainfall for each month and (B) annual rainfall totals for each year, compared to the long-term annual rainfall mean (dashed line) (County of Santa Barbara, 2017a).

Air temperatures in the study area, based on downscaled global climate model data for the time period from 1985-2014, have an annual mean for daily minimum temperature of 10°C and an annual mean for daily maximum temperature of 21.8°C (Myers et al. 2017).

Seasonal variation between summer and winter in daily minimum air temperature and daily maximum air temperature are about 7°C and 6°C, respectively (Table 1).

Table 1: Average minimum and maximum daily air temperatures across seasons and the year over the Santa Barbara south coast region, for the period from 1985-2014 (Myers et al., 2017)

	Annual	DJF (Winter)	MAM (Spring)	JJA (Summer)	SON (Fall)
Daily Minimum Temperature (°C)	10.0	6.0	9.1	13.7	11.1
Daily Maximum Temperature (°C)	21.8	18.7	20.5	24.6	23.5

2.2. Land Use

The study area encompasses gradients of urban and agricultural land use across coastal watersheds. Urban development is concentrated in the cities of Santa Barbara, Goleta, and Carpinteria, with a combined population of approximately 220,000, including unincorporated areas. Most urban development in this region occurs at lower elevations on the coastal plain, with few people living in the steep headwater areas of watersheds (Figure 2). Agricultural land use occurs primarily in the foothills on the northern boundary of Goleta, in the valleys and foothills of the watersheds west of Goleta, and surrounding Carpinteria to the north and east (Figure 2, Panel A). The Carpinteria area also has a large number of greenhouse operations.

Undeveloped land is concentrated at higher elevations in the watersheds that have urban or agricultural development at lower elevations, although there are some entire watersheds with minimal development. Undeveloped areas are covered by a mix of native and non-native vegetation types, including grassland, oak woodland, shrub (chaparral and coastal sage scrub), and riparian habitats.

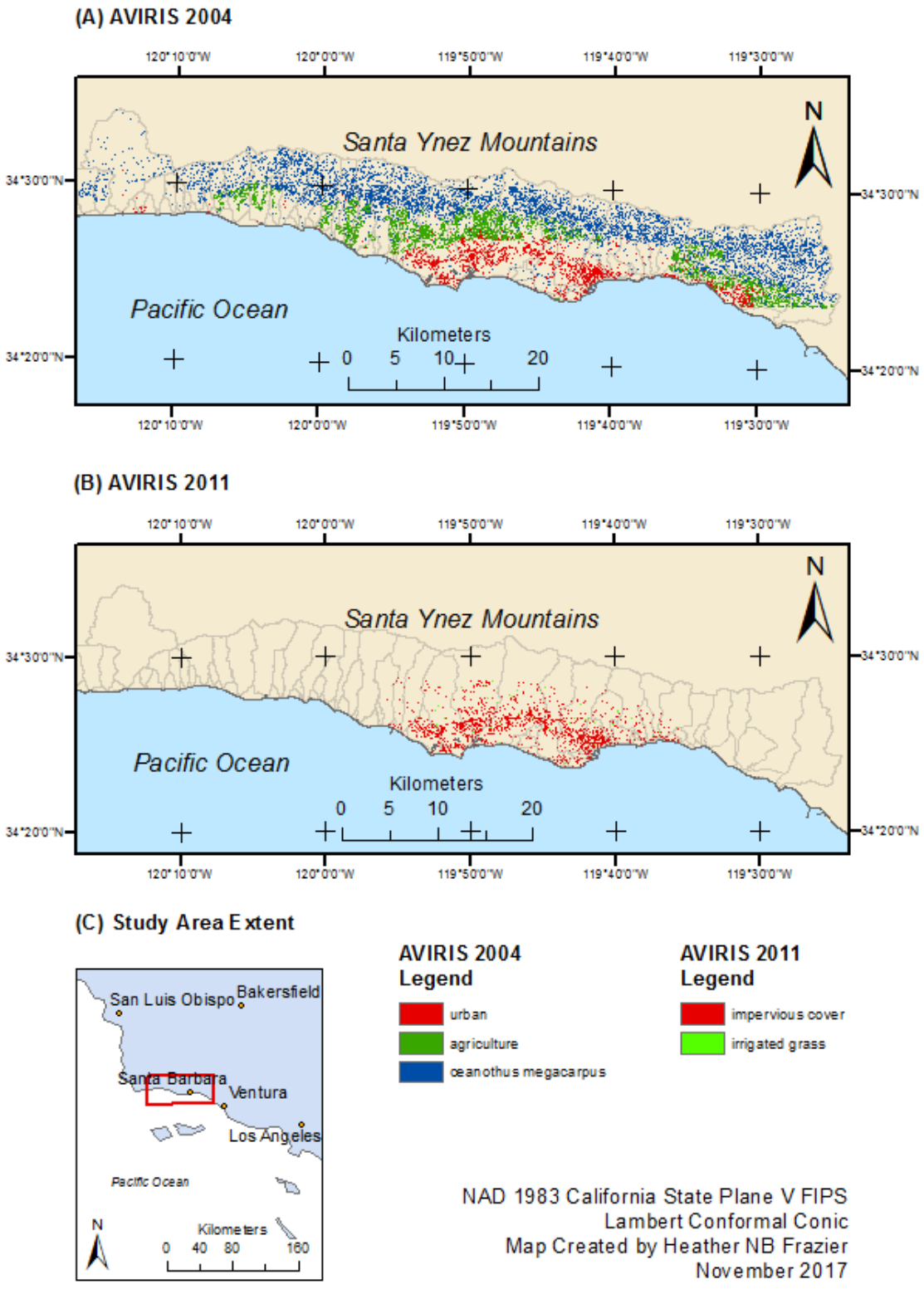

Figure 2: Land use classification maps for (A) the whole study area based on AVIRIS imagery collected in 2004 and (B) the Goleta and Santa Barbara urban areas, based on AVIRIS data collected in 2011.

Land use for each watershed and for each upstream area of influence were extracted from a land use classification map derived from Airborne Visible-Infrared Imaging Spectrometer (AVIRIS) Classic data collected in 2004 and 2011. AVIRIS Classic is a hyperspectral optical sensor that collects radiance reflected from the Earth surface in the visible and near infrared range of the electromagnetic spectrum, including 224 bands for wavelengths between 400 nm and 2500 nm.

The 2004 AVIRIS data were collected on August 6, 2004 with the classification map having a spatial resolution of 16 m and covering the entire coast from Gaviota to Carpinteria between the ocean and the crest of the Santa Ynez Mountains (about 8.7 km^2 is missing for the RN01 watershed; Figure 2, Panel A). The 2011 AVIRIS imagery was collected on July 19, 2011, has a 7.5 m spatial resolution, and covers the Santa Barbara and Goleta urban areas, allowing the discrimination of manmade from natural surfaces (Figure 2, Panel B). The 2004 AVIRIS imagery is the main source of land use data for comparisons among watersheds in the region, whereas the 2011 AVIRIS imagery provided more detailed information about variations within urban areas. The reflectance data for the two sets of imagery were processed using multiple end-member spectral analysis (MESMA) and a library of known spectral signatures for each land use class were used to create the final maps of land use and land cover (Roberts et al., 1998). Additional details on the processing methods for the 2011 AVIRIS imagery are provided in Roberts et al. (2017).

The specific classes from each image were combined into broader categories to represent the general urban and agricultural characteristics of the landscape. The 2004 AVIRIS classification map included urban and agricultural classes, constituting the main indicators

of urban and agricultural development, respectively. Where 2004 AVIRIS data were cut-off in the Rincon watershed, USGS NLCD data was used instead (Homer et al., 2015). Prior work by Robinson et al. (2005) provided a detailed description of land use in the Carpinteria area, so these data were used to determine impervious cover for the Franklin Creek and Carpinteria Creek watersheds. The 2011 AVIRIS classification map included a number of urban classes, including various roofing types, paved surfaces, and artificial turf, which were combined into a single class, along with rock cover, to arrive at an impervious cover class for the 2011 AVIRIS imagery. The 2011 AVIRIS map also included an irrigated grass category, which included golf courses or playing fields. Undeveloped, non-agricultural, and non-urban land uses from the 2004 AVIRIS map were lumped together in an undeveloped class, excluding irrigated grass and unknown classes.

2.3. References

Baldwin, B. 2014. Origins of plant diversity in the California floristic province. Annual Review of Ecology, Evolution, and Systematics 45: 347-369. https://doi.org/10.1146/annurev-ecolsys-110512-135847

Beighley, R.E., T. Dunne, and J.M. Melack. 2005. Understanding and modeling basin hydrology: interpreting the hydrogeological signature. Hydrological Processes 19: 1333-1353. Doi: 10.1002/hyp.5567.

Cincotta, R.P., J. Wisnewski, and R. Engelman. 2000. Human populations in the biodiversity hotspots. Nature 404: 990-992.

County of Santa Barbara, Department of Public Works Water Resources Hydrology. September 2017a. Official monthly and yearly rainfall record, station 234. Accessed October 25, 2017. http://www.countyofsb.org/pwd/water/downloads/hydro/234mdd.pdf

County of Santa Barbara Department of Public Works Water Resources Hydrology. September 2017b. Official monthly and yearly rainfall record, station 212. Accessed October 26, 2017. http://www.countyofsb.org/pwd/water/downloads/hydro/212mdd.pdf

Homer, C.G., Dewitz, J.A., Yang, L., Jin, S., Danielson, P., Xian, G., Coulston, J., Herold, N.D., Wickham, J.D., and Megown, K., 2015, Completion of the 2011 National Land Cover Database for the conterminous United States-Representing a decade of land cover change information. *Photogrammetric Engineering and Remote Sensing*, v. 81, no. 5, p. 345-354

Minor, S.A., K.S. Kellogg, R.G. Stanley, L.D. Gurrola, E.A. Keller, and T.R. Brandt. 2009. Geologic Map of the Santa Barbara Coastal Plain Area, Santa Barbara County, California: U.S. Geological Survey Scientific Investigations Map 3001, scale 1:25,000, 1 sheet, pamphlet, 39 p.

Myers, M.R., D.R. Cayan, S.F. Iacobellis, J.M. Melack, R.E. Beighley, P.L. Barnard, and J.E. Dugan, H.M. Page. 2017. Santa Barbara Coastal Ecosystem Vulnerability Assessment. CASG-17-009.

Myers, N., R.A. Mittermeier, C.G. Mittermeier, G.A.B. da Fonseca, and J.Kent. 2000. Biodiversity hotspots for conservation priorities. Nature 2000 403: 853-858.

Roberts, D.A., M. Gardner, R. Church, S. Ustin, G. Scheer, and R.O. Green.1998. Mapping chaparral in the Santa Monica Mountains using multiple endmember spectral mixture models. Remote Sensing of Environment 65: 267-279.

Roberts, D., M. Alonzo, E.B. Wetherley, K.L. Dudley, and P.E. Dennison. 2017. Multiscale Analysis of Urban Areas Using Mixing Models. Pages 247-282 in D.A. Quattrochi, E. Wentz, N. Siu-Ngan Lam, and C.W. Emerson (Eds.) Integrating Scale in Remote Sensing and GIS. Routledge, London.

Robinson, T.H., A. Leydecker, J.M. Melack, and A.A. Keller. 2005. Steps toward modeling nutrient export in coastal Californian streams with a Mediterranean climate. Agricultural Water Management 77:144-158.

3. Stream metabolism in coastal streams: Increased productivity related to urban landscapes

3.1. Introduction

Urban land use is a particular problem for stream ecosystems, leading to several consistent, well-documented changes in the physical, chemical, and biological conditions of receiving streams, often called the 'urban stream syndrome' (Paul and Meyer 2001; Allan 2004; Walsh et al., 2005; Cooper et al., 2013). The interacting effects of land use and climate threaten stream ecosystems in areas with Mediterranean climates, creating a critical need to measure and understand the extent of the urban influence in these streams (Felipe et al., 2013; Cooper et al., 2013). Stream metabolism, the rates and balance of primary productivity and respiration in a stream, describes the fundamental dynamics of organic matter creation and consumption in a stream ecosystem and is sensitive to many of the changes commonly associates with urbanization, including loss of riparian vegetation, increased nutrients and temperatures, and changes in hydrology and organic matter inputs (Bernot et al., 2010). However, prior studies have demonstrated inconsistent responses of GPP, CR, P/R, and NEP to urban development (Bott et al., 2006a; von Schiller et al., 2008; Bernot et al., 2010), indicating that stream metabolism studies in urban streams are warranted, particularly in areas with Mediterranean climates.

In my research, I seek to answer the question of how GPP, CR, NEP, and P/R change among catchments with different extent of urban development and to determine environmental variables (e.g., nutrients, light, temperature, organic matter) that influence those changes. I predict that increased nutrients and light availability associated with urban

development will lead to higher GPP in urban catchments. I expect that some drivers of CR will be enhanced (temperature and nutrients), but that others will be variable (availability of organic matter) among sites with varying urban land use, leading to inconsistent responses in CR. I expect the resulting NEP and P/R will be more positive in urban streams than non-urban streams, indicating an overall increase in autotrophy and the decreased importance of external sources (allochthonous sources) of organic matter in the stream ecosystem. I also expect that the changes in GPP, CR, NEP, and P/R among catchments will be associated with differences in metrics (e.g., impervious cover, human population density) of urban land use across watersheds.

To assess these predictions, I used a comparative design across multiple watersheds with varying urban land use but with similar geology, climate, and size, matching, as closely as possible, the geomorphic setting across sites. At each location, stream metabolism was measured using an open-system diel oxygen change method and relevant environmental variables, including physical, chemical, and biological parameters, were collected at each site. To capture a range of environmental conditions, the measurements were repeated through time coinciding with the seasonal shift from the cool rainy season to the warm dry season. The resulting data were compared between urban and non-urban locations and to gradients in land use between sites.

3.2. Study Sites and General Study Design

Six streams were selected for this study, including 2 sites in undeveloped watersheds (Arroyo Hondo (HO) and Rattlesnake (RS) creeks) and 4 sites with varying urban/suburban development (Phelps (PH), Atascadero (AT), Arroyo Burro (AB), and Sycamore (SY) creeks) (Figure 4). The watersheds draining to the study sites ranged in area from 3.3 to 23.6

km^2 and had urban land use varying from 0-24% (Table 3, Table 5). Study sites were chosen based on their accessibility, base flow conditions, and land use targets.

Table 2: Metabolism schedule of data collection

Deployment	Range of data collection dates
1	March 11, 2014 – March 29, 2014
2	April 2, 2014 – April 15, 2014
3	April 22, 2014 – May 6, 2014
4	May 20, 2014 – June 5, 2014
5	June 13, 2014 – June 30, 2014
6	July 8, 2014 – July 22, 2014

Data collection commenced in March 2014 and continued in 6 staggered deployments (Table 2) of at least 3 days duration per site through July 2014, except for RS, which had only 3 deployments because it dried at the beginning of May. Rainfall during the study period was limited, but data collection began soon after the largest rainfall event of the year (Figure 3). During each deployment, at least three consecutive days of dissolved oxygen, temperature, photosynthetically active radiation (PAR), and water level data were collected to allow the calculation of daily gross primary production (GPP), community respiration (CR), and net ecosystem production (NEP) rates, as well as primary production to respiration ratios (P/R), for each stream ecosystem. A 100 m reach upstream from the oxygen logger attachment location was used to sample additional variables. Data on benthic algal biomass, nutrient (N, P) and dissolved organic carbon (DOC) concentrations, canopy cover, conductivity, total suspended solids (TSS), water velocity, water depth, water width, and discharge were collected once during each deployment, usually at the end of the deployment. Additionally, data for benthic organic matter (FBOM and CBOM), channel slope, and general site mapping were collected once during the study. Metabolism values

were then compared to the environmental and land use variables across sites to assess the influences of environmental and land use variables on metabolism.

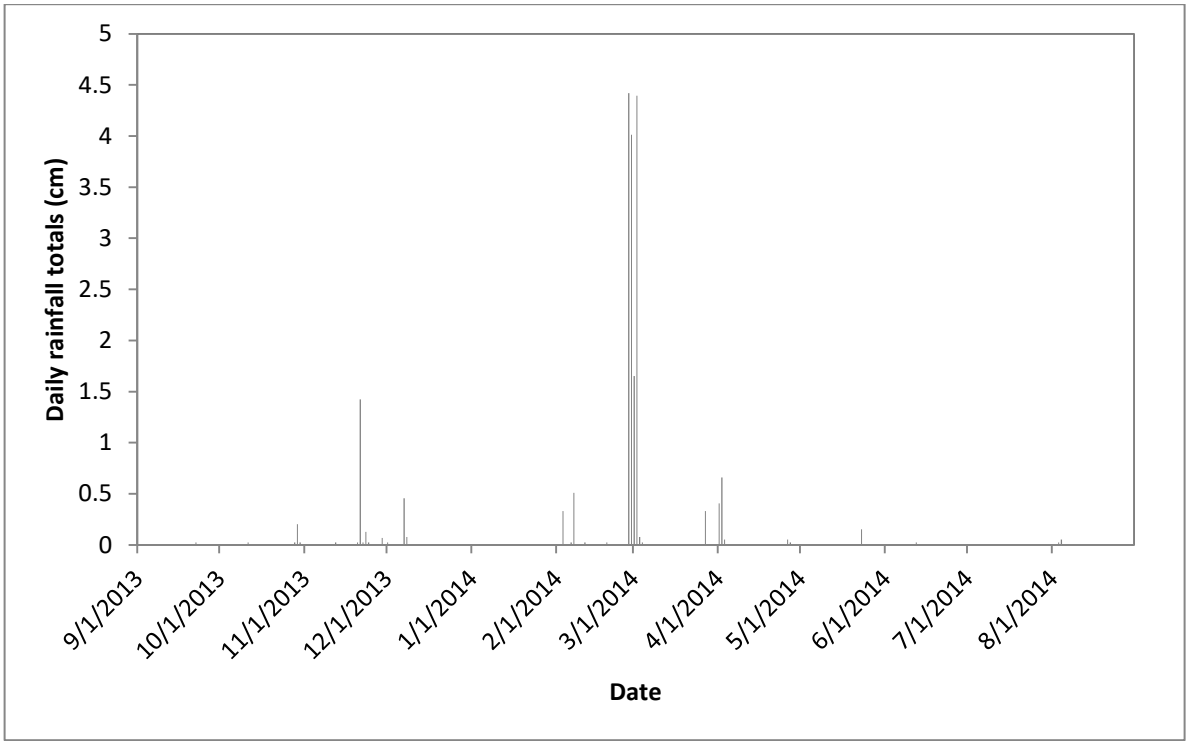

Figure 3: Rainfall in downtown Santa Barbara during the 2014 water year (County of Santa Barbara, 2016b)

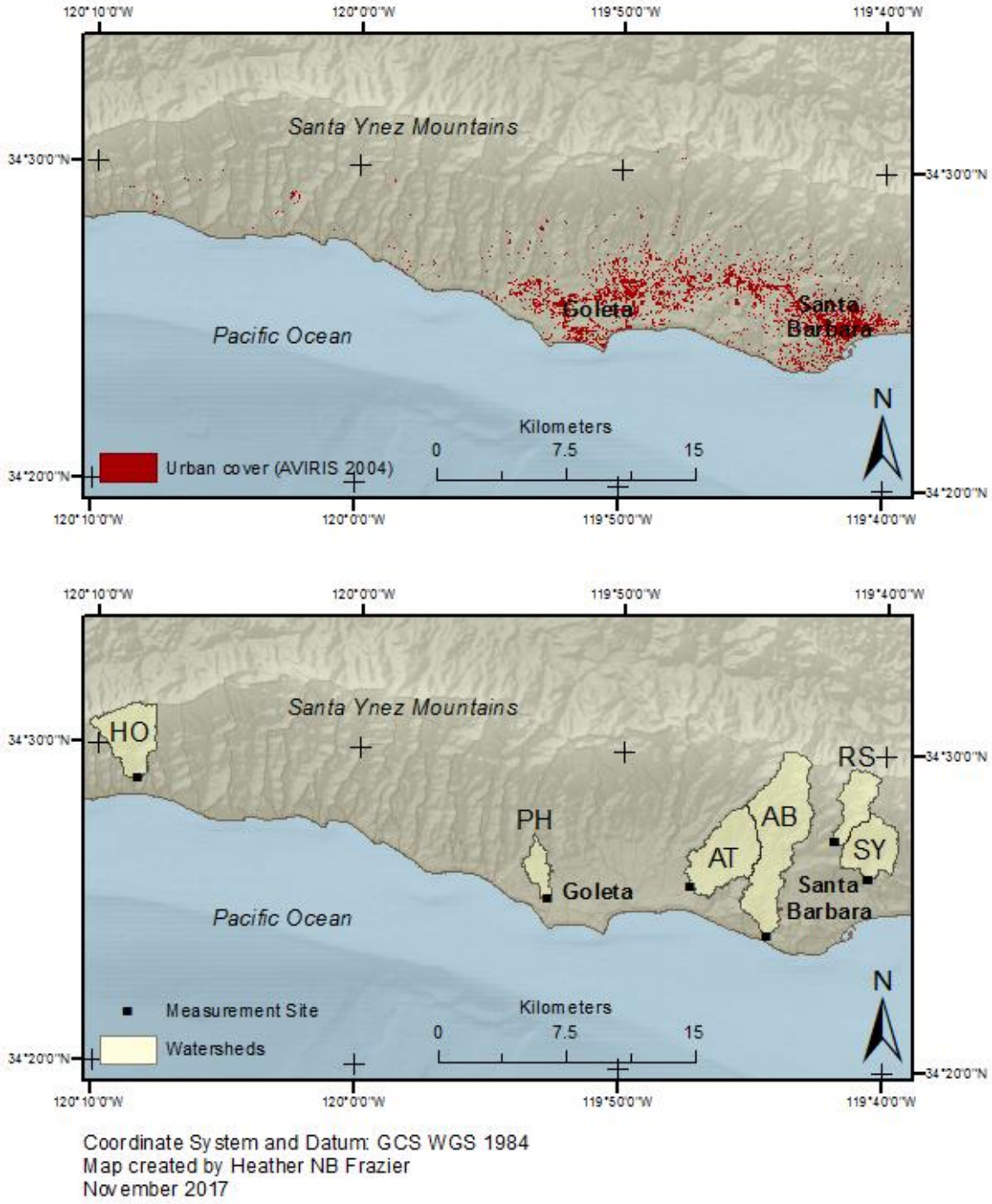

Figure 4: Map of metabolism study sites. Urban cover shown is the urban class from the 2004 AVIRIS classification map, described in the study area description. Watershed areas draining to each study site are shown.

Table 3: Site locations and characteristics

Site	Latitude	Longitude	Elevation (m)	Drainage Area (km^2)	Channel slope (%)	Water Slope (%)
HO	34.482000	-120.140606	35	10.5	1.4	0.16
RS	34.455400	-119.698936	230	6.3	4.8	--
SY	34.435150	-119.676744	35	8.8	3.1	2.9
AB	34.405192	-119.740178	5	23.6	0.3	0.02
AT	34.430097	-119.789497	10	13.9	0.03	0.001
PH	34.422812	-119.879836	5	3.3	0.15	0.17

3.2.1. Watershed delineation and determination of upstream riparian area of influence (AOI)

The watershed draining to each study reach was delineated using the ArcGIS Spatial Analyst and ArcHydro Toolboxes (version 10.0, ESRI, Redlands, CA) on a NOAA DEM of southern Santa Barbara County (Carignan et al., 2009). Using the ArcHydro Toolbox, sinks in the DEM (cells with no neighboring cells at lower elevations) were filled, flow directions were calculated for each cell, and flow accumulation for each cell was calculated (the number of upslope cells draining to a given cell). The downstream end of each study reach identified the pour point for watershed delineation at each site, while also determining the upstream cells contributing flow to the study reach. Because initial watershed delineations were unrealistic for Phelps Creek, likely owing to low slopes and the presence of obfuscating bridges or buildings, stream channels were "burned in" using the ArcHydro DEM reconditioning tool to force flow to the channel within a given buffer distance based on the AGREE protocol's default settings, producing more realistic demarcations. Watershed land use metrics were extracted using shapefiles of the delineated watersheds.

Because all metabolism and environmental measurements were made during a dry period, it may not be inappropriate to assume that processes in the entire watershed influenced measurements within the reach (Goodridge and Melack, 2012). As a

consequence, a localized riparian area of influence (AOI) and associated land use metrics for this zone were delineated for each study reach. For metabolism estimates, the upstream distance (X in m) integrated by the measurements made by the dissolved oxygen sensor can be estimated based on the velocity of flow (v in m s^{-1}) and the reaeration rate (gas transfer velocity divided by average depth, K_{O2} in s^{-1}) using the following equation (Chapra and DiToro, 1991; discussed in Grace and Imberger, 2006):

$$X = 3v/K_{O2}. \quad \text{(Eq. 1)}$$

This estimate of upstream influence was calculated for each deployment at each site using the same velocity and gas transfer velocities used to calculate metabolism, as described in the methods. The average upstream distance of influence for all deployments, buffered by 50 m on each site of stream, was used to define the AOI at each site and the land use characteristics in the AOI were determined. The distances of upstream influence for each site are listed in Table 4.

Table 4: Upstream Influence for each site

Site	HO	RS	SY	AB	AT	PH
Distance of Upstream Influence (m)	480	210	300	2850	1570	770

3.2.2. Land use characteristics

The 2004 AVIRIS classification map, as described in the study area description, was used to extract cover by land use classes for entire watersheds, whereas the 2011 AVIRIS classification map, also described in the study area description, was used to extract land use cover information for the upstream area of influence (AOI). For Arroyo Hondo, which was

outside the spatial extent of the 2011 AVIRIS data, the impervious and irrigated grass areas were assumed to be 0.

The number of septic parcels in or touching each watershed or AOI was determined from a shapefile of septic parcels provided by the County of Santa Barbara Public Health Department. In addition, the number of street crossings was counted manually for each AOI; the length of a channelized section was divided by the total stream length in the AOI to get proportion stream channelization; and areas of parcels identified as golf courses falling within each watershed or AOI were calculated (using shapefiles provided by the County of Santa Barbara). The human population in each watershed and AOI were calculated from 2010 Census TIGER data at the census block level. Population densities were calculated for each census block by dividing by census block area. These densities were used to calculate the population in each watershed and AOI by assuming an even spatial distribution of population and using the area of each census block intersecting a watershed or AOI to calculate the number of people expected in that portion of the census block. Values for the portions of all census blocks intersecting the watershed or AOI were summed to get the total population, which was then divided by the watershed or AOI area to get population density (Table 5).

Table 5: Watershed and AOI land use characteristics.

Watershed Characteristic	HO	RS	SY	AB	AT	PH
Area (km^2)	10.5	6.3	8.8	23.6	13.9	3.3
Urban area (hectares, AVIRIS 2004)	1	1	11	166	225	80
Impervious area (heactares, AVIRIS 2011)	0	6	50	216	268	77
Ceanothus megacarpus area (hectares, AVIRIS 2004)	262	198	194	458	43	4
Population	1	91	2276	12718	15072	6583
Golf parcel area (hectares)	0.0	0.0	0.0	57.7	3.1	40.7
Septic parcels (count)	1	9	173	308	495	173
% Urban Cover (AVIRIS 2004)	0	0	1	7	16	24
% Impervious Cover (AVIRIS 2011)	0	1	6	9	19	23
% Ceanothus megacarpus cover (AVIRIS 2004)	25	31	22	19	3	1
Population density (people/km^2)	0	14	259	539	1084	1995

AOI Characteristic	HO	RS	SY	AB	AT	PH
Area (hectares)	4.6	1.5	2.9	39.5	26.3	7.3
Urban area (m^2, AVIRIS 2004)	0	512	0	27648	13312	19200
Impervious Area (m^2, AVIRIS 2011)	0	225	1350	36731	58781	14006
Population	0	3	17	358	412	134
Irrigated grass area (m^2, AVIRIS 2011)	0	169	2363	26100	14513	4781
Septic parcels (count)	1	0	0	13	1	0
% Urban Cover (AVIRIS 2004)	0	3	0	7	5	26
% Impervious Cover (AVIRIS 2011)	0	1	5	9	22	19
% Irrigated grass cover (AVIRIS 2011)	0	1	8	7	6	7
% AOI length channelized	0	0	0	13	69	63
Population density (people/km^2)	0	200	586	906	1567	1836

3.3. Methods

3.3.1. Continuously monitored variables: Dissolved oxygen, temperature, and photosynthetically available radiation

Dissolved oxygen concentrations and water temperature measurements were made with D-Opto Oxygen Loggers (Zebra-Tech Ltd., Nelson, New Zealand; DO: 0.02 ppm accuracy, 0.001 ppm resolution; temperature: ±0.1°C accuracy, 0.01°C resolution) placed at mid-depth (ranging 0.03-0.37 m across all times and sites) at a location where cross-sectional mixing was most likely (e.g., a confined riffle without major surface disturbances where flow was confined to a single channel). Water depth and the depth of the probe were measured at the

time of each deployment. Prior to deployment, the oxygen loggers were calibrated in the laboratory at sea level according to the manufacturer's instructions. In addition, two TidbiT v2 temperature loggers (Onset Corp., Cape Cod, MA, USA; ±0.21°C accuracy, 0.02°C resolution, 5 minute response time, 0.1°C per year drift) were deployed upstream of the oxygen logger, with one in the nearest riffle and the other in the nearest pool. If nearby pools or riffles were not present, loggers were placed within the first 50 meters upstream of the oxygen logger. Tidbit loggers were inter-calibrated in the laboratory (Table 6), with the range of temperature values among loggers averaging 0.32°C, when times of rapid change (8°C in a day) were included, but averaging 0.18°C, when changes were more gradual (three days of data when daily temperature changes were < 3°C per day). In some cases, a level logger, which also recorded temperature (Solonist Levellogger, various models, ±0.1°C accuracy, 0.1°C resolution), was deployed within 50 m upstream of the oxygen logger with temperature loggers being spaced to provide coverage in a different pool or riffle from the level logger. All temperature loggers were secured at the bed surface, zip tied to bricks or helical screw anchors, and protected from direct sunlight using manufacturer-provided solar covers or by leaning a rock over the sensor. Water depth at each logger was recorded at the time of deployment.

Table 6: Correlation coefficients for tidbit temperature logger test data

Last two digits of Tidbit serial number	74	75	76	77	78	79	80	81	82	83
74	0	0.990	0.984	0.983	0.982	0.988	0.998	0.998	0.983	0.993
75	0.990	0	0.996	0.997	0.996	0.997	0.984	0.987	0.997	0.997
76	0.984	0.996	0	0.999	0.999	0.998	0.975	0.982	0.998	0.995
77	0.983	0.997	0.999	0	0.999	0.998	0.975	0.981	0.999	0.996
78	0.982	0.996	0.999	0.999	0	0.998	0.973	0.979	0.998	0.996
79	0.988	0.997	0.998	0.998	0.998	0	0.981	0.985	0.998	0.998
80	0.998	0.984	0.975	0.975	0.973	0.981	0	0.997	0.976	0.987
81	0.998	0.987	0.982	0.981	0.979	0.985	0.997	0	0.980	0.989
82	0.983	0.997	0.998	0.999	0.998	0.998	0.976	0.980	0	0.995
83	0.993	0.997	0.995	0.996	0.996	0.998	0.987	0.989	0.995	0

Light available for photosynthesis was measured at the oxygen logger location for each deployment with an Odyssey Photosynthetic Irradiance Logger (Dataflow Systems Pty Ltd., Christchurch, New Zealand), which is a cosine corrected light sensor that measured light levels between 400 and 700 nm. The logger was attached using pipe clamps to a helical screw anchor or rebar driven into the channel such that the light diffusion disc was above the top of the anchor, but within 0.5 meters of the water surface. To maintain consistent logger orientation to the incoming light, the light loggers were leveled at the diffusion disk using a multi-directional bubble level at the time of deployment.

To calibrate logger counts to photosynthetically available radiation (PAR) levels, logger measurements at 5-minutes intervals were compared to instantaneous measurements made using a LI-COR LI-190S quantum sensor attached to a LI-COR LI-185A quantum meter (LI-COR, Inc., Lincoln, NE, USA), averaged over the same time increments. Calibration measurements were made during three separate sessions under natural sunlight, generating a total of 31 datapoints for each logger (Figure 5) producing tight linear relationships between each Odyssey logger and the LI-COR meter data ($R^2 > 0.99$ for all the loggers, Figure 6).

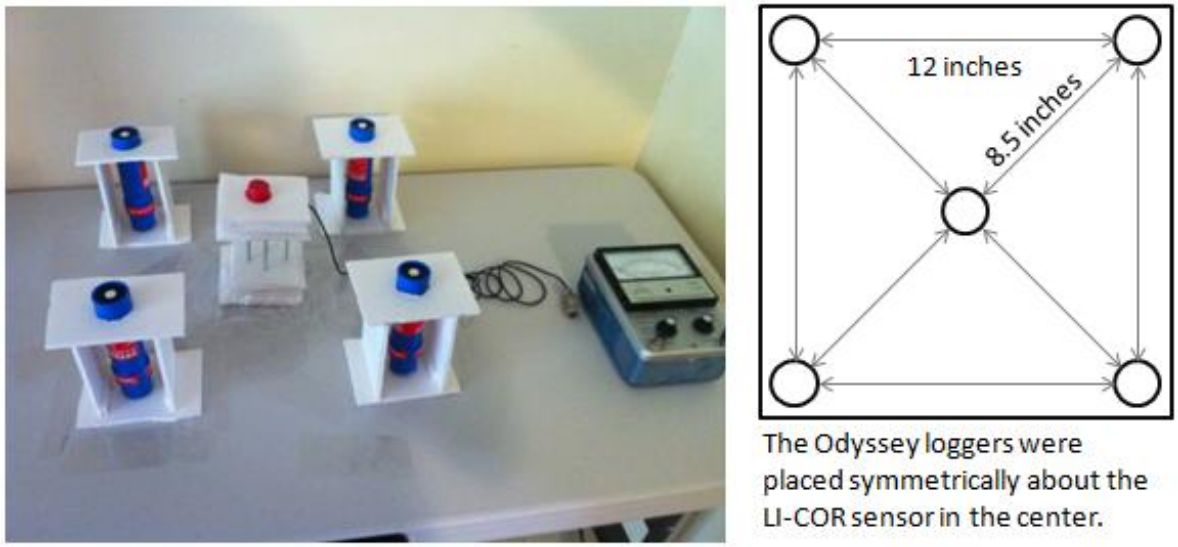

Figure 5: PAR logger calibration design

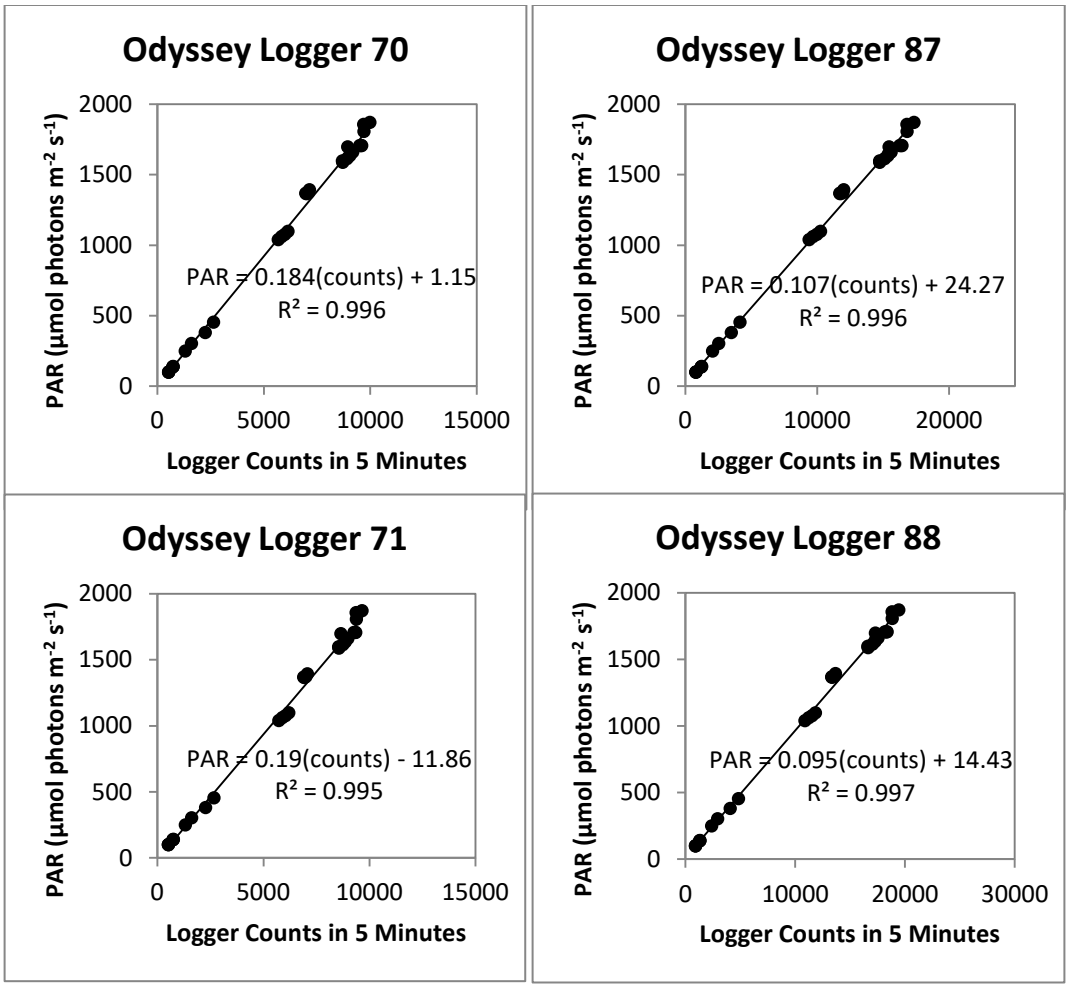

Figure 6: Calibration curves for the Odyssey loggers

Water level was monitored every five minutes using a Solonist Levelogger pressure transducer (Solonist Canada Ltd. Georgetown, Ontario, Canada, various models, minimum accuracy 1 cm) installed in a perforated pipe at each location, except Phelps and Arroyo Burro creeks, which had leveloggers installed by the Santa Barbara Coastal Long Term Ecological Research Project or the Cheadle Center for Biodiversity and Biological Restoration. Manual stage measurements at the level logger location were taken at least twice during each deployment, and usually more frequently, to tie level logger records to

direct depth measurements. All loggers, which collected data at 5-minute intervals, were synchronized to the same computer clock to ensure agreement among measurement times.

3.3.2. Collection of depth, velocity, and substratum data

Several variables were collected, throughout each reach, one time per deployment, using a distributed sampling strategy, which was adapted from Klose et al. (2012) and Ode (2007). All samples were collected within the 100 m reach upstream from the oxygen logger location. This 100 m study reach was split into 10 equal 10 m segments. In each 10 m segment, the location for a single cross section was randomly selected using a random numbers table. For each study reach, the 10 stream segments did not change from one deployment to the next, but a new randomly-selected cross-section was chosen for each section for each deployment. For each cross-sectional transect, then, width was measured, recorded, and split into 4 even segments, with the inter-segment boundaries providing 3 evenly-spaced sampling locations for substratum characterization, algal sampling, and depth and velocity measurements (Figure 7). If the selected sampling location was dry, then the next nearest possible location was measured.

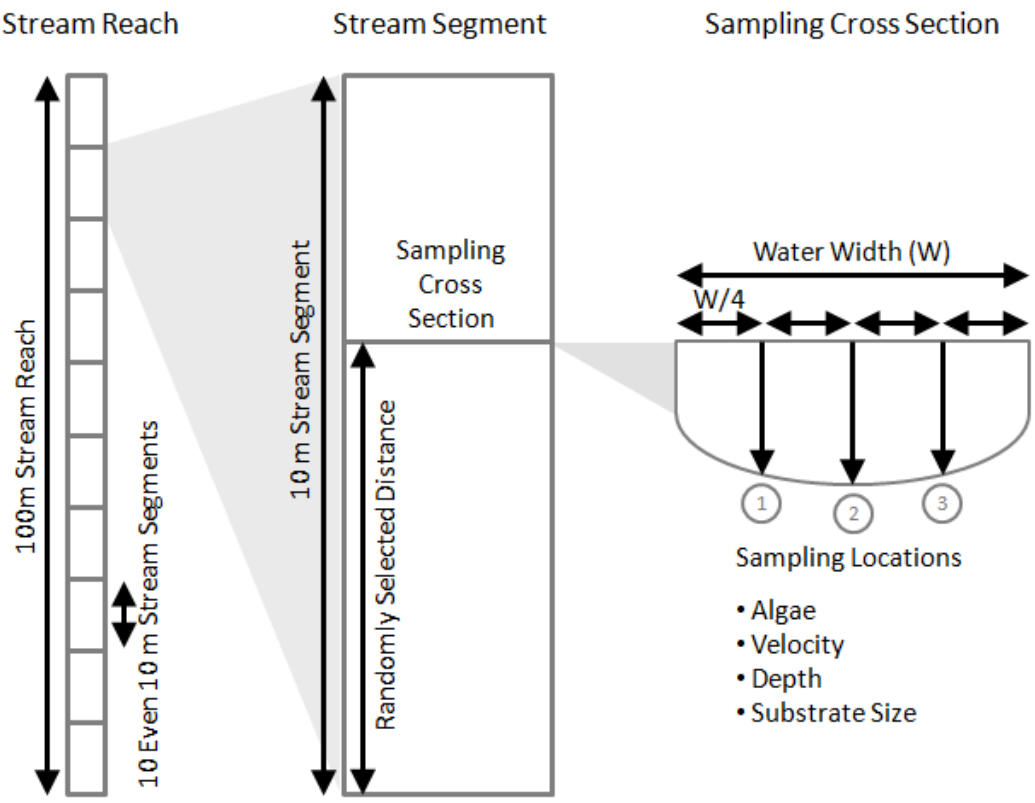

Figure 7: Schematic of the distributed sampling strategy

Water depth and velocity were measured at the thirty distributed sampling locations for each deployment with an additional pair of measurements made at the thalweg along each segment's cross-sectional transect. Water depth was measured to the nearest 0.3 cm at each location with a Lufkin1066D Red End engineer's folding wood rule (Apex Tool Group LLC., Sparks, MD, USA) and the average reach water depth was calculated by averaging all 30 depth measurements. Velocity was measured at 0.6 of total depth from the surface using a Flo-mate 2000 portable flowmeter and wading rod (Marsh-McBirney, Inc, Frederick, MD, USA). In some cases, flow was visible but registered 0 velocity using the current meter; for these sites and times, a value of 0.005 m s^{-1} was recorded. Negative measured velocities were replaced with 0's. Average reach velocity was calculated by averaging the 30

distributed velocity measurements and the 10 thalweg velocity measurements. The width from the left bank to the right bank water edges was measured for each segment cross-section, then the 10 sampling transect widths were averaged to obtain a water width for each deployment.

Substratum size was evaluated during each deployment by visually assessing the long axis length of substratum particles at the locations identified by the distributed sampling strategy (Table 7, Ode, 2007). Due to the lack of storm flows during the study period, substratum composition within the reach was expected to remain stable, so the observations from all the deployments were pooled and the percentages of total observations in each category were calculated to characterize substratum size composition for each site.

Table 7: Benthic substratum size categories

Substrate Identification Category	Size
Clay/hardpan	<0.06mm, hard, smooth, and consolidated
Fines	<0.06mm, not gritty
Sand	0.06 – 2mm, gritty to ladybug
Fine gravel	2 – 16mm, ladybug to marble
Coarse gravel	16 – 64mm, marble to tennis ball
Cobble	64 – 250mm, tennis ball to basketball
Small boulder	25cm – 1m, basketball to meter stick
Large boulder	1 – 4m, meter stick to car
Human-made	Concrete, asphalt (channelized)

3.3.3. Algal biomass

Two benthic algal biomass samples, one for chlorophyll and one for AFDM, were also taken at each of the 30 distributed sampling sites for each deployment, with the 3 samples

for chlorophyll, and separate 3 samples for AFDM, from each cross-stream transect being combined to create amalgamated samples for each transect.

At each sampling location with large substrata, such as cobbles and boulders, hereafter referred to as hard substrata, samples were collected using the Davies and Gee (1993) sampler. The sampler was made from a syringe with the end cut off, with a neoprene collar added to prevent algae loss during scrubbing (Figure 8). The diameter of the tube was 28 mm, providing a sampling area of about 6.2 cm^2 for each sample location. A 4 mm thick neoprene disk was glued to the end of the syringe plunger, a piece of Velcro was glued to the neoprene, and a circular 0.8-cm thick abrasive disk (Glit/Microtron White Super Polishing floor buffing pad, Continental Commercial Products, GA; now produced by Americo, GA) was attached to the Velcro. Each abrasive disk was used to scrape algae from rock surfaces by placing the apparatus against a rock, pressing the plunger with the scouring pad against the rock, and rotating 10 full turns in both directions. The abrasive pad, which captured the scrubbed algae, was removed from the apparatus and stored in a plastic canister.

For reaches with substrata such as sand and gravel (soft substrata), a 50 mL centrifuge tube cylinder was used to core the sediments to a depth of 0.8 cm (Figure 8). A small spatula was placed under the coring device cylinder, and then the core was transferred to a plastic canister. If floating algae were present immediately above the sampling location, they were cored with the soft-substrate sampler tube, then added to the canister with the rest of the algal sample from that location. Algal sample canisters were stored on ice in the field, and then frozen at -20°C until analysis. If both hard- and soft-substrata were present along the

same cross-stream transect, the cores and abrasive pads were combined and processed as soft-substrate samples.

Figure 8: Benthic algae sampling tools. The sampler and spatula used to collect soft substrate algae samples is on the left. An example of the sampler used to collect algae samples from cobbles and boulders is on the right, along with an example of an abrasive scrubbing disc. The penny (diameter of 1.9 cm) is included for scale.

Algal chlorophyll samples from hard substrata were thawed in the dark in a refrigerator and excess water was filtered through a Pall Brand A/E filter under vacuum (1 µm nominal pore size). After removing excess water from each scouring pad, any material on sample containers and handling apparati was filtered through the AE filter, then the filter was dried under vacuum. Soft-substratum algal samples were covered with aluminum to exclude light and freeze-dried in a Labconco FreezeZone Bulk Tray Dryer (Labconco Corp, Kansas City, MO, USA) for 1-3 days to remove excess water. Any materials in the storage container or

on handling apparati were washed through a Pall Brand A/E filter under vacuum (1 μm nominal pore size) using nanopure water. The filter and scrubbing discs from hard substrata samples, and the filter and freeze-dried material from soft-substrata samples, were each transferred to 50 mL polypropylene conical centrifuge tubes.

For both soft- and hard- substratum sample centrifuge tubes, pigments were extracted in ca. 25-ml of 90% acetone for 2 days in the dark in the refrigerator. Each sample was homogenized three times for 30 seconds per time with a Fisher Vortex Genie 2 (Fisher Scientific International, Inc., Hampton, NH, USA) during extractions. At the end of the extraction period, each sample was shaken vigorously and centrifuged at 5000 rpm for 20 minutes in a Sorvall RC 5B plus (Sorvall UK Ltd., Cambrige, UK; brand now owned by Thermo Fisher Scientific). A 3 ml extract from each sample was transferred to a 1 cm path-length glass cuvette, then optical density (OD) at 664 nm, 665 nm, and 750 nm was analyzed on a Shimadzu UV-1800 spectrophotometer (Shimadzu Co., Kyoto, Japan). A blank of 90% acetone was analyzed at the same wavelengths and with the same acidification procedures after every 4-6 sample sets. If sample optical densities were greater than 1.0 for a sample, the sample was diluted with 90% acetone and reanalyzed. Some samples were re-centrifuged and re-analyzed due to high turbidity.

Chlorophyll *a* and pheophytin *a* were calculated using the following equations (based on APHA 2012c; Steinman et al. 2006):

$$Chlorophyll\ a,\ \frac{mg}{m^2} = \frac{26.7(664_b - 665_a)\times V}{A\times L}, \qquad \text{(Eq. 2)}$$

$$Pheophytin\ a,\ \frac{mg}{m^2} = \frac{26.7[1.7(665_a) - 664_b]\times V}{A\times L}, \qquad \text{(Eq. 3)}$$

where V is the volume of the extract in liters, A is the area of the substratum sampled in m^2, L is the light path length through the cuvette in cm, 664_b is the OD of the 90% acetone extract at 664 nm before acidification, and 665_a is the OD of the 90% acetone extract at 665 nm after acidification. Before calculations were made, the corresponding blank OD and the 750 OD were subtracted from the 664OD and 665OD values.

3.3.4. Discharge

At least once per deployment, discharge was estimated at 3 or more cross sections within each 100 m reach. Each cross-section was subdivided into one to five subsections, depending on width, in which cross-sectional areas were measured (width X depth) and multiplied by current velocity; then the flow in all subsections was summed to obtain a discharge estimate for each cross section. Discharge estimates were averaged over cross-sections to obtain a mean discharge for each deployment.

3.3.5. Water chemistry collection and analysis

Water samples were collected one time during each deployment, with dissolved organic carbon (DOC) samples being collected first. Prior to field collection, glass EPA screw thread water analysis vials were pre-combusted at 500°C for 12 hours while the vial caps, collection syringes, and plastic filter housing components were acid washed in 10% HCl, then triple rinsed in nanopure water. After drying and cooling in the lab, the glass vials were capped and the syringes and filter housings were stored in sealed plastic bags. Several Whatman GF/F filters (0.7 μm pore size) were combusted at 500°C for 2 hours, then stored in foil envelopes inside clean plastic bags. Water for DOC samples was collected from the thalweg of the stream with a clean 120 mL syringe, then filtered through a pre-combusted GF/F filter into a clean glass vial, which had been triply washed with filtered sample water.

A water sample for nutrient (nitrate, phosphate, ammonium) analysis was collected using the same filter and syringe, filling a new 60 mL HDPE triply-rinsed screw-cap vial (Nalgene Brand). A 2-L bulk water sample was collected in a HDPE bottle that was triple-rinsed in stream water for analysis of total suspended solids (TSS). The nutrient and DOC samples were stored on ice, in the dark, for transportation to the laboratory, then DOC samples were frozen at -20°C and nutrient and TSS samples at 4°C until analysis. Specific conductance and water temperature were measured in the main channel with an Orion, model 140 conductivity/salinity meter, which was calibrated in the lab using a 1413 μS cm^{-1} standard solution and which automatically computed specific conductance at 25°C in the field.

DOC samples were analyzed using the high temperature combustion method on a Shimadzu TOC-V (Shimadzu Co., Kyoto, Japan), with modifications as described in Carlson et al. (2010). Samples were analyzed for dissolved NH_4^+, NO_3^-, and PO_4^{3-} concentration on a Lachat Automated Ion Analyzer (Hach Company, Loveland, CO, USA). Ammonium was measured by adding base to the sample stream, converting ammonium to ammonia (Lachat Instruments Inc., 1995), which then diffuses across a Teflon membrane into phenol red pH indicator, which is then analyzed colorimetrically at 570 nm (detection limit 0.5 μM, sensitivity ±0.2 μM, accuracy ±5%; Willason and Johnson, 1986). Nitrate was measured using a standard Griess-Ilosvay reaction after cadmium reduction (0.5 μM detection limit, ±0.2μM sensitivity, ±5% accuracy; USEPA, 1983; Lachat Instruments Inc., 1996). Phosphate was measured as soluble reactive phosphorus (SRP) after reaction with ammonium molybdate and antimony potassium tartrate (Lachat Instruments Inc., 1996b) and reduction by ascorbic acid with heating (45°C), then assessed colorimetrically at 880 nm (0.3 μM detection limit, ±0.2 μM sensitivity, ±10% accuracy; Grasshoff, 1976).

The method for analyzing total suspended solids (TSS) was adapted from APHA (2012a) and APHA (2012b). Several A/E filters were triply rinsed with nanopure water before being combusted at 500°C for 1 hour then weighed on an analytical balance (Mettler-Toledo AB-S, Mettler-Toledo International Inc., Columbus, OH, USA). The bulk TSS sample was thoroughly shaken and poured into a large plastic bucket on a stir plate, and then 250 mL to 1.5 L of sample water, depending on TSS concentrations, were removed and passed through a prepared filter. The filter was dried under vacuum at ambient temperature to remove excess water and transferred to an assigned weigh boat, then placed in a drying oven at 105°C for 1 hour and weighed to the nearest 0.1 mg. After repeated drying and weighing to a constant weight, filters were repeatedly combusted at 500°C for 1 hour, cooled, and weighed to the nearest 0.1 mg until the weight measurement fell within 0.5 mg of the previous weight. The difference between the mass of the initial prepared filter and the mass of the dried filter with residue was considered the total suspended solids for the volume of water passing through that filter. The difference between the mass of the dried filter with residue and the mass of the combusted filter with residue was considered the volatile suspended solids for the volume of water passing through that filter

3.3.6. Canopy characterization

Data on canopy cover was collected at each site during each deployment, using the methods for hemispherical imagery collection and processing described by Alonzo et al. (2015). Hemispherical canopy images were collected at the upper and lower ends of each stream reach and at the center of each cross-stream transect for a total of 12 locations. Creating a binary image of foliage using images collected in near-infrared wavelengths can be more efficient and accurate than using images collected in visible wavelengths

(Chapman, 2007), a useful feature in urban settings where images may contain both built structures and foliage (Osmond, 2009). As a consequence, hemispherical images were collected using a Nikon Coolpix 5400 digital camera (Nikon Corp., Tokyo, Japan), altered to record red and infrared light by replacing the manufacturer's infrared-blocking filter with a filter that blocks wavelengths shorter than 590 nm (as in Alonzo et al. 2015). The camera was fitted with a Nikon LC-ER2 hemispherical lens using a Nikon UR-E10 adapter and was fixed to a 3-way tripod so that the camera pointed upward. The top of the camera lens was adjusted to be 1 m above the streambed, a compass was used to align the top of the camera to magnetic north, and a bubble level was used to insure the camera lens was level. A set of three bracketed exposures was collected at each of 12 photographic locations: an automatic exposure (+0), a 1-stop underexposure (-1), and a 1-stop overexposure (+1).

Using Dynamic-Photo HDR 5 for Windows (Mediachance, Ottawa, Canada), the three exposures were aligned and combined into a single high dynamic range (HDR) image. Creating an HDR image increases the contrast between the sky and foliage and mitigates pixel saturation in images captured in direct sunlight (Jonckheere et al. 2004). Canopy elements were separated from sky elements in each HDR file using an image segmentation rule-set routine in eCognition Developer Version 8.64.1 (Trimble Navigation Ltd, Sunnyvale, CA, USA; Build 1765 x64; Mar 24, 2011). After automatic segmentation and classification, manual editing was used to correct errors in image class assignment. The final binary images were analyzed for canopy openness using Gap Light Analyzer v2 (©1999 Simon Frazer University, Cary Institute of Ecosystem Studies). The images were made binary in the eCognition processing step, so the GLA threshold was arbitrarily set at 160 and

canopy calculations were made using simple default settings (not tied to latitude, longitude, or date of the image acquisition) (Figure 9).

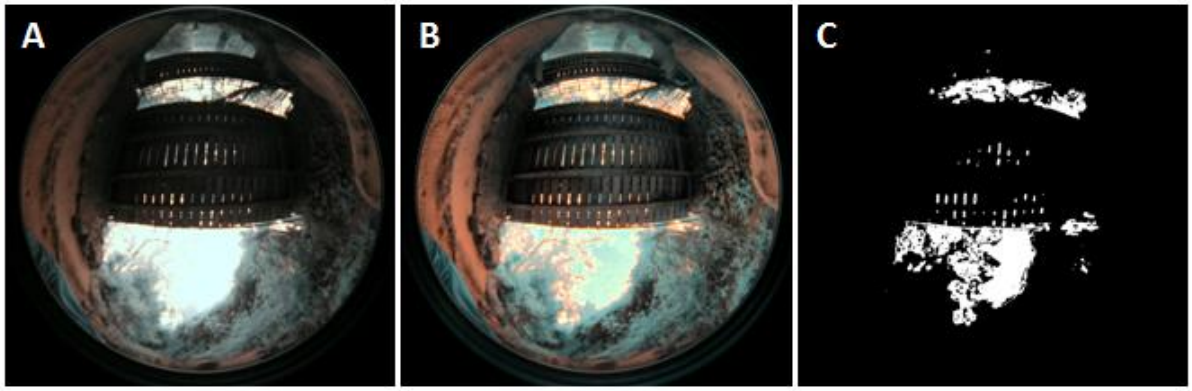

Figure 9: Example of hemispherical photo processing, showing (A) a normal exposure hemispherical image collected by the camera in the field, (B) the same hemispherical image in HDR after processing in Dynamic Photo HDR 5, and (C) the same image in binary format after processing in eCognition.

3.3.7. Benthic organic matter

Samples of benthic organic matter (BOM) were collected once during the study period at each site, except at RS, which dried before sampling occurred. BOM was assumed to remain consistent through the study period due to the lack of storm flow, so the timing of sample collection varied at each site during the study period. A random sample was obtained from each cross-stream transect by taking soft substrata core samples from each corner of a 30.5 cm x 30.5 cm area (4 samples per transect) by pressing a 107 mm diameter PVC pipe to a depth of 4.5 cm, then sliding a piece of flat plastic under the pipe before sample removal. If roots or other organic matter prevented the pipe from sliding easily into the substratum, a serrated knife was used to cut around the outside of the pipe. The 4 core samples from each cross-stream transect were placed in a single bucket. In sampling locations with hard (cobble and boulder) substrata, a 250 μm mesh Surber sampler was used to collect benthic organic

matter by manually disturbing upstream substrata in the 30.5 cm x 30.5 cm frame for 3 minutes, allowing suspended organic matter to be swept into the net. Samples from the first 5 cross-stream transects in each creek were composited into one large sample and samples from the second 5 transects were composited into a separate large sample, noting the total surface area sampled, then each sample was poured through a 250 μm mesh net. Samples were transferred to 2 L wide-mouth HDPE bottles, transported to the lab, and stored at 4°C until processing.

In the laboratory, BOM samples were passed through 4.75 mm, 1 mm, and 250 μm mesh sieves (Humbolt Mfg Corp, Elgin, IL, USA), with each size fraction being placed in a labeled aluminum pan. Sample size fractions were repeatedly dried at 105°C for 24 hours and weighed, until constant weight was achieved (within 0.5 g of the previous weight), then repeatedly combusted at 500°C for a minimum of 12 hours and weighed to achieve constant weight (as above). The difference in mass between the dried sample and the combusted sample represented organic mass loss and was divided by the sampled area to obtain the benthic organic content per area (g m^{-2}).

3.3.8. Additional site mapping

A map of each site was created by mapping major features of consecutive 10 m segments, adjoined at the end-points, within each 100 m reach. A central reference line running approximately along the thalweg of the main channel was mapped in each section using a compass and measuring tape, and the end points were mapped to a benchmark location. The elevation of the channel at the thalweg and the water level were surveyed at 2.5 m intervals along the entire 100 m chain of mapping segments using a model AZ-1S Nikon Automatic Level (Nikon Corp., Tokyo, Japan) and surveying stadia. These

measurements were used to estimate a slope for the channel bed and the water surface for each site. In each 10 m segment, 2 transects, placed perpendicular to the central line, were used to map the water edge and the estimated boundaries of common storm flow events, as indicated by slope and vegetation changes along the banks. Detailed notes were recorded about locations of major physical features, such as boulders, trees, large debris, deep pools, and important changes in the bed substratum. At least 3 detailed cross sections were surveyed perpendicular to flow at each site to map channel geomorphology; these were distributed throughout the reach and were also referenced to the mapping center line. The resulting map for each site can be found in Appendix I.

3.3.9. Gas change method for estimating ecosystem metabolism

Metabolism estimates were calculated using the single-station dissolved oxygen gas change method, which assumes that dissolved oxygen concentrations in the water column are influenced by photosynthesis (P), respiration (R), and gas exchange with the atmosphere (E) (Odum,1956). The method assumes that photosynthetic activity (carbon fixation) increases dissolved oxygen concentrations (see Equations 4 and 5) whereas respiration decreases dissolved oxygen concentrations:

$6CO_2 + 6H_2O + \text{light} \rightarrow C_6H_{12}O_6 + 6O_2$ (photosynthesis), (Eq. 4)

$C_6H_{12}O_6 + 6O_2 \rightarrow 6H_2O + 6CO_2 + \text{heat}$ (respiration). (Eq. 5)

Gas exchange with the atmosphere, noted as E, can either increase or decrease oxygen concentrations in the water column depending on the relationship between the water column concentration and the saturation concentration. If no other processes alter oxygen

concentrations, dissolved oxygen changes (ΔDO) in the water column can be represented by the equation:

$$\Delta DO = P - R \pm E. \quad \text{(Eq. 6)}$$

Oxygen concentration changes then are primarily related to the balance between photosynthesis and respiration, and oxygen fluxes are often converted to carbon units using a photosynthetic quotient and a respiratory quotient (see Bott, 2006b).

3.3.10. Calculation of the gas transfer velocity

Gas exchange across the air-water interface is related to the difference between the measured dissolved oxygen concentration, C, and the calculated saturation value, C_s. This difference is termed the saturation deficit (D_{sd}, see Equation 7) with its sign indicating whether oxygen is being added or lost from the water column:

$$D_{sd} = C - C_s \quad \text{(Eq. 7)}$$

When the water column is undersaturated (Cs > C, D_{sd} is negative), oxygen is added to the system from the atmosphere, whereas oxygen is lost from the water to the atmosphere when the water column is supersaturated (Cs < C, D_{sd} is positive). When the saturation deficit is multiplied by an appropriate gas transfer velocity (K, discussed below, in units of length per time), an estimated gas flux across the air-water surface, E (see Equation 8) can be calculated:

$$E = K \times D_{sd} \quad \text{(Eq. 8)}$$

Gas exchange calculations in streams generally use a reaeration coefficient, K_2, which has units of time^{-1} and is not corrected for depth; however, the mass of gas required to aerate a system is related to the depth of the water column (Raymond et al. 2012). The gas transfer velocity, K, which has units of distance per time, is often used and is tied to the physical processes that cause turbulence at the air-water interface (Zappa et al. 2007).

Two approaches were used to estimate gas transfer velocity. If a given deployment had an average water velocity greater than 1.5 cm s^{-1} and the reach had a water surface slope greater than 1%, then model 2 from Table 2 in Raymond et al. (2012) was used to calculate K (Equation 8): This model was selected for its high R^2 value and because Raymond et al. (2012) argued that it was appropriate for small systems.

$$K_{600} = 5937 \times (1 - 2.54 \times Fr^2) \times (VS)^{0.89} \times D^{0.58}, \quad \text{(Eq. 9)}$$

where K_{600} is the gas transfer velocity (m d^{-1}) normalized to a Schmidt number of 600, corresponding to a temperature of 17.5°C, V is the water velocity (m s^{-1}), S is the energy slope (unitless, approximately the water surface slope with uniform flow), D is the water depth (m), and Fr is the dimensionless Froude number that classifies stream flow as subcritical, critical, or supercritical. The Schmidt number influences gaseous mass transfer (Monteith and Unsworth, 2008). The Froude number is calculated using Equation 10 (Chow, 1959):

$$Fr = V/(gD)^{0.5}, \quad \text{(Eq. 10)}$$

where g is the gravitational constant (9.80665 m s^{-2}). The K600 was adjusted to a temperature of 20°C:

$$K_{(20°C)} = (Sc_{T2}/Sc_{600})^{-0.5} \times K_{600} \quad \text{(Eq. 11)}$$

where $K_{(20°C)}$ is the K value for the desired Schmidt number, corresponding to 20°C, K_{600} is the K value for a Schmidt number of 600, and Sc_{600} and $Sc_{(20°C)}$ denote the Schmidt numbers associated with the old temperature and the new temperature, respectively. Dissolved oxygen concentration given a Schmidt number temperature was calculated as in Raymond et al. (2012):

$$Sc = 1801 - 120.10T + 3.782T^2 - 0.0476T^3, \quad \text{(Eq. 12)}$$

where Sc is the Schmidt number and T is the water temperature in °C.

An alternative approach was used when deployments occurred during stagnant conditions (slopes < 1%, average water velocity < 1.5 cm s^{-1}). In these cases, a simple stagnant boundary layer model (Lewis and Whitman, 1924; see Equation 13) was used to estimate a gas transfer velocity, using experimental data from Emerson (1975) to guide the selection of the stagnant boundary layer (thin film) thickness:

$$K = D_{md}/z, \quad \text{(Eq. 13)}$$

where K is the mass transfer coefficient (gas transfer velocity) in cm h^{-1}, D_{md} is the molecular diffusion coefficient of oxygen in water at a specified temperature in cm^2 hr^{-1}, and z is the stagnant boundary layer thickness, which is measured in μm but converted to cm for the calculation. Because the study streams were protected from strong winds by riparian vegetation, a stagnant boundary layer thickness of 350 μm was selected for wind speeds less than 2 m s^{-1} (Figure 4 in Emerson, 1975). An oxygen diffusivity of 1.978 x 10^{-5} cm^2 s^{-1} at 20°C was used based on the following equation in Langø et al. (1996):

$$D_{od} = 1.2\, e^{0.026T}, \qquad \text{(Eq. 14)}$$

Where D_{od} is the oxygen diffusivity constant in cm^2 s^{-1} and T is the water temperature in °C. The method used for each deployment can be found in Table 8.

Table 8: Table of gas exchange method used in each deployment at each site. Deployments where K was calculated using the stagnant boundary layer model are indicated as TF. Deployments where K was calculated using model 2 in Raymond et al. (2012) are indicated as R.

Site	**AB**	**AT**	**PH**	**HO**	**RS**	**SY**
Deployment 1	TF	TF	TF	R	R	R
Deployment 2	TF	TF	TF	R	R	R
Deployment 3	TF	TF	TF	R	TF	R
Deployment 4	TF	TF	TF	R	--	R
Deployment 5	TF	TF	TF	R	--	R
Deployment 6	TF	TF	TF	R	--	TF

After a method for calculating the gas transfer velocity had been selected and a K value had been calculated for the deployment corresponding to the Schmidt number at a temperature of 20°C, a temperature correction was made using the following equation originally developed in Elmore and West (1961) and described in Bott (2006b):

$$K_{(T°C)} = K_{(20°C)} \times 1.024^{Tave-20}, \quad \text{(Eq. 15)}$$

where $K_{(T°C)}$ is the gas transfer velocity for the temperature at the time of the oxygen measurement, $K_{(20°C)}$ is the gas transfer velocity for a temperature of 20°C, and T_{ave} is the reach-averaged water temperature in °C at the time of the oxygen measurement. This time series of instantaneous, temperature-corrected gas transfer velocities could then be used to estimate gas exchange at each measurement time, using Equation 8.

3.3.11. Metabolism calculation procedure

Metabolism rates were calculated in Matlab R2010a as shown in Figure 10 (Mathworks, Inc., Natick, MA, USA). The 5-minute interval oxygen data were averaged into 15 minute intervals and differences between consecutive dissolved oxygen data points were calculated to determine a ΔDO for each time step. Oxygen changes per unit volume were converted to oxygen changes per unit area by multiplying by the average reach depth. For each measurement time, saturated dissolved oxygen concentration was linearly interpolated between the values in a dissolved oxygen solubility table (USGS, 2013) using the temperature, specific conductance, and atmospheric pressure at each site. The temperature used was an average over 15-minute intervals from the two tidbit loggers and oxygen logger locations; specific conductance was measured for that deployment; and atmospheric pressure was estimated from elevation using a standard elevation-pressure relationship curve. The saturation concentration and the measured concentration at every time were used to calculate the saturation deficit using Equation 7. A K value was calculated for each deployment using either the thin film model or the Raymond et al. (2012) equation, as

described in the previous section. The saturation deficit for each time was multiplied by the temperature-corrected K value for that time, resulting in an estimate of gas exchange. The gas exchange estimates for consecutive 15-minute dissolved oxygen data points were averaged to determine the gas exchange for the 15-minute time step. The gas exchange value was used to correct the ΔDO to determine net oxygen changes due only to metabolic processes (P and R).

Each time step was classified as either daytime or nighttime using the PAR data and nighttime time steps were assumed to have photosynthesis rates of zero, allowing the calculation of respiration rates (Equation 6). Respiration rates for the 90 minutes before daybreak were averaged and interpolated through the daytime to the average respiration rate for the 90 minutes after sunset. A community respiration rate (CR) for each deployment date was determined by integrating the respiration curve from midnight to midnight and gross primary productivity (GPP) was calculated as the integrated area between the respiration curve and the photosynthesis curve.

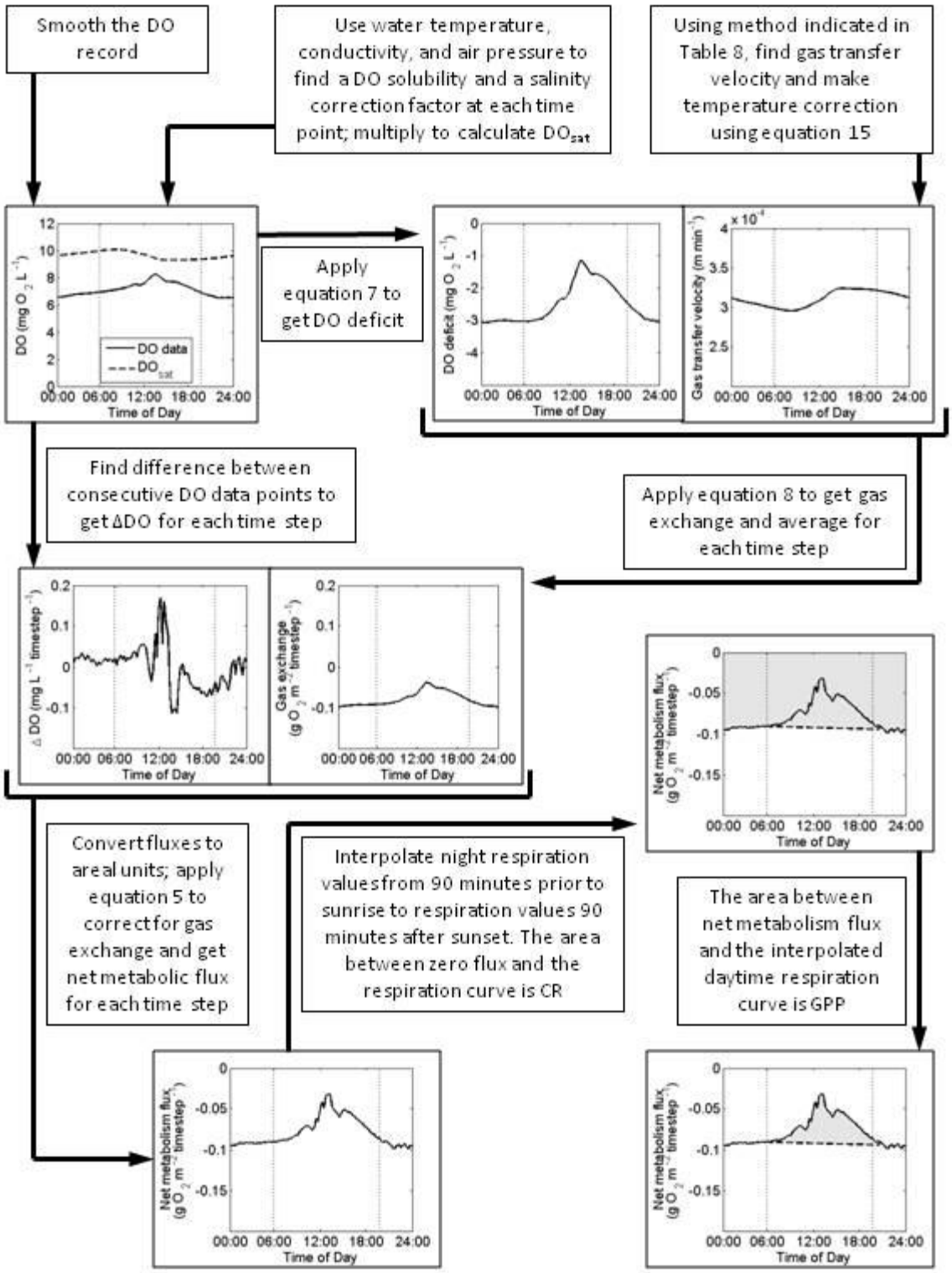

Figure 10: Diagram demonstrating metabolism calculation process. Example data are from Sycamore Creek on April 30, 2014.

3.3.12. Data issues

The oxygen loggers appeared to malfunction for a few times during the day in Arroyo Burro Creek, presumably owing to supersaturation. In these cases, negative oxygen values were removed and resulting gaps were filled using linear interpolation from the nearest times with reasonable dissolved oxygen values. Although temperature was logged by the oxygen logger and two other temperature loggers, then averaged, for each deployment, one temperature logger failed during two of the deployments (once at Rattlesnake, once at Atascadero). In these cases, the two remaining locations were averaged to obtain a deployment temperature. Because loggers at different locations showed different maximum and mean temperatures at different sites and times, daily temperature minima, maxima, means, and ranges for each temperature logger dataset were found and averages of these values were calculated to obtain average minimum, maximum, mean, and range values across loggers in each deployment.

PAR logger data were used to determine day length for each day of metabolism calculations and raw light counts were converted to μmol photons m^{-2} s^{-1} using the calibration curves presented in Figure 6. The PAR data were summarized as total daily PAR (referred to later as total PAR or tPAR) and daily peak PAR (referred to as peak PAR or pPAR). Total PAR was calculated by multiplying the PAR level by the time length for each measurement period, then summing over measurement periods to obtain the total incoming energy per day (expressed as mol photons m^{-2} d^{-1}). The peak PAR rate was determined by identifying the maximum PAR measurement on each deployment day.

3.3.13. Data analysis

The averages of the first three deployments for each metabolism estimate for each site (the site-averages) were used as dependent variables in examining the effects of urban versus non-urban sites on metabolic rates (unbalanced, one-way ANOVA), including the site SY as an undeveloped site and a developed site in separate analyses.

Relationships between metabolism estimates and corollary environmental data collected during each deployment were also examined. Because a number of environmental variables were likely inter-related, a principal component analysis (PCA) was performed on the environmental data, then the PCA axis scores were used as independent variables in subsequent multiple regression analyses. Prior to analysis, proportion variables were logit-transformed and all other variables, except metabolism estimates, were log-transformed. The cross correlation matrix between all environmental variables was examined and redundant variables were excluded. The environmental variables included in the PCA were nitrate, phosphate, DOC, benthic chlorophyll *a*, total PAR, specific conductance, total suspended solids, mean water temperature, discharge, thalweg water velocity, water depth, and water width. For these analyses, the variable value for each deployment at each site was considered a single observation, so variables with multiple measurements during a deployment were averaged to arrive at a deployment-averaged value. Because there was no flow in Rattlesnake Creek during the third deployment, this produced 32 site-time observations (6 sites with 6 deployments at each site except Rattlesnake).

The PCA was performed in Matlab. All variables were centered (the mean was subtracted from each observation) and standardized by the standard deviation in preparation for the PCA. Principal components were retained for regression analysis if they explained at

least 5% of the variance in the multivariate data and also had an eigenvalue greater than one. For relationships between metabolic rate estimates and PCA axis scores, correlation coefficients of 0.35 or greater were significant ($p < 0.05$). Regressions were calculated using the 32 site-time observations for each metabolism parameter and the retained principal components. Pearson correlation analyses were performed between the metabolism estimates and environmental variables that were identified as important by the PCA regression analysis and that only had single measurement values for each site during the study (e.g., bed substratum, BOM variables, and elevation). For variables with data from multiple deployments, the average of the first three deployments was used for each site (n = 6). The metabolism values, along with the environmental variables identified by the previous analyses, were then compared to land use at each site using time-averaged values from the first three deployments or the single site values as replicates (n=6).

3.4. Results

3.4.1. Environmental characteristics of sites

Oxygen concentrations ranged from 0 to 31.9 mg L^{-1} across all sites with ranges from 2.6 to 31.9 mg L^{-1} at Arroyo Burro Creek, 0.4 to 25.7 mg L^{-1} at Atascadero Creek, 0 to 14.9 mg L^{-1} at Phelps Creek, 7.8 to 9.0 mg L^{-1} at Arroyo Hondo Creek, 4.2 to 10.5 mg L^{-1} at Sycamore Creek, and 4.0 to 9.1 mg L^{-1} at Rattlesnake Creek (Appendix II). Across deployments, dissolved oxygen minima were consistently lower and dissolved oxygen maxima were generally higher at the low elevation, developed sites than at the higher elevation sites, with Sycamore Creek being similar to Arroyo Hondo and Rattlesnake creeks (Table 9). As a consequence, dissolved oxygen concentration ranges over each deployment were consistently higher at the low elevation (> 5 mg L^{-1}) than at the high elevation (< 4 mg

L^{-1}) sites. Mean dissolved oxygen levels were consistently lower at Atascadero and Phelps Creeks than at the other four sites across deployments (Table 9).

Table 9: Summary of dissolved oxygen data

	HO	RS	SY	AB	AT	PH
Dissolved Oxygen Minima (mg L^{-1})						
(1) March 11-March 29	8.6	8.6	8.5	5.6	1.3	3.4
(2) April 2-April 15	8.3	7.6	7.9	5.5	1.1	2.5
(3) April 22 - May 6	8.3	4.8	6.4	4.8	0.9	0.6
(4) May 20 - June 5	8.1	--	4.9	3.6	1.3	0.8
(5) June 13 - June 30	7.8	--	4.6	3.3	1.5	1.7
(6) July 8 - July 22	7.2	--	4.5	3.6	1.7	0.2
Site Average	**8.1**	**7.0**	**6.1**	**4.4**	**1.3**	**1.5**
Dissolved Oxygen Maxima (mg L^{-1})						
(1) March 11-March 29	9.3	9.0	10.4	28.8	7.1	5.9
(2) April 2-April 15	9.3	8.4	10.1	16.4	19.0	6.6
(3) April 22 - May 6	8.9	7.5	8.6	15.8	12.6	9.3
(4) May 20 - June 5	8.8	--	8.3	17.9	12.3	9.5
(5) June 13 - June 30	8.7	--	8.2	23.1	12.4	12.4
(6) July 8 - July 22	8.4	--	6.9	17.2	9.8	7.8
Site Average	**8.9**	**8.3**	**8.7**	**19.9**	**12.2**	**8.6**
Dissolved Oxygen Means (mg L^{-1})						
(1) March 11-March 29	8.9	8.8	9.2	10.5	3.0	4.4
(2) April 2-April 15	8.9	8.1	8.6	8.3	5.3	4.2
(3) April 22 - May 6	8.6	6.1	7.1	7.4	5.1	3.8
(4) May 20 - June 5	8.4	--	6.3	6.8	5.5	3.8
(5) June 13 - June 30	8.2	--	6.0	7.2	5.7	6.0
(6) July 8 - July 22	7.9	--	5.4	7.4	4.6	2.6
Site Average	**8.5**	**7.6**	**7.1**	**7.9**	**4.9**	**4.1**
Dissolved Oxygen Ranges (mg L^{-1})						
(1) March 11-March 29	0.7	0.4	1.9	23.2	5.8	2.5
(2) April 2-April 15	1.0	0.8	2.2	10.9	17.9	4.2
(3) April 22 - May 6	0.6	2.6	2.2	11.0	11.7	8.7
(4) May 20 - June 5	0.7	--	3.4	14.4	11.0	8.6
(5) June 13 - June 30	0.9	--	3.6	19.9	10.9	10.7
(6) July 8 - July 22	1.1	--	2.5	13.6	8.1	7.6
Site Average	**0.8**	**1.3**	**2.6**	**15.5**	**10.9**	**7.1**

Water temperatures ranged from 10.7 to 26.0°C across all sites with ranges from 12.3 to 22.7°C at Arroyo Burro Creek, 11.0 to 26.0°C at Atascadero Creek, 10.7 to 24.9°C at Phelps Creek, 12.4 to 19.5°C at Arroyo Hondo Creek, 12.6 to 19.5°C at Sycamore Creek, and 12.0 to 20.2°C at Rattlesnake Creek (Appendix II). Temperature minima showed no consistent patterns across sites during the first three deployments (March 11 – May 6), but were higher at the low than higher elevation sites during the last three deployments (May 20 – July 22) (Table 10). Temperature maxima, were consistently higher at the developed than undeveloped sites at all elevations, including the higher elevation Sycamore Creek site. Temperature means for each deployment were higher at the developed than undeveloped sites for the first two deployments (March 11- April 15) and higher at the low elevation than high elevation sites for the remainder of deployments (April 22 – July 22). Temperature ranges were higher at the developed than undeveloped sites for the first three deployments (March 11 – May 6) and higher at low than high elevation sites throughout the study (Table 10). Minimum, maximum, and mean temperatures generally increased across deployments, but the timing of the peak temperature range was not consistent across sites (Table 10).

Table 10: Summary of water temperature data

	HO	RS	SY	AB	AT	PH
Temperature Minima (°C)						
(1) March 11-March 29	13.8	12.9	13.3	13.0	12.5	12.8
(2) April 2-April 15	13.0	12.7	13.2	13.6	11.9	11.9
(3) April 22 - May 6	13.8	15.4	14.8	14.4	14.8	14.3
(4) May 20 - June 5	14.6	--	15.1	16.0	17.0	16.4
(5) June 13 - June 30	14.6	--	15.9	17.5	17.4	16.2
(6) July 8 - July 22	16.0	--	17.9	18.3	20.1	18.4
Site Average	**14.3**	**13.7**	**15.0**	**15.5**	**15.6**	**15.0**
Temperature Maxima (°C)						
(1) March 11-March 29	15.8	14.5	16.9	17.2	19.2	17.6
(2) April 2-April 15	15.0	15.3	16.3	17.1	17.9	17.1
(3) April 22 - May 6	16.7	18.1	18.5	19.6	20.1	19.5
(4) May 20 - June 5	17.5	--	18.7	20.3	22.2	20.8
(5) June 13 - June 30	17.9	--	19.3	21.6	23.2	20.6
(6) July 8 - July 22	18.7	--	20.2	21.5	24.5	22.6
Site Average	**16.9**	**16.0**	**18.3**	**19.6**	**21.2**	**19.7**
Temperature Means (°C)						
(1) March 11-March 29	14.7	13.6	15.1	14.8	15.9	15.2
(2) April 2-April 15	13.9	13.8	14.9	15.2	14.8	14.4
(3) April 22 - May 6	14.9	16.5	16.5	16.7	17.3	16.7
(4) May 20 - June 5	15.8	--	16.7	17.8	19.3	18.2
(5) June 13 - June 30	16.0	--	17.4	19.3	19.7	18.1
(6) July 8 - July 22	17.3	--	18.8	19.6	21.7	20.2
Site Average	**15.4**	**14.6**	**16.6**	**17.2**	**18.1**	**17.1**
Temperature Ranges (°C)						
(1) March 11-March 29	2.1	1.6	3.6	4.3	6.7	4.8
(2) April 2-April 15	2.0	2.6	3.1	3.4	6.0	5.2
(3) April 22 - May 6	2.8	2.7	3.7	5.2	5.3	5.2
(4) May 20 - June 5	2.9	--	3.5	4.3	5.2	4.4
(5) June 13 - June 30	3.3	--	3.3	4.1	5.9	4.4
(6) July 8 - July 22	2.7	--	2.4	3.2	4.4	4.3
Site Average	**2.6**	**2.3**	**3.3**	**4.1**	**5.6**	**4.7**

The method used for characterizing canopy openness was sensitive to overall light conditions, often producing different results at the same site under full sun versus full cloud cover. The shortcomings of this method made it difficult to distinguish between seasonal changes in weather versus vegetation growth. As a consequence, only a single canopy openness value was determined for each site based on the hemispherical images captured between the third and fourth deployment, between May 6 and May 18, 2014, which had similar overall light conditions across all the sites. Canopy openness averaged over each study reach was similar among sites regardless of urban development, ranging from 2% at Arroyo Hondo Creek to 14% at Atascadero Creek (Table 11). Average reach canopy openness differed only slightly from canopy openness measurements taken at the downstream end of the reach, where PAR and oxygen sensors were deployed.

Table 11: Summary of canopy and PAR data

	HO	RS	SY	AB	AT	PH
Average Whole-site Canopy Openness (%)						
	2	10	5	5	14	12
Instrument Location Canopy Openness (%)						
	2	6	6	4	24	6
Peak PAR (µmol photons m^{-2} s^{-1})						
(1) March 11-March 29	351	548	1268	562	1279	627
(2) April 2-April 15	423	814	1172	774	1602	816
(3) April 22 - May 6	1288	1194	1549	813	1579	896
(4) May 20 - June 5	1349	--	1125	1476	1702	833
(5) June 13 - June 30	1115	--	1003	1311	1749	1119
(6) July 8 - July 22	652	--	963	1021	1709	949
Site Average	**863**	**852**	**1180**	**993**	**1603**	**873**
Total PAR (mol photons m^{-2} d^{-1})						
(1) March 11-March 29	2.95	5.63	2.90	5.54	13.83	5.73
(2) April 2-April 15	3.40	7.29	5.32	4.47	23.30	5.69
(3) April 22 - May 6	4.66	11.26	6.37	4.09	28.36	5.64
(4) May 20 - June 5	6.21	--	5.52	4.74	29.50	4.75
(5) June 13 - June 30	5.29	--	5.22	5.73	32.13	5.40
(6) July 8 - July 22	4.59	--	4.50	4.07	27.91	4.19
Site Average	**4.52**	**8.06**	**4.97**	**4.77**	**25.84**	**5.24**

Site averages for daily total PAR, which integrates the incoming light throughout the daytime, ranged from 4.52 to 25.84 mol photons m^{-2} d^{-1}, while site averages for peak PAR, which shows only the most intense rate of incoming radiation during the day, ranged from 852-1603 µmol photons m^{-2} d^{-1}. The tPAR and pPAR values measured on individual days at each site can be found in Appendix II. Both tPAR and pPAR were not consistently different among sites. The maximum pPAR and tPAR levels were observed between the 3rd and 5th deployments (April 22-June 30) across most sites, with the exception of the Phelps site, which had maximum total PAR during the first deployment (before March 29) (Table 11).

Both pPAR and tPAR have better correlation to the canopy openness at the location where each logger was installed (n = 6, pPAR: Pearson R = 0.81, p = 0.05; tPAR Pearson R = 0.95, p = 0.004, respectively) as opposed to the average canopy openness across the entire reach (no significant correlation), although the values at Atascadero Creek may be outliers (Figure 11). The much higher pPAR and tPAR values at Atascadero Creek indicate that the logger was installed at a location that had a more open canopy compared to the rest of the reach. The relationship between tPAR and canopy cover is better than the relationship between pPAR and canopy cover, likely because tPAR reflects incoming radiation throughout the day, whereas pPAR reflects radiation at the time of day when the position of the sun aligns with gaps in the canopy, which varies across sites and is not necessarily related to measurements of canopy openness.

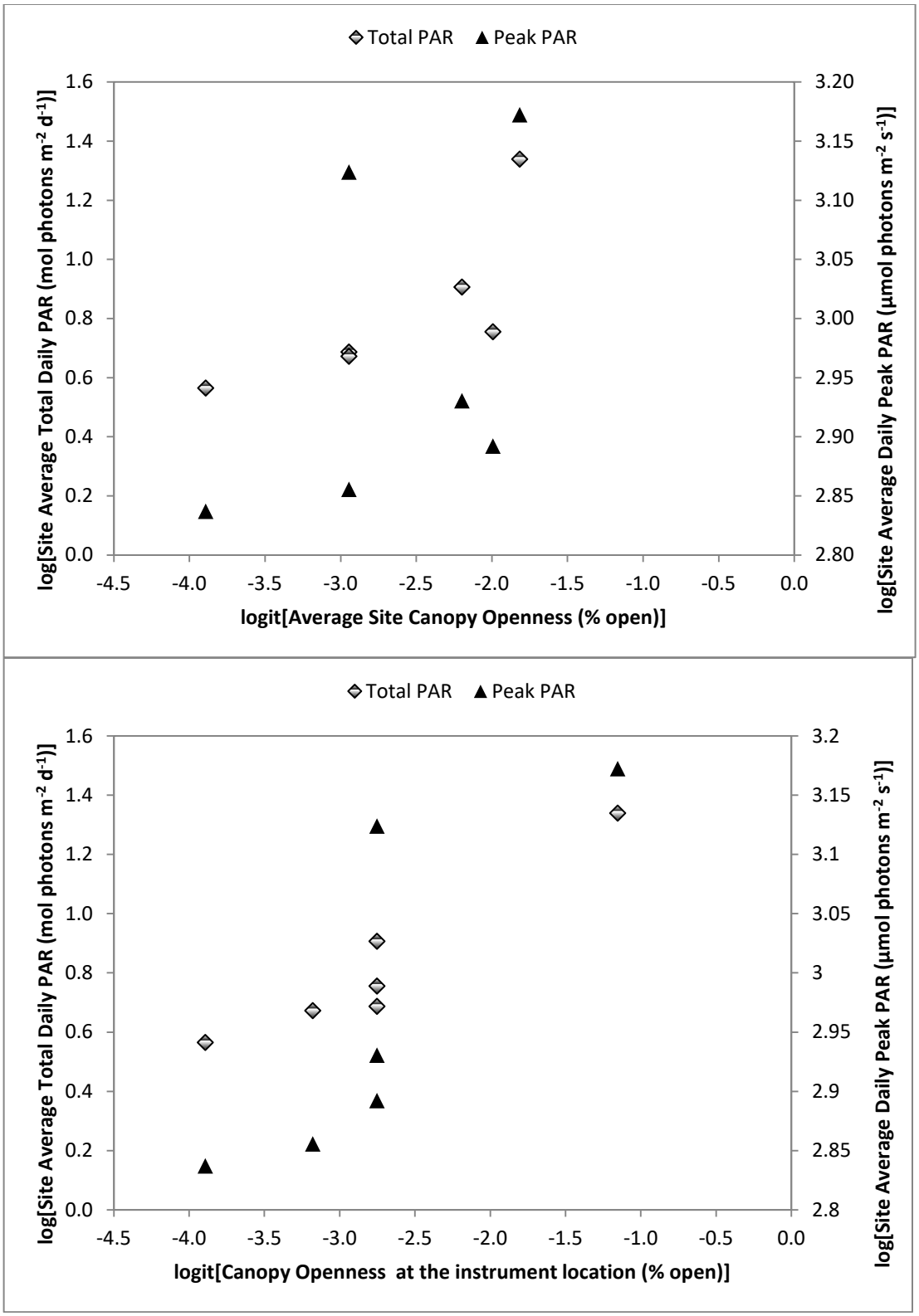

Figure 11: Peak PAR (pPAR) and total PAR (tPAR) levels, averaged for the first three deployments at each site, compared to canopy openness in (A) the entire reach and (B) at the oxygen instrument location only

Discharge generally decreased from the first to the last deployment across sites, ranging from 0.1–7.0 L s^{-1} across all sites and times with flow (excluding Rattlesnake Creek in the third deployment). The highest discharge was found for Arroyo Burro Creek, the site with the largest watershed, and the smallest discharges were found at the three sites with the smallest watersheds: Phelps, Rattlesnake, and Sycamore Creeks (Table 12). Water depths were greatest at Arroyo Burro Creek and lowest at Rattlesnake Creek, which dried after the third deployment (after May 6); average widths were greatest at Atascadero Creek and least at Rattlesnake Creek; and average current velocity was greatest at Arroyo Hondo Creek and least at Phelps Creek (Table 12). In general, there was little consistent relationship between discharge, velocity, depth, or width and elevation or land use pattern; however, site-average thalweg velocity was higher at high than low elevation sites and water depth was greater at the low than high elevation sites after April 22.

Table 12: Summary of discharge, flow velocity, and water depth data

	HO	RS	SY	AB	AT	PH
Discharge (L s^{-1})						
(1) March 11-March 29	6.5	1.1	1.7	7.0	4.0	0.7
(2) April 2-April 15	4.0	0.9	1.5	7.6	2.1	0.5
(3) April 22 - May 6	2.2	0.0	1.0	3.8	2.6	1.3
(4) May 20 - June 5	1.0	--	0.3	4.1	3.2	0.8
(5) June 13 - June 30	1.4	--	0.2	4.7	0.8	0.5
(6) July 8 - July 22	0.3	--	0.1	4.7	0.5	0.2
Site Average	**2.6**	**0.7**	**0.8**	**5.3**	**2.2**	**0.7**
Thalweg Velocity (cm s^{-1})						
(1) March 11-March 29	7.8	4.0	6.1	0.8	3.7	2.0
(2) April 2-April 15	3.6	6.4	4.6	4.0	3.1	0.8
(3) April 22 - May 6	7.5	1.0	3.2	3.5	1.3	1.3
(4) May 20 - June 5	3.7	--	2.6	2.0	1.5	1.4
(5) June 13 - June 30	2.9	--	2.4	2.3	0.8	0.4
(6) July 8 - July 22	1.9	--	1.0	2.5	1.8	0.6
Site Average	**4.6**	**3.8**	**3.3**	**2.5**	**2.0**	**1.1**
All Locations Velocity (cm s^{-1})						
(1) March 11-March 29	4.4	3.1	3.4	0.7	2.2	1.2
(2) April 2-April 15	3.2	3.3	2.5	2.6	2.0	0.4
(3) April 22 - May 6	3.3	0.2	2.2	1.9	0.7	0.8
(4) May 20 - June 5	1.8	--	1.1	1.4	1.5	1.3
(5) June 13 - June 30	1.2	--	1.4	1.6	0.5	0.2
(6) July 8 - July 22	1.0	--	0.6	1.3	0.8	0.2
Site Average	**2.5**	**2.2**	**1.9**	**1.6**	**1.3**	**0.7**
Water Depth (m)						
(1) March 11-March 29	0.14	0.11	0.15	0.23	0.15	0.11
(2) April 2-April 15	0.16	0.07	0.13	0.21	0.13	0.13
(3) April 22 - May 6	0.10	0.06	0.10	0.21	0.14	0.15
(4) May 20 - June 5	0.13	--	0.12	0.23	0.15	0.15
(5) June 13 - June 30	0.13	--	0.08	0.22	0.15	0.16
(6) July 8 - July 22	0.10	--	0.08	0.20	0.16	0.13
Site Average	**0.13**	**0.08**	**0.11**	**0.22**	**0.15**	**0.14**
Wetted Width (m)						
(1) March 11-March 29	3.4	1.7	2.8	4.1	5.9	1.7
(2) April 2-April 15	3.4	1.7	2.8	4.1	5.5	1.7
(3) April 22 - May 6	3.4	0.9	2.7	4.1	5.1	1.7
(4) May 20 - June 5	3.1	--	2.6	4.1	4.9	1.7
(5) June 13 - June 30	2.9	--	2.5	4.0	4.8	1.6
(6) July 8 - July 22	2.6	--	2.3	4.0	4.6	1.6
Site Average	**3.1**	**1.4**	**2.6**	**4.1**	**5.1**	**1.7**

Overall, there were few consistent temporal trends across sites in nitrate, phosphate, DOC, benthic chlorophyll, TSS, and conductivity levels. However, across deployments, nitrate levels tended to decline and chlorophyll levels to increase in Atascadero and Phelps creeks, whereas phosphate, TSS, and conductivity increased in Sycamore Creek (Table 13 and Table 14). Average nitrate concentrations were greatest at Arroyo Burro Creek (30.3 μM), average phosphate concentrations were highest at Atascadero Creek (12.4 μM), and average DOC (954 μM), chlorophyll (68 mg m^{-2}), TSS (12.4 mg L^{-1}), and specific conductance (4298 μS cm^{-1}) levels were highest in Phelps Creek, with the lowest average values of these variables being measured at Rattlesnake (nitrate, 0.2 μM) or Arroyo Hondo (phosphate, 0.2 μM; DOC 66 μM; chlorophyll, 4.2 mg m^{-2}; TSS, 0.8 mg L^{-1}; specific conductance 1207 μS cm^{-1}) creeks (Table 13 and Table 14). Across deployments, phosphate levels were generally higher at sites in basins with some development than at the two sites (Arroyo Hondo, Rattlesnake) draining undeveloped catchments. Log-transformed nitrate, log-transformed DOC, and log-transformed specific conductance were significantly higher in developed (AT, AB, PH, and SY) than undeveloped basins (HO and RS) based on time-averaged data from the first three deployments (one-way ANOVAs, n = 6: $F_{1,4} = 9.3$, $p = 0.04$; $F_{1,4} = 16.8$, $p = 0.01$; $F_{1,4} = 15.3$, $p = 0.02$, respectively). Chlorophyll levels were greater and TSS levels were lower at low than high elevation sites (one-way ANOVA on averaged deployment 1-3 data, log-transformed: $F_{1,4} = 93.3$, $p = 0.0006$ and $F_{1,4} = 8.7$, $p = 0.04$, respectively), although Sycamore Creek had intermediate chlorophyll levels between the undeveloped and other developed sites in the first two deployments (March 11 – April 15).

Table 13: Summary of nitrate, phosphate, DOC, and benthic chlorophyll data

	HO	RS	SY	AB	AT	PH
Nitrate (µM)						
(1) March 11-March 29	0.2	0.1	4.5	35.8	11.2	5.3
(2) April 2-April 15	0.7	0.0	0.9	43.4	4.9	1.5
(3) April 22 - May 6	0.3	0.5	1.1	38.6	1.5	1.8
(4) May 20 - June 5	0.5	--	0.7	22.6	0.9	0.8
(5) June 13 - June 30	0.0	--	1.1	18.2	0.9	1.4
(6) July 8 - July 22	0.3	--	0.4	23.1	1.0	1.3
Site Average	**0.3**	**0.2**	**1.4**	**30.3**	**3.4**	**2.0**
Phosphate (µM)						
(1) March 11-March 29	0.1	0.9	1.0	0.2	15.8	0.8
(2) April 2-April 15	0.1	0.8	1.2	1.6	15.5	3.7
(3) April 22 - May 6	0.3	1.7	1.7	0.8	15.3	2.6
(4) May 20 - June 5	0.2	--	2.4	0.9	9.6	3.3
(5) June 13 - June 30	0.2	--	3.1	0.9	7.5	0.8
(6) July 8 - July 22	0.2	--	3.7	1.1	10.9	4.4
Site Average	**0.2**	**1.1**	**2.2**	**0.9**	**12.4**	**2.6**
DOC (µM)						
(1) March 11-March 29	93.0	192.2	570.4	344.5	592.1	706.2
(2) April 2-April 15	93.4	181.4	579.0	378.0	696.3	1209.5
(3) April 22 - May 6	53.3	216.0	740.0	421.7	685.4	859.0
(4) May 20 - June 5	53.4	--	795.0	386.8	472.6	1014.3
(5) June 13 - June 30	47.8	--	806.6	394.5	555.1	822.9
(6) July 8 - July 22	54.5	--	826.4	393.4	553.4	1111.8
Site Average	**65.9**	**196.6**	**719.6**	**386.5**	**592.5**	**953.9**
Benthic Chlorophyll a (mg m^{-2})						
(1) March 11-March 29	1.6	2.3	3.4	26.6	9.3	24.1
(2) April 2-April 15	2.6	4.6	8.3	44.1	26.9	40.2
(3) April 22 - May 6	4.7	9.2	3.0	55.0	49.1	59.2
(4) May 20 - June 5	2.8	--	4.6	38.1	50.8	60.7
(5) June 13 - June 30	6.2	--	5.4	39.6	54.6	118.4
(6) July 8 - July 22	7.1	--	2.1	54.2	54.4	104.0
Site Average	**4.2**	**5.4**	**4.5**	**42.9**	**40.8**	**67.8**

Table 14: Summary of total suspended solids and specific conductance data

	HO	RS	SY	AB	AT	PH
TSS (mg L^{-1})						
(1) March 11-March 29	1.0	2.0	1.5	3.2	3.3	11.0
(2) April 2-April 15	0.3	1.4	1.6	2.8	6.1	20.5
(3) April 22 - May 6	0.9	1.8	2.4	2.2	24.7	8.7
(4) May 20 - June 5	1.2	--	1.8	2.1	3.1	7.3
(5) June 13 - June 30	0.8	--	2.5	2.0	3.5	5.1
(6) July 8 - July 22	0.6	--	11.2	1.7	3.1	22.0
Site Average	**0.8**	**1.7**	**3.5**	**2.3**	**7.3**	**12.4**
Volatile Solids (% of TSS)						
(1) March 11-March 29	55%	44%	35%	42%	42%	28%
(2) April 2-April 15	65%	48%	63%	37%	37%	32%
(3) April 22 - May 6	70%	58%	51%	48%	23%	33%
(4) May 20 - June 5	78%	--	45%	65%	59%	34%
(5) June 13 - June 30	86%	--	45%	70%	59%	52%
(6) July 8 - July 22	93%	--	32%	66%	61%	42%
Site Average	**74%**	**50%**	**45%**	**55%**	**47%**	**37%**
Specific Conductance (µS cm^{-1})						
(1) March 11-March 29	1153	1280	3200	2360	2610	4920
(2) April 2-April 15	1200	1310	3230	2180	1961	2660
(3) April 22 - May 6	1217	1405	3890	2340	2500	4720
(4) May 20 - June 5	1222	--	4410	2250	2160	4470
(5) June 13 - June 30	1230	--	4580	2310	2290	3950
(6) July 8 - July 22	1219	--	4690	2290	2240	5070
Site Average	**1207**	**1332**	**4000**	**2288**	**2294**	**4298**

The developed, low elevation sites were dominated by sand or finer substrata, whereas the higher elevation sites were dominated by gravel, cobble, and boulders (Table 15). Total BOM, CBOM, and FBOM levels were higher at the low elevation, developed sites than the higher elevation sites, with the developed Sycamore Creek site being more similar to the other higher elevation, undeveloped site, Arroyo Hondo Creek, for which BOM data were obtained (Table 15). Log-transformed levels of FBOM and TBOM were significantly higher

at low than high elevation sites (AT, AB, PH > RS, SY; one-way ANOVA, $F_{1,4} = 29.0$, $p = 0.01$ and $F_{1,4} = 11.8$, $p = 0.04$, respectively).

Table 15: Substrata and benthic organic matter characteristics at each site

		HO	RS	SY	AB	AT	PH
		(n = 149)	(n = 60)	(n = 149)	(n = 144)	(n = 140)	(n = 148)
Substrata	**Sand and finer (%)**	0	17	9	80	81	93
	Gravel (%)	26	35	32	19	19	5
	Cobbles (%)	31	18	28	1	0	1
	Boulders (%)	44	30	32	0	0	0
Benthic Organic Matter	**fBOM (g m^{-2})**	24	--	53	298	205	407
	cBOM (g m^{-2})	348	--	277	527	616	1308
	Total BOM (g m^{-2})	372	--	329	825	821	1715

3.4.2. PCA results

A PCA on values of 12 environmental variables measured at 32 sites-times produced four significant PCA axes (eigenvalues > 1 and explained variance >5%, Table 16), together explaining 88% of the variation in the multivariate dataset. The first PCA axis (PC-1), explaining 40% of the variation in the multivariate dataset, was positively correlated with phosphate, DOC, chlorophyll *a*, TSS, and specific conductance; the second PCA axis (PC-2), which explained 25% of the variation, was positively related to discharge, nitrate concentration, water width, and water depth; the third PCA axis (PC-3), which accounted for another 14% of the multivariate variation, was positively related to total PAR level, water width, and phosphate concentration; and the fourth PCA axis (PC-4), accounting for 9% of the variation, was positively related to mean temperature and negatively related to thalweg velocity and DOC concentration (Table 17).

Table 16: Eigenvalues and variance explained for each principal component

	Variance Explained	Eigenvalue
PC-1	**0.40**	**4.79**
PC-2	**0.25**	**2.99**
PC-3	**0.14**	**1.65**
PC-4	**0.09**	**1.04**
PC-5	0.06	0.67
PC-6	0.02	0.28
PC-7	0.02	0.19
PC-8	0.01	0.16
PC-9	0.01	0.10
PC-10	0.00	0.05
PC-11	0.00	0.04
PC-12	0.00	0.03

*Bolded numbers represent values that meet the thresholds required to retain the component for analysis (>5% variance explained and eigenvalue >1)

Table 17: Principal component coefficients for each variable

	PC-1	PC-2	PC-3	PC-4
log(total PAR)	0.2	0.12	**0.64**	0
log(mean temp)	0.29	0.05	0.13	**0.53**
log(discharge)	-0.14	**0.5**	-0.08	-0.19
log(thalweg velocity)	-0.35	0.08	0.1	**-0.45**
log(depth)	0.1	**0.49**	-0.27	0.18
log(width)	-0.01	**0.46**	**0.37**	-0.08
log(nitrate)	0.19	**0.4**	-0.32	-0.22
log(phosphate)	**0.36**	-0.01	**0.37**	-0.31
log(DOC)	**0.4**	-0.07	-0.11	**-0.36**
log(chlorophyll a)	**0.35**	0.22	-0.1	0.27
log(TSS)	**0.38**	-0.12	-0.03	-0.18
log(Specific Conductance)	**0.35**	-0.18	-0.27	-0.24

*Coefficients highlighted in bold meet the criteria described in the methods for significance.

3.4.3. Metabolism results

Reaeration coefficients, calculated from gas transfer velocities and average water depths at each site, varied across sites and deployments. In general, reaeration coefficients were relatively constant at the developed sites (AB, AT, PH), but generally declined across deployments at Sycamore Creek and the undeveloped sites (HO, RS, although peaks occurred during the 3rd deployment for HO and the 2nd deployment for RS) (Table 18). Reaeration coefficients were consistently lower across deployments at the developed, low elevation sites (AB, AT, PH) than at the high elevation sites (HO, RS, SY).

Table 18: Summary of reaeration coefficients and gas transfer velocities

	HO	RS	SY	AB	AT	PH
Reaeration Coefficients (d^{-1})						
(1) March 11-March 29	37.1	60.7	49.4	2.1	3.3	4.4
(2) April 2-April 15	17.8	110.2	40.9	2.3	3.8	3.8
(3) April 22 - May 6	41.1	8.1	33.1	2.3	3.5	3.3
(4) May 20 - June 5	19.9	--	25.5	2.1	3.3	3.3
(5) June 13 - June 30	16.0	--	28.2	2.2	3.3	3.1
(6) July 8 - July 22	12.3	--	6.1	2.4	3.1	3.8
Gas Transfer Velocities (cm hr^{-1})						
(1) March 11-March 29	21.6	27.8	30.9	2.0	2.0	2.0
(2) April 2-April 15	11.9	32.2	22.2	2.0	2.0	2.0
(3) April 22 - May 6	17.1	2.0	13.8	2.0	2.0	2.0
(4) May 20 - June 5	10.8	--	12.8	2.0	2.0	2.0
(5) June 13 - June 30	8.7	--	9.4	2.0	2.0	2.0
(6) July 8 - July 22	5.1	--	2.0	2.0	2.0	2.0

Daily estimates of GPP ranged from 0.1 to 6.1 g O_2 m^{-2} d^{-1} across all measurement days and sites (Appendix II). Arroyo Burro Creek had the largest single estimated daily GPP and time-averaged GPP (3.5 g O_2 m^{-2} d^{-1}), whereas Rattlesnake Creek had the lowest (average =

0.5 g O_2 m^{-2} d^{-1}, Table 19). GPP estimates were consistently lower at Arroyo Hondo and Rattlesnake creeks (means = 0.5 g O_2 m^{-2} d^{-1}) than at the other sites (means = 2.0 to 3.5 g O_2 m^{-2} d^{-1}), with average GPP at Sycamore Creek being less than average GPP at the other developed sites during the 3rd, 5th, and 6th deployments (April 22- May 6 and after June 13).

Daily estimates of CR were variable across sites, ranging from 2.0 at Rattlesnake Creek to 15.9 g O_2 m^{-2} d^{-1} at Sycamore Creek (Appendix II, Table 19). On average, CR was higher in Rattlesnake and Sycamore creeks (8.2 g O_2 m^{-2} d^{-1}) than at the other sites (means = 4.2 to 4.5 g O_2 m^{-2} d^{-1}), but there were no consistent patterns across time. High elevation sites had higher average CR values during the first deployment (March 11-29) and lower than average CR values during the last deployment (July 8-22) compared to low elevation sites. Daily estimates of NEP ranged from -14.8 to 0.8 g O_2 m^{-2} d^{-1} across sites and were negative (net heterotrophy) for all dates, except for 2 days during the first deployment at Arroyo Burro Creek (March 18-19, Appendix II). Across all deployments, NEP was lowest at Rattlesnake and Sycamore creeks (-7.6 and -6.2 g O_2 m^{-2} d^{-1}), had intermediate values at Arroyo Hondo, Phelps, and Atascadero creeks (-3.7, -2.5, and -2.1 g O_2 m^{-2} d^{-1}, respectively), and was highest (least negative) at Arroyo Burro Creek (-0.7 g O_2 m^{-2} d^{-1}). Daily estimates of P/R ranged from 0.0 to 1.2 across all times and sites (Appendix II), with values less than 1 on all but two days at Arroyo Burro Creek. Average P/R across deployments ranged from 0.1 at both sites in undeveloped basins (Arroyo Hondo, Rattlesnake) to 0.2 at Sycamore Creek to 0.4 and 0.5 at Phelps and Atascadero creeks to 0.8 at Arroyo Burro Creek (Table 19).

Table 19: Summary of metabolism estimates

	HO	RS	SY	AB	AT	PH
GPP ($g\ O_2\ m^{-2}\ d^{-1}$)						
(1) March 11-March 29	0.5	0.3	2.8	4.8	0.8	0.6
(2) April 2-April 15	0.4	1.0	2.3	2.8	2.5	1.4
(3) April 22 - May 6	0.8	0.2	1.6	2.3	2.7	3.0
(4) May 20 - June 5	0.6	--	2.7	3.6	3.3	2.5
(5) June 13 - June 30	0.4	--	2.0	4.0	3.0	2.7
(6) July 8 - July 22	0.3	--	0.5	3.4	2.4	2.2
Site Average	**0.5**	**0.5**	**2.0**	**3.5**	**2.4**	**2.1**
CR ($g\ O_2\ m^{-2}\ d^{-1}$)						
(1) March 11-March 29	5.8	7.8	7.7	4.4	3.7	3.0
(2) April 2-April 15	3.7	14.6	8.8	3.4	4.6	4.1
(3) April 22 - May 6	6.1	2.1	9.3	3.3	4.7	5.6
(4) May 20 - June 5	4.1	--	12.0	4.8	4.9	5.0
(5) June 13 - June 30	3.4	--	9.2	5.0	4.6	4.4
(6) July 8 - July 22	2.1	--	2.2	4.2	4.5	5.3
Site Average	**4.2**	**8.2**	**8.2**	**4.2**	**4.5**	**4.5**
NEP ($g\ O_2\ m^{-2}\ d^{-1}$)						
(1) March 11-March 29	-5.2	-7.4	-4.9	0.5	-3.0	-2.4
(2) April 2-April 15	-3.3	-13.6	-6.5	-0.5	-2.1	-2.7
(3) April 22 - May 6	-5.3	-1.9	-7.7	-1.0	-2.0	-2.6
(4) May 20 - June 5	-3.4	--	-9.3	-1.2	-1.6	-2.5
(5) June 13 - June 30	-2.9	--	-7.2	-1.0	-1.6	-1.7
(6) July 8 - July 22	-1.9	--	-1.8	-0.8	-2.1	-3.0
Site Average	**-3.7**	**-7.6**	**-6.2**	**-0.7**	**-2.1**	**-2.5**
P/R (unitless)						
(1) March 11-March 29	0.1	0.0	0.4	1.1	0.2	0.2
(2) April 2-April 15	0.1	0.1	0.3	0.8	0.5	0.3
(3) April 22 - May 6	0.1	0.1	0.2	0.7	0.6	0.5
(4) May 20 - June 5	0.2	--	0.2	0.7	0.7	0.5
(5) June 13 - June 30	0.1	--	0.2	0.8	0.6	0.6
(6) July 8 - July 22	0.1	--	0.2	0.8	0.5	0.4
Site Average	**0.1**	**0.1**	**0.2**	**0.8**	**0.5**	**0.4**

3.4.4. Metabolism relationships to site characteristics and environmental variables

Using averages for each deployment at each site as replicates in multiple regression analyses (n = 32, excludes RS deployment 3), GPP, NEP, and P/R were significantly and positively correlated with principal component 1, which was positively related to phosphate, TSS, and DOC concentrations, chlorophyll *a*, and specific conductance (Table 20). All four metabolism parameters were related to PC-2: GPP, NEP, and P/R positively and CR negatively. PC-2 was positively related to discharge, water depth, wetted width, and nitrate concentration. Only P/R was related, negatively, to PC-3 (Table 20), which was related to total PAR levels, water width, and phosphate concentration. CR, NEP, and P/R, but not GPP, were related to PC-4 (NEP and P/R positively, CR negatively), which was related to mean temperature, thalweg velocity and DOC. The most significant relationships were found for PC-2 (Table 20), suggesting that although individual metabolism parameters were related to a variety of environmental variables, all the metabolism parameters were related to nitrate, discharge, water width, and water depth. Strong relationships were also found for PC-1, suggesting that other stream chemical characteristics also played an important role in metabolism.

Table 20: Multivariate regression model results comparing metabolism values at each site-deployment (n = 32), to principle component axes 1 through 4

GPP	R Square	Adjusted R Square	F Stat	p-value	MSE	dfe	dfr	N
	0.63	0.58	11.7	1.2E-05	0.64	27	4	32
	Coefficient	**SE**	**t Stat**	**p-value**	**lower 95%**	**Upper 95%**		
β_o (intercept)	2.01	0.14	14.2	5.2E-14	1.71	2.30		
β_1 (PC-1)	0.31	0.07	4.7	6.0E-05	0.18	0.45		
β_2 (PC-2)	0.39	0.08	4.6	8.2E-05	0.21	0.56		
β_3 (PC-3)	-0.19	0.11	-1.7	0.11	-0.42	0.04		
β_4 (PC-4)	0.06	0.14	0.4	0.69	-0.24	0.35		

CR	R Square	Adjusted R Square	F Stat	p-value	MSE	dfe	dfr	N
	0.33	0.23	3.3	2.4E-02	5.85	27	4	32
	Coefficient	**SE**	**t Stat**	**p-value**	**lower 95%**	**Upper 95%**		
β_o (intercept)	5.50	0.43	12.9	5.1E-13	4.61	6.38		
β_1 (PC-1)	-0.24	0.20	-1.2	0.23	-0.65	0.17		
β_2 (PC-2)	-0.59	0.25	-2.4	0.03	-1.11	-0.08		
β_3 (PC-3)	0.21	0.34	0.6	0.54	-0.49	0.91		
β_4 (PC-4)	-1.03	0.43	-2.4	0.02	-1.91	-0.15		

NEP	R Square	Adjusted R Square	F Stat	p-value	MSE	dfe	dfr	N
	0.66	0.61	13.0	5.2E-06	3.49	27	4	32
	Coefficient	**SE**	**t Stat**	**p-value**	**lower 95%**	**Upper 95%**		
β_o (intercept)	-3.49	0.33	-10.6	4.2E-11	-4.17	-2.81		
β_1 (PC-1)	0.55	0.15	3.6	1.2E-03	0.24	0.87		
β_2 (PC-2)	0.98	0.19	5.1	2.6E-05	0.58	1.38		
β_3 (PC-3)	-0.40	0.26	-1.5	0.14	-0.94	0.14		
β_4 (PC-4)	1.08	0.33	3.3	2.8E-03	0.40	1.76		

P/R	R Square	Adjusted R Square	F Stat	p-value	MSE	dfe	dfr	N
	0.84	0.82	36.0	1.9E-10	0.01	27	4	32
	Coefficient	**SE**	**t Stat**	**p-value**	**lower 95%**	**Upper 95%**		
β_o (intercept)	0.41	0.02	19.2	2.7E-17	0.36	0.45		
β_1 (PC-1)	0.07	0.01	7.1	1.1E-07	0.05	0.09		
β_2 (PC-2)	0.11	0.01	9.0	1.3E-09	0.09	0.14		
β_3 (PC-3)	-0.05	0.02	-2.8	0.01	-0.08	-0.01		
β_4 (PC-4)	0.04	0.02	2.1	0.05	0.00	0.09		

Correlations were examined between the metabolism parameters and the environmental variables based on the averages for the first three deployments (March 11 to May 6) at each site (n = 6 except for correlations including BOM variables, where n = 5) to help interpret the results of the PCA regressions and to assess relationships between metabolism and environmental variables averaged over time. These results confirm that GPP, NEP, and P/R

were positively related to nitrate ($p = 0.003$, $p = 0.03$, and $p = 0.001$, respectively, Figure 12) and depth ($p = 0.03$, $p = 0.03$, $p = 0.02$, respectively), but there were no relationships between these metabolic parameters and the other variables that were related to PC-2 (Table 21). Also, CR was not related to the environmental variables related to PC-2 or PC-4, but CR and NEP were related to elevation, which was not included in the PCA (Table 21). NEP also was positively related to chlorophyll concentration and negatively related to cobble coverage.

Table 21: Significant ($p<0.05$) Pearson correlation coefficients for the relationships between metabolism estimates and environmental variables using time-averaged data over the first three deployments at each site as replicates (n=6).

	GPP	CR	NEP	P/R
log(depth)	0.85		0.87	0.89
log(nitrate)	0.96		0.86	0.97
log(chla)			0.83	
logit(cobbles)			-0.83	
logit(channel slope)		0.82		
log(elevation)		0.83	-0.93	

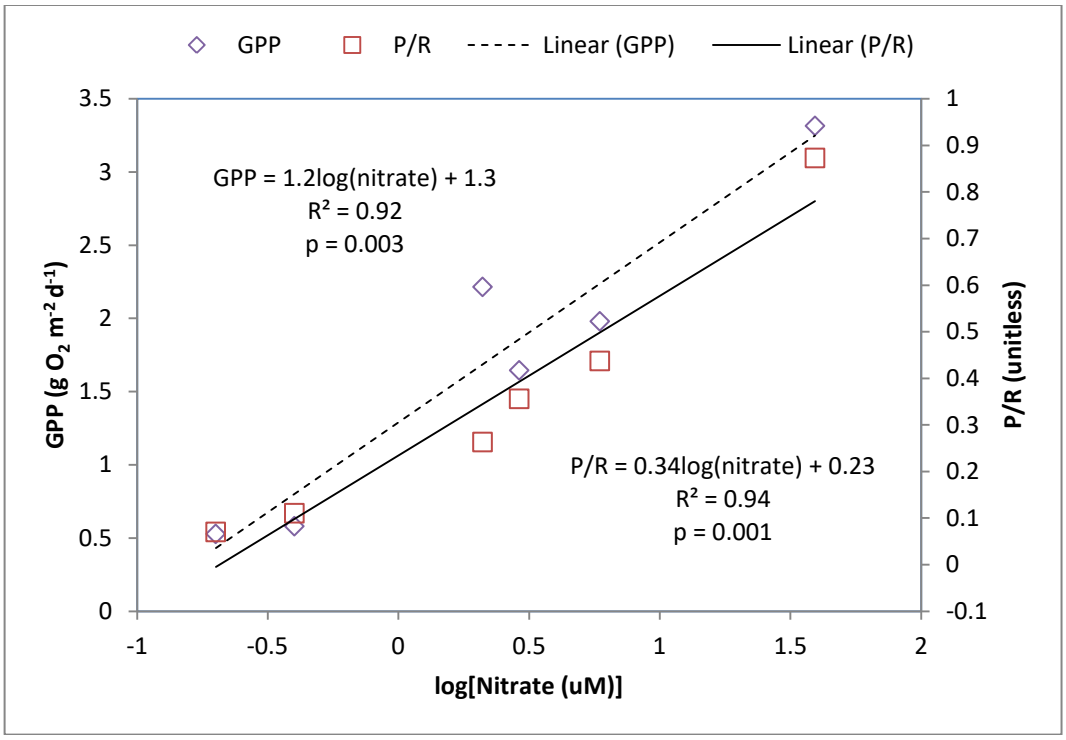

Figure 12: GPP and P/R versus log-transformed nitrate concentration using time-averaged site data from the first three deployments as replicates.

3.4.5. Comparison of metabolism estimates between developed and undeveloped sites

Time-averaged metabolism values from the first three deployments (March 11- May 6, Figure 13) were compared between undeveloped (HO, RS) and developed (AB, AT, PH) sites, with Sycamore included as either an undeveloped or a developed site in two separate analyses. When Sycamore Creek was included as a developed site, GPP was significantly greater at developed than undeveloped sites (one-way ANOVAs, $p = 0.03$, $F_{1,4} = 10.23$) (Table 22), but CR, NEP, and P/R were not different between land use categories. When Sycamore Creek was included as an undeveloped site (aligning with elevation differences between the groups), NEP was significantly more positive and CR was significantly lower at developed than undeveloped sites (one-way ANOVAs for NEP, $p = 0.02$, $F_{1,4} = 15.76$ and

CR, p = 0.04, $F_{1,4}$ = 8.93) (Table 22), but GPP and P/R were not different between land use categories.

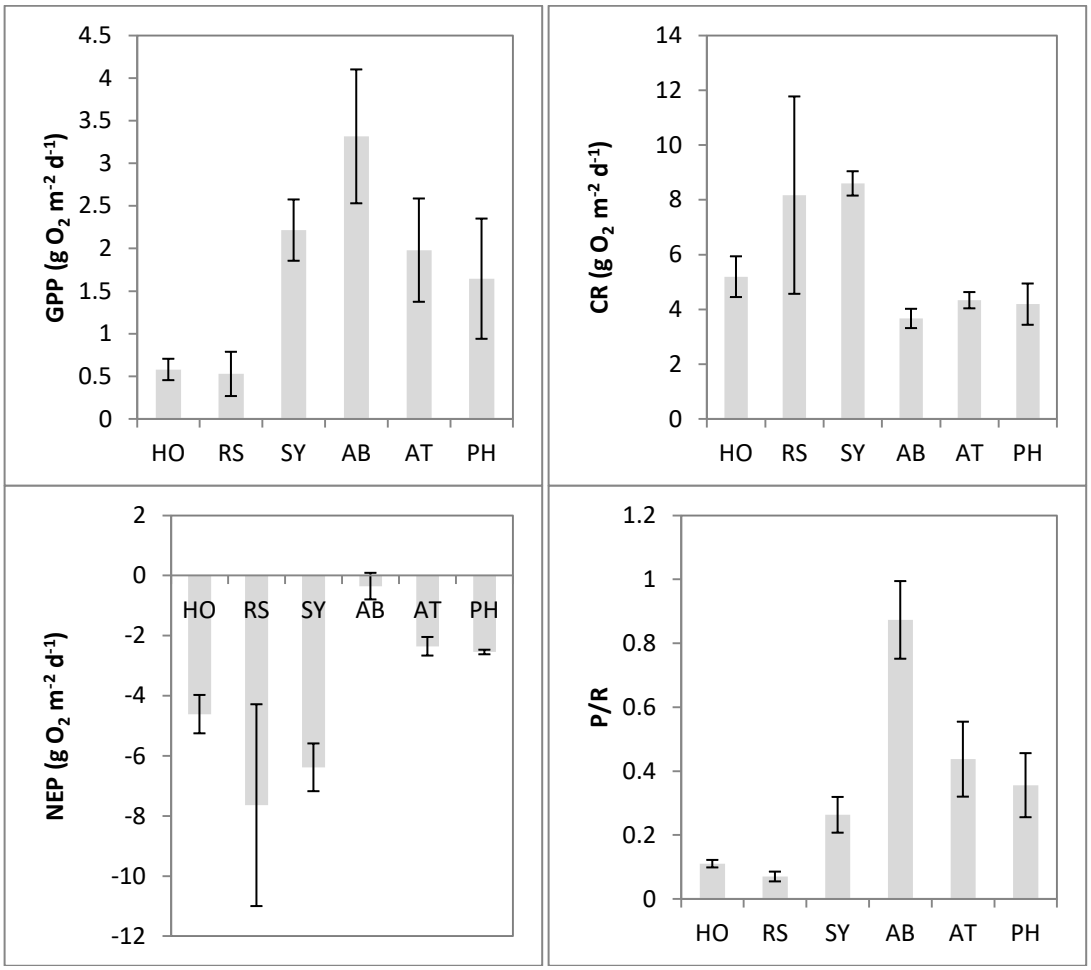

Figure 13: Time-averaged metabolism values for the first three deployments at each site (±1 SE)

Table 22: One-way ANOVA comparing metabolism values at developed (AB, AT, PH) and undeveloped (HO, RS) sites, including SY as either a developed or undeveloped site in two separate analyses.

	HO/RS v. SY/AB/AT/PH					
GPP	**Source**	**SS**	**df**	**MS**	**F**	**Prob>F**
	Groups	4.0	1	4.0	10.23	**0.03**
	Error	1.6	4	0.4		
	Total	5.6	5			
CR	**Source**	**SS**	**df**	**MS**	**F**	**Prob>F**
	Groups	2.9	1	2.9	0.58	0.49
	Error	20.1	4	5.0		
	Total	23.0	5			
NEP	**Source**	**SS**	**df**	**MS**	**F**	**Prob>F**
	Groups	13.8	1	13.8	2.34	0.20
	Error	23.6	4	5.9		
	Total	37.4	5			
P/R	**Source**	**SS**	**df**	**MS**	**F**	**Prob>F**
	Groups	0.2	1	0.2	3.74	0.13
	Error	0.2	4	0.1		
	Total	0.4	5			

	HO/RS/SY v. AB/AT/PH					
GPP	**Source**	**SS**	**df**	**MS**	**F**	**Prob>F**
	Groups	2.2	1	2.2	2.56	0.18
	Error	3.4	4	0.9		
	Total	5.6	5			
CR	**Source**	**SS**	**df**	**MS**	**F**	**Prob>F**
	Groups	15.9	1	15.9	8.93	**0.04**
	Error	7.1	4	1.8		
	Total	23.0	5			
NEP	**Source**	**SS**	**df**	**MS**	**F**	**Prob>F**
	Groups	29.8	1	29.8	15.76	**0.02**
	Error	7.6	4	1.9		
	Total	37.4	5			
P/R	**Source**	**SS**	**df**	**MS**	**F**	**Prob>F**
	Groups	0.2	1	0.2	5.68	0.08
	Error	0.2	4	0.0		
	Total	0.4	5			

3.4.6. Comparison of metabolism to land use

That the regression analyses indicated that nitrate concentration was an important driver of GPP, NEP, and P/R, motivated examination of differences among land use variables, nitrate concentration, and metabolism variables across sites. These analyses indicated that Arroyo Burro Creek was an outlier compared to the other creeks, with nitrate levels, number of septic parcels, GPP, and P/R being higher at this site than the other sites (Table 5, Table 13, and Table 19). If Arroyo Burro is removed, both GPP and P/R continue to show a significant relationship with nitrate ($n = 5$, Pearson's $r = 0.91$, $p = 0.03$ and Pearson's $r = 0.98$, $p = 0.002$, respectively).

Several of the land use variables were significantly inter-correlated (Appendix III). Although none of the land use variables were related to total watershed area, almost all were

related to the total urban area in the watershed. Despite inter-correlation among the land use variables, only a subset demonstrated significant correlations with metabolism metrics or log nitrate (Table 23). Of the land use variables that showed significant relationships with metabolism metrics, only the number of septic parcels in the AOI was not related to any other land use variables.

At the AOI scale, CR, NEP, P/R and log nitrate levels were related to AOI area (CR negatively, NEP, P/R, and log nitrate positively); NEP, P/R, and log nitrate levels were positively related to human population numbers; P/R and log nitrate levels were positively related to impervious area; GPP, P/R, and log nitrate levels were positively related to irrigated grass area; GPP was positively related to proportionate irrigated grass coverage; NEP was positively related to urban area; and P/R was positively related to number of septic parcels (Table 23). At the watershed scale, NEP, P/R, and log nitrate levels were positively related to urban area, GPP and log nitrate levels were positively related to impervious area, and GPP was positively related to septic parcels. CR had no significant relationships to any land use variables at either the AOI or watershed scales, other than AOI area. Some of these land use variables were related to log-transformed elevation, but elevation was not significantly related to the land use variables with which GPP demonstrated a significant relationship (Table 23). The relationships for P/R and log nitrate concentrations with land use were similar (Table 23, Figure 14), and GPP, P/R, and nitrate levels were most strongly related to the area of irrigated grass in the AOI, which was not significantly related to elevation (Table 23).

Table 23: Significant correlation coefficients (p<0.05) between time-averaged metabolism estimates and log nitrate from the first three deployments, and log elevation, versus land use variables (n=6) (ws = watershed, aoi = riparian area of influence).

	GPP	CR	NEP	P/R	log(nitrate)	log(elevation)
log(ws urban area)			0.83	0.82	0.90	-0.87
log(ws impervious area)	0.86				0.90	
log(ws septic)	0.82					
log(aoi urban area)			0.87			-0.82
log(aoi impervious area)				0.81	0.89	-0.83
log(aoi population)			0.81	0.83	0.90	-0.83
log(aoi irrigated grass area)	0.90			0.87	0.94	
log(aoi septic)				0.86		
logit(aoi irrigated grass %)	0.83					
log(aoi area)		-0.85	0.95	0.88	0.89	-0.84
logit(ws %urban)						-0.86

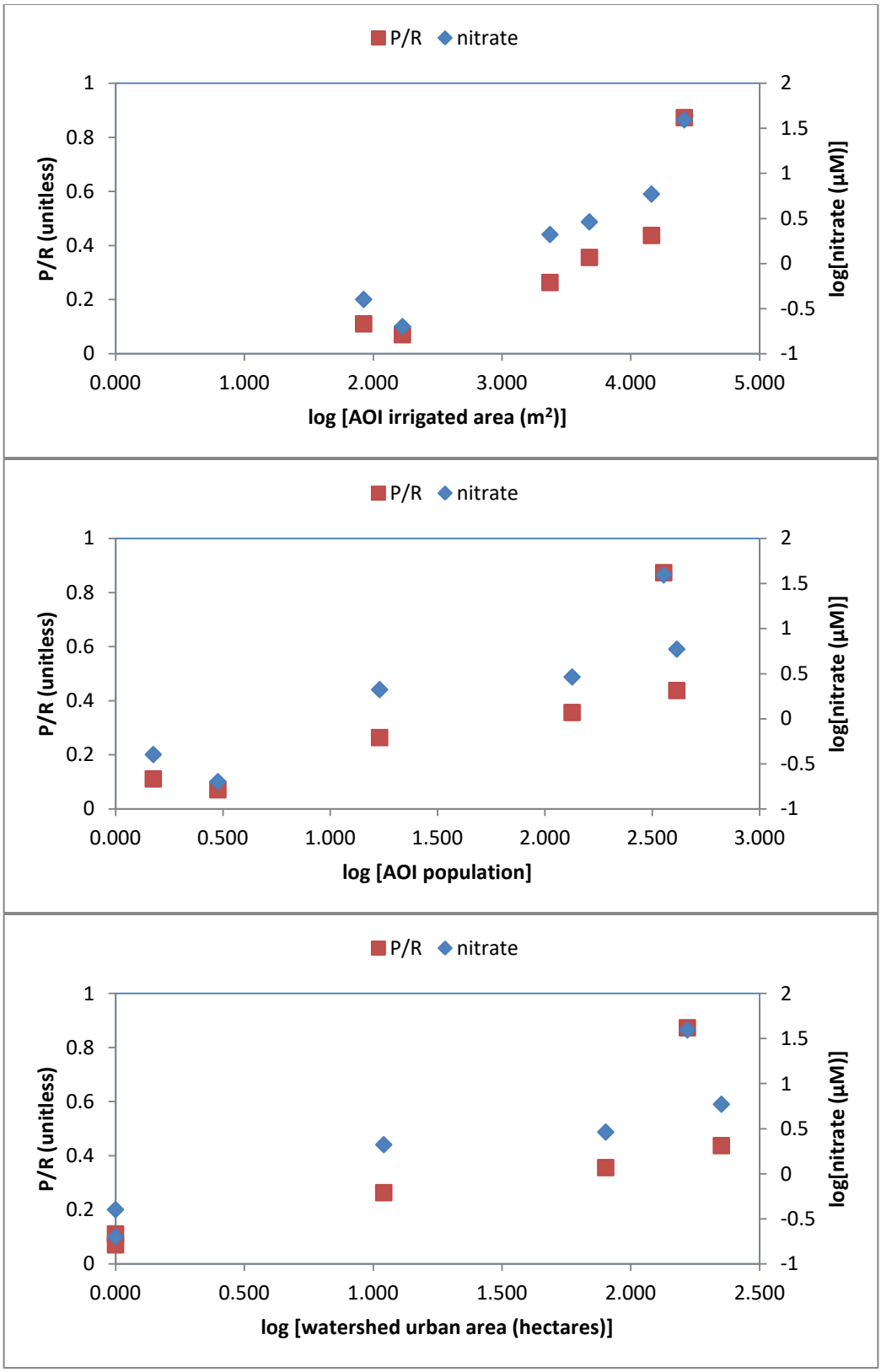

Figure 14: Relationships of P/R and log nitrate versus various land use variables

3.5. Discussion

3.5.1. Comparison of results to other systems

The creeks in this study are small and relatively steep, with closed riparian canopy in their headwaters, and probably representative of low-order streams under the River Continuum Concept (Vannote et al., 1980; Dodds et al., 2015). Average GPP values for reference sites in this study (0.5 g O_2 m^{-2} d^{-1}) were similar to the GPP values found in forested streams in other forested regions (less than 2.0 g O_2 m^{-2} d^{-1}), which were lower than those recorded from open canopy grasslands and desert shrublands (between 3-5 g O_2 m^{-2} d^{-1}) (Bernot et al., 2010). Average GPP values for the urban sites in this study (2-3.5 g O_2 m^{-2} d^{-1}) were higher than GPP values found in deciduous forested streams and lower than values found in systems with more open canopies, being most similar to values recorded at sites in a wet coniferous-deciduous mixed forest (about 2 g O_2 m^{-2} d^{-1}) (Bernot et al., 2010). When GPP values from the sites in this study are compared to values at sites with similar land uses across multiple biomes, values from reference sites in this study fall within the middle third of values (0.2-1.8 g O_2 m^{-2} d^{-1}) from reference sites across biomes, and values of GPP from urban sites, except Arroyo Burro Creek, fall within the middle third of values (0.7-3.3 g O_2 m^{-2} d^{-1}) from urban sites across biomes (Bernot et al., 2010). Although CR rates across all sites in this study are also within ranges for deciduous forest sites studied by Bernot et al. (2010), the authors of that study found high CR variability across biomes, resulting in no significant CR differences among regions or land use types. Stream NEP values in this study were mostly negative, indicating net heterotrophy, which is common across most metabolism studies and most regions with closed canopy conditions (Bernot et al., 2010;

Mulholland et al., 2001). NEP rates for forested reference streams fell between the average values for the two undeveloped sites, Arroyo Hondo and Rattlesnake creeks.

Streams in the study area have highly seasonal flows, with generally low discharge, sometimes leading to drying, except during rainy periods, similar to streams found in arid regions. However, the sites in this study have high riparian canopy cover, which is frequently absent in desert streams, limiting the similarity between desert and this Mediterranean region. GPP rates in an Arizona headwater desert stream (Mulholland et al., 2001) were much higher than those found in all the streams in this study. Rates of GPP in desert shrubland streams of Arizona and New Mexico, including sites with urban and agricultural land use, were higher than the values measured in this study, except those measured at Arroyo Burro Creek. CR values from desert systems cited in Dodds et al. (2015), Mulholland et al. (2001), and Bernot et al. (2010) were larger than those measured at Arroyo Hondo Creek, and more similar to those measured at Rattlesnake and Sycamore Creeks. Some studies of NEP in desert regions have found autotrophic conditions (positive NEP, Mulholland et al., 2001), but others have generally found heterotrophic conditions (negative NEP), similar to values found in other regions (Bernot et al., 2010).

Light availability is recognized as a critical driver of metabolic differences across regions (Mulholland et al., 2001; Bernot et al., 2010; Lamberti and Steinman, 1997). A key difference between the systems studied here and the forested streams studied in other regions is that the streams studied had fairly continuous riparian canopy cover over time, whereas riparian canopy in other regions showed pronounced seasonality (open in winter, closed in summer). Desert regions are often reported as having minimal riparian vegetation and grassland regions can have spatially variable riparian vegetation (Dodds et al., 2015)

whereas the studied Mediterranean sites had intact, mostly closed riparian canopies (2-14% openness in each reach = 86 to 98% canopy cover). Probably owing to continuous riparian canopy cover, the streams in the study area have small annual temperature ranges compared to those in deciduous forest and desert regions, and the study area streams never freeze.

Because of these differences in the characteristics of streams in the study area to those of streams in other biomes, probably the streams most comparable are those in other regions with a Mediterranean climate. The range of GPP values from undeveloped sites in this study were similar to, or at the lower end of, values reported for undeveloped sites in Spain (Acuña et al., 2004; Acuña et al., 2005; von Schiller et al., 2008; Aristi et al., 2014; Aristi et al., 2015). However, GPP rates from the undeveloped sites in this study were lower than those measured at oligotrophic sites in Basque Country (NE Spain, Izagirre et al., 2008). A wide range and high variability of stream CR values have been reported from Mediterranean areas. In one study, the highest CR values approximated 30 g O_2 m^{-2} d^{-1} in late autumn/winter, with values as low as 0.4 g O_2 m^{-2} d^{-1} in the late spring and summer (Acuña et al. 2004). Daily values of CR reported in early spring from Spain were both greater (Acuña et al., 2004) and lower (von Schiller et al., 2008) than those measured, whereas those reported for late spring and summer from Spain were generally lower (Acuña et al., 2004; Acuña et al., 2005). CR values from oligotrophic streams in NE Spain were higher than the CR values measured in this study (Izagirre et al., 2008). As reported here, heterotrophy typified Spanish streams.

3.5.2. Relevance of the timing of the measurements

Droughts are common in regions with Mediterranean climates and the study was conducted during one of the driest years on record and was part of the driest five year period

recorded in the study region (County of Santa Barbara, 2016a). Drought conditions likely influenced the magnitude and variability in metabolic parameters among the study sites. During extended droughts, debris, litter, and algae accumulate and longitudinal and lateral hydrological connectivity diminishes, in some cases leading to isolated pools or complete drying (e.g., Acuña et al., 2004, 2005). Also, in the study region, low flow conditions have been shown to enhance differences in nitrate concentrations between urban and undeveloped streams because the undeveloped headwaters contribute a lower proportion of stream flow than during wet periods and urban development occurs at low elevations on the coastal plain (Goodridge and Melack, 2012). Similarly, a study in the nearby Ventura River found that the spatial scale of land use affecting benthic algal levels changed seasonally, with patterns reflecting whole catchment land use during the wet season but only local conditions, such as wastewater treatment plant inputs, during the dry season (Klose et al., 2012). Mediterranean-climate streams experience high inter-annual variability in rainfall, so if the study had been conducted in a wet year, there may have been less of a difference among sites with different land uses owing to more significant contributions from headwater areas, which are more similar across stream systems than lower developed catchment areas.

Although conducted in a dry year, the study started shortly after a large storm event, during which about 70% of the rainfall for the year fell in less than a week (County of Santa Barbara, 2016b). This area is typified by flashy hydrographs, which are more pronounced in urban areas (Walsh et al., 2005), allowing for the flushing of materials that accumulated through the extended dry season. Storms alter metabolic rates, scouring algae and depressing GPP (e.g., Uehlinger and Naegeli, 1998), which would make the streams more similar for a short recolonization period; however, storms after extended dry periods also can deliver

pollutants and nutrients to streams that have accumulated on the landscape during the dry period (Lee and Bang, 2000). Depending on the source of contaminants, storms could also accentuate differences in contaminant loading to streams draining basins with different land uses, setting the stage for differences among streams through the dry season caused by land use.

3.5.3. Differences in metabolic parameters between developed and undeveloped sites

During the first deployment, some of the developed sites had low GPP rates, similar to those at undeveloped sites, probably because they were measured shortly after storms. Several studies have reported a depression in GPP for several days following storms (Beaulieu et al., 2013; Roberts et al., 2007; Uehlinger and Naegeli, 1998). After the first week or two following a storm, the influence of the storm disturbance is expected to have less influence on metabolic responses. Roberts et al. (2007) found that stream GPP levels returned to pre-storm values around 5 days after a storm, suggesting that any storm influences would have diminished by the second deployment. Future research should further focus on GPP across land use types as a function of time since disturbance (Izagirre et al., 2008). Despite the similarity between sites in the first deployment, developed sites had higher GPP than undeveloped sites when the first three deployments were averaged (March 11 – May 6), as expected. Significant differences between developed and undeveloped sites were measured for nitrate, DOC, and specific conductance, suggesting changes in water chemistry due to urban development, even at low levels of urban development, such as those observed at SY.

There was a greater range of CR rates compared to GPP rates across sites, similar to prior studies (Bernot et al., 2010). However, CR tended to be higher at high than low

elevation sites during the first three deployments (March 11 – May 6), perhaps reflecting the effects of the storm on lowland sites, and higher at low than high elevation sites during the last deployment (July 8 – July 22), perhaps owing to higher FBOM levels at the lowland sites. Because these streams are almost exclusively heterotrophic, rates of NEP generally reflected the magnitude of CR, which is larger than GPP, resulting in similar patterns in NEP and CR across sites, though NEP and CR have different relationships to environmental variables. Also, drying and system fragmentation appeared to reduce metabolic rates substantially at RS in deployment 3 (April 22 – May 6) and SY in deployment 6 (July 8 – July 22), a pattern observed in other studies of stream metabolism in regions with Mediterranean climate (Acuña et al., 2005). The results of this study did not demonstrate a significant difference in NEP between developed and undeveloped sites, but did demonstrate that NEP was significantly higher at low than high elevation sites. There was also not a significant difference in P/R between developed and undeveloped sites or between high and low elevation sites.

Due to the pattern of urban development in this area, the gradient from urban to non-urban sites tends to co-vary with elevation changes, which have a clear influence on some of the environmental variables, such as benthic organic matter, bed substrata, and chlorophyll. Although there are low-elevation, non-urban streams in the area, many of these sites dry during the summer and fall, constraining conclusions that can be drawn from the data due to the small number of sites and the confounding influences of elevation and slope differences between the developed and undeveloped sites. The metabolism results from SY also suggest that GPP may be sensitive to low levels of urban development regardless of elevation and that CR is probably more sensitive to differences in elevation than differences in land use.

3.5.4. Pathways of urban influence on stream metabolism

Nutrients play an important role in algal growth (Borchard, 1996) and urbanization is associated with nutrient pollution, although the amounts and sources of various nutrients can vary widely depending on the specific activities occurring on the landscape. Many studies have shown that stream phosphate, nitrate, and ammonium concentrations increase with urban development, even when only a small proportion of the catchment is urbanized (Paul and Meyer, 2001; Osborne and Wiley, 1988). Although urban development appears to increase nutrient concentrations and, hence, algal growth and GPP (Mulholland et al., 2001; Lamberti and Steinman, 1997; Clapcott et al., 2010; Lee and Bang, 2000; Walsh et al., 2005), other factors, such as flow, light, depth, toxins, and turbidity, may limit the extent of this response (Paul and Meyer, 2001).

Studies in the study region have shown that stream nitrogen concentrations are higher in urban creeks than undeveloped creeks during low flow conditions when headwater areas have less hydrological influence (Goodridge and Melack, 2012). The results highlight nitrate as a potential critical driver of GPP rates and the P/R balance, consistent with a study in the nearby Ventura River basin that showed nitrogen limited or co-limited algal growth at most study sites (Klose et al., 2012), and a study including streams in the study area that found nitrate enrichment resulted in increased ecosystem productivity (Nelson et al., 2013). Nitrate concentrations, P/R, and GPP were all highest at Arroyo Burro Creek (AB), which also had the greatest number of septic parcels touching the riparian AOI. Poorly designed or malfunctioning septic tanks may be nitrate sources, which stimulated GPP (Wakida and Lerner, 2005; Kaushal et al., 2011). It is possible, however, that other sources of nitrate pollution from the urban areas along this creek may also have contributed to high GPP.

When the data for AB were removed, there was still a significant difference in nitrate, P/R, and GPP levels between developed and undeveloped sites and significant correlations between nitrate and both P/R and GPP. Because GPP, P/R, and nitrate concentrations were related indicators of total urban area and the amount of irrigated grass area near the stream, there are likely other sources of urban nitrate pollution, other than septic fields, that drive GPP and P/R across the study sites. Although phosphate concentrations were not clearly related to GPP in this study, and phosphate concentrations were not related to the number of septic parcels, prior studies indicate that septic fields may contribute both phosphorus and nitrogen to streams (Hoare, 1984; Gerritse et al., 1995).

Although not identified as a key factor in this study, light availability is often one of the key factors controlling algal growth (Hill, 1996). Urban development is often expected to reduce or remove riparian vegetation, thus increasing light availability, but human impacts on riparian vegetation can vary (Cooper et al., 2013). Urban encroachment into the riparian zone may alter the amount or species composition of vegetation, whereas channelization or channel hardening can reduce or eliminate riparian vegetation (Walsh et al., 2005). Several studies have demonstrated a connection between increased light availability and higher GPP rates with urbanization (Beaulieu et al., 2013; Bernot et al., 2010; Mulholland et al., 2001). In this study, light levels were similar across sites and were not related to GPP rates, with the site (AT) with the greatest light availability and least canopy cover (AT) being different from the site with the highest GPP rates (AB). This suggests that these streams are not affected or affected equally by light limitation, so variation in metabolic parameters may be driven by N availability.

The significant relationships of CR, P/R, and NEP with principal component 4 in the regression analysis suggest that temperature may play a role in stream metabolism in the area, although it may not be a primary metabolic driver in these streams. Both cellular and ecosystem respiration are expected to increase with increasing temperature (Gillooly et al., 2001; Allen et al., 2005; Yvon-Durocher et al., 2012). Several studies have demonstrated a relationship between temperature and CR rates (e.g. Bernot et al., 2010), but this relationship is not always evident (Young and Huryn, 1999; Mulholland et al., 2001; Roberts et al., 2007). Temperature is considered one of the primary drivers of CR, but the relationship between CR and temperature in the PCA regression analysis is the opposite of what would be expected, with increased temperatures associated with decreased CR. This may be an elevation effect because CR was higher at high than low elevation sites, but temperature was higher at low than high elevation sites.

The positive relationship between temperature and P/R or NEP is more in line with expectations. Water temperatures are generally expected to increase with urbanization (Walsh et al., 2005), but few studies demonstrate this relationship (see examples in Pluhowski, 1970; Kaushal et al, 2010), and examples in Medtiterranean streams are even rarer. Water temperature metrics in this study were related to both land use and elevation, with higher temperatures at low elevation, developed sites and with lower temperatures at higher elevation, undeveloped sites. Increased temperatures can stimulate algal growth directly and indirectly, depending on the species, as well as increase GPP responses to increasing PAR levels (Denicola, 1996; Beaulieau et al 2013). Evidence of increased growth rates in green algae was observed in streams in the study area after riparian removal by fires led to increased stream temperatures (Klose et al., 2015).

Organic matter levels also are expected to affect CR rates. The link between organic matter levels and CR rates may be especially strong in urban areas due to anthropogenic sources of DOC and POC, such as organic carbon inputs from septic systems, lawn and impervious surface runoff, and wastewater treatment plants (Beaulieu et al., 2013; Paul and Meyer, 2001, Walsh et al., 2005). Also, in areas where urbanization promotes algal blooms, DOC may increase owing to the increased production of algal exudates. Kaplan and Bott (1982), for example, observed diel changes in DOC due to algal exudates, accounting for up to 20% of total DOC export. Urbanization can also affect POC inputs and it is well-known that inputs of one form of POC, i.e. leaf litter, can increase CR rates (Acuña et al., 2004). Urban inputs of DOC and POC provide substrates for microbial growth with subsequent effects on CR rates (Uehlinger et al., 2000; Uehlinger, 2006).

Because there were no wastewater treatment plants in the study catchments, there were probably diffuse sources of organic contamination, such as septic systems, sewer leaks, or fecal runoff from streets, to the study streams. The results of this study demonstrate increases in DOC with increased urban cover and higher BOM at lower elevation, low gradient sites, where most of the developed sites were located. However, CR rates were not found to be correlated to either DOC or BOM. This suggests that either organic matter availability was not a primary driver of CR across the study streams, or that the POC and BOM variables measured do not adequately characterize the labile portion of the organic matter pool, which may be relatively small (Mayorga et al., 2005). A study in Switzerland over 15 years showed a decrease in CR with decreasing loads of wastewater treatment plant effluent, but overall DOC did not change, suggesting that overall DOC was not a good measure of the DOC pool being used by microbes (Uehlinger, 2006). Although a

relationship between CR rates and temperature or organic carbon levels was not found, this may be owed to the complex interaction among factors driving CR rates (Yvon-Durocher et al., 2012; Beaulieu et al., 2013; Walsh et al., 2005).

Because indices of stream autotrophy (NEP, P/R) are based on GPP and CR, similar considerations can apply to the explanation of the NEP and P/R results. Although the regression analyses produced tighter relationships between P/R and environmental principal components than between GPP or CR and principal components, it would be difficult to determine if primarily GPP or CR were driving P/R if P/R results were presented alone. In this study, P/R appeared to be driven primarily by GPP, whereas NEP showed similarities to different aspects of the CR and GPP results.

3.5.5. Effects of land use on stream metabolism

Conclusions about the influence of land use change on stream metabolism have ranged from those finding no relationship (Meyer et al., 2005; von Schiller et al., 2008) to those that found that metabolism was sensitive to land use patterns (Clapcott et al., 2010; Bernot et al., 2010). A number of authors have found stream metabolism to be sensitive to local riparian conditions (light availability) as opposed to the availability of nutrients, but some have found that riparian conditions are not necessarily related to catchment urbanization (von Schiller et al., 2008). A study in central Japan (Iwata et al., 2007) reported that urban streams were more autotrophic (higher GPP/CR) than other streams, including agricultural streams, which they attributed to higher organic matter loading (higher CR) in agricultural streams and lower organic carbon inputs (lower CR) to urban streams due to wastewater treatment practices. Both von Schiller et al. (2008) and Iwata et al. (2007) studied streams

that were affected by both agricultural and urban activity, making it difficult to disentangle the effects of different land uses on stream metabolism, as noted by Clapcott et al. (2010).

In a large inter-biome study of stream metabolism and land use in the United States, Bernot et al. (2010) found that GPP was elevated in streams with substantial urban or agricultural development in their drainage basins compared to reference streams across multiple biomes, but that a land use effect on CR was not apparent. A study in a tropical system found that urban riparian land use affected CR rates through nitrogen enrichment, even at low levels of urban cover (Silva-Junior et al., 2014). Clapcott et al. (2010) reported that GPP and CR were more strongly related to native vegetation removal than to impervious cover. The authors also argued that other studies of stream metabolism responses to land use did not consider a broad enough land use gradient or large enough datasets. In general, studies of stream metabolism in urban areas have been inconsistent in method and purpose, which may have contributed to inconsistencies in observed stream metabolic responses to urbanization.

Another potential reason for inconsistencies may be that common proportional measures of urban land cover or impervious cover (% impervious cover) may not approximate the key drivers of stream GPP and CR in all systems. In this study, metabolism parameters and nitrate were not related to per cent urban cover, but were related to total urban area, which is probably related to the total mass of nitrogen exported from the landscape to streams. Differences in the primary drivers of metabolism across regions may result in relationships with per cent land use cover in some areas but not others. For example, nitrogen limitation is common in algal communities in this study region (Klose et al., 2012, Nelson et al., 2013), but if light is a limiting factor in a different region, then the relationship between

metabolism and urban indicators may differ from this study based on the local relationship between urbanization and riparian cover. Analysis of the effects of urban development on stream metabolism is complicated because multiple urban characteristics may be related to each other, confounding the clarity or interpretation of relationships between stream metabolism and urban population or land use variables. More explicit information about urban structures and activities, and their effects on stream ecosystems, may allow us to better disentangle the direct and indirect effects of urban features and processes on streams. Further, a better understanding of the mechanistic pathways whereby urbanization affects stream processes may allow the construction of better models of urban-stream interactions, providing more robust predictions of urbanization effects on a variety of streams.

Some past studies have incorporated alternative measures of urban development (e.g., human population densities) or have examined the influence of specific features in the urban landscape on streams (e.g., wastewater outfalls). In a study of 19 streams in NE Spain, the authors divided their study sites into groups using nutrient and chlorophyll criteria, as well as population density (Izagirre et al., 2008). They found lower rates of GPP in eutrophic streams with high human populations densities than in eutrophic streams with low human densities. In a different approach, Aristi et al. (2015) found that both GPP and CR increased below a treated wastewater effluent point source. Other studies have specifically measured metabolism in streams with significant underground piped flows, a common occurrence in urban streams (Hope et al., 2014; Pennino et al., 2014). Viewed together, studies that focus on specific urban processes or characteristics rather than just impervious cover may contribute to a broader understanding of the complexities of the effects of urbanization on streams.

Another limitation of previous studies examining stream metabolism and land use is that many rely on one-time stream metabolism measurements over one or a few days. Owing to advances in sensor technology and data processing methods, more stream studies are using continuous sensors to monitor metabolic rates frequently through time to identify specific controls on metabolic rates. Studies of single urban streams through time (e.g., Beaulieu et al. 2013) have provided insights into factors controlling changes in metabolism, but the results have limited applicability to other systems and times and do not allow evaluations of land use influences. Simultaneous measurements of metabolism in many streams through time, a strategy applied in Izagirre et al. (2008), allows the evaluation of stream metabolism, and potential drivers, in individual systems through time and of the influence of land use patterns across multiple streams. Although the work described here was at a more limited spatial and temporal scale than the Izagirre et al. (2008) study, the strategy of collecting metabolism data through time allowed for patterns to emerge in the time-averaged data that were obscured by short-term events in individual deployments. This thesis work and the Izagirre et al. (2008) study provide a better assessment of stream metabolic responses through both time and across land uses, providing a large improvement over studies that based comparisons on a single or limited number of days or sites.

Ultimately, it will be necessary to have a much larger number of study locations and catchments, each with detailed information on ambient environmental conditions, landscape development, and specific human activities, to draw more definitive conclusions regarding land use effects on stream ecosystems. Although such information is beyond the scope of this study, this study does provide information on the effects of urban land use on stream

metabolism, as well as possible mechanisms for these effects, acting as a foundation for future, more comprehensive studies.

3.6. References

Acuña, V., A. Giorgi, I. Muñoz, U. Uehlinger, and S. Sabater. 2004. Flow extremes and benthic organic matter shape the metabolism of a headwater Mediterranean stream. Freshwater Biology 49: 960-971.

Acuña, V., I. Muñoz, A. Giorgi, M. Omella, F. Sabater, and S. Sabater. 2005. Drought and postdrought recovery cycles in an intermittent Mediterranean stream: structural and functional aspects. Journal of the North American Benthological Society 24: 919-933.

Allan, J.D. 2004. Landscapes and riverscapes: The influence of land use on stream ecosystems. Annual Review of Ecology, Evolution, and Systematics 35: 257-284.

Allen, A.P., J.F. Gillooly, and J.H. Brown. 2005. Linking the global carbon cycle to individual metabolism. Functional Ecology 19: 202-213.

Aristi, I., M. Arroita, A. Larrañaga, L. Ponsatí, S. Sabater, D. von Schiller, A. Elosegi, and V. Acuña. 2014. Flow regulation by dams affects ecosystem metabolism in Mediterranean rivers. Freshwater Biology 59: 1816-1829.

Aristi, I., D. von Schiller, M. Arroita, D. Barceló, L. Ponsatí, M.J. García-Galán, S. Sabater, A. Elosegi, and V. Acuña. 2015. Mixed effects of effluents from wastewater treatment plants on river ecosystem metabolism: subsidy or stress? Freshwater Biology 60: 1398-1410.

Alonzo, M., Bookhagen, B., McFadden, J.P., Sun, A., and Roberts, D.A. 2015. Mapping urban forest leaf area index with airborne lidar using penetration metrics and allometry. Remote Sensing of Environment, 162: 141-153.

APHA, 2012a, Method 2540 D. Total Suspended Solids Dried at 103-105°C. Standard Methods for the Examination of Water and Wastewater (22nd Ed.). American Public Health Association, Washington, DC. 2-66.

APHA, 2012b. Method 2540 E. Fixed and Volatile Solids Ignited at 550°C. Standard Methods for the Examination of Water and Wastewater (22nd Ed.). American Public Health Association, Washington, DC. 2-67.

APHA, 2012c. Method 10200 H. Chlorophyll. Standard Methods for the Examination of Water and Wastewater (22nd Ed.). American Public Health Association, Washington, D.C. 10-22 – 10-30.

Beaulieu, J.J., C.P. Arango, D.A. Balz, and W.D. Shuster. 2013. Continuous monitoring reveals multiple controls on ecosystem metabolism in a suburban stream. Freshwater Biology 58: 918-937.

Bernot, M.J., D.J. Sobota, O. Hall Jr., P.J. Mulholland, W.K. Dodds, J.R. Webster, J.L. Tank, L.R. Ashkenas, L.W. Cooper, C.N. Dahm, S.V. Gregory, N.B. Grimm, S.K. Hamilton, S.L. Johnson, W.H. McDowell, J.L. Meyer, B. Peterson, G.C. Poole, H.M. Valett, C. Arango, J.J. Beaulieu, A.J. Burgin, C. Crenshaw, A.M. Helton, L. Johnson, J. Merriam, B.R. Niederleehner, J.M. O'Brien, J.D. Potter, R.W. Sheibley, S.M. Thomas, and K. Wilson. 2010. Inter-regional comparison of land-use effects on stream metabolism. Freshwater Biology 55:1874-1890.

Borchard, M.A. 1996. Nutrients. Pages 183-227 in R.J. Stevenson, M.L. Bothwell, and R.L. Lowe (Eds.) Algal Ecology. Academic Press, San Diego.

Bott, T.L., D.S. Montgomery, J.D. Newbold, D.B. Arscott, C.L. Dow, A.K. Aufdenkampe, J.K. Jackson, and L.A. Kaplan. 2006a. Ecosystem metabolism in streams of the Catskill

Mountains (Deleware and Hudson River watersheds) and Lower Hudson Valley. Journal of the North American Benthological Society 25:1018-1044.
Bott, T.L. 2006b. Primary Productivity and Community Respiration. Pages 663-690 in F.R. Hauer and G.A. Lamberti (Eds.) Methods in Stream Ecology, 2nd ed. Academic Press, San Diego.
Carignan, K.S., L.A. Taylor, B.W. Eakins, R.R. Warnken, E. Lim, and P.R. Medley, 2009. Digital Elevation Model of Santa Barbara, California: Procedures, Data Sources and Analysis, NOAA Technical Memorandum NESDIS NGDC-29, U.S. Dept. of Commerce, Boulder, CO, 30 pp. Accessed May 5, 2015. http://www.ngdc.noaa.gov/dem/squareCellGrid/download/603
Carlson, C.A., D.A. Hansell, N.B. Nelson, D.A. Siegel,W.M. Smethie, S. Khatiwala, M.M. Meyers, and E. Halewood. 2010. Dissolved organic carbon export and subsequent remineralization in the mesopelagic and bathypelagic realms of the North Atlantic basin. Deep-Sea Res. II, 57:1433-1445.
Chapman, L. 2007. Potential applications of near infra-red hemispherical imagery in forest environments. Agricultural and Forest Meteorology, 143:151–156.
Chapra, S.C. and D.M. Di Toro. 1991. Delta method for estimating primary production, respiration, and reaeration in streams. Journal of Environmental Engineering 117: 640-655.
Chow, V.T. 1959. Open channel hydraulics. McGraw-Hill Kogakusha Ltd., Tokyo.
Clapcott J.E., R.G. Young, E.O. Goodwin, and J.R. Leathwick. 2010. Exploring the response of functional indicators of stream health to land-use gradients. Freshwater Biology 55: 2181-2199.
Cooper, S.D., P.S. Lake, S. Sabater, J.M. Melack, and J.L. Sabo. 2013. The effects of land use changes on streams and rivers in Mediterranean climates. Hydrobiologia 719:383-425.
County of Santa Barbara, Department of Public Works Water Resources Hydrology. June 1, 2016a. Historical driest four consecutive years. Accessed June 9, 2016. http://www.countyofsb.org/uploadedFiles/pwd/Content/Water/Documents/Historical%20Driest%20Four%20Consecutive%20Years.pdf
County of Santa Barbara, Department of Public Works Water Resources Hydrology. June 1, 2016b. Historical Rainfall Information – Daily Rainfall XLS, station 234. Accessed June 9, 2016. http://www.countyofsb.org/pwd/dailyrainfall.sbc
Davies, A.L. and J.H.R. Gee. 1993. A simple periphyton sampler for algal biomass estimates in streams. Freshwater Biology 30: 47-51.
Denicola, D.M. 1996. Periphyton response to temperature at different ecological levels. Pages 149-181 in R.J. Stevenson, M.L. Bothwell, and R.L. Lowe (Eds.) Algal Ecology. Academic Press, San Diego.
Dodds, W.K., K. Gido, M.R. Whiles, M.D. Daniels, and B.P. Grudzinski. 2015. The Stream Biome Gradient Concept: factors controlling lotic systems across broad biogeographic scales. Freshwater Science, 34: 1-19.
Elmore, H.L., and W.F. West. 1961. Effect of water temperature on stream reaeration. Journal of the Sanitary Engineering Division, 87(SA6):59-71.
Emerson, S. 1975. Gas exchange in small Canadian Shield lakes. Limnology and Oceanography, 20: 754-761.

Felipe, A.F., J.E. Lawrence, and N. Bonada. 2013. Vulnerability of stream biota to climate change in mediterranean climate regions: a synthesis of ecological responses and conservation challenges. Hydrobiologia 719: 331-352.
Gerritse, R.G., J.A. Adeney, G.M. Dommock, and Y.M. Oliver. 1995. Retention of nitrate and phosphate in soils of the Darling Plateau in Western Australia: implications for domestic septic tank systems. Australian Journal of Soil Research 33: 353-367.
Gillooly, J.F., J.H. Brown, G.B. West, V.M. Savage, and E.L. Charnov. 2001. Effects of size and temperature on metabolic rate. Science 293: 2248-2251.
Goodridge, B.M. and J.M. Melack. 2012. Land use control of stream nitrate concentration in mountainous coastal California watersheds. Journal of Geophysical Research 117: G02005, doi: 10.1029/2011JG001833.
Grace, M.R. and S.J. Imberger. 2006. Stream Metabolism: Performing & Interpreting Measurements. Water Studies Centre Monash University, Murray Darling Basin Commission and New South Wales Department of Environment and Climate Change. 204 pp. Accessed at http://www.sci.monash.edu.au/wsc/docs/tech-manual-v3.pdf
Grasshoff, K. 1976. Methods of Seawater Analysis, Verlag Chemie, New York, New York.
Hill, W.R. 1996. Effects of light. Pages 121-148 in R.J. Stevenson, M.L. Bothwell, and R.L. Lowe (Eds.) Algal Ecology. Academic Press, San Diego.
Hoare, R.A. 1984. Nitrogen and phosphorus in Rotorua urban streams. New Zealand Journal of Marine and Freshwater Research 18: 451-454.
Hope, A.J., W.H. McDowell, and W.M. Wollheim. 2014. Ecosystem metabolism and nutrient uptake in an urban piped headwater stream. Biogeochemistry 121: 167-187.
Iwata, T., T. Takahashi, F. Kazama, Y. Hiraga, N. Fukuda, M. Honda, Y. Kimura, K. Kota, D. Kubota, S. Nakagawa, T. Nakamura, M. Shimura, S. Yanagida, L. Xeu, E. Fukasawa, Y. Hirasuka, T. Ikebe, N. Ikeno, A. Kohno, K. Kubota, K. Kuwata, T. Misonou, Y. Osada, Y. Sato, R. Shimizu, and K. Shindo. 2007. Metabolic balance of streams draining urban and agricultural watersheds in central Japan. Limnology 8: 243-250.
Izagirre, O., U. Agirre, M. Bermejo, J. Pozo, and A. Elosegi. 2008. Environmental controls of whole-stream metabolism identified from continuous monitoring of Basque streams. Journal of the North American Benthological Society 27: 252-268.
Jonckheere, I., S. Fleck, K. Nackaerts, B. Muys, P. Coppin, and M. Weiss. 2004. Review of methods for in situ leaf area index determination. Agricultural and Forest Meteorology, 121: 19–35.
Kaplan, L.A, and T.L. Bott. 1982. Diel fluctuations of DOC generated by algae in a piedmont stream. Limnology and Oceanography 27: 1091-1100.
Kaushal S.S., G.E. Likens, N.A. Jaworski, M.L. Pace, A.M. Sides, D. Seekell, K.T. Belt, D.H. Secor, and R.L. Wingate. 2010. Rising stream and river temperatures in the United States. Frontiers in Ecology and the Environment 8: 461-466.
Kaushal, S.S., P.M. Groffman, L.E. Band, E.M. Elliott, C.A. Shields, and C. Kendall. 2011. Tracking nonpoint source nitrogen pollution in human-impacted watersheds. Environmental Science and Technology 45: 8225-8232.
Klose, K., S.D. Cooper, A.D. Leydecker, and J. Kreitler. 2012. Relationships among catchment land use and concentrations of nutrients, algae, and dissolved oxygen in a southern California river. Freshwater Science 31: 908-927.

Klose, K., S.D. Cooper, and D. Bennett. 2015. Effects of wildfire on stream algal abundance, community structure, and nutrient limitation. Freshwater Science 34: 1494-1509.
Lachat Instruments Inc. 1995. Ammonia in surface water, wastewater (gas diffusion): Method 10-107-06-5-A. Milwaukee, WI.
Lachat Instruments Inc. 1996. Nitrate/Nitrite, nitrite in surface water, wastewater: Method 31-107-04-1-C, Milwaukee, WI.
Lachat Instruments Inc. 1996b. Phosphate in brackish water or seawater: Method 31-115-01-3-A.
Lamberti, G.A. and A.D. Steinman. 1997. A comparison of primary production in stream ecosystems. Journal of the North American Benthological Society 16: 95-104.
Langø, T., T. Mørland, and A.O. Brubakk. 1996. Diffusion coefficients and solubility coefficients for gases in biological fluids and tissues: A review. Undersea and Hyperbaric Medicine, 23: 247-272.
Lee, J.H., and K.W. Bang. 2000. Characterisation of urban stormwater runoff. Water Research 34: 1773-1780.
Lewis, W.K., and W.C. Whitman. 1924. Principles of gas adsorption. Industrial and Engineering Chemistry, 17:1215-1220.
Mayorga, E., A.K. Aufdenkampe, C.A. Masiello, A.V. Krusche, J.I. Hedges, P.D. Quay, J.E. Richey, and T.A. Brown. 2005. Young organic matter as a source of carbon dioxide outgassing from Amazonian rivers. Nature 436: 538 – 541.
Meyer, J.L., M.J. Paul, and W.K. Taulbee. 2005. Stream ecosystem function in urbanizing landscapes. Journal of the North American Benthological Society 24: 602-612.
Monteith, J.L. and M.H. Unsworth. 2008. Environmental Physics, 3rd ed. Academic Press, Amsterdam.
Mulholland, P.J., C.S Fellows, J.L. Tank, N.B. Grimm, J.R. Webster, S.K. Hamilton, E. Marti, L. Ashkenas, W.B. Bowden, W.K. Dodds, W.H. McDowell, M.J. Paul, and B.J. Peterson. 2001. Inter-biome comparison of factors controlling stream metabolism. Freshwater Biology 46: 1503-1517.
Nelson, C.E., D.M. Bennett, and B.J. Cardinale. 2013. Consistency and sensitivity of stream periphyton community structural and functional responses to nutrient enrichment. Ecological Applications 23: 159-173.
Ode, P.R. 2007. Standard operating procedures for collecting macroinvertebrate samples and associated physical and chemical data for ambient bioassessments in California. California State Water Resources Control Board Surface Water Ambient Monitoring Program (SWAMP) Bioassessment SOP 001.
Odum, H.T. 1956. Primary production in flowing waters. Limnology and Oceanography 1: 102-117.
Osborne, L.L., and M.J. Wiley. 1988. Empirical relationships between land use/cover and stream water quality in an agricultural watershed. Journal of Environmental Management 26: 9-27.
Osmond, P. 2009. Application of near-infrared hemispherical photography to estimate leaf area index of urban vegetation. International conference on urban climate, 29 June-3 July, 2009, Yokohama, Japan. pp. 1–4.
Paul, M.J., and J.L. Meyer. 2001. Streams in the urban landscape. Annual Review of Ecology and Systematics 32: 333-365.

Pennino, M.J., S.S. Kaushal, J.J. Beaulieu, P.M. Mayer, and C.P. Arango. 2014. Effects of urban stream burial on nitrogen uptake and ecosystem metabolism: implications for watershed nitrogen and carbon fluxes. Biogeochemistry 121: 247-269.

Pluhowski, E.J. 1970. Urbanization and its effect on the temperature of streams in Long Island, New York. USGS Professional Paper 627–D

Raymond, P.A., C.J. Zappa, D. Butman, T.L. Bott, J. Potter, P.J. Mulholland, A.E. Laursen, W.H. McDowell, and D. Newbold. 2012. Scaling the gas transfer velocity and hydraulic geometry in streams and small rivers. Limonology and Oceanography, Fluids & Environments, 2:41-53, doi: 10.1215/21573689-1597669.

Roberts, B.J., P.J. Mulholland, and W.R. Hill. 2007. Multiple scales of temporal variability in ecosystem metabolism rates: results from 2 years of continuous monitoring in a forested headwater system. Ecosystems 10: 588-606.

Silva-Junior E.F., T.P. Moulton, I.G. Boëchat, and Björn Gücker. 2014. Leaf decomposition and ecosystem metabolism as functional indicators of land use impacts on tropical streams. Ecological Indicators 36: 195-204.

Steinman, A.D., G.A. Lamberti, and P.R. Leavitt. 2006. Biomass and Pigments of Benthic Algae. Pages 357-380 in F.R. Hauer and G.A. Lamberti (Eds.) Methods in Stream Ecology, 2nd ed. Academic Press, San Diego.

Uehlinger, U., and M.W. Naegeli. 1998. Ecosystem metabolism, disturbance, and stability in a prealpine gravel bed river. Journal of the North American Benthological Society 17: 165-178.

Uehlinger, U., C. König, and P. Reichert. 2000. Variability of photosynthesis-irradiance curves and ecosystem respiration in a small river. Freshwater Biology 44: 493-507.

Uehlinger, U. 2006. Annual cycle and inter-annual variability of gross primary production and ecosystem respiration in a floodprone river during a 15-year period. Freshwater Biology 51: 938-950.

USEPA. 1983. Nitrogen, Nitrate-Nitrite. Method 353.2 (Colorimetric, Automated, Cadmium Reduction). Methods for Chemical Analysis of Water and Wastes, (EPA-600/ 4-79-020): 353-2.1 – 353-2.5.

USGS. 2013. DOTABLES: Dissolved oxygen solubility tables, Version 3.5. Generated online on 10/24/2013. Available at http://water/usgs.gov/software/DOTABLES.

Vannote, R.L., G.W. Minshall, K.W. Cummins, J.R. Sedell, and C.E. Cushing. 1980. The river continuum concept. Canadian Journal of Fisheries and Aquatic Sciences 37: 130-137.

von Schiller, D., E. Marti, J.L. Riera, M. Ribot, J.C. Marks, and F. Sabater. 2008. Influence of land use on stream ecosystem function in a Mediterranean catchment. Freshwater Biology 53: 2600-2612.

Wakida, F.T., and D.N. Lerner. 2005. Non-agricultural sources of groundwater nitrate: a review and case study. Water Research 39: 3-16.

Walsh, C.J., A.H. Roy, J.W. Feminella, P.D. Cottingham, P.M. Groffman, and R.P. Morgan II. 2005. The urban stream syndrome: current knowledge and the search for a cure. Journal of the North American Benthological Society 24: 706-723.

Willason, S. W. and K.S. Johnson. 1986. A rapid, highly sensitive technique for the determination of ammonia in seawater. Marine Biology, 91: 285-290.

Young, R.G. and A.D. Huryn. 1999. Effects of land use on stream metabolism and organic matter turnover. Ecological Applications 9: 1359-1376.

Yvon-Durocher, G., J.M. Caffrey, A. Cescatti, M. Dossena, P. del Giorgio, J.M. Gasol, J.M. Montoya, J. Pumpanen, P.A. Staehr, M. Trimmer, G. Woodward, and A.P. Allen. 2012. Reconciling the temperature dependence of respiration across timescales and ecosystem types. Nature 487: 472-476.

Zappa, C.J., W.R. McGillis, P.A. Raymond, J.B. Edson, E.J. Hintsa, H.J. Zemmelink, J.W.H. Dacey, and D.T. Ho. 2007. Environmental turbulent mixing controls on air-water gas exchange in marine and aquatic systems. Geophysical Research Letters, 34: L10601, doi: 10.1029/2006GL028790.

4. Thermal characteristics and urban warming in Santa Barbara streams

4.1. Introduction

Temperature affects many chemical and biological processes in stream ecosystems. Temperature affects oxygen dynamics, chemical toxicity, cellular and ecosystem metabolism, and the diversity and community structure of organisms (Benson and Krause, 1980; Cairns et al., 1975; Gillooly et al., 2001; Demars et al., 2011; Hawkins et al., 1997). Heat fluxes that influence temperature, such as solar radiation, evaporation and condensation, bed conduction, sensible heat transfer with the atmosphere, friction, and advection from upstream or adjacent water bodies (Webb, 1996) make temperature sensitive to some land use changes, such as hydrological alterations and riparian canopy loss. Previous studies have found increased stream temperatures due to land use changes, particularly urbanization (Pluhowski et al., 1970; Galli, 1990), but there is limited information about stream temperature dynamics in urban areas with Mediterranean climates.

Although stream temperatures can change rapidly through time, many ecological studies continue to measure temperature at specific points in time, limiting the availability of long-term, high frequency temperature records, which are necessary to understand long-term patterns in temperature and the effects of changes in temperature at all temporal scales on biological processes (Arismendi et al, 2012). As climate changes, it is critical to characterize thermal regimes in streams through both time and space, especially in regions where the interactions of climate and land use change are expected to have a significant impact on stream ecosystems, such as regions with Mediterranean climates (Felipe et al., 2013; Cooper

et al., 2013). In Santa Barbara, California, specifically, water temperature data are also important because studies in nearby streams have recorded water temperatures exceeding the thermal tolerances of the southern California steelhead trout *(Oncorhynchus mykiss)*, a native, federally-listed, anadromous fish that is the focus of many conservation and management efforts (Matthews and Berg, 1997; Sloat and Osterback, 2013).

My research has 3 objectives: (1) to describe spatial and temporal variation in the thermal characteristics of Santa Barbara streams, (2) to assess whether water temperature is likely to limit the distribution of the southern California steelhead trout in Santa Barbara streams, and (3) to assess whether agricultural and urban development affect temperatures in Santa Barbara streams. I expected that temperatures would be elevated to levels dangerous to steelhead trout in some but not all of the streams and that locations in urban areas would have temperatures higher than those in undeveloped or agricultural areas, particularly during the daytime.

To address my objectives and evaluate these expectations, I examined water temperature data from 21 streams in Santa Barbara County, CA, USA, with varying urban and agricultural land use, collected between 2001 and 2015 and ranging in duration across sites from 2 to 14 years. Water temperatures were assessed using 5-minute, daily, and seasonal values, both regionally and at individual sites, to address the first objectives. The occurrence of temperatures exceeding 25°C, associated with significant steelhead mortality (Myrick and Cech, 2001), was assessed for each site to address the second objective. To address the third objective, a comparative design was used to determine if sites in basins with agricultural or urban development had higher temperatures than those in undeveloped areas. I also examined other important potential sources of stream thermal variability in the region,

including wild fires and rainfall patterns, and explored the implications of the results for the effects of projected changes in climate on streams.

4.2. Description of study sites and water temperature data

As part of the SBC-LTER project, which began in 2001, temperature data were collected at 21 locations across 14 separate watersheds, each of which drains to the Santa Barbara Channel (Figure 15). Water level pressure transducers (Solonist LevelLogger, various models, ±0.1°C sensor accuracy, 0.1°C sensor resolution, -20°C to 80°C operating range) at each monitored site recorded water temperatures at 5-minute intervals. This analysis used data from the 2002-2015 water years (each water year runs from October 1st to September 30th). The duration and timing of data collection were not consistent across sites (Table 24), but each site used in these analyses had data from at least two water years, albeit with some data gaps, especially for sites with short records. Data collection was discontinued at some of the sites during the study period due to frequent or prolonged drying, which is common in this region. Rainfall was variable during the study period, which included both dry and wet years. Based on the rainfall record in downtown Santa Barbara (County of Santa Barbara, 2017a), spanning 1900-2017, annual rainfall in 2007 was the lowest recorded whereas annual rainfall in 2005 was in the 95th percentile for the historical record (Table 24). The last 4 years of the study period occurred during a prolonged regional drought, which lasted from 2012 to 2016 and included the driest 5 consecutive years on record in the Santa Barbara area (County of Santa Barbara, 2017b).

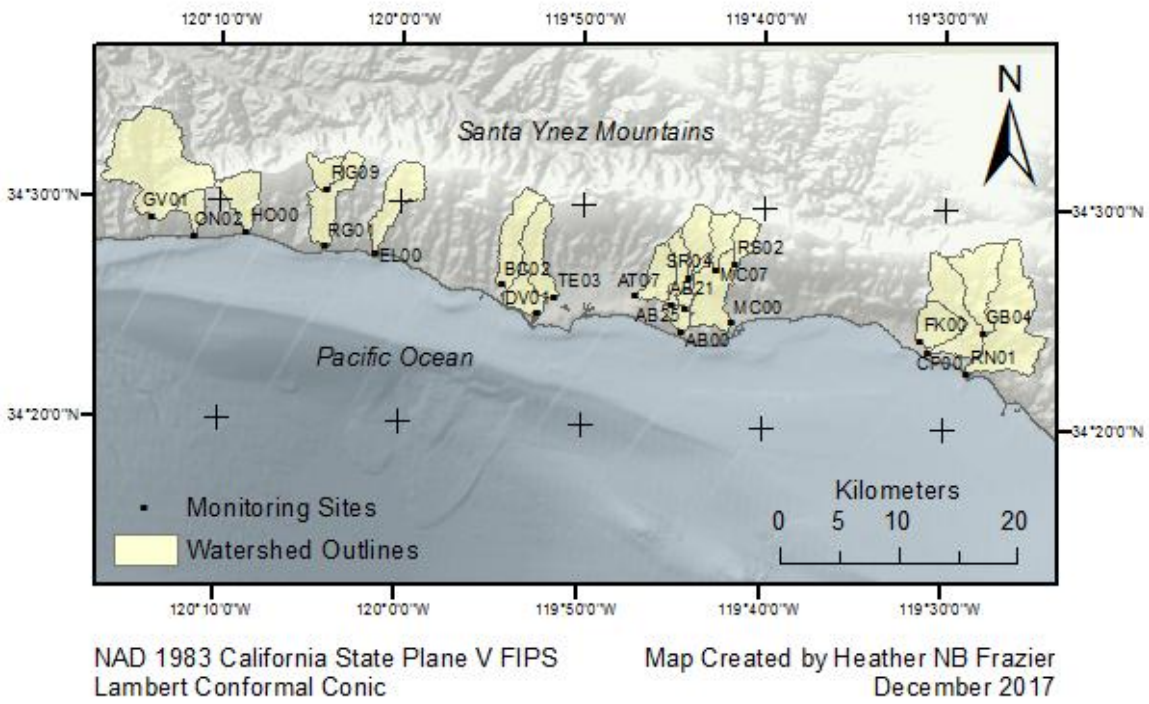

Figure 15: Temperature monitoring sites

Table 24: Water temperature data collection sites and data availability. Sites with data in a given year are marked with 'X'. The annual rainfall percentile is provided for each water year, based on the 1900-2017 record in downtown Santa Barbara (County of Santa Barbara, 2017a). Years during which wild fire occurred in the study area and sites downstream from those fires are marked with an asterisk.

Watershed	Site ID	Water year													
		2002	2003	2004*	2005	2006	2007	2008*	2009*	2010	2011	2012	2013	2014	2015
		Annual rainfall percentile													
		6	82	13	95	74	0	57	21	67	88	17	5	2	11
Arroyo Burro	SR04		X	X	X				*						
	AB21	X	X	X					*						
	AB25	X	X												
	AB00	X	X	X	X	X	X	X	X*	X	X	X	X	X	X
Arroyo Hondo	HO00	X	X	X*	X	X	X		X	X	X	X	X	X	X
Atascadero	AT07			X	X	X	X	X	X*	X					
Bell Canyon	BC02				X	X	X	X*	X	X	X	X	X	X	X
Carpinteria	GB04	X	X												
	CP00	X	X	X	X	X	X	X	X						
Devereux	DV01			X	X	X	X								
El Capitan	EL00	X	X	X	X	X	X	X							
Franklin	FK00	X	X	X	X	X	X	X							
Gaviota	GV01	X	X	X*	X	X	X	X	X	X	X	X	X	X	X
Mission	RS02	X	X	X	X	X	X	X*	X*	X	X	X	X	X	X
	MC07	X	X	X	X				*						
	MC00	X	X	X	X	X	X	X*	X*	X	X	X	X	X	X
Refugio	RG09	X	X	X											
	RG01	X	X	X	X	X	X	X	X	X	X	X	X	X	X
Rincon	RN01	X	X	X	X	X	X	X	X						
San Onofre	ON02			*	X	X	X	X	X						
Tecolotito	TE03			X	X	X		*							

The catchments draining to each temperature measurement location and the elevation of each location were extracted from a 30 m digital elevation model using ArcGIS (ESRI, Redlands, CA) (Table 25). The watershed outlines were used to measure watershed area and to extract land use cover information for each site. Urban, agricultural, and undeveloped land uses for each site were extracted from the 2004 AVIRIS classification map, described

in the study area overview. In addition, data from the AVIRIS 2011 classification map was available for ten sites (AB00, AB21, AB25, AT07, BC02, DV01, MC00, MC07, RS02, SR04), allowing the amounts of impervious cover for those watersheds to be estimated. Detailed impervious cover information was created for the Carpinteria area watersheds (CP00, FK00, GB04) in Robinson et al. (2005). These two datasets provided coverage for all the watersheds with urban development, so for this analysis the impervious cover totals from these two sources were considered the best available data and were used instead of the AVIRIS 2004 urban cover data. Land use for each site was characterized separately for each land use category by percent cover of each land use category (urban, agricultural, and undeveloped) for each watershed (Table 25). Because stream ecosystems may be altered by even low development levels (0-10%, Paul and Meyer, 2001), a site was considered urban if the percent impervious cover was >5%, a site was considered agricultural if the percent agricultural cover was >5%, and a site was considered developed if it was designated as either urban or agricultural, or both.

Table 25: Watershed and land use characteristics at each site. Sites are designated as urban (Urb) or non-urban (NUrb), as agricultural (Ag) or non-agricultural (NAg), and as developed (Dv) or undeveloped (UDv).

Site ID	Elevation (m)	Upstream area (km^2)	Impervious Cover (%)	Agricultural Cover (%)	Undeveloped Cover (%)	Urb/ NUrb	Ag/ NAg	Dv/ UDv
AB00	5	24.0	7%	8%	60%	Urb	Ag	Dv
AB21	15	18.6	7%	11%	63%	Urb	Ag	Dv
AB25	25	1.7	20%	0%	29%	Urb	NAg	Dv
AT07	15	9.6	14%	8%	43%	Urb	Ag	Dv
BC02	20	15.1	1%	20%	69%	NUrb	Ag	Dv
CP00	10	38.4	3%	8%	83%	NUrb	Ag	Dv
DV01	5	8.2	21%	6%	40%	Urb	Ag	Dv
EL00	20	16.0	0%	0%	92%	NUrb	NAg	UDv
FK00	10	11.4	29%	23%	50%	Urb	Ag	Dv
GB04	105	18.6	0%	0%	93%	NUrb	NAg	UDv
GV01	25	49.6	0%	0%	95%	NUrb	NAg	UDv
HO00	15	11.2	0%	0%	94%	NUrb	NAg	UDv
MC00	10	30.4	11%	3%	57%	Urb	NAg	Dv
MC07	185	7.3	1%	4%	83%	NUrb	NAg	UDv
ON02	10	5.3	0%	0%	98%	NUrb	NAg	UDv
RG01	15	20.8	0%	9%	85%	NUrb	Ag	Dv
RG09	155	6.2	0%	0%	96%	NUrb	NAg	UDv
RN01	15	39.7	1%	15%	77%	NUrb	Ag	Dv
RS02	275	5.8	0%	0%	87%	NUrb	NAg	UDv
SR04	75	9.6	1%	8%	81%	NUrb	Ag	UDv
TE03	5	13.9	4%	22%	63%	NUrb	Ag	Dv

Riparian canopy data were not available for all measurement locations, so a broad assessment of site characteristics, particularly the presence or absence of riparian vegetation, was conducted by viewing the location of each site in Google Earth (Google, Inc., Mountain View, CA) using imagery available throughout the study period. For each site and 100 m upstream, the presence of riparian vegetation or other shading features (e.g., highway overpass) were noted, as were other stream characteristics, such as channelization (Table 26).

Table 26: Site locations and characteristics.

Site ID	Latitude	Longitude	Seasonal Median Logger Depth (cm)				Other Site Characteristics
			W	Sp	Su	F	
AB00	34.40505027	-119.74020603	6	6	5	4	Bank vegetation present, little or no creekbed visible in Google Earth within 100 m upstream.
AB21	34.42654104	-119.75020527	8	8	6	6	Bank vegetation present, creekbed partially visible in Google Earth within 100 m upstream.
AB25	34.42277778	-119.73805556	2	3	4	7	Bank vegetation present, little or no creekbed visible in Google Earth within 100 m upstream.
AT07	34.43226376	-119.78413910	5	6	6	6	Located in concrete flood control channel, no bank vegetation and few shading features within 100 m upstream, except a bridge. Channel is clearly visible in Google Earth. No groundwater inputs expected due to concrete lining. Few stormwater outfalls obvious in immediate upstream reach.
BC02	34.43903000	-119.90566000	11	11	9	9	Bank vegetation present, thick canopy and little or no channel visible in Google earth within 100 m upstream, some creekbed visible in Google earth at attachment location.
CP00	34.39301245	-119.51412680	19	19	18	19	Bank vegetation present, creekbed partially visible in Google Earth within 100 m upstream.
DV01	34.41746000	-119.87399000	23	14	15	9	Located in wetland area with low gradient. Minimal bank vegetation present: no canopy vegetation. Pooling of water apparent, creek clearly visible in Google Earth.
EL00	34.46072662	-120.02232819	7	---	---	---	Bank vegetation present, creekbed partially visible in Google Earth within 100 m upstream.
FK00	34.40164787	-119.52144830	11	10	11	8	Located in concrete flood control channel, no bank vegetation but some bridges and channel-side trees in area 100 m upstream. No groundwater inputs expected due to concrete lining, but potential inputs from stormdrain outfalls.
GB04	34.40836434	-119.46373860	16	16	14	14	Bank vegetation present, creekbed partially visible in Google Earth within 100 m upstream.
GV01	34.48550000	-120.22916667	8	8	4	4	Bank vegetation present, but gaps in vegetation. Creekbed is visible in Google Earth within 100 m upstream.
HO00	34.47528580	-120.14121564	8	8	6	6	Located in culvert under highway. Bank vegetation present at upstream end of culvert. No creekbed is visible in Google Earth within 100m upstream from culvert. Site moved from upstream end of culvert to inside culvert in 2008.

Site ID	Latitude	Longitude	Seasonal Median Logger Depth (cm)				Other Site Characteristics
			W	Sp	Su	F	
MC00	34.41307303	-119.69499174	2	3	2	2	Multiple bridges in 100 m upstream. Cobbled creekbed with concrete sides form channel. Some channel-side trees above walls on banks. Creekbed clearly visible on Google Earth within 100 m upstream
MC07	34.45223050	-119.70931153	8	7	5	6	Bank vegetation present, no creekbed visible in Google Earth within 100 m upstream.
ON02	34.47196000	-120.18867000	3	2	9	3	Bank vegetation present, creekbed partially or fully visible in Google Earth within 100 m upstream. Sensor located at upstream end of highway culvert.
RG01	34.46573164	-120.06932215	10	11	7	8	Patches of bank vegetation present within 100 m upstream, creekbed partially or fully visible in Google Earth within 100 m upstream. Sensor located under highway overpass.
RG09	34.50944444	-120.06750000	5	2	---	4	Bank vegetation present, little or no creekbed visible in Google Earth within 100 m upstream.
RN01	34.37730000	-119.47793840	8	7	4	3	Vegetation and canopy present. Sensor located at upstream end of highway culvert. Creekbed visible in Google Earth at culvert opening, but little or no creekbed visible in Google Earth for 100m upstream.
RS02	34.45761111	-119.69222222	9	9	8	6	Bank vegetation present, creekbed partially visible in Google Earth within 100 m upstream.
SR04	34.44716151	-119.73502593	12	13	12	---	Bank vegetation present, creekbed partially visible in Google Earth within 100 m upstream.
TE03	34.43055000	-119.85762000	5	8	4	3	Bank vegetation present, creekbed partially visible in Google Earth within 100 m upstream.

Four wildfires occurred in study watersheds during the study period, the Gaviota Fire (2004), the Gap Fire (2008), the Tea Fire (2008), and the Jesusita Fire (2009). Few sites were located within the footprints of the fires, but sites within or downstream from the footprints of these fires are indicated in Table 24. Additional information related to these fires is provided in the Methods section.

4.3. Methods

4.3.1. Data preparation and considerations

Due to the challenges of collecting and managing temperature datasets over multiple years, pre-processing was required to prepare the data for analysis. All data pre-processing was completed using MATLAB (The MathWorks, Inc., Natick, MA). As necessary, Excel (Microsoft Corp., Redmond, WA) was used to prepare files for import into MATLAB. In addition to temperature data, available water level data, corrected or uncorrected, were also imported. After data were imported into MATLAB, formatting inconsistencies in timestamps were corrected and all timestamps were converted to Coordinated Universal Time (UTC), and then to local standard time (UTC-8h).

A supervised routine was used to eliminate errors from the temperature records. Data were compared to reasonable limits on water temperature for the region, with unreasonable or nonsensical data, owing to excessively cold (<0°C) or warm (>50°C) temperatures, being eliminated. In addition, given the 5-minute measurement time step, data were eliminated if a data point was greater than 1°C different from an adjacent data point, or, based on visual assessment of temperature patterns, if the average of three consecutive data points was greater than 35°C or less than 4°C. Data gaps less than 2 hours in duration were filled using linear interpolation. Finally, each record was visually inspected and additional data were removed manually to eliminate remaining errors.

Intermittent drying, particularly in the summer and early fall, and during dry years, is common in streams in the study area. Temperature data from times when stream sites were obviously dry, as determined from stage data and field notes, were eliminated. Manual water level data were collected when transducer data were downloaded, usually every 2 - 6

months. Additional manual measurements were made every 1-4 weeks, starting in 2007, when baseflow water samples were collected. Combined with field notes, the manual stage data were used to create a record of dry periods at each site, representing times when the temperature sensor was not submerged. When air pressure compensated stage data from the pressure transducers were available, these records were also used to identify and eliminate dry periods. Because transducer data were highly variable through time, the data were smoothed using a 48 hour moving average window, which prevented data from being removed at times when water levels were low but the sensor was still submerged, as indicated by the manual stage record. After dry period temperature data were removed, the result was a record of water temperature measurements at five-minute intervals over the period of monitoring for each site. The total number of observations across all sites and years varied from 23766 observations on September 30 to 42912 observations on February 24 (Figure 16).

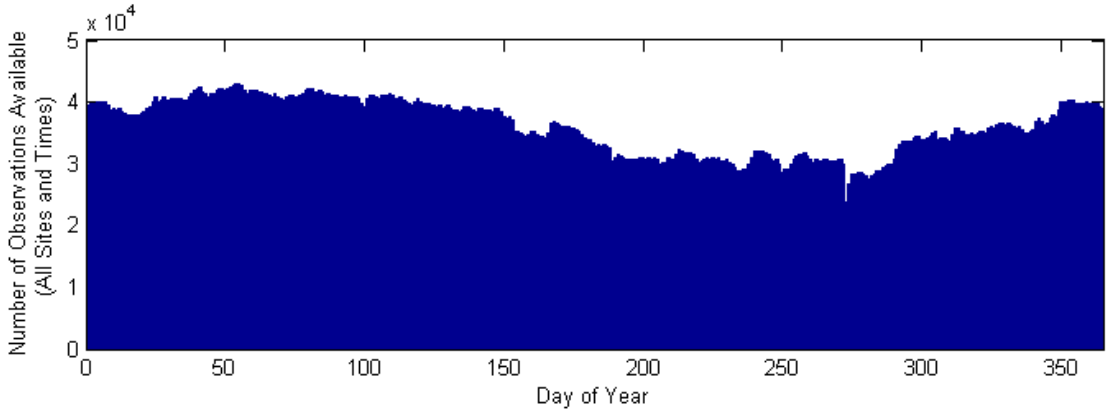

Figure 16: The availability of data for each DOY, pooling data from all sites and all years.

For each site and date (00:00 to 23:55), daily mean temperature (Dmean), daily minimum temperature (Dmin), daily maximum temperature (Dmax), and daily temperature

range (Drange = Dmax – Dmin) were calculated. To minimize the influence of missing data on the daily summary statistics, the daily summary statistics were only calculated for days that were missing 2 hours of data or less. The multi-year record of daily summary statistics was divided into individual calendar years from 2001 to 2015. Leap days were removed so that each year had 365 days and all data could be compared for the same day of the year (DOY). Data were then divided among months and seasons (winter = December – February (DJF); spring = March – May (MAM); summer = June – August (JJA); and fall = September – November (SON)). The winter season for a given calendar year included the December data from the previous calendar year so that data from consecutive winter months were grouped. If temperature data covered less than 30 days of seasonal data, those data were not used for further seasonal analysis. For each year, the seasonally grouped daily data were used to calculate a seasonal average ($\pm$ SD and CV) for each of the four daily metrics.

There were some potential problems with the temperature data. No information was available about the calibration among sensors or potential sensor drift through time, aside from what was provided by the sensor manufacturer for the sensor model series. Also, over the course of data collection, sensors were replaced with new models, so all data were considered using the manufacturer-reported accuracy for the least accurate sensor models. The placement of the sensors in streams may have resulted in direct solar heating of the sensors at some sites for parts of the day or year, which should only affect daytime data. Minimum daily temperatures, because they were collected at night, should not be influenced by this type of error. The potential for direct solar heating is more likely at sites that had limited shading, including AT07, FK00, DV01, MC00, and GV01. There are few options for correcting this kind of error or estimating the magnitude of the error resulting from this

source, so this aspect of the temperature data must be considered when interpreting the analysis results.

4.3.2. Characterization of the thermal environment

Because the annual temperature cycle was similar across the region, the data for all sites and years was combined to provide a broad description of the regional thermal environment throughout the study period. For each DOY, data from all sites and years was combined to create a full temperature record, which was summarized by finding the 5^{th} percentile, 95^{th} percentile, median, minimum, maximum, and mean temperature values for the dataset. The resulting annual patterns for each summary metric were used to demonstrate the regional thermal regime during the study period. Because there were differences in periods of data coverage among sites, direct comparisons of temperature data between sites were performed using data collected at the same time across sites.

Although the majority of site records were too short to examine long-term trends in water temperature, a subset of 9 sites had measurement periods covering at least 8 years, albeit with data gaps. These sites, with the span of water years in parentheses, were AB00 (2002-2015), BC02 (2005-2015), CP00 (2002-2009), GV01 (2002-2014), HO00 (2002-2015, missing all of 2008), MC00 (2002-2015), RG01 (2002-2015), RN01 (2002-2009), and RS02 (2002-2015). These sites spanned the east-west geographical extent of the study region and included sites from each of the land use categories, so were used to examine decadal-scale linear trends in temperature across the region. Simple linear regression models were fit to daily summary data for each of these sites to determine long-term trends in temperature and whether they varied among sites. Linear regressions were also applied to seasonal summary data for this subset of sites.

Comparison of wet and dry years

To assess whether wet years had different temperatures from dry years, seasonal temperature data were compared between a wet year, 2005, and two dry years, 2002 and 2007, using paired t-tests. Based on the historical annual rainfall record (118 years) at a rain gauge in downtown Santa Barbara, the 2005 water year was the wettest year during the study period, falling with the 95th percentile of data from the historical record (Table 24, County of Santa Barbara, 2017a). At the same rain gauge, the rainfall for four years during the study period fell below the 10th percentile of data from the historical record (Table 24). Two of these years, 2002 and 2007, allowed a comparison with 2005 data for at least 6 sites in every season. Both of these water years rank among the 5 driest years on record at rain gauges in Carpinteria (68 year record), Goleta (76 years), and San Marcos Pass (52 years) (County of Santa Barbara, 2017c). The analysis could not be repeated to include other wet years because fewer than 6 sites had data for both dry and wet years when wet years other than 2005 were considered.

Assessing the potential influence of upstream wild fire

Fire is a recurring disturbance in the Santa Barbara area that can alter stream ecosystems in similar ways as urban development, through processes such as the loss of canopy cover or changes in sediment transport and deposition (Walsh et al., 2005; Barro and Conard, 1991). During the study period, 4 fires occurred in the study area, burning portions of the basins upstream from some of the study sites. Increases in stream temperatures resulting from fire are expected to occur for streams within burn areas if riparian vegetation burned, as seen in prior studies (e.g., Cooper et al., 2015). Only two of the measurement sites fell within the burn perimeters of these fires (GV01 in the Gaviota fire and RS02 in the Tea Fire), but the

potential for changes in riparian shading, sediment transport, and stream geomorphology still may lead to downstream temperature effects.

To increase sample sizes for analysis of fire effects on stream temperature, temperature data for all 4 fires were considered together, standardizing all data relative to the timing of the fire (i.e., pre-fire and post-fire years, Table 27). For each fire, pre-fire temperatures from the two years prior to the fire were compared to temperatures in the year after the fire. At least one fire site and one non-fire site were included for each fire based on the availability of data, but the non-fire sites for the Gap and Tea fires were shared due to the similar timing of those events. The average stream temperature metric for the two pre-fire years was subtracted from the temperature metric value in the post-fire year. Two sites, MC00 and RS02, burned in both the Tea and Jesusita fires but were only assessed based on the earlier Tea fire in order to maintain consistent before-after data timing compared to the other sites during the other fires. The before-after temperature difference was calculated for all sites with upstream burning and all sites without upstream burning for each of the four fires, and mean temperature differences between sites in burned versus unburned basins were compared using one-way ANOVA.

Table 27: Description of fire events and water temperature sites used for analysis. Sites marked with an asterisk were burned in both the Tea and Jesusita fires.

Fire Name	Site ID	Fire Year	Fire/ Non-Fire	Proportion of watershed burned	Distance from fire perimeter (km)	-2 year	-1 year	+1 year
Gaviota	GV01	June 2004	F	0.04	0	2003	2004	2005
Gaviota	HO00	June 2004	F	0.44	0.6	2003	2004	2005
Gaviota	AB00	June 2004	N	---	---	2003	2004	2005
Gaviota	CP00	June 2004	N	---	---	2003	2004	2005
Gaviota	EL00	June 2004	N	---	---	2003	2004	2005
Gaviota	FK00	June 2004	N	---	---	2003	2004	2005
Gaviota	MC00	June 2004	N	---	---	2003	2004	2005
Gaviota	MC07	June 2004	N	---	---	2003	2004	2005
Gaviota	RG01	June 2004	N	---	---	2003	2004	2005
Gaviota	RN01	June 2004	N	---	---	2003	2004	2005
Gaviota	RS02	June 2004	N	---	---	2003	2004	2005
Gaviota	DV01	June 2004	N	---	---	2003	2004	2005
Gaviota	SR04	June 2004	N	---	---	2003	2004	2005
Gaviota	TE03	June 2004	N	---	---	2003	2004	2005
Gap	BC02	July 2008	F	0.56	4.1	2007	2008	2009
Gap/Tea	GV01	July 2008	N	---	---	2007	2008	2009
Gap/Tea	RG01	July 2008	N	---	---	2007	2008	2009
Gap/Tea	AT07	July 2008	N	---	---	2007	2008	2009
Tea	RS02*	November 2008	F	0.09	0.5	2007	2008	2009
Tea	MC00*	November 2008	F	0.02	8.5	2007	2008	2009
Jesusita	AB00	May 2009	F	0.47	6.3	2008	2009	2010
Jesusita	GV01	May 2009	N	---	---	2008	2009	2010
Jesusita	AT07	May 2009	F	0.23	4.2	2008	2009	2010

Assessing thermal conditions for steelhead trout

Because temperatures above 25°C are associated with significant rates of steelhead mortality (Myrick and Cech, 2001), all 5-minute data at each site were screened for measurements exceeding 25°C. The number of observations exceeding this threshold was recorded for each year and summed over all years to find the total number of observations

over 25°C at each site, then averaged over the years with available data. It was assumed that each observation represented 5 minutes of time when temperature exceeded the threshold, allowing for an estimate of the total number of hours exceeding 25°C per year. The number of hours per year above the threshold provides a metric of the proportion of the time temperatures were above the threshold, but it may underestimate the proportion due to missing data. The occurrence of measurements exceeding the threshold was visualized to allow general patterns in the timing and duration of near-lethal temperatures to be assessed.

4.3.3. Comparison of temperatures across sites

Two strategies were used to compare seasonal water temperature across all the sites. First, for each day of the study period from 2001 to 2015, an average (± SD) across all sites with available data for each daily temperature summary statistic was calculated, producing a regional average temperature and daily temperature range. Then, differences between the daily temperature statistics at each site and the daily averages across sites were calculated, standardized by the common daily SD across sites. These values will be referred to as the daily temperature deviations for each site from the daily all-site averages, or just deviations. Average DOY temperature deviations were calculated over all years of record and plotted for each daily summary statistic to create an annual deviation pattern for each site, which will be referred to as the thermal signature. Annual deviation patterns for all sites were compared visually to identify sites with similar patterns throughout the year for each of the daily temperature metrics. A second strategy was used to check the deviation patterns. For each daily summary statistic, the seasonal average temperatures across all available sites were ranked for the years 2002-2007, when the largest numbers of sites were measured

concurrently. The ranking results for each site were compared to the deviation results to check whether the same patterns across sites were evident.

4.3.4. Comparison of temperatures across sites based on land use

To determine if sites with different land uses had different thermal regimes, temperatures were compared across sites based on the areal proportion of each land use type and land use classification for each site's drainage basin. For the categorical analysis, urban (Urb) versus non-urban (NUrb), agricultural (Ag) versus non-agricultural (NAg), and developed (Dv) versus undeveloped (UDv) sites were compared (Table 25). Comparisons across sites in different land use categories were made for the years 2002-2008 for the winter and spring, for the years 2002-2007 in the summer, and for the years 2002-2006 in the fall to concentrate on years with at least 10 available sites. The seasonal average data for each daily temperature metric were compared between land use groups using one-way ANOVAs. The results were assessed for consistent, statistically significant ($\alpha = 0.05$) differences between groups through time, indicating whether sites with different land uses had different temperature characteristics.

Also, linear regression analyses were conducted of relationships between seasonal temperature data for each daily summary statistic and the logit-transformed proportion of land use cover in each category. The logit transformation ($\ln(p/1-p)$) was used to meet the assumptions of the applied parametric analyses (Wharton and Hui, 2011). Regressions were calculated using the same ranges of years used for the one-way ANOVAs, and the average ($\pm$ SD) slope for the relationship across all years was calculated. A matrix plot was constructed to display when and for which daily summary statistics the regressions were significant ($\alpha = 0.05$). Both the ANOVA results and the regression results were corrected for

comparison-wise error using the Bonferroni correction, such that spring and winter comparisons required a p-value of 0.007, summer comparisons required a p-value of 0.008, and fall comparisons required a p-value of 0.01 to be considered significant.

4.4. Results

4.4.1. Description of regional thermal characteristics

Throughout the study region, peak temperatures occurred in July and minimum temperatures occurred in December and January. Based on all available observations (5-minute data), water temperatures in the study area usually ranged from 7.4°C (5th percentile on January 20) to 25.2°C (95th percentile on July 25) across all sites throughout the year. The average of all mean daily temperatures varied from 11.0°C (January 4) to 20.1°C (July 25) with an annual average of 15.5°C (Figure 17). Maximum, mean, and minimum temperature metrics were correlated with each other, whereas daily temperature ranges were most closely related to maximum temperature (Table 28).

Table 28: Correlations between the daily temperature metrics. For all correlations, n = 45,301 and p<<<0.001.

		Daily Temperature Metric		
		Minimum	Mean	Maximum
Daily Temperature Metric	Mean	0.95		
	Maximum	0.78	0.92	
	Range	0.04	0.33	0.66

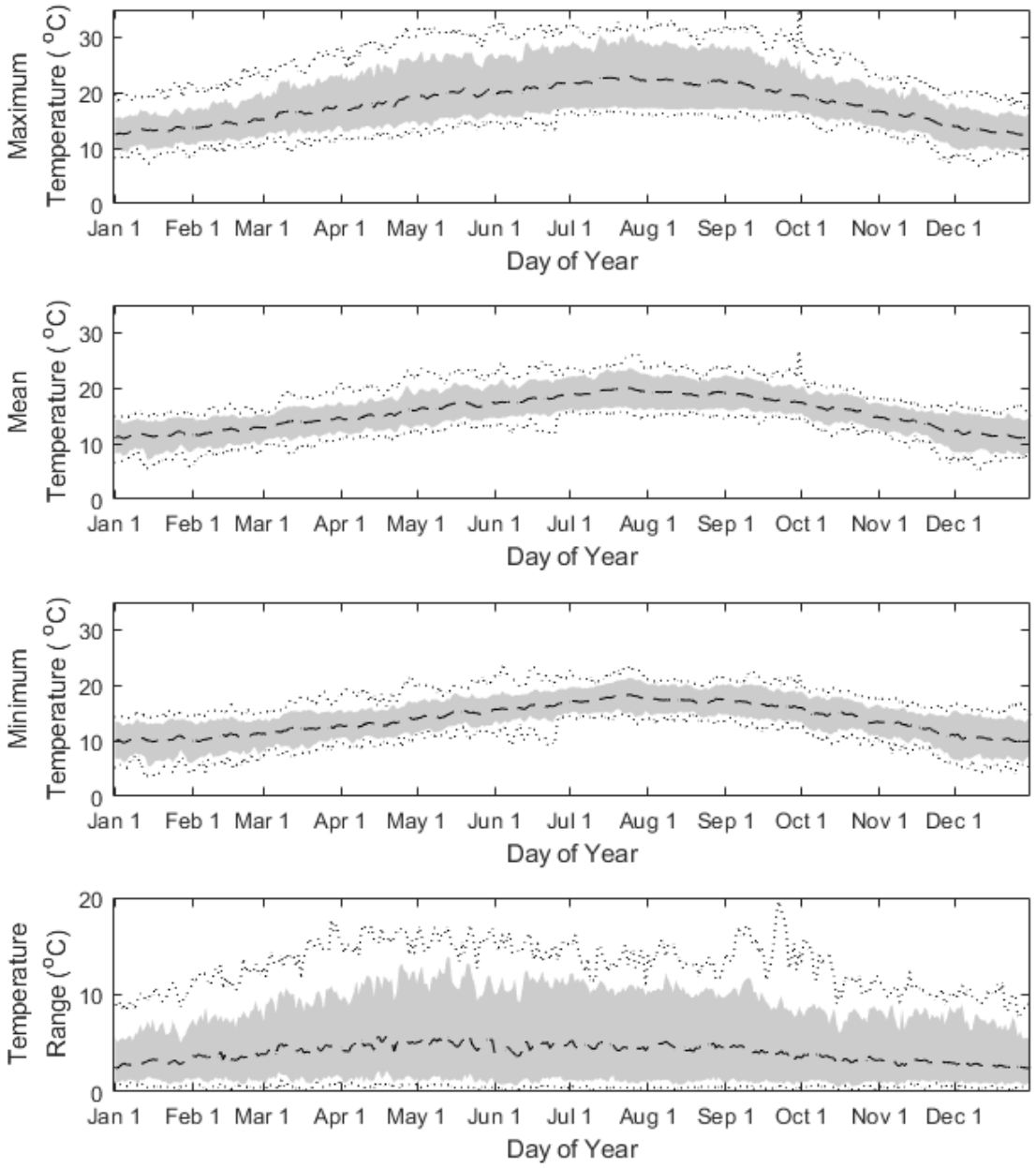

Figure 17: Annual cycle of each daily temperature metric using data from all sites and years. Dashed lines are the mean, dotted lines are the minimum and maximum values, and the grey area stretches from the 5th to the 95th percentile of the data.

Average daily maximum temperature was 17.9°C, ranging, from 12.4°C to 23.0°C throughout the year, whereas average daily minimum temperature was 13.9°C, ranging from 9.7°C to 18.3°C throughout the year. Average daily temperature ranges were smallest in the

winter (average of 2.4°C on December 30) and largest in the spring (average of 5.8°C on April 19), with an overall average of 4.0°C for the whole year. There was broad variation in daily ranges, with the smallest 5^{th} percentile daily range of 0.5°C occurring on November 8 and the largest 95^{th} percentile daily range of 13.9°C occurring on May 13. Temperatures varied significantly within and across sites for each season (Table 29).

Table 29: Average seasonal temperature and the number of available years of data at each site for the four daily temperature metrics. Standard deviations are given in parentheses. The nine sites with the longest records are indicated in bold. Data that are missing or not applicable are indicated with '—'.

Site ID	Winter					Spring				
	Min	Mean	Max	Range	Years	Min	Mean	Max	Range	Years
AB00	**9.7 (0.8)**	**10.9 (0.7)**	**12.3 (0.8)**	**2.7 (0.4)**	**14**	**13.5 (0.6)**	**15.0 (0.6)**	**17.3 (0.9)**	**3.8 (0.9)**	**14**
AB21	12.1 (0.5)	12.9 (0.5)	13.9 (0.5)	1.8 (0.2)	3	15.2 (0.8)	16.3 (0.7)	17.6 (0.6)	2.4 (0.2)	3
AB25	9.9 (1.3)	12.1 (0.7)	15.3 (0.5)	5.5 (1.8)	2	12.6 (0.4)	15.0 (0.3)	18.4 (0.2)	5.8 (0.6)	2
AT07	9.3 (0.7)	11.8 (0.5)	16.1 (0.6)	6.8 (1.0)	6	12.8 (0.5)	16.7 (0.6)	22.7 (1.3)	9.8 (1.6)	6
BC02	**9.1 (0.9)**	**10.6 (0.8)**	**12.3 (0.8)**	**3.2 (0.7)**	**11**	**12.3 (0.5)**	**14.2 (0.5)**	**16.5 (1.0)**	**4.1 (1.1)**	**11**
CP00	**10.5 (0.9)**	**12.0 (0.7)**	**13.7 (0.7)**	**3.2 (0.8)**	**8**	**13.3 (0.7)**	**15.7 (0.6)**	**18.5 (1.0)**	**5.2 (1.1)**	**8**
DV01	11 (1.0)	12.4 (0.9)	13.8 (0.9)	2.8 (0.5)	4	16.1 (1.3)	18.1 (1.3)	20.4 (1.9)	4.2 (2.0)	4
EL00	11.6 (0.8)	12.9 (0.7)	14.3 (0.8)	2.7 (0.4)	5	13.1 (0.8)	14.8 (0.6)	17.1 (0.8)	4.0 (0.9)	4
FK00	10.6 (1.1)	13.0 (0.7)	17.4 (1.4)	6.8 (2.0)	5	13.5 (1.3)	17.1 (0.9)	23.6 (2.4)	10.1 (3.2)	7
GB04	9.0 (1.2)	10.2 (1.0)	12.0 (0.8)	3.0 (0.4)	2	11.4 (0.4)	13.4 (0.1)	16.3 (0.8)	4.9 (1.2)	2
GV01	**10.4 (1.1)**	**11.7 (0.9)**	**13.3 (1.0)**	**2.8 (1.0)**	**13**	**13.5 (0.7)**	**15.7 (0.6)**	**18.9 (1.5)**	**5.4 (1.6)**	**13**
HO00	**13.1 (0.9)**	**13.9 (0.8)**	**14.9 (0.8)**	**1.7 (0.3)**	**12**	**13.9 (1.0)**	**14.7 (0.8)**	**15.8 (0.7)**	**1.9 (0.5)**	**11**
MC00	**11.2 (0.8)**	**12.5 (0.7)**	**14.1 (0.7)**	**2.9 (0.4)**	**14**	**14.9 (0.8)**	**16.8 (0.6)**	**20.3 (1.4)**	**5.5 (1.3)**	**14**
MC07	9.6 (0.9)	10.6 (0.7)	11.8 (0.5)	2.3 (0.4)	4	12.2 (0.6)	13.7 (0.6)	15.4 (0.6)	3.2 (0.5)	4
ON02	12.5 (0.8)	13.5 (0.8)	14.9 (0.7)	2.4 (0.2)	5	12.9 (0.6)	14.6 (0.5)	17.1 (0.4)	4.3 (0.6)	4
RG01	**10.1 (0.7)**	**11.8 (0.6)**	**13.8 (0.8)**	**3.7 (1.0)**	**13**	**13.2 (0.5)**	**15.2 (0.6)**	**17.9 (1.4)**	**4.8 (1.6)**	**12**
RG09	10.7 (0.3)	11.6 (0.6)	12.4 (0.9)	1.6 (0.6)	2	12.8 (1.2)	14.0 (1.3)	15.6 (2.0)	2.7 (0.8)	2
RN01	**9.2 (0.8)**	**11.1 (0.7)**	**13.2 (0.8)**	**4.0 (0.7)**	**7**	**12.3 (0.6)**	**14.8 (0.8)**	**17.8 (1.6)**	**5.5 (1.5)**	**8**
RS02	**9.7 (0.9)**	**10.8 (0.7)**	**12.3 (0.9)**	**2.6 (0.7)**	**13**	**12.0 (0.4)**	**13.4 (0.7)**	**15.7 (1.8)**	**3.8 (1.5)**	**12**
SR04	9.5 (1.0)	10.7 (1.0)	12.2 (1.0)	2.7 (0.3)	3	12.2 (0.3)	14.0 (0.5)	16.2 (0.7)	4.0 (0.4)	3
TE03	10 (0.7)	11.2 (0.7)	12.4 (0.7)	2.3 (0.1)	3	14.5 (1.4)	16.2 (1.3)	18.2 (1.4)	3.7 (0.3)	3
Site ID	**Summer**					**Fall**				
	Min	Mean	Max	Range	Years	Min	Mean	Max	Range	Years
AB00	**17.2 (0.9)**	**18.5 (0.9)**	**20.6 (1.4)**	**3.4 (1.3)**	**14**	**14.5 (1.6)**	**15.6 (1.7)**	**17.0 (2.0)**	**2.5 (0.5)**	**14**
AB21	19.4 (0.8)	20.2 (0.8)	21.3 (0.7)	1.9 (0.1)	2	16.0 (0.5)	16.7 (0.4)	17.4 (0.4)	1.4 (0.1)	2
AB25	16.1 (0.02)	17.8 (0.1)	20.0 (0.2)	3.8 (0.2)	2	13.6 (--)	15.2 (--)	17.3 (--)	3.7 (--)	1
AT07	17.4 (0.8)	21.6 (0.9)	28.3 (1.1)	10.9 (0.9)	6	12.8 (1.7)	15.9 (1.8)	21.3 (1.7)	8.6 (0.9)	6
BC02	**16.1 (0.7)**	**17.7 (0.6)**	**20.3 (1.5)**	**4.3 (1.9)**	**11**	**13.2 (0.9)**	**14.6 (1.0)**	**16.1 (1.4)**	**2.9 (1.0)**	**10**
CP00	**17.4 (0.6)**	**19.3 (0.8)**	**21.5 (1.4)**	**4.1 (1.0)**	**8**	**14.6 (0.6)**	**16.1 (0.5)**	**17.7 (0.7)**	**3.0 (0.7)**	**7**
DV01	19.9 (1.5)	21.5 (1.5)	23.5 (1.5)	3.6 (1.0)	3	14.5 (1.3)	16.0 (1.1)	17.6 (1.1)	3.2 (0.6)	4
EL00	16.5 (0.3)	18.0 (0.5)	20.0 (0.6)	3.5 (0.3)	3	14.7 (0.9)	16.1 (0.9)	17.7 (1.2)	3.0 (0.3)	2
FK00	17.9 (1.0)	20.9 (0.5)	26.4 (3.1)	8.5 (4.0)	5	14.9 (1.5)	17.7 (1.3)	22.9 (1.6)	8.0 (0.7)	4
GB04	15.1 (--)	16.4 (--)	18.0 (--)	2.9 (--)	1	11.6 (--)	13.4 (--)	16.1 (--)	4.5 (--)	1
GV01	**17.2 (0.6)**	**19.7 (0.7)**	**24.0 (1.7)**	**6.8 (1.8)**	**10**	**14.2 (0.5)**	**15.9 (0.7)**	**18.4 (1.4)**	**4.2 (1.1)**	**11**
HO00	**15.5 (0.7)**	**16.2 (0.5)**	**17.2 (0.4)**	**1.7 (0.5)**	**12**	**15.2 (0.9)**	**15.9 (0.7)**	**16.7 (0.6)**	**1.6 (0.5)**	**13**
MC00	**19.0 (0.6)**	**20.6 (0.6)**	**24.4 (1.7)**	**5.5 (1.6)**	**13**	**16.6 (1.3)**	**17.9 (1.5)**	**20.1 (2.5)**	**3.5 (1.3)**	**14**
MC07	15.5 (1.0)	17.2 (0.9)	19.6 (1.6)	4.1 (1.7)	3	12.8 (1.4)	14.1 (1.5)	15.9 (2.0)	3.1 (1.2)	3
ON02	17.5 (0.5)	18.5 (0.5)	19.8 (0.9)	2.3 (0.3)	2	15.7 (2.2)	16.6 (1.7)	17.6 (1.4)	2.0 (0.8)	3
RG01	**16.3 (0.9)**	**18.5 (0.8)**	**21.7 (1.5)**	**5.4 (1.8)**	**11**	**14.4 (1.2)**	**16.5 (1.0)**	**19.6 (2.1)**	**5.2 (2.3)**	**10**
RG09	--	--	--	--	0	13.7 (--)	14.4 (--)	15.0 (--)	1.3 (--)	1
RN01	**16.4 (0.5)**	**18.6 (1.0)**	**21.4 (2.0)**	**5.0 (1.6)**	**8**	**13.2 (0.3)**	**15.2 (0.3)**	**17.6 (1.0)**	**4.4 (1.2)**	**7**
RS02	**16.1 (0.8)**	**17.6 (0.9)**	**20.0 (2.0)**	**3.9 (1.9)**	**8**	**13.6 (0.8)**	**14.8 (1.0)**	**16.7 (1.5)**	**3.1 (1.1)**	**10**
SR04	15.8 (0.7)	17.6 (1.1)	19.5 (1.4)	3.7 (0.7)	2	--	--	--	--	0
TE03	18.7 (0.6)	20.1 (0.7)	21.5 (0.5)	2.8 (0.5)	3	14.7 (0.1)	15.7 (0.1)	16.8 (0.4)	2.1 (0.3)	2

Trends in temperature during the study period

Temporal trends in daily water temperature metrics varied in magnitude and direction for the 9 sites with the longest data records (Figure 18). When considering data from all seasons, daily minimum, mean, maximum, and range in temperature increased through the study period at some sites (MC00, RN01), whereas other sites showed increasing trends for only a subset of the daily temperature metrics (GV01, BC02, AB00, RS02, CP00, HO00). All four summary temperature metrics declined over time at one site (RG01). There appears to be a geographical pattern in the direction of the temperature trends, with western sites decreasing and eastern sites increasing over the study period. Because there were gaps in the temperature data at some sites, particularly in the summer, temporal trends for every daily summary statistic in each season were also examined (Figure 18).

The direction of seasonal trends at each site generally agree with the annual trends, although many of the seasonal trends are not significantly different from zero due to the small number of years of seasonal data available at each site (Table 29 includes the number of years of data available for each season). The strongest trends in seasonal temperature data across years were observed for daily maximum temperatures and temperature ranges, and trends were generally stronger in the fall. Inter-annual trends for temperature metrics in the winter and for seasonal mean temperatures were generally not significant. Most sites showed a mix of positive and negative temperature trends across seasons and daily summary metrics; however, maximum temperature and temperature range generally increased across the study period in all seasons at MC00, whereas GV01 generally showed declining maximum temperature and temperature range in all seasons.

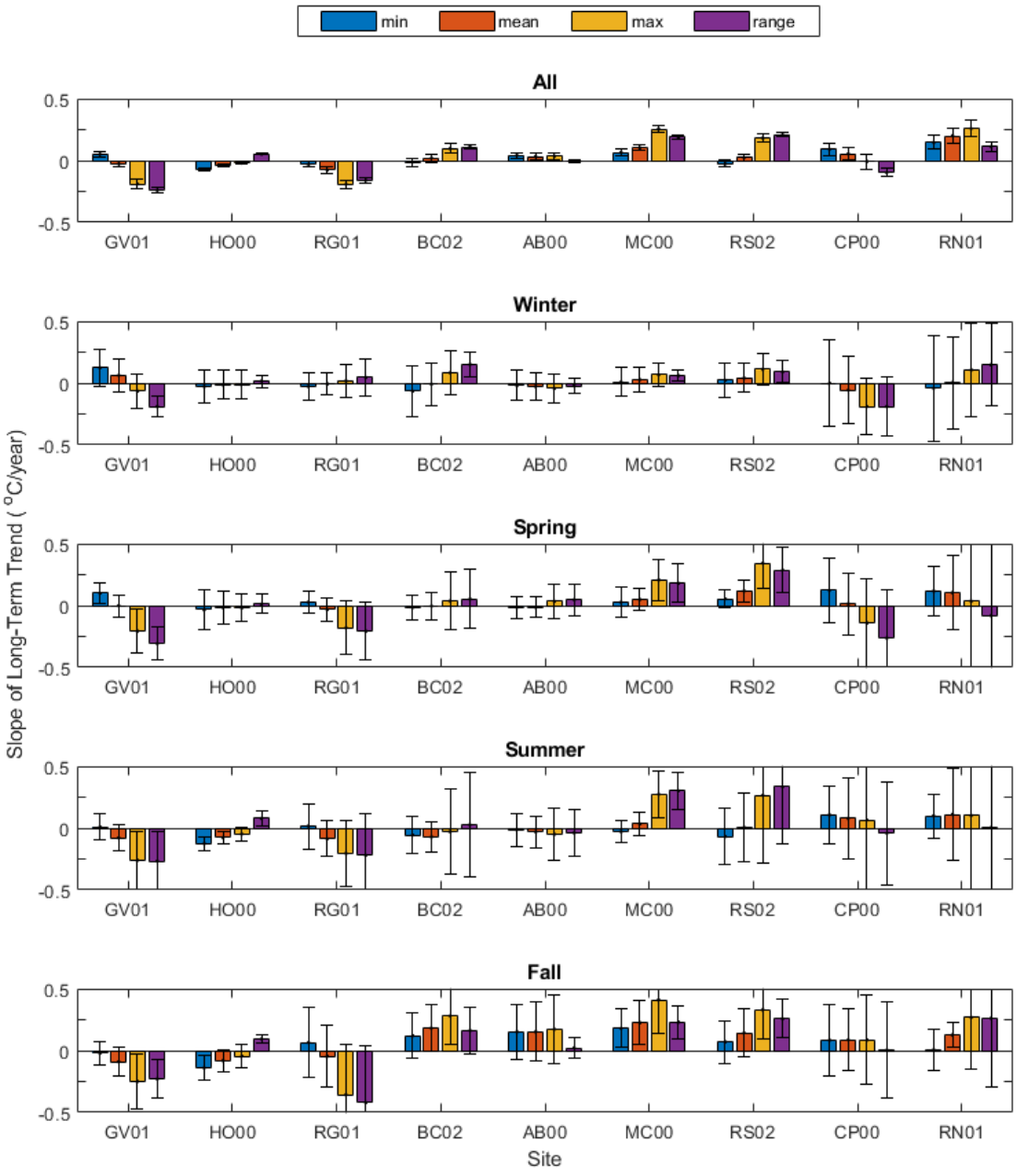

Figure 18: For all data and for each season, the slope of the multi-year trend in each daily summary statistic for the 9 long-term sites. The sites are arranged geographically from west to east. The error bars represent the 95% confidence interval for each slope estimate. The number of years available for each season at each site is described in Table 29.

Temperature response to upstream burning

The difference between spring temperature in the year after a fire and the average spring temperature in the two years before a fire were compared between sites with burning in the upstream basin and sites without burning in the upstream basin. The mean differences at fire sites were not significantly different from the mean differences at non-fire sites (Table 30).

Table 30: ANOVA results comparing pre- and post-fire temperatures between sites with and without upstream catchment burning.

		N		Mean Difference (°C)		ANOVA result	
		Fire	No Fire	Fire	No fire	$F_{1, 21}$	p
Daily temperature metric	Minimum	7	16	-0.2	0.1	0.533	0.473
	Mean	7	16	-0.1	-0.2	0.145	0.707
	Maximum	7	16	0	-0.8	0.812	0.378
	Range	7	16	0.2	-0.8	1.09	0.308

Temperatures in wet and dry years

Paired t-tests comparing seasonal temperatures in 2005 (a wet year) to seasonal temperatures in 2002 and 2007 (wet years) indicate no significant difference between wet and dry years for spring, summer, or fall temperatures. T-tests, however, indicated significant differences between 2005 and 2002 for daily minimum and mean temperatures and temperature ranges in winter, along with a significant difference between 2005 and 2007 in daily temperature range (Table 31). Daily minimum and mean temperatures for winter 2005 were warmer than those for 2002, and daily temperature ranges in winter 2005 were smaller than those in both 2002 and 2007. Additional data at a sufficient number of sites during multiple wet and dry years would be required to further generalize these results.

Table 31: Significant differences between winter wet year and winter dry year data

Years (wet, dry)	Daily Metric	N	Mean (wet)	Mean (dry)	df	CI		tstat	p
2005, 2002	Minimum	9	11.1	9.9	8	-1.9	-0.5	-3.89	0.005
2005, 2002	Mean	9	12.1	11.5	8	-1.1	-0.1	-2.90	0.02
2005, 2002	Range	9	2.4	3.9	8	0.5	2.6	3.32	0.01
2005, 2007	Range	12	2.7	3.4	11	0.0	1.3	2.37	0.04

Suitability of thermal regime for steelhead trout

Temperatures exceeding the 25°C lethal steelhead threshold were observed at 15 of the 21 study sites (Table 32).The average number of observations exceeding 25°C each year was low at 10 of these sites, corresponding to less than 30 cumulative hours over the entire year. Five sites, however, exceeded 25°C more frequently: FK00, DV01, AT07, MC00, and GV01. Temperatures at both AT07 and FK00, in particular, were above 25°C, on average, for hundreds of hours each year.

Table 32: Number of temperature observations exceeding 25°C at each site. Sites are listed in order of decreasing watershed percent urban cover.

Site ID (in order of decreasing %urban cover)	Total Observations Exceeding 25°C	Average Observations Each Year Exceeding 25°C	Estimated Hours Per Year Exceeding 25°C
FK00	25443	3180	265
DV01	5532	1106	92
AB25	0	0	0
AT07	45548	6507	542
MC00	16137	1076	90
AB00	108	7	1
AB21	0	0	0
TE03	40	10	1
CP00	1173	130	11
BC02	1253	104	9
SR04	6	2	0
RN01	2754	306	26
MC07	220	44	4
RS02	2039	136	11
GB04	91	30	3
EL00	0	0	0
GV01	13770	918	77
HO00	0	0	0
ON02	0	0	0
RG09	0	0	0
RG01	4170	278	23

Generally, at sites that exceeded temperature thresholds, temperatures exceeded 25°C in the afternoon and the amount of time spent above the threshold was limited to a few hours (Figure 19). The total numbers of observations exceeding the threshold varied among years, but most were concentrated in the dry season, particularly during the summer. Four of the five sites that exceeded 25°C most frequently had urban development in their watersheds, and all had no or interrupted canopy cover. The two channelized sites, FK00 and AT07, showed longer stretches of time above the threshold compared to other sites and

temperatures on most days in the summer season at these sites exceeded 25°C (Figure 19). Due to missing data, this assessment may underestimate the amount and proportion of time spent above the threshold at each site.

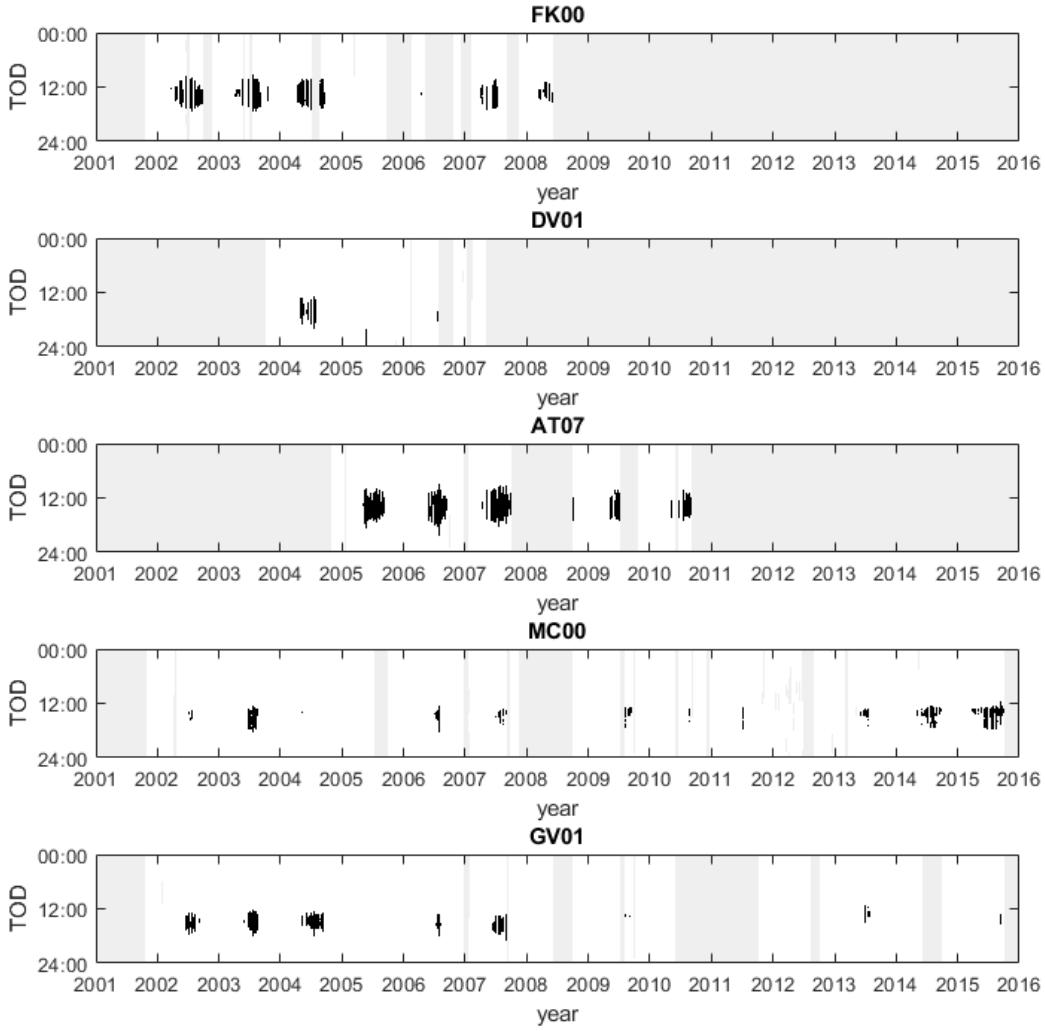

Figure 19: Temperature measurements exceeding the 25°C threshold. Black indicates measurements exceeding the threshold; grey areas are missing data. Sites are presented from top to bottom in order of decreasing percent urban cover in their basins.

4.4.2. Comparison of temperatures across sites

The temperatures at each site were compared to other sites by examining deviations of individual sites from the all-site average (Figure 20) and ranking seasonal site averages for temperature metrics for years with data available at the largest number of sites (2002-2007) (Appendix IV). When considered together, these results show which sites are warmest and coolest for different parts of the day and different parts of the year, while also allowing sites to be grouped based on similarities in their thermal regimes.

Sites MC00, DV01, and FK00 had consistently higher minimum, mean, and maximum daily temperatures compared to the all-site averages throughout the year (Figure 20A), indicating that these sites were consistently warmer than other sites. An additional two sites, AT07 and GV01, had consistently higher mean and maximum daily temperatures, but not minimum daily temperatures, compared to the all-site averages, indicating these sites were warmer than other sites during the day, but not necessarily at night. The higher temperatures at these 5 sites compared to other sites is supported by the ranking results from 2002-2007 and by the frequency that these temperatures exceeded the 25°C temperature threshold (Table 32, Figure 19).

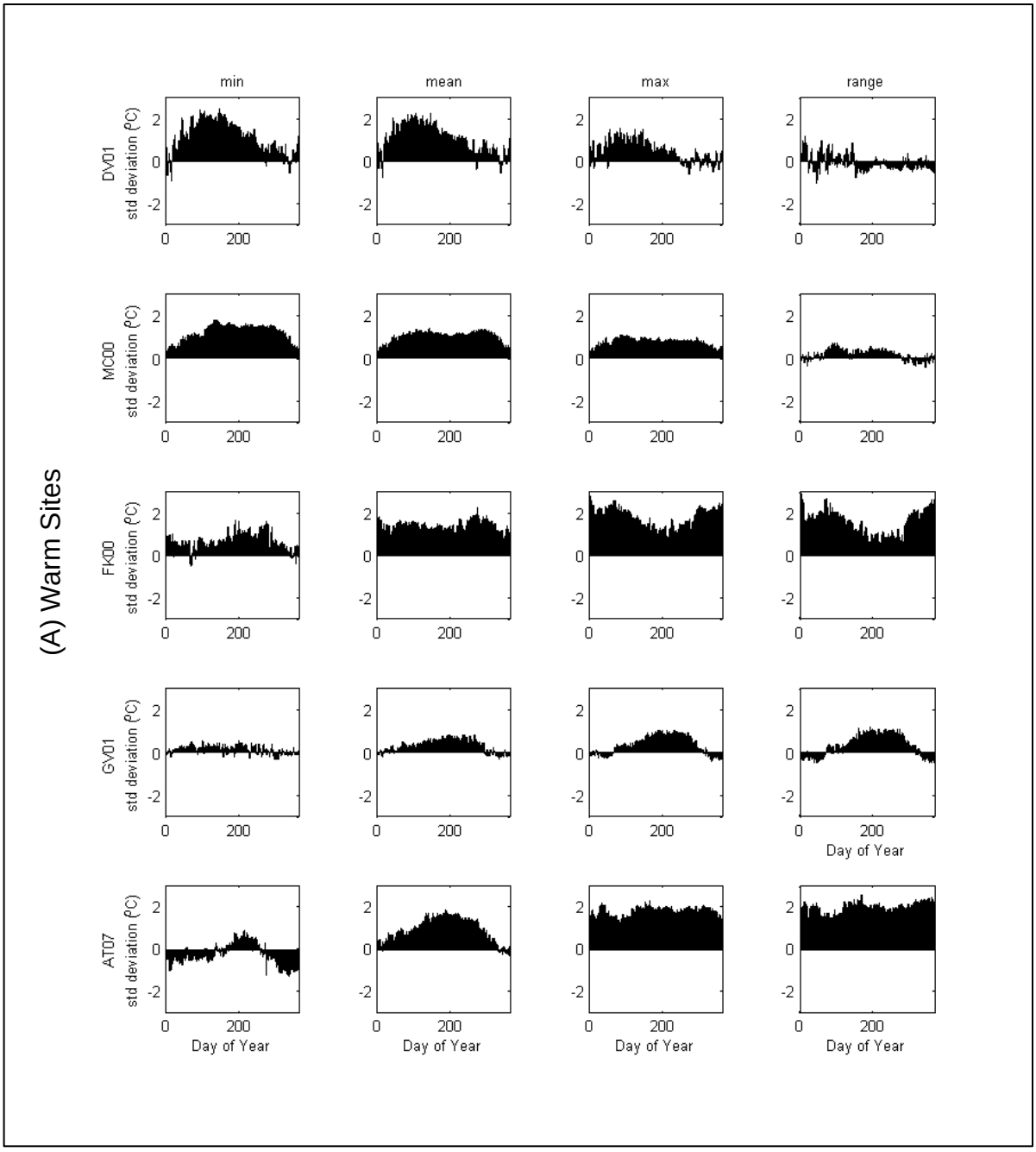

Figure 20: Annual patterns of temperature deviations from the all-site mean at each site.

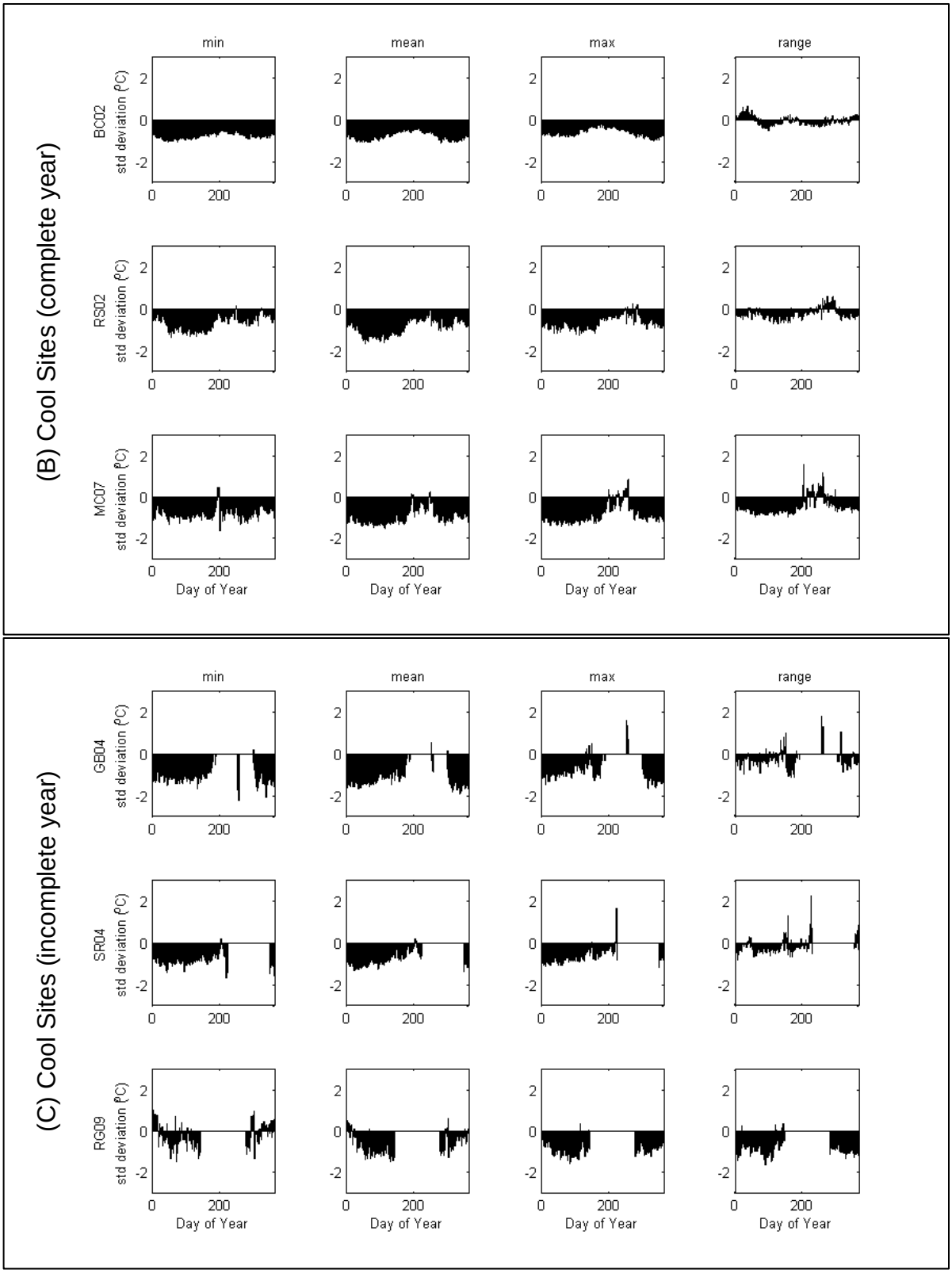

Figure 20 (continued): Annual patterns of temperature deviations from the all-site mean at each site.

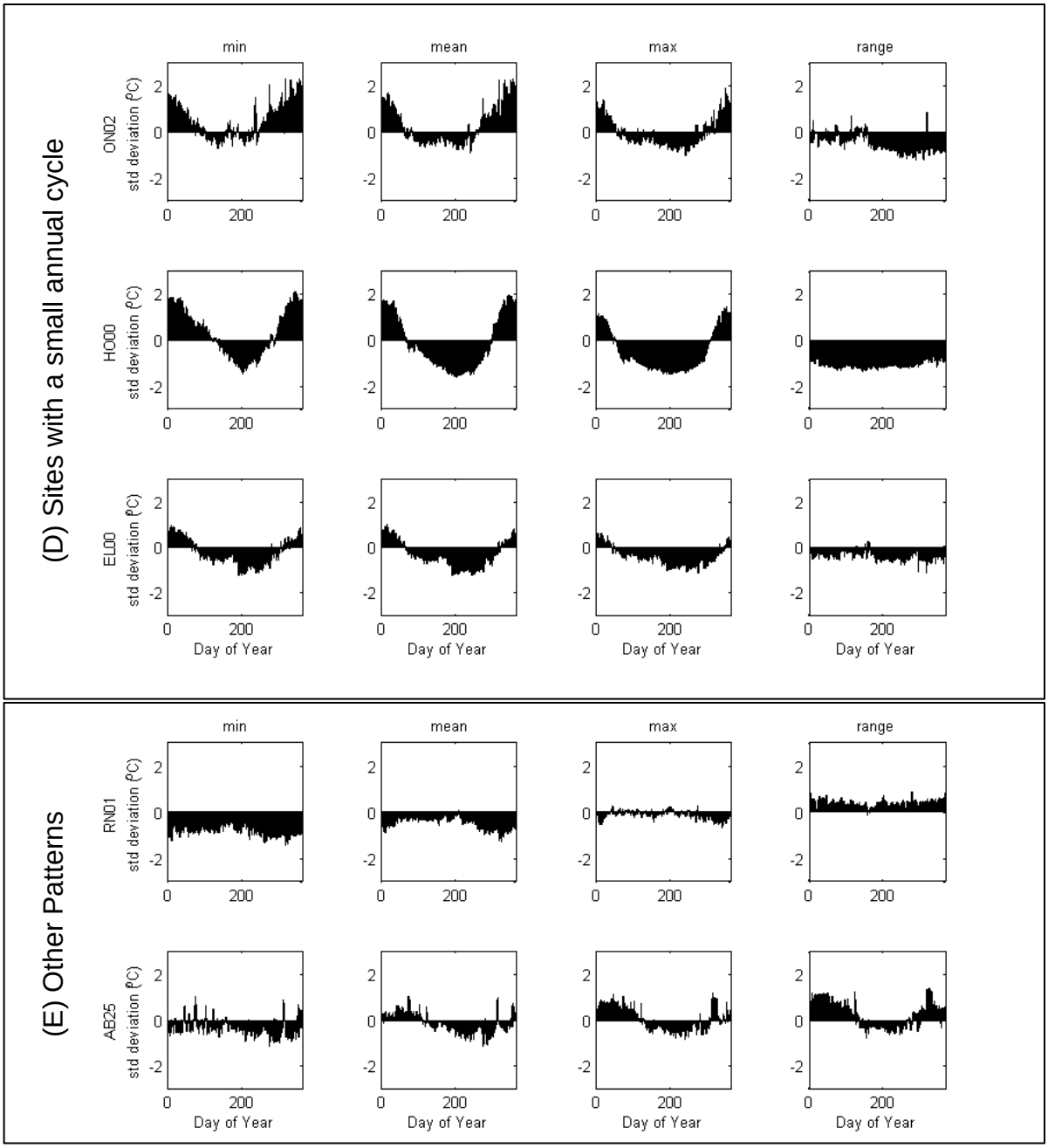

Figure 20 (continued): Annual patterns of temperature deviations from the all-site mean at each site.

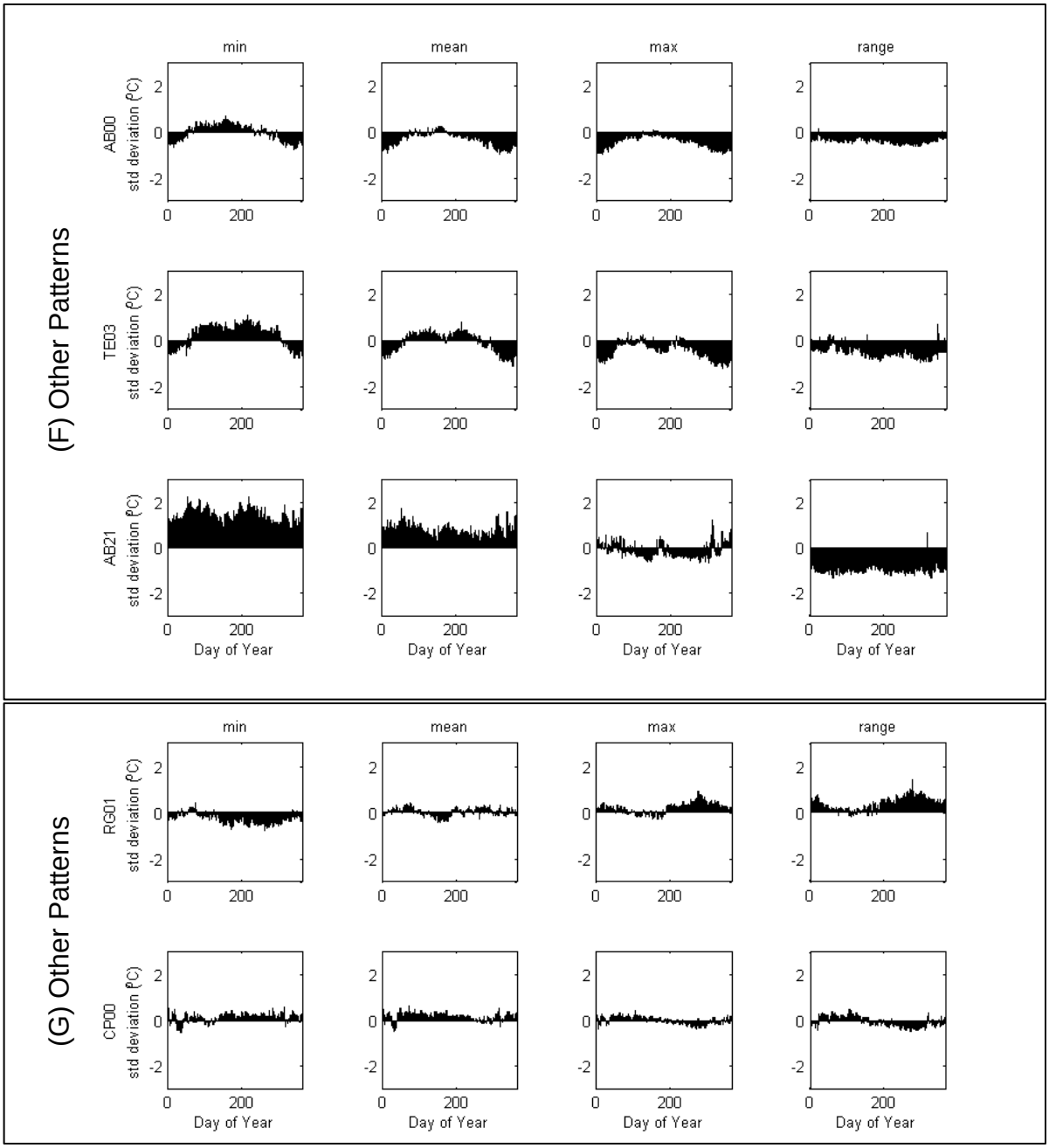

Figure 20 (continued): Annual patterns of temperature deviations from the all-site mean at each site.

Although these 5 sites are the warmest sites in the region, there are differences among these sites in the magnitude of the daily temperature range. Two of these sites, MC00 and DV01, had warm minimum daily temperatures compared to other sites, but maximum daily temperatures that, although above the average across sites, were closer to average than the

minimum temperatures, resulting in daily temperature ranges that were near or smaller than average ranges for all sites. At the other three sites, especially AT07 and FK00, maximum daily temperatures were relatively warm, often 2 standard deviations higher than other sites, compared to minimum daily temperatures, resulting in near to or larger than average daily temperature ranges compared to other sites. These assessments of deviations of temperature ranges from average are supported by the rankings for temperature ranges for FK00 and AT07, and to a lesser degree for GV01. Of the 5 warm sites, all except GV01 are located in urban basins and all lack significant shading from riparian vegetation. The two sites with particularly warm daytime temperatures, AT07 and FK00 (Appendix IV), are the two sites located in concrete channels.

Sites BC02, RS02, and MC07 had consistently cooler minimum, mean, and maximum daily temperatures throughout the days, months, seasons, and years compared to other sites (Figure 20B), which resulted in lower daily temperature ranges. RS02 and MC07 differed from BC02 in that both were cooler in the winter and spring, but mean and maximum daily temperatures increased at these sites in the late summer and into the fall to become closer to the all-site average, producing greater temperature ranges in the fall, near or above the all-site average range. Sites GB04, SR04, and RG09 also were cooler than other sites throughout the day (Figure 20C), but gaps in the summer or fall record for these sites prevented extrapolation through the entire year. Available winter and summer ranking results did indicate that GB04 and SR04 were colder than most other sites during years with available data (Appendix IV). All the cold sites except BC02 were at elevations at least 50 m higher than the rest of the sites, suggesting that temperature decreases with increasing elevation in this region.

Sites HO00, EL00, and ON02 were relatively cool during the summer and relatively warm during the winter compared to the other sites in the study area (Figure 20D), consistent with the seasonal rankings from 2002-2007 (Appendix IV). Summer minimum, mean, and maximum daily temperatures were consistently lower at HO00 than at other sites, with EL00 and ON02 showing similar tendencies. In the winter, however, HO00, ON02, and EL00 were among the warmest sites, particularly for minimum and mean daily temperature. From 2002-2007 HO00 ranked as the warmest site every year for winter minimum and mean temperature (Appendix IV). All of these sites also had a smaller than average daily temperature range. Overall, the deviation and rank results indicate that the temperatures at these sites do not vary as much as those at other sites throughout the year, either between seasons or daily, providing a relatively stable thermal environment compared to the other sites.

Other sites (AB00, AB21, AB25, CP00, RG01, RN01, and TE03) had less consistent patterns relative to other sites over time (Figure 20 E-G). Cooler than average mean and minimum temperatures at RN01, coupled with larger than average daily ranges, reflected cooler temperatures at night, compared to other sites (Figure 20E). Site AB25, on the other hand, was generally cooler than the all-site average at night throughout the year, generally cooler than other sites throughout the day during the summer, and generally warmer than other sites during the day in the winter (Figure 20E). Sites AB00, TE03, and AB21 had smaller than average daily ranges (Figure 20F). Both AB00 and TE03 were relatively warmer than other sites in the summer and relatively cooler than other sites in the winter for each daily summary statistic, the opposite pattern from that seen at HO00, ON02, and EL00. Overall, the most prominent feature of the deviations indicate that temperatures at these sites

were relatively warm at night in the summer, and cooler at mid-day in winter, compared to other sites.

AB21 was anomalous in that minimum temperatures were consistently higher than the all-site average, whereas temperatures during mid-day were near or below average, resulting in consistently smaller-than-average temperature ranges throughout the year. Sites RG01 and CP00 showed no consistent patterns in temperature statistics relative to other sites (Figure 20G). The RG01 data suggest cooler-than-average minimum temperatures in the summer and warmer-than-average maximum temperatures in the summer. Both RG01 and CP00 were among the 5 sites with the largest winter ranges for 5 out of the 6 years from 2002-2007, whereas RG01 was also among the 5 sites with the largest summer ranges for all 6 years (Appendix IV).

4.4.3. Comparison of temperatures across sites in basins with different land use patterns

Relationships between seasonal temperature metrics and land use cover, particularly impervious cover, were strongest in the spring and summer (Figure 21A). Seasonal temperature metrics were not consistently related to agricultural or undeveloped land use, but were related to urban cover in spring and summer, particularly for minimum, mean, and maximum temperatures in the spring and minimum and mean temperatures in the summer. In general, stream temperatures increased with increasing urban cover in the spring and summer (Figure 21 and Figure 22).

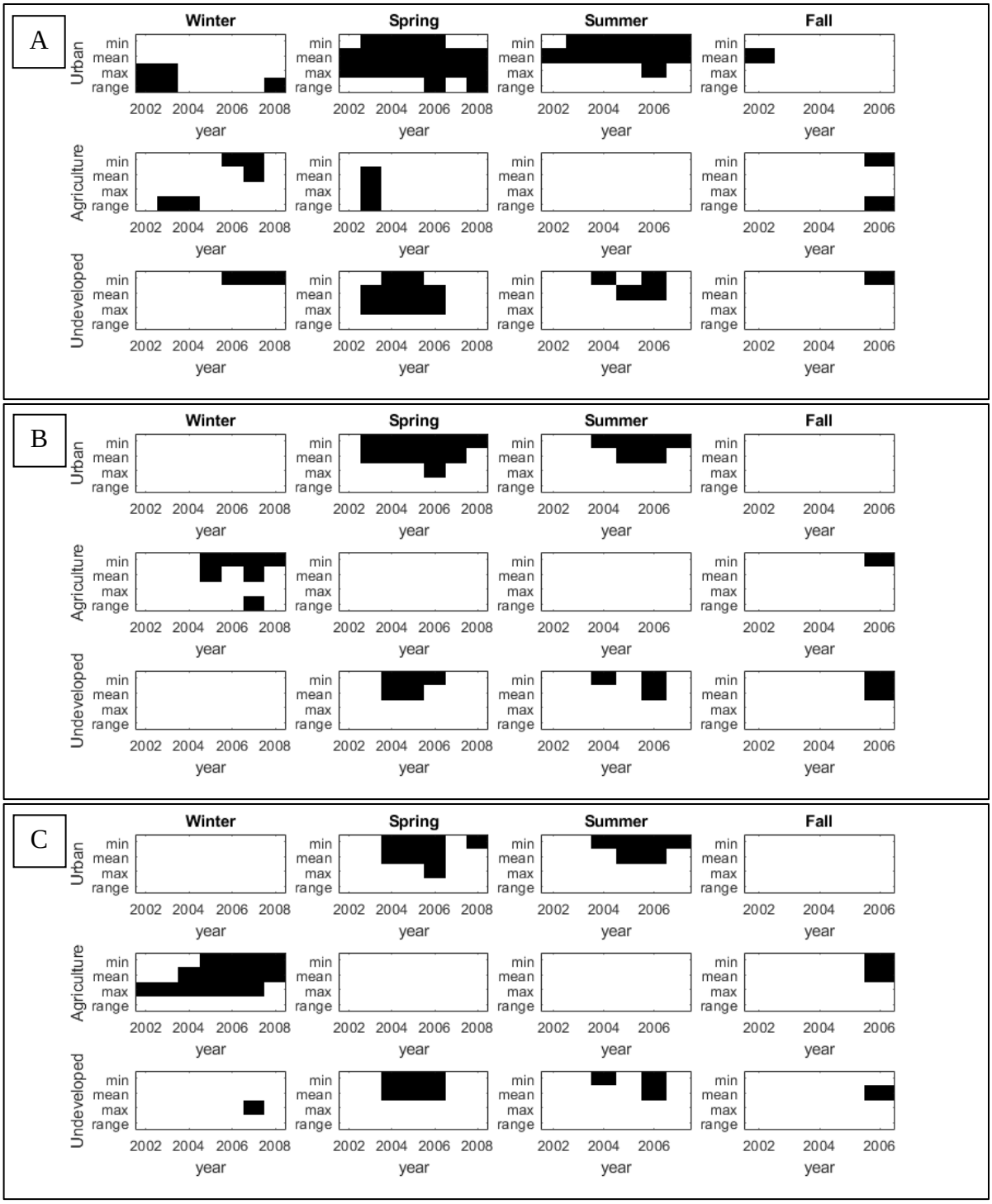

Figure 21: Significant regressions (uncorrected α = 0.05) between temperature and logit transformed proportion of land use cover for all seasons and summary statistics using (A) all available sites for each year, (B) all available sites except channelized sites, and (C) all available sites except channelized and high elevation sites. Significant relationships are indicated in black.

Spring mean temperatures demonstrated a particularly strong relationship with urban cover, with each year from 2002-2008 demonstrating a significant relationship, with p-values ranging from <<0.001 to 0.034 (see Table 33 for spring and summer urban regression metrics). When Bonferroni corrections for comparison-wise error were applied, significant relationships for all years remained, except for 2002. The average slope for the relationship between spring mean daily temperature and urban cover was 0.61 (SD = 0.13), indicating that doubling the proportion of impervious cover resulted in temperatures increases of 2 - 5%. Spring maximum temperatures also demonstrated a consistent, strong relationship with urban cover (p-values from 0.001 to 0.04, Table 33), with 2004 and 2006-2008 remaining significant with Bonferroni corrections. The slope of the relationship between spring maximum temperature and urban cover was 1.09 (SD = 0.26), suggesting that doubling the proportion of impervious cover in a catchment would lead to a temperature increase of about 3 - 6%. After adjustments for comparison-wise error for spring minimum, summer minimum, and summer maximum temperature relationships with urban cover, two years still showed significant relationships (Table 33).

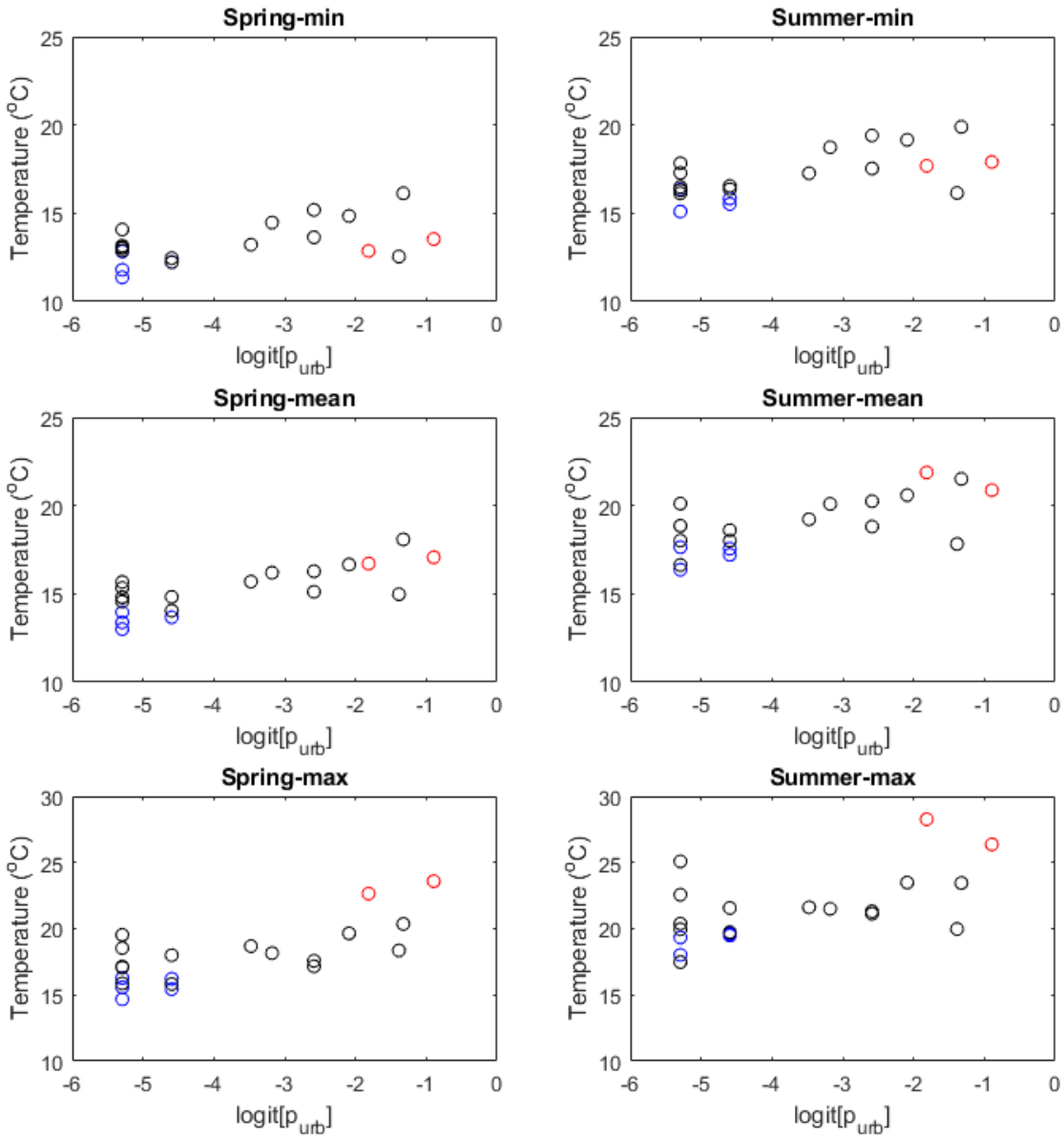

Figure 22: Spring and summer average temperatures for minimum, mean, and maximum daily temperature metrics, plotted against the logit transformed proportion of impervious cover in each basin. Values for each site are the average of all available seasonal averages from 2002-2008 for spring or from 2002-2007 for summer. Channelized sites are marked in red; high elevation sites are marked in blue.

The general comparison of temperatures across sites indicated that two of the urban sites, AT07 and FK00, were usually much warmer than the other sites during the daytime in the spring and summer. These sites are channelized, which appears to dramatically alter the

thermal regime compared to other sites. Minimum temperatures at the channelized sites were similar to sites with less development and lower than many of the sites with more urban cover, with the opposite being true for spring maximum temperatures. The channelized sites, then, had unique thermal regimes, with higher daytime temperatures and lower nighttime temperatures compared to other sites. Both channelized sites also had high exposure to solar radiation owing to a lack of riparian canopy, raising the possibility that the data at these sites are affected by direct solar heating of the temperature sensor. The extent of direct solar heating is unknown, but more likely for daytime spring and summer data when solar radiation is high. Because of these issues, the regression analyses were repeated, excluding these two sites.

With the channelized sites excluded, spring minimum and mean, and summer minimum temperatures still were consistently, significantly positively related to urban cover (Figure 21B, Table 33), but spring maximum temperatures were not. The exclusion of the channelized sites resulted in significant regressions for spring minimum temperature with urban cover for all years except 2002, of which 2004-2006 remained significant with Bonferroni corrections (Table 33). Average regression slopes were 0.57 (SD = 0.16) for spring minimum temperatures, 0.59 (SD = 0.16) for spring mean temperatures, and 0.68 (SD = 0.17) for summer minimum temperatures versus urban cover. These relationships suggested temperature increases of 3-5% when the proportion of urban cover was doubled.

Table 33: Regression summaries for spring and summer minimum and mean temperatures, and spring maximum temperatures with transformed extent of impervious cover. Bolded p-values are significant after correcting for comparison-wise error using the Bonferroni correction ($p < 0.007$ in spring, $p < 0.008$ in summer).

		All Available Sites								Excluding AT07 and FK00								Excluding AT00, FK00, RS02, MC07, RG09, SR04, and GB04							
		Year	N	dfe	dfr	β_0	β_1	F	p	R^2	Year	N	dfe	dfr	β_0	β_1	F	p	R^2	Year	N	dfe	dfr	β_0	β_1	F	p	R^2
Spring Min, Urban		2002	13	11	1	13.6	0.25	1.14	0.308	0.09	2002	12	10	1	14.0	0.34	1.52	0.246	0.13	2002	9	7	1	13.5	0.12	0.14	0.718	0.02
		2003	16	14	1	14.4	0.37	7.45	0.016	0.35	2003	15	13	1	14.8	0.45	8.17	0.013	0.39	2003	10	8	1	14.4	0.27	2.57	0.148	0.24
		2004	16	14	1	16.7	0.62	10.66	**0.006**	0.43	2004	15	13	1	17.6	0.83	17.83	**0.001**	0.58	2004	11	9	1	17.4	0.69	13.16	**0.006**	0.59
		2005	17	15	1	15.9	0.59	29.77	**0.000**	0.66	2005	15	13	1	15.9	0.59	20.88	**0.001**	0.62	2005	12	10	1	15.8	0.52	16.74	**0.002**	0.63
		2006	15	13	1	13.8	0.29	8.31	0.013	0.39	2006	13	11	1	14.7	0.49	25.07	**0.000**	0.70	2006	12	10	1	14.6	0.43	29.58	**0.000**	0.75
		2007	13	11	1	14.7	0.30	1.57	0.237	0.12	2007	11	9	1	16.4	0.66	5.93	0.038	0.40	2007	10	8	1	16.3	0.59	4.33	0.071	0.35
		2008	11	9	1	13.8	0.23	1.74	0.220	0.16	2008	9	7	1	15.8	0.65	11.63	0.011	0.62	2008	8	6	1	15.7	0.62	8.52	**0.027**	0.59
Spring Mean, Urban		2002	13	11	1	16.4	0.45	5.82	0.034	0.35	2002	12	10	1	16.0	0.36	2.60	0.138	0.21	2002	9	7	1	15.5	0.12	0.33	0.586	0.04
		2003	16	14	1	17.1	0.55	13.27	**0.003**	0.49	2003	15	13	1	16.9	0.50	7.57	0.016	0.37	2003	10	8	1	16.3	0.23	2.90	0.127	0.27
		2004	16	14	1	19.6	0.87	21.79	**0.000**	0.61	2004	15	13	1	19.7	0.90	16.12	**0.001**	0.55	2004	11	9	1	19.3	0.68	11.04	**0.009**	0.55
		2005	17	15	1	18.2	0.66	32.18	**0.000**	0.68	2005	15	13	1	18.0	0.64	16.39	**0.001**	0.56	2005	12	10	1	17.8	0.51	25.44	**0.001**	0.72
		2006	15	13	1	16.6	0.55	19.92	**0.001**	0.61	2006	13	11	1	16.9	0.61	14.34	**0.003**	0.57	2006	12	10	1	16.7	0.52	16.52	**0.002**	0.62
		2007	13	11	1	17.6	0.58	11.42	**0.006**	0.51	2007	11	9	1	17.5	0.58	5.73	0.040	0.39	2007	10	8	1	17.3	0.48	4.28	0.072	0.35
		2008	11	9	1	17.8	0.61	11.78	**0.007**	0.57	2008	9	7	1	17.5	0.55	3.62	0.099	0.34	2008	8	6	1	17.1	0.42	2.33	0.177	0.28
Spring Max, Urban		2002	13	11	1	21.2	0.89	5.38	0.041	0.33	2002	12	10	1	16.3	-0.34	0.41	0.537	0.04	2002	9	7	1	15.3	-0.89	3.91	0.089	0.36
		2003	16	14	1	21.5	0.97	9.28	0.009	0.40	2003	15	13	1	19.4	0.68	1.86	0.196	0.13	2003	10	8	1	19.0	0.26	0.36	0.563	0.04
		2004	16	14	1	24.2	1.32	10.74	**0.006**	0.43	2004	15	13	1	20.4	0.61	0.85	0.372	0.06	2004	11	9	1	20.1	0.21	0.09	0.772	0.01
		2005	17	15	1	21.1	0.75	8.23	0.012	0.35	2005	15	13	1	19.5	0.56	1.80	0.202	0.12	2005	12	10	1	19.3	0.29	0.71	0.420	0.07
		2006	15	13	1	21.0	1.03	18.58	**0.001**	0.59	2006	13	11	1	17.7	0.39	0.82	0.384	0.07	2006	12	10	1	17.2	0.11	0.09	0.773	0.01
		2007	13	11	1	22.5	1.18	9.78	**0.010**	0.47	2007	11	9	1	15.8	-0.43	0.68	0.431	0.07	2007	10	8	1	15.0	-0.83	3.41	0.102	0.30
		2008	11	9	1	24.7	1.49	12.53	**0.006**	0.58	2008	9	7	1	18.6	0.21	0.12	0.744	0.02	2008	8	6	1	17.5	-0.29	0.25	0.632	0.04
Summer Min, Urban		2002	12	10	1	18.2	0.45	4.83	0.053	0.33	2002	11	9	1	18.5	0.53	4.52	0.062	0.33	2002	9	7	1	18.5	0.47	2.75	0.141	0.28
		2003	15	13	1	18.8	0.46	5.21	0.040	0.29	2003	14	12	1	19.0	0.51	4.42	0.057	0.27	2003	10	8	1	18.8	0.40	1.95	0.201	0.20
		2004	10	8	1	19.2	0.56	10.41	0.012	0.57	2004	9	7	1	20.2	0.78	26.74	**0.001**	0.79	2004	9	7	1	20.2	0.78	26.74	**0.001**	0.79
		2005	17	15	1	19.5	0.58	14.80	**0.002**	0.50	2005	15	13	1	19.6	0.60	9.63	0.008	0.43	2005	12	10	1	19.5	0.51	8.48	0.016	0.46
		2006	13	11	1	21.2	0.84	26.12	**0.000**	0.70	2006	12	10	1	21.9	0.97	37.99	**0.000**	0.79	2006	11	9	1	22.0	0.99	33.79	**0.000**	0.79
		2007	10	8	1	18.5	0.40	9.02	0.017	0.53	2007	8	6	1	19.9	0.71	23.20	**0.003**	0.79	2007	8	6	1	19.9	0.71	23.20	**0.003**	0.79
Summer Mean, Urban		2002	12	10	1	20.4	0.54	6.78	0.026	0.40	2002	11	9	1	18.5	0.10	0.06	0.816	0.01	2002	9	7	1	18.3	-0.06	0.02	0.899	0.00
		2003	15	13	1	21.1	0.59	6.04	0.029	0.32	2003	14	12	1	20.4	0.58	1.73	0.213	0.13	2003	10	8	1	20.8	0.55	1.29	0.288	0.14
		2004	10	8	1	21.4	0.64	7.80	0.023	0.49	2004	9	7	1	19.0	-0.02	0.00	0.974	0.00	2004	9	7	1	19.0	-0.02	0.00	0.974	0.00
		2005	17	15	1	21.4	0.63	13.00	**0.003**	0.46	2005	15	13	1	19.9	0.41	1.60	0.228	0.11	2005	12	10	1	19.8	0.27	0.80	0.393	0.07
		2006	13	11	1	23.4	0.90	17.85	**0.001**	0.62	2006	12	10	1	20.9	0.43	0.94	0.354	0.09	2006	11	9	1	20.7	0.32	0.43	0.527	0.05
		2007	10	8	1	21.5	0.63	6.59	0.033	0.45	2007	8	6	1	18.1	-0.20	0.17	0.692	0.03	2007	8	6	1	18.1	-0.20	0.17	0.692	0.03

The five undeveloped sites were generally at higher elevations and were consistently cooler than most other sites throughout the year. Because of this elevation confound, the regression analyses were repeated, excluding both high elevation and channelized sites. Excluding the high elevation and channelized sites produced similar results to those obtained for the entire dataset excluding the channelized sites for the relationship between temperature and impervious cover. Spring minimum and mean temperatures were significantly positively related to urban cover from 2004 to 2006 and summer minimum temperatures were related to urban cover in 2004 and 2006-2007 (Table 33, Figure 21C). Spring maximum and summer mean temperatures were unrelated to urban cover.

Similar to the regression analyses, when data on temperature metrics from all available sites were included in one-way ANOVAs, minimum and mean temperatures in spring and summer, and spring maximum temperatures, were higher at urban than non-urban sites. When data from channelized sites were removed from analyses, consistent differences between urban and non-urban sites remained for spring and summer minimum temperatures and spring mean temperatures. When data from high elevation sites were also removed from analyses, only minimum temperatures were consistently different between urban and non-urban sites over more than one year (2005 and 2006 for spring minimum temperature and 2006 and 2007 for summer minimum temperature, with Bonferroni corrections, see Appendix V).

4.5. Discussion

The research was designed to describe water temperature regimes in the coastal region of central California, including variations in daily and seasonal temperature through time and

across sites, thermal conditions for steelhead trout, and differences between wet and dry years. This information, then, provided background for the primary focus of this chapter, which was to examine the effects of land use changes, and secondarily wildfire, on stream temperature regimes. Water temperatures were dynamic, varying widely during the day and between seasons both within and across sites, although temperature patterns were generally consistent through time within individual sites. Most measured temperatures fell below 25°C, the assumed upper threshold of steelhead trout thermal tolerance, except for brief periods at a subset of sites. Two channelized sites, however, had frequent warm periods, including temperatures in excess of 30°C. There was little evidence for temperature differences between a wet year (2005) and two dry years (2002, 2007), except for winter temperature ranges, which were smaller in 2005. Across the study region, a subset of sites was consistently warmer, other higher elevation sites were consistently cooler, and still others had limited seasonal variability compared to other sites in this region. Some of the variation in thermal regimes across sites could be attributed to the degree of urban land use, with evidence for increased minimum and mean temperatures in the spring and summer, and increased maximum temperatures in the spring, at urbanized sites.

4.5.1. Characteristics of the thermal environment

Santa Barbara stream temperatures follow air temperature dynamics in this region. Compared to regional atmospheric temperatures for the period from 1985-2014, extracted from downscaled global climate model data, the average daily range of measured water temperatures throughout the year was smaller than the average range of atmospheric temperatures throughout the year (Myers et al., 2017). Annual average atmospheric daily minimum temperatures for the region are 10°C, whereas the corresponding value for water

temperatures was 13.9°C. Annual average atmospheric daily maximum temperatures for the region are 21.8°C, whereas the corresponding value for water temperatures was 17.9°C. The water temperatures presented here are similar to other water temperature measurements made in this area, (e.g. Sloat and Osterback, 2013; Boughton et al., 2015; Matthews and Berg, 1997), although there was significant variation among sites. A significant temperature difference between wet and dry years was not found, except for winter temperature ranges, but the analysis was limited to a single wet year, so results from additional sites during additional wet and dry years would be required to further this analysis.

Trends in temperature during the study period

Effects of changing climate on water temperatures and how these, in turn, will affect aquatic organisms and communities is of wide interest. In California, climate change is expected to increase air temperatures by 1.5°C to 4.5°C by the end of the twenty-first century, with more warming in the summer than winter and significant variation across locations (Cayan et al., 2008). In Santa Barbara, based on a business-as-usual emissions scenario, temperatures are expected to increase by up to 3.3 - 3.9°C by the end of the twenty-first century with the number of extreme hot days (equal or exceeding ~31.3°C) is expected to increase six fold or more (Myers et al. 2017). Owing to heat exchange between the atmosphere and streams, stream temperatures should generally increase in the future, mirroring projected increases in local air temperatures. Modeling of Sierra Nevada streams suggests that each 2°C increase in air temperature is expected to cause a 1.6°C increase in stream temperature, with variation across individual watersheds (Null et al., 2013).

Some streams in the U.S.A. are beginning to warm (e.g. Kaushal et al., 2010; Arismendi et al., 2012), but the ability to detect warming trends depends on the length of the

temperature record and when temperature data were collected. For example, a study of stream temperature trends across the Pacific coast of the U.S.A. found warming trends in the longest records (>30 years), but cooling trends at many sites with shorter records (13-30 years), with the direction of trends relating to the length and specific timing of data collection, highlighting the sensitivity of trend analysis to short-term patterns and temporal scale (Arismendi et al., 2012). Because the longest temperature record in this study encompasses 14 years and because of high inter-annual climatic variability, it is not surprising that the Santa Barbara stream temperature data does not show consistent trends. During the study period, the direction and magnitude of stream temperature changes over years varied across sites and seasons, although individual sites often showed consistent trends throughout the year.

Because all of the study streams responded to similar climatic conditions throughout the study period, the high site-to-site variability in short-term temporal patterns suggests that different sites will respond to climate change in different ways. This observation emphasizes the importance of local site characteristics, such as groundwater inflows or the presence and extent of riparian vegetation, for moderating relationships between stream and atmospheric temperatures. As a consequence, land use changes that modify local environmental conditions may interact with climate change to affect stream water temperatures. For example, a study of water temperatures in Tokyo streams found that increases in wastewater effluent altered the relationship between air temperature and water temperature (Kinouchi et al., 2007).

Although this dataset provides important information about water temperature conditions in the Santa Barbara area and how they change from year to year, the dataset is too short to

provide definitive evidence of climate change-induced warming in local streams, highlighting the importance of collecting and maintaining long-term water temperature datasets. The variability in temperature patterns across sites also stresses the importance of collecting long-term datasets at multiple locations in a region to understand how different local conditions alter the responsiveness of stream temperatures to climatic change.

Implications of thermal characteristics for steelhead trout

The study area lies near the southern range limits of anadromous southern California steelhead trout (*Oncorhynchus mykiss*), which require cool temperatures for growth and development. Water temperatures in the study area were typically warmer than the optimum temperature ranges for this species, which are generally below 15°C for most life stages (Carter, 2005). However, steelhead occur in watersheds as far south as Baja California (Moyle, 2002, cited in Myrick and Cech, 2004), and steelhead trout populations in a number of creeks in the study area, such as GV01, HO00, TE03, AT07, MC07, RS02, MC00, CP00, GB04, and RN01, have been given a high priority for steelhead recovery efforts (NMFS, 2012).

Generally, steelhead mortality is expected to be significant at temperatures exceeding 25°C (Myrick and Cech, 2001) with this threshold frequently being used as an index of the highest thermal conditions allowing steelhead survival through the warm season (e.g. Matthews and Berg, 1997; Boughton et al., 2015). The lethal threshold for steelhead throughout this region is often placed around 24°C, but higher upper thermal tolerances have been found (Myrick and Cech, 2004). In some California locations, steelhead can persist even as temperatures approach 30°C, with instantaneous maximum temperatures near this value being observed in some specific systems (Myrick and Cech, 2001; Sloat and

Osterback, 2013; Boughton et al., 2015). However, variations in reported critical thermal maxima for steelhead have been explained by the duration and level of acclimation temperatures, suggesting limited local adaptation to high temperatures within the species (Sloat and Osterback, 2013).

Throughout the Santa Barbara region, temperatures exceeding the presumed 25°C threshold for steelhead survival were observed at 15 of the 21 study sites. For 10 of these sites, the number of measurements exceeding 25°C represented a small proportion of all measurements and corresponded to less than 30 hours, and typically much less, of the entire year. The duration of individual warm events was typically less than a few hours and warm events do not occur regularly at most sites in this study. Steelhead are known to use cooler thermal refugia in pools, seeps, tributaries, or at depth, when temperatures warm to about 25°C (Nielsen et al., 1994, Brewitt and Danner, 2014; Matthews and Berg, 1997; Sloat and Osterback, 2013; Boughton et al., 2015), so the occurrence of occasional short-term warming is unlikely to exclude steelhead from most sites.

The remaining 5 sites, however, had conditions that may have been problematic for steelhead. Water temperatures at two sites, AT07 and FK00, frequently exceeded 25°C and frequently remained above this threshold for periods of 4-7 hours, accumulating hundreds of hours per year above the threshold. Average summertime maximum temperatures are often above 25°C at these sites; however, both of these sites are channelized and lack essential habitat, such as cover and pools, so habitat considerations may be more important in excluding steelhead from these sites than temperature (Thompson et al., 2012).

Temperatures at three additional sites, MC00, GV01, and DV01, may also be problematic for steelhead, with each site accumulating an estimated 77 - 92 hours per year

above 25°C. Even if each individual event exceeding the threshold is limited to a few hours or less, during which steelhead may find thermal refuge, the temperature records indicate the potential for chronic warm temperature exposure at these sites. The thermal regimes at the MC00 and GV01 locations should be a concern for natural resource managers because both are in watersheds designated as a high priority for steelhead management and restoration efforts (NMFS, 2012).

It should be noted that some of the sites were missing significant amounts of data, particularly during the warmer portions of the year, often owing to seasonal drying. Drying would also exclude fish from these sites, but gaps during the warm season when water was still present may lead to an underreporting of dangerously high temperatures, which should be considered when interpreting these results for particular research or management uses.

Wildfire Influence

Wildfires, due to natural or human causes, are an important element of the ecosystems in this region, with 15 major wildfires in Santa Barbara County between 1955 and 2016 (SB County Fire, 2016). Generally, the areal extent of wildfires and the duration of the fire season, particularly in spring and summer, are expected to increase in southwest California owing to climate and land use changes (Cayan et al., 2008; Yue et al., 2014; Keeley et al., 2016). The size and distribution of the human population, in particular, are expected to be more important than climate in determining the extent of fire in low-elevation, low-latitude portions of California (Keeley et al., 2016).

The chaparral vegetation common in the study region is highly flammable and the warm, dry climate makes wildfire inevitable, so many plant species are well-adapted to the periodic occurrence of fire and vegetation recovery may be rapid (Barro and Conard, 1991). For the

short-term, however, the loss of vegetation destabilizes hillslopes, leading to rilling and gully erosion and increased sediment deliveries downstream, which can cause significant alteration to the stream channel, increased stream flow, and a higher risk of flooding (Barro and Conard, 1991; Lavabre et al., 1993; Loaiciga et al., 2001; Benda et al., 2003; Cannon et al., 2008, Verkaik et al., 2013). In the Santa Barbara area, specifically, a study of the Maria Ygnacio watershed following the Painted Cave Fire of 1990 found that sediment transport and accumulation in the 3 years after a fire filled pools and smoothed the longitudinal and cross-sectional profiles of the channel (Keller et al., 1997). There are important implications of these fire-induced conditions for aquatic ecosystems (Verkaik et al., 2013), and some of the changes following wildfire will likely lead to changes in stream temperature.

Where the riparian vegetation burned and canopy cover was reduced, as seen in Cooper et al. (2015), increased solar radiation may lead to warmer water temperatures. In the Idaho River network, basin-scale water temperature increases were observed for over a decade after a fire, of which 9% could be attributed to light level increases after wildfire, with the remaining increases attributable to air temperature and stream flow differences (Isaak et al., 2010). In the same study, sites within fire perimeters had water temperatures much higher than basin-wide averages and 50% of that warming was attributed to light level increases after wildfire (Isaak et al., 2010). Regarding immediate effects, stream temperatures were almost 10°C higher in a stream in an area that was burning compared to a stream outside the burned area. Immediately after the fire, even though temperature minima were similar in streams in the burned and unburned areas, maximum temperatures continued to be higher in the stream in the burned area than in the stream in the unburned area (Hitt et al., 2003).

Compared to the results of these past studies, there was no consistent response of water temperature to fire in this study, probably because few of the study sites lay within wildfire footprints. Elevated stream temperatures after fire reported in the literature were primarily recorded at sites where riparian vegetation burned, reducing shading and increasing light levels. Although changes in sediment accumulation and increased stream flow downstream of fires could alter temperatures at downstream sites, the effects of these changes to stream heat budgets were probably minor compared to the effects of canopy conditions on stream temperature. Although heated water in the burned area could affect temperatures in downstream areas, this was not observed, perhaps because of the distance (up to several kilometers) between fire perimeters and several of the study sites influenced by fire. In addition, the comparative methods employed may not have been adequate to detect subtle changes in temperature regimes downstream from burned areas.

Many of the conditions that change in a stream as a result of wildfire are similar to the changes that occur due to land use, including riparian vegetation removal, changes to the sediment budget, and higher storm flows (Walsh et al., 2005). The resulting changes in stream ecosystems and water temperature are expected to be similar, except that wildfires are a short-term disturbance: the vegetation will re-grow and sediment and hydrological conditions will stabilize. Land use changes are more permanent, so resulting impacts on stream ecosystems will persist.

4.5.2. Patterns in temperature across sites

The analyses suggest that urban development elevates stream temperature, particularly in the spring and summer of most years, concordant with the results of previous studies. Pluhowski et al. (1970) found that human alterations to streams in urbanized areas of Long

Island, NY resulted in significant increases in stream temperature. Kaushal et al. (2010) found that river temperatures were increasing across the U.S (records of 24 - 98 years duration), with the greatest increases occurring in urbanizing areas, whereas an analysis of USGS data found a positive association between urban cover and both summer and winter stream temperatures (Hill et al., 2013). Rice et al. (2011) found a 0.37°C increase in summer mean temperature for each 1% increase in impermeable surface coverage in North Carolina, and Galli (1990) reported a 0.08°C increase per 1% increase in impervious cover in Maryland.

The temperature-urban cover relationships found for the study streams indicate that 1% incremental increases in impervious cover yielded similar magnitudes of temperature increase as those found in other studies, but only when the initial proportion of impervious cover was low: less than 15% impervious cover for spring maximum temperatures, less than 10% for spring and summer mean temperatures, and less than 5% for spring and summer minimum temperatures. Temperature increases resulting from 1% increases in impervious cover became smaller with higher proportions of initial impervious cover. That a relationship was found for the spring and summer but not the fall or winter may be related to seasonal changes in stream flow across sites. Fall stream flow may be very low at some typically cool sites, potentially leading to warmer temperatures in non-urban streams, and seasonal drying may limit site availability for analysis. In the winter, lower ambient temperatures, less solar radiation, and greater stream flow may lead to more uniform thermal conditions among streams, leading to weaker relationships with urban development.

Prior studies have explored pathways by which urban development influences stream temperatures. A number of studies have found that paved surfaces can lead to heated runoff,

which can lead to rapid increases in stream temperatures during summer storms (Nelson and Palmer, 2007; Rice et al., 2011; Somers et al., 2013; Sabouri et al., 2013) and modeling efforts have corroborated the physical underpinnings of these observations (Van Buren et al., 2000; Janke et al., 2008). However, the effects of runoff with high temperatures are expected to be minimal in Santa Barbara streams because most rainfall occurs during cooler times of the year. Another potential pathway of urban influence on stream temperature is through the addition of heated effluents from wastewater treatment plants, which have been shown to increase water temperatures in receiving waters in the Tokyo urban area (Kinouchi et al., 2007; Xin and Kinouchi, 2013). However, treated wastewater effluents are not discharged into Santa Barbara streams. In addition to heated wastewater effluent, Xin and Kinouchi (2013) determined that water abstractions and associated decreases in stream flow also increased summer water temperatures in Tokyo streams. Changes to stream base flows are known to be a potential consequence of urbanization (Allan, 2004). In Santa Barbara, water is not directly drawn from local streams for municipal use, but groundwater pumping, and landscape, golf course, and residential and agricultural irrigation have the potential to alter surface runoff and groundwater levels and, in turn, stream flow in local streams, particularly at sites positioned lower in the watersheds, where most development occurs.

One of the more common explanations for the impacts of urbanization on stream temperatures pertains to human impacts on riparian vegetation. It is well-known that clear-cut tree harvesting without leaving a riparian bufferstrip leads to increased stream temperatures (Moore et al., 2005). Although clear-cut forestry does not occur in Santa Barbara watersheds, the importance of riparian vegetation in reducing solar radiation inputs to streams is easily extrapolated to other land uses, including agricultural and urban

development, which have been shown to alter riparian vegetation (Webb et al., 2008). Previous urban and agricultural stream studies have highlighted the role of riparian vegetation loss in causing water temperature increases (Krause et al., 2004; Nelson and Palmer, 2007; Webb et al., 2008; Goss et al., 2014).

Although urban development has been shown to influence stream temperatures, it cannot explain all of the temporal and spatial variation in temperature, at least in some cases. In the Puget Lowlands of Washington, urbanization patterns in entire catchments were not the most important factor determining summer stream temperatures (Booth et al., 2014). In this case, stream temperatures appeared to be driven by a combination of watershed and local conditions. In this study region, factors that are potentially altered by urbanization, such as riparian vegetation and groundwater inputs, are already naturally variable across locations. By considering the results of the urban analysis along with general site characterizations and inter-site patterns in thermal signatures, some clues emerge about possible drivers of temperatures across this region.

The potential influence of canopy cover on stream temperature was illustrated by the lack of riparian vegetation at the five warmest sites, which were predominately (4 of 5) urban sites. Riparian vegetation can be locally variable, owing to different past activities and current conditions (Allan, 2004), so it is not clear that increasing urbanization always results in the loss of riparian vegetation. In Santa Barbara, some urban reaches have extensive riparian vegetation and natural channels whereas others have minimal vegetation and/or hardened banks. If riparian vegetation coverage is the main driver of local thermal regimes but is not necessarily related to urban development, which was the case for the metabolism sites described in the previous chapter, it is not clear why a relationship between stream

temperature and impervious cover exists. Although riparian vegetation coverage was apparently an important driver of thermal regimes, particularly daily maximum temperatures, across the region, it did not fully explain the relationship between temperature and urban cover in this area. Urban cover may be both an indicator of hydrological routing, that affects surface and groundwater inputs and, hence, temperature conditions, as well as a general proxy for geomorphology and local riparian vegetation cover, despite local variation in riparian conditions.

Two of the study sites in drainage basins with high urban cover, AT07 and FK00, were channelized and their thermal regimes were much different than those at other sites, being among the warmest sites with the largest daily temperature ranges. Flows through concrete channels are likely to be shallow, exposed to high solar radiation owing to a lack of riparian vegetation, and isolated from groundwater exchanges, all of which can lead to higher temperatures during the day and lower temperatures at night. The effects of channelization on stream temperature have received limited attention in the ecological literature, perhaps because such effects are usually assumed. One study, however, showed that modeled in-stream temperatures declined when concrete channels were removed (Anderson et al., 2010). At present, however, the distance downstream affected by temperature alterations in channelized reaches is unclear, but may produce altered thermal regimes in downstream natural channels with intact riparian vegetation. The relationships between urban cover and spring maximum or summer mean temperatures disappeared when channelized sites were excluded from analyses, indicating that the effect of urbanization on these metrics was driven by channelization.

Interestingly, the positive relationships between minimum stream temperatures and impervious cover were strengthened or extended when channelized sites were excluded, indicating that urbanization did affect water temperature at sites with natural channels, during the night when riparian shading influences would be minimal. Urban areas often have warmer air and surface temperatures, described as the urban heat island, which can conduct heat to shallow groundwater below urban centers (Zhu et al., 2015), perhaps explaining why increases in minimum stream temperatures were found at urban sites connected to the groundwater (i.e., sites with natural channels) rather than at sites that were disconnected from subsurface water (i.e., sites with concrete channels).

The role of riparian vegetation and other shading features in driving thermal regimes across sites is also suggested by the characteristics of the cool sites (RS02, MC07, BC02, and potentially RG09, SR04, and GB04), which were typified by high shading, either from canopy cover or steep local geomorphology. The cool thermal environments at these sites also suggest that cool groundwater inputs at higher elevations play a role in differentiating thermal regimes across locations. Except for BC02, these cooler sites are located at higher elevations than the rest of the sites and have step-pool geomorphologies with deep pools that perhaps receive groundwater inputs. Although site BC02 occurred at lower elevations than the other cool sites, it had a deep channel and a well-vegetated riparian zone. Also, this site is surrounded by agricultural land, so agricultural runoff, likely from groundwater sources, may have contributed cool water to the stream throughout the warm season. Cool temperatures throughout the day and year at all the cool sites suggest that, if fish have physical access to these sites, temperature conditions are likely to be suitable for fish survival and steelhead trout have been observed in some of these streams in the past.

However, many of these sites, except BC02, often dry seasonally, so fish habitat may become fragmented and limited to isolated pools for a portion of the year, potentially limiting steelhead survival despite appropriate temperatures. Despite the potentially confounding influence of elevation, removal of the high elevation sites from analyses still produced significant relationships between spring minimum and mean temperatures, and summer minimum temperature, versus impervious cover.

Sites EL00, HO00, and ON02 with low seasonal variability in temperature and cooler summer temperatures compared to other sites also likely provide good thermal environments for steelhead. These sites are located at the west end of the study area at low elevations, suggesting that their low thermal variability may result from significant groundwater inputs, as well as riparian or geomorphic shading. HO00 has both extremely low daily and intra-annual variability, probably owing to a combination of groundwater inputs and extensive shading, and is known to support healthy steelhead populations.

To fully understand variation in temperature among sites, additional information about each site is necessary, such as information on canopy conditions, groundwater inputs, atmospheric heat exchange, basin aspect, flow depth and velocity, channel geomorphology, and slope. Additional integrative analysis of this dataset and other datasets, such as those for air temperature and cloud cover, may provide context and explanations for the temperature results. Information needed to calculate heat budgets for each of the study sites was not available, but the temperature data, themselves, provide directions for useful future research.

4.6. Conclusion

Water temperatures generally reflected air temperatures in the study area. For most study sites, temperatures rarely or never exceeded upper thermal thresholds for steelhead trout,

indicating that temperature was unlikely to limit the abundance or distribution of steelhead in most Santa Barbara streams. Although there were positive relationships between urban land cover versus spring and summer minimum and spring mean stream temperatures, these relationships were often not observed at other times of the year. Channelized sections of urban study streams exhibited extremely high temperatures and large daily temperature variation. Differences in thermal characteristics across the sites suggest, but do not confirm, that cover by riparian vegetation and groundwater inputs likely play a significant role in determining temperature variation across sites. In general, a more detailed analysis of local temperature data, combined with additional data needed to calculate heat budgets and to provide an environmental context for measurements, can improve our understanding of spatial variability in temperature regimes.

This analysis addresses a gap in our knowledge of the role of land use in determining stream temperatures in areas with Mediterranean climates. Locally, this dataset provides background on thermal patterns across the area and demonstrates the dynamic nature of stream temperature, confirming the importance of frequently collect temperature data over long periods of time. Long-term data collection across a wide range of sites is critical to furthering our understanding of how water temperatures change in response to interacting stressors such as land use and climate change. Although this dataset has gaps and requires additional considerations for some sites, data collection is ongoing at some of the sites (AB00, BC02, GV01, HO00, MC00, RG01, and RS02) and this analysis provides a foundation for future analyses of an increasingly valuable dataset.

4.7. References

Allan, J.D. 2004. Landscapes and riverscapes: The influence of land use on stream ecosystems. Annual Review of Ecology, Evolution, and Systematics 35: 257-284.

Anderson, W.P., J.L. Anderson, C.S. Thaxton, and C.M. Babyak. 2010. Changes in stream temperatures in response to restoration of groundwater discharge and solar heating in a culverted, urban stream. Journal of Hydrology 393: 309-320.

Arismendi, I., S.L. Johnson, J.B. Dunham, and R. Haggerty. 2012. The paradox of cooling streams in a warming world: Regional climate trends do not parallel variable local trends in stream temperature in the Pacific continental United States. Geophysical Research Letters 39: L10401. doi: 10.1029/2012GL051448

Barro, S.C. and S.G. Conard. 1991. Fire effects on California chaparral systems: An overview. Environment International 17: 135-149.

Benda, L., D. Miller, P. Bigelow, and K. Andras. 2003. Effects of post-wildfire erosion on channel environments, Boise River, Idaho. Forest Ecology and Management 178: 105-119.

Benson, B.B. and D. Krause. 1980. The concentration and isotopic fractionation of gases dissolved in freshwater in equilibrium with the atmosphere. 1. Oxygen. Limnology and Oceanography 25: 662-671.

Boughton D.A., L.R. Harrison, A.S. Pike, J.L Arriaza, and M. Mangel. 2015. Thermal potential for steelhead life history expression in a southern California alluvial river. Transactions of the American Fisheries Society 144: 258-273. doi: 10.1080/00028487.2014.986338

Booth D.B., K.A. Kraseski, and C.R. Jackson. 2014. Local-scale and watershed-scale determinants of summertime urban stream temperatures. Hydrological Processes 28: 2427-2438. doi: 10.1002/hyp.9810

Brewitt, K.S. and E.M. Danner. 2014. Spatio-temporal temperature variation influences juvenile steelhead (*Oncorhynchus mykiss*) use of thermal refuges. Ecosphere 5:92. http://dx.doi.org/10.1890/ES14-00036.1

Cairns, J., A.G. Heath, and B.C. Parker. 1975. The effects of temperature upon the toxicity of chemicals to aquatic organisms. Hydrobiologia 47: 135-171.

Cannon, S.H., J.E. Gartner, R.C. Wilson, J.C. Bowers, and J.L. Laber. 2008. Storm rainfall conditions for floods and debris flows from recently burned areas in southern Colorado and southern California. Geomorphology 96: 250-269.

Carter, K. 2005. The Effects of Temperature on Steelhead Trout, Coho Salmon, and Chinook Salmon Biology and Function by Life Stages: Implications for Klamath Basin TMDLs. California Regional Water Quality Control Board, North Coast Region. 26p.

Cayan, D.R., E.P. Maurer, M.D. Dettinger, M. Tyree, and K. Hayhoe. 2008. Climate change scenarios for the California region. Climate Change 87(Suppl 1): S21-S42.

Cooper, S.D., P.S. Lake, S. Sabater, J.M. Melack, and J.L. Sabo. 2013. The effects of land use changes on streams and rivers in Mediterranean climates. Hydrobiologia 719:383-425.

Cooper, S.D., H.M. Page, S.W. Wiseman, K. Klose, D. Bennett, T. Even, S. Sadro, C.E. Nelson, and T.L. Dudley. 2015. Physicochemical and biological responses of streams to wildfire severity in riparian zones. Freshwater Biology 60: 2600-2619.

County of Santa Barbara, Department of Public Works Water Resources Hydrology. September 2017a. Official monthly and yearly rainfall record, station 234. Accessed October 25, 2017. http://www.countyofsb.org/pwd/water/downloads/hydro/234mdd.pdf
County of Santa Barbara, Department of Public Works Water Resources Hydrology. September 2017b. Driest consecutive years – Santa Barbara, 118 years of rainfall (1900-2017). Accessed November 13, 2017. http://www.countyofsb.org/uploadedFiles/pwd/Content/Water/Documents/Historical%20Driest%20Four%20Consecutive%20Years.pdf
County of Santa Barbara, Department of Public Works Water Resources Hydrology. September 2017c. Historical Driest Years. Accessed November 13, 2017. http://www.countyofsb.org/uploadedFiles/pwd/Content/Water/Documents/Historical%20Driest%20Years.pdf
Demars, B.O.L., J.R. Manson, J.S. Olafsson, G.M. Gislason, R.Gudmundsdottir, G. Woodward, J. Reiss, D.E. Pichler, J.J. Rasmussen, and N. Friberg. 2011. Temperature and the metabolic balance of streams. Freshwater Biology 56: 1106-1121.
Felipe, A.F., J.E. Lawrence, and N. Bonada. 2013. Vulnerability of stream biota to climate change in mediterranean climate regions: a synthesis of ecological responses and conservation challenges. Hydrobiologia 719: 331-352.
Galli, J. 1990. Thermal impacts associated with urbanization and stormwater management best management practices. Metropolitan Washington Council of Governments, Maryland Department of Environment, Washington, D.C. pp. 157. Accessed on October 4, 2017. https://www.mwcog.org/documents/1990/12/12/thermal-impacts-associated-with-urbanization-and-stormwater-management-best-management-practices/
Gillooly, J.F., J.H. Brown, G.B. West, V.M. Savage, and E.L. Chamov. 2001. Effects of size and temperature on metabolic rate. Science 293:2248-2251.
Goss, C.W., P.C. Goebel, S. Mazeika, and P. Sullivan. 2014. Shifts in attributes along agriculture-forest transitions of two streams in central Ohio, USA. Agriculture, Ecosystems, and Environment 197: 106-117.
Hawkins, C.P., J.N. Hogue, L.M. Decker, and J.W. Feminella. 1997. Channel morphology, water temperature, and assemblage structure of stream insects. Journal of the North American Benthological Society 16:728-749.
Hill, R.A., C.P. Hawkins, and D.M. Carlisle. 2013. Predicting thermal reference conditions for USA streams and rivers. Freshwater Science 32: 39-55. https://doi.org/10.1899/12-009.1
Hitt, N.P. 2003. Immediate effects of wildfire on stream temperature. Journal of Freshwater Ecology 18: 171-173.
Isaak, D.J., C. H. Luce, B. E. Rieman, D.E. Nagel, E.E. Peterson, D.L. Horan, S. Parkes, and G. L. Chandler. 2010. Effects of climate change and wildfire on stream temperatures and salmonid thermal habitat in a mountain river network. Ecological Applications 20: 1350-1371.
Janke B.D., W.R. Herb, O. Mohseni, and H.G. Stefan. 2009. Simulation of heat export by rainfall-runoff from a paved surface. Journal of Hydrology 365: 195-212. doi: 10.1016/j.jhydrol.2008.11.019
Kaushal, S.S., G.E. Likens, N.A. Jaworski, M.L. Pace, A.M. Sides, D. Seekell, K.T. Belt, D.H. Secor, and R.L. Wingate. 2010. Rising stream and river temperature in the United

States. Frontiers in Ecology and the Environment 8: 461-466. http://www.jstor.org/stable/29546160
Keeley, J.E. and A.D. Syphard. 2016. Climate change and future fire regimes: Examples from California. Geosciences 6. Doi: 10.3390/geosciences6030037
Keller, E.A., D.W. Valentine, and D.R. Gibbs. 1997. Hydrological response of small watersheds following the southern California Painted Cave Fire of June 1990. Hydrological Processes 11: 401-414.
Kinouchi, T., H. Yagi, and M. Miyamoto. 2007. Increase in stream temperature related to anthropogenic heat input from urban wastewater. Journal of Hydrology 335: 78-88. doi: 10.1016/j.jhydrol.2006.11.002
Krause, C.W., B. Lockard, T.J. Newcomb, D. Kibler, V. Lohani, and D.J. Orth. 2004. Predicting influences of urban development on thermal habitat in a warm water stream. Journal of the American Water Resources Association. 40: 1645-1658.
Lavabre, J., D.S. Torres, and F. Cernesson. 1993. Changes in the hydrological response of a small Mediterranean basin a year after a wildfire. Journal of Hydrology 142: 273-299.
Loáiciga, H.A., D. Pederos, and D.Roberts. 2001. Wildfire-streamflow interactions in a chaparral watershed. Advances in Environmental Research 5:295-305.
Matthews, K.R. and N.H. Berg. 1997. Rainbow trout responses to water temperature and dissolved oxygen stress in two southern California stream pools. Journal of Fish Biology 50: 50-67.
Moore, R.D., D.L. Spittlehouse, and A. Story. 2005. Riparian microclimate and stream temperature response to forest harvesting: a review. Journal of the American Water Resources Association 41: 813-834.
Myers, M.R., D.R. Cayan, S.F. Iacobellis, J.M. Melack, R.E. Beighley, P.L. Barnard, J.E. Dugan, and H.M. Page. 2017. Santa Barbara Coastal Ecosystem Vulnerability Assessment. CASG-17-009.
Myrick, C.A. and J.J. Cech. 2001. Temperature effects on Chinook salmon and steelhead: a review focusing on California's Central Valley populations. Bay-Delta Modeling Forum. Technical Publication 01-1.57pp. Accessed online on October 4, 2017 www.cwemf.org/Pubs/TempReview.pdf
Myrick, C.A. and J.J. Cech . 2004. Temperature effects on juvenile anadromous salmonids in California's central valley: what don't we know? Reviews in Fish Biology and Fisheries 14: 113-123.
National Marine Fisheries Service. 2012. Southern California Steelhead Recovery Plan Summary. Accessed online October 4, 2017 http://www.westcoast.fisheries.noaa.gov/publications/recovery_planning/salmon_steelhead/domains/south_central_southern_california/southern_california_steelhead_recovery_plan_executive_summary_012712.pdf
Nelson, K.C. and M.C. Palmer. 2007. Stream temperature surges under urbanization and climate change: Data, models, and responses. Journal of the American Water Resources Association. 43:440-452.
Nielsen J.L., T.E. Lisle, and V. Ozaki. 1994. Stratified pools and their use by steelhead in northern California streams. Transactions of the American Fisheries Society 123: 613-626.

Null, S.E., J.H. Viers, M.L. Deas, S.K. Tanaka, and J.F. Mount. 2013. Stream temperature sensitivity to climate warming in California's Sierra Nevada: impacts to coldwater habitat. Climatic Change 116: 149-170. doi: 10.1007/s10584-012-0459-8

Paul, M.J., and J.L. Meyer. 2001. Streams in the urban landscape. Annual Review of Ecology and Systematics 32: 333-365.

Pluhowski, E.J. 1970. Urbanization and its effect on the temperature of streams in Long Island, New York. USGS Professional Paper 627-D.

Rice, J.S., W.P. Anderson, Jr., and C.S. Thaxton. 2011. Urbanization influences on stream temperature behavior within low-discharge headwater streams. Hydrological Research Letters 5: 27-31. doi: 10.3178/HRL.5.27

Robinson, T.H., A. Leydecker, J.M. Melack, and A.A. Keller. 2005. Steps toward modeling nutrient export in coastal Californian streams with a Mediterranean climate. Agricultural Water Management 77:144-158.

Sabouri, F., B Gharabaghi, A.A. Mahboubi, and E.A. McBean. 2013. Impervious surfaces and sewer pipe effects on stormwater runoff temperature. Journal of Hydrology 502:10-17. http://dx.doi.org/10.1016/j.jhydrol.2013.08.016

Santa Barbara County Fire Department. August 3, 2016. Major wildfires in Santa Barbara County 1955-2016. Accessed October 3, 2017. http://www.sbcfire.com/major-wildfires-in-santa-barbara-county-1955-2016/

Sloat, M.R. and A.K. Osterback. 2013. Maximum stream temperature and the occurrence, abundance, and behavior of steelhead trout (*Oncorhynchus mykiss*) in a southern California stream. Canadian Journal of Fisheries and Aquatic Sciences 70:64-73. dx.doi.org/10.1139/cjfas-2012-0228

Somers, K.A., E.S. Bernhardt, J.B. Grace, B.A. Hassett, E.B. Sudduth, S. Wang, and D.L. Urban. 2013. Streams in the urban heat island: spatial and temporal variability in temperature. Freshwater Science 32: 309-326. http://dx/doi/org/10.1899/12-046.1

Thompson, L.C., J.L. Voss, R.E. Larsen, W.D. Tietje, R.A. Cooper, and P.B. Moyle. 2012. Southern steelhead, hard woody debris, and temperature in a California central coast watershed. Transactions of the American Fisheries Society 141:275-284.

Van Buren, M.A., W.E. Watt, J. Marsalek, and B.C. Anderson. 2000. Thermal enhancement of storwmwater runoff by paved surfaces. Water Research 34: 1359-1371.

Verkaik, I., M. Rieradevall, S.D. Cooper, J.M. Melack, T.L. Dudley, N. Prat. 2013. Fire as a disturbance in Mediterranean climate streams. Hydrobiologia 719: 353-382. DOI 10.1007/s10750-013-1463-3.

Walsh, C.J., A.H. Roy, J.W. Feminella, P.D. Cottingham, P.M. Groffman, and R.P. Morgan II. 2005. The urban stream syndrome: current knowledge and the search for a cure. Journal of the North American Benthological Society 24: 706-723.

Warton, D.I. and F.K.C. Hui. 2011. The arcsine is asinine: the analysis of proportions in ecology. Ecology, 92: 3-10.

Webb, B.W. 1996. Trends in stream and river temperature. Hydrological Processes 10: 205-226.

Webb, B.W., D.M. Hannah, R.D. Moore, L.E. Brown, and F. Nobilis. 2008. Recent advances in stream and river temperature research. Hydrological Processes 22: 902-918. Doi: 10.1002/hyp.6994

Xin, Z. and T. Kinouchi. 2013. Analysis of stream temperature and heat budget in an urban river under strong anthropogenic influences. Journal of Hydrology 489: 16-25. http://dx.doi.org/10.1016/j.jhydrol.2013.02.048

Yue, X., L.J. Mickley, and J.A. Logan. 2014. Projection of wildfire activity in southern California in the mid-21st century. Climate Dynamics 43: 1973-1991. Doi: 10.1007/s00382-013-2022-3.

Zhu, K., P. Bayer, P. Grathwohl, and P. Bunn. 2015. Groundwater temperature evolution in the subsurface urban heat island of Cologne, Germany. Hydrological Processes 29: 965-978.

Appendix I: Metabolism site maps

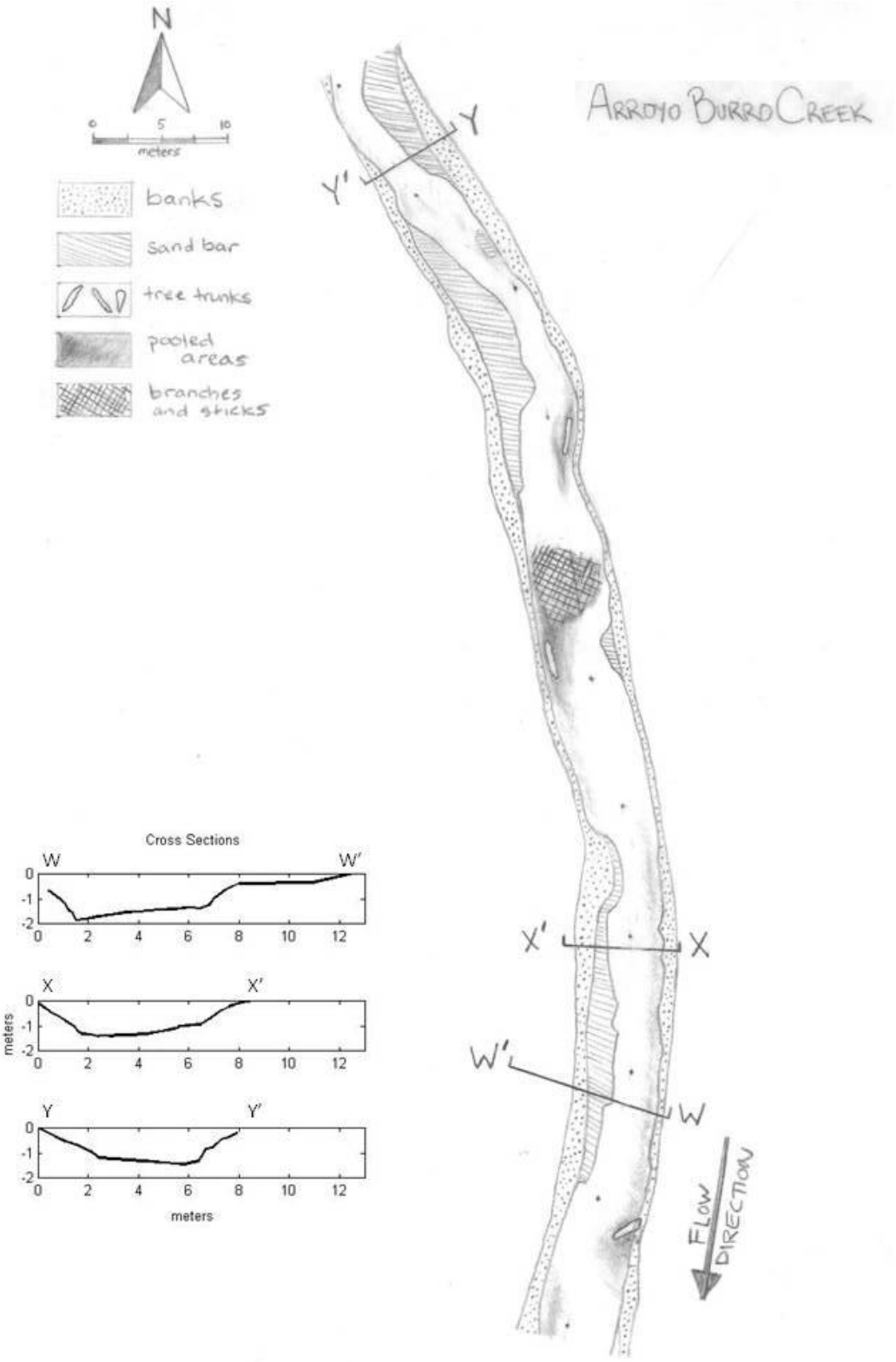

Appendix I: Metabolism site maps (continued)

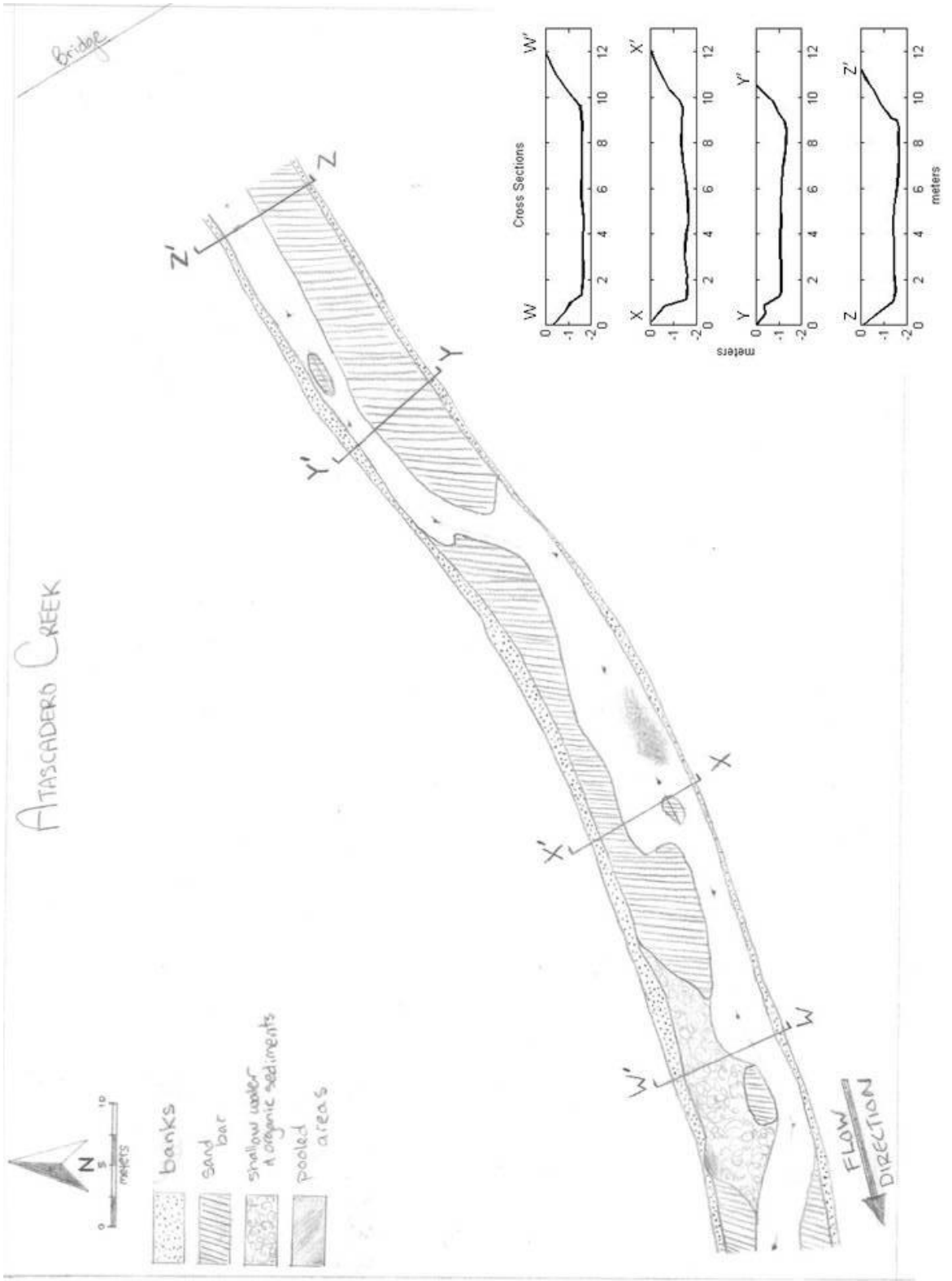

Appendix I: Metabolism site maps (continued)

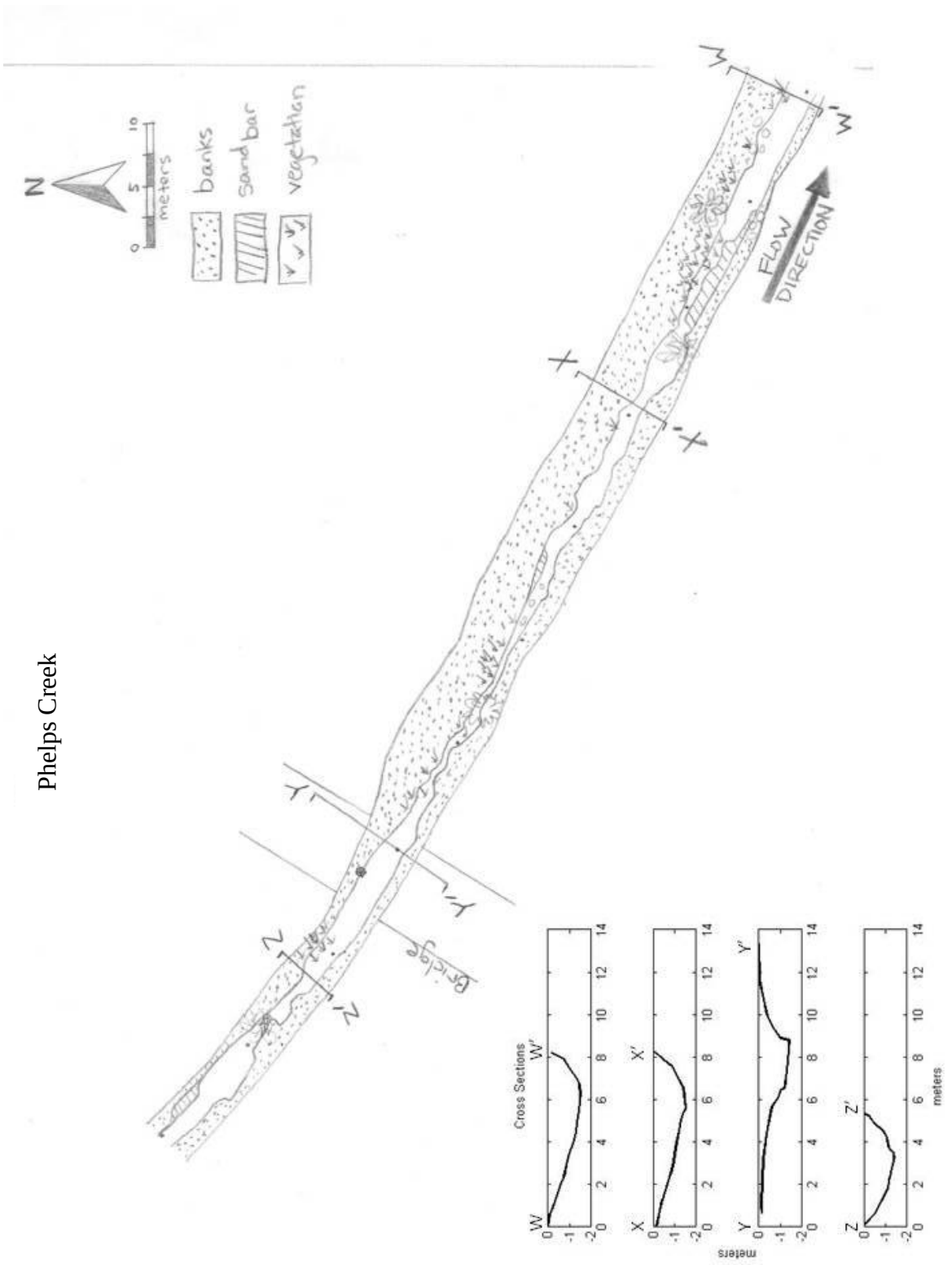

Appendix I: Metabolism site maps (continued)

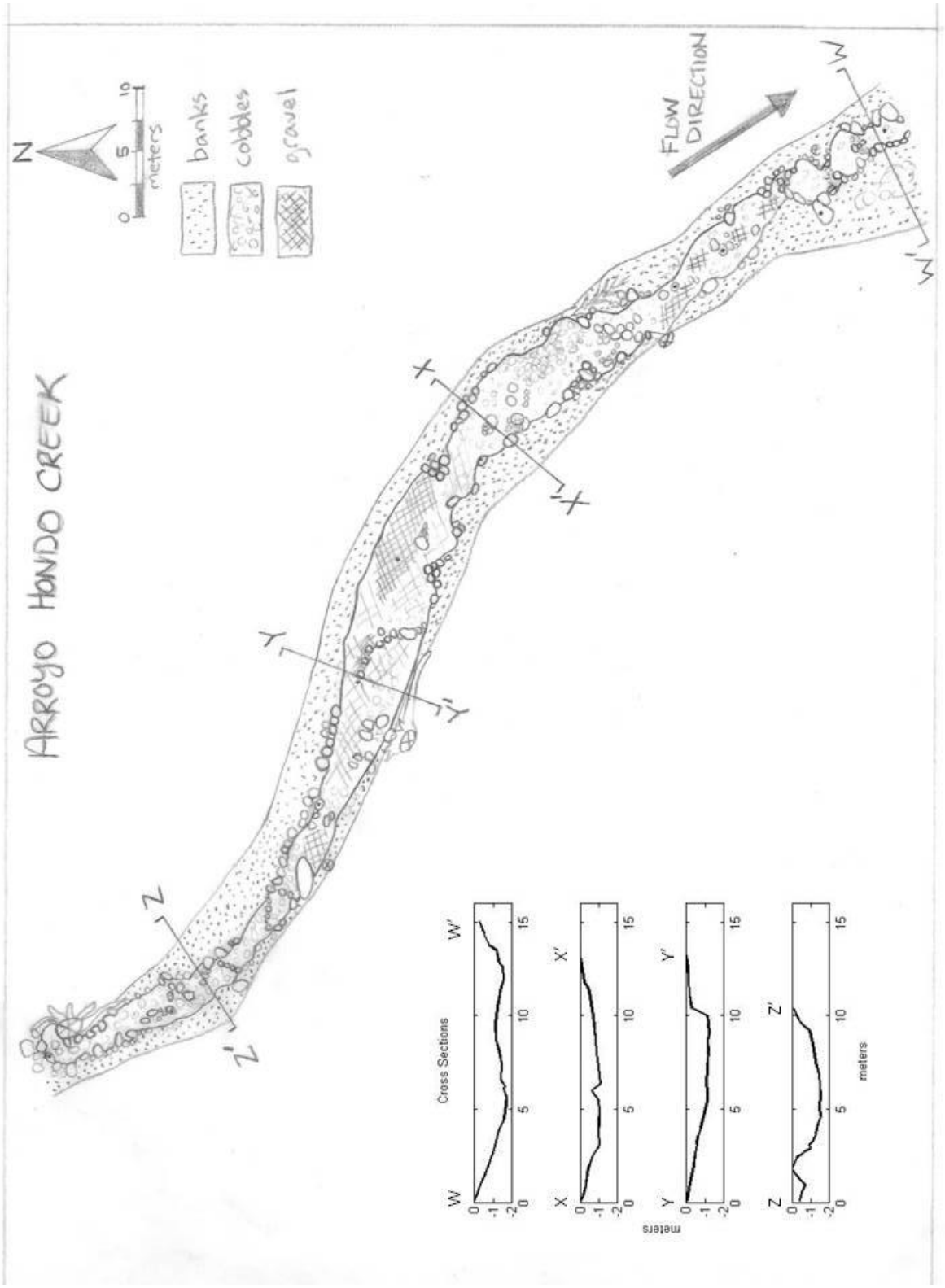

Appendix I: Metabolism site maps (continued)

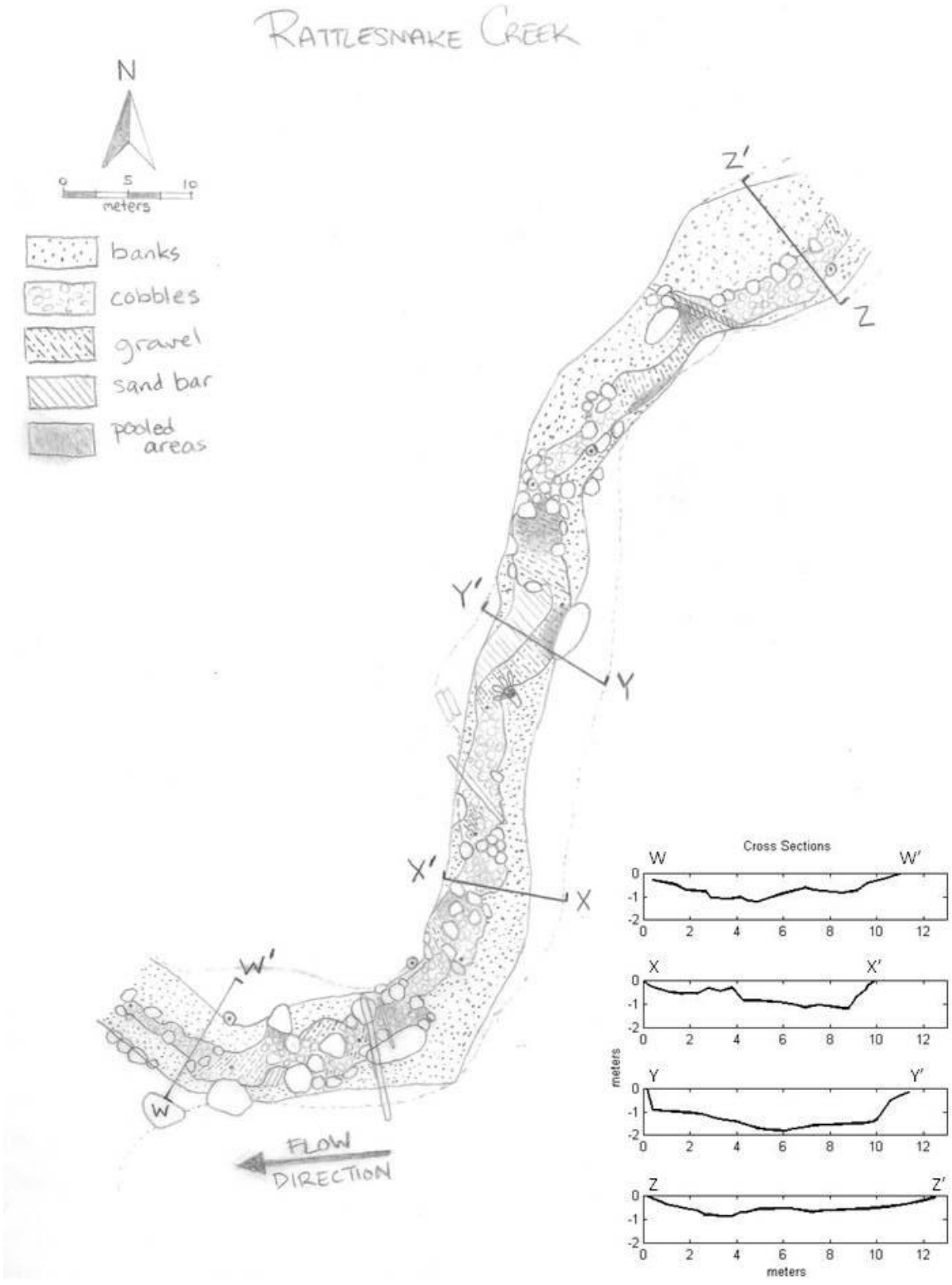

Appendix I: Metabolism site maps (continued)

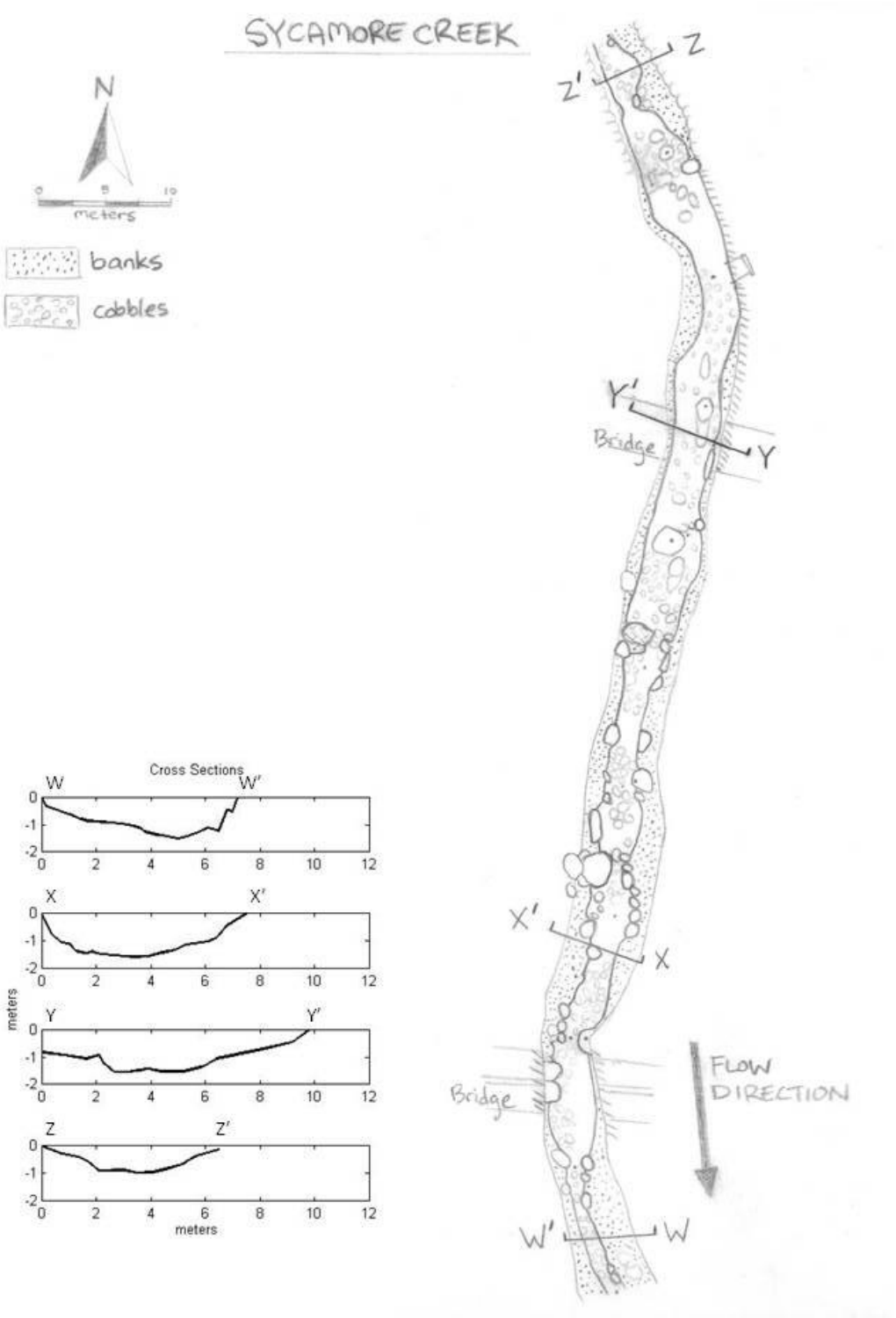

Appendix II: Daily metabolism data

Arroyo Burro Creek daily data

	Date	Day of year	Metabolism				Dissolved Oxygen				PAR	
			GPP	CR	NEP	P/R	Mean	Minimum	Maximum	Range	Peak	Total
			g O_2 m^{-2} d^{-1}	g O_2 m^{-2} d^{-1}	g O_2 m^{-2} d^{-1}	unitless	mg L^{-1}	mg L^{-1}	mg L^{-1}	mg L^{-1}	µmol photons m^{-2} s^{-1}	mol photons m^{-2} d^{-1}
Deployment 1	March 17, 2014	76	3.2	-3.4	-0.2	0.9	10.0	6.6	22.9	16.3	665	5.86
	March 18, 2014	77	5.2	-4.4	0.8	1.2	11.1	5.7	31.6	26.0	481	5.37
	March 19, 2014	78	6.1	-5.3	0.8	1.2	10.6	4.6	31.9	27.4	542	5.37
Deployment 2	April 8, 2014	98	3.2	-3.4	-0.2	0.9	8.6	4.7	23.1	18.4	853	5.07
	April 9, 2014	99	2.5	-3.4	-0.8	0.8	8.0	6.0	12.5	6.6	1139	4.64
	April 10, 2014	100	2.8	-3.3	-0.4	0.9	8.5	5.8	13.5	7.7	331	3.71
Deployment 3	April 29, 2014	119	2.3	-3.6	-1.3	0.6	7.0	5.1	11.1	6.0	1142	4.61
	April 30, 2014	120	1.5	-2.6	-1.0	0.6	7.7	5.1	15.6	10.5	689	3.96
	May 1, 2014	121	2.9	-3.7	-0.8	0.8	7.6	4.2	20.7	16.5	608	3.71
Deployment 4	May 30, 2014	150	3.2	-4.6	-1.5	0.7	6.6	4.1	11.0	6.9	1432	4.44
	May 31, 2014	151	3.0	-4.4	-1.4	0.7	6.5	3.9	14.0	10.1	1363	4.63
	June 1, 2014	152	3.4	-4.8	-1.4	0.7	6.4	3.3	18.4	15.1	1496	4.71
	June 2, 2014	153	4.1	-5.4	-1.3	0.8	7.0	3.3	23.5	20.3	1500	4.62
	June 3, 2014	154	4.2	-5.0	-0.8	0.8	7.1	2.8	27.3	24.4	1530	5.06
	June 4, 2014	155	3.4	-4.4	-1.0	0.8	7.1	4.0	13.3	9.3	1532	5.00
Deployment 5	June 25, 2014	176	4.2	-5.6	-1.4	0.8	7.4	4.1	18.6	14.5	1205	5.81
	June 26, 2014	177	4.2	-4.9	-0.7	0.9	7.0	2.6	27.3	24.7	1188	5.50
	June 27, 2014	178	4.1	-4.9	-0.9	0.8	7.4	3.2	27.5	24.3	1461	5.73
	June 28, 2014	179	3.6	-4.6	-1.1	0.8	6.9	3.1	19.1	16.0	1388	5.87
Deployment 6	July 16, 2014	197	3.1	-4.3	-1.1	0.7	6.7	3.2	12.1	8.9	77	2.22
	July 17, 2014	198	4.1	-4.3	-0.2	1.0	8.2	3.4	25.7	22.3	1474	4.92
	July 18, 2014	199	3.0	-4.0	-1.0	0.8	7.4	4.2	13.8	9.7	1513	5.07

Arroyo Burro Creek daily data (continued)

	Date	Day of Year	T1 logger Temperature				T2 logger Temperature				Toxy logger Temperature			
			Mean	Minimum	Maximum	Range	Mean	Minimum	Maximum	Range	Mean	Minimum	Maximum	Range
			°C	°C	°C	°C	°C	°C	°C	°C	°C	°C	°C	°C
Deployment 1	March 17, 2014	76	15.3	13.5	17.6	4.1	15.2	13.6	17.7	4.1	15.3	13.4	18.0	4.6
	March 18, 2014	77	14.8	13.0	17.1	4.1	14.8	13.1	16.9	3.8	14.8	12.9	17.3	4.4
	March 19, 2014	78	14.4	12.5	16.7	4.2	14.5	12.6	16.8	4.2	14.5	12.4	17.1	4.8
Deployment 2	April 8, 2014	98	14.9	12.8	17.1	4.2	14.9	12.9	17.5	4.6	14.9	12.6	17.6	5.0
	April 9, 2014	99	15.6	13.7	17.4	3.7	15.7	14.1	18.0	3.9	15.6	13.6	17.9	4.3
	April 10, 2014	100	15.1	14.3	15.9	1.6	15.2	14.4	16.2	1.8	15.1	14.1	16.0	1.8
Deployment 3	April 29, 2014	119	16.5	14.6	18.6	4.0	16.8	14.6	19.9	5.4	16.8	14.4	19.8	5.4
	April 30, 2014	120	16.4	14.4	18.7	4.4	16.8	14.2	20.4	6.2	16.8	14.0	20.1	6.1
	May 1, 2014	121	16.6	14.6	18.8	4.2	17.0	14.5	20.1	5.6	16.9	14.2	20.3	6.0
Deployment 4	May 30, 2014	150	17.8	15.9	20.1	4.2	18.0	16.2	20.7	4.6	17.9	15.9	20.5	4.6
	May 31, 2014	151	18.0	16.4	20.1	3.7	18.2	16.6	21.2	4.6	18.1	16.4	20.6	4.2
	June 1, 2014	152	17.7	15.9	19.8	3.9	17.9	16.2	20.7	4.6	17.8	15.9	20.1	4.2
	June 2, 2014	153	17.6	16.3	19.7	3.4	17.8	16.5	20.8	4.3	17.7	16.2	20.1	3.9
	June 3, 2014	154	17.4	15.6	19.8	4.2	17.7	15.8	20.9	5.0	17.6	15.6	20.2	4.6
	June 4, 2014	155	17.4	15.7	19.7	4.0	17.6	15.8	20.8	5.0	17.5	15.6	20.0	4.4
Deployment 5	June 25, 2014	176	18.5	16.5	21.0	4.5	18.6	16.7	21.2	4.5	18.5	16.6	20.9	4.4
	June 26, 2014	177	19.2	17.4	21.7	4.3	19.3	17.6	21.9	4.3	19.3	17.4	21.6	4.3
	June 27, 2014	178	19.6	18.1	21.6	3.5	19.8	18.1	22.4	4.3	19.8	18.1	22.0	3.9
	June 28, 2014	179	19.3	17.9	21.2	3.3	19.8	18.1	22.3	4.2	19.6	17.9	21.7	3.8
Deployment 6	July 16, 2014	197	19.9	19.5	20.5	1.0	20.1	19.7	20.7	1.0	20.0	19.5	20.5	1.0
	July 17, 2014	198	19.3	17.5	21.7	4.2	19.6	17.7	22.7	5.0	19.4	17.5	21.7	4.2
	July 18, 2014	199	19.3	17.7	21.4	3.7	19.6	17.8	22.3	4.5	19.5	17.7	21.7	4.0

Appendix II: Daily metabolism data (continued)

Atascadero Creek daily data

	Date	Day of year	Metabolism				Dissolved Oxygen				PAR	
			GPP	CR	NEP	P/R	Mean	Minimum	Maximum	Range	Peak	Total
			g O_2 m^{-2} d^{-1}	g O_2 m^{-2} d^{-1}	g O_2 m^{-2} d^{-1}	unitless	mg L^{-1}	mg L^{-1}	mg L^{-1}	mg L^{-1}	µmol photons m^{-2} s^{-1}	mol photons m^{-2} d^{-1}
Deployment 1	March 11, 2014	70	0.2	-3.6	-3.4	0.1	2.4	1.3	7.6	6.4	1016	11.01
	March 12, 2014	71	1.0	-3.8	-2.8	0.3	2.9	0.4	6.1	5.6	1420	15.00
	March 13, 2014	72	1.1	-3.9	-2.7	0.3	3.7	2.1	7.6	5.5	1403	15.48
Deployment 2	April 3, 2014	93	1.9	-4.2	-2.3	0.5	4.8	1.8	14.0	12.2	1625	23.91
	April 4, 2014	94	2.4	-4.7	-2.3	0.5	4.8	1.0	17.1	16.1	1577	20.81
	April 5, 2014	95	3.1	-4.8	-1.7	0.6	6.3	0.4	25.7	25.3	1604	25.17
Deployment 3	April 22, 2014	112	2.1	-4.3	-2.2	0.5	4.6	1.4	9.9	8.5	1626	29.11
	April 23, 2014	113	2.8	-4.9	-2.0	0.6	5.0	0.6	11.8	11.2	1576	28.00
	April 24, 2014	114	3.2	-4.8	-1.7	0.7	5.9	0.6	16.0	15.3	1535	27.96
Deployment 4	May 20, 2014	140	4.2	-5.7	-1.5	0.7	5.4	1.1	12.7	11.6	1780	32.28
	May 21, 2014	141	2.9	-4.5	-1.6	0.6	5.6	0.8	12.8	12.0	1717	34.94
	May 22, 2014	142	3.0	-4.9	-1.9	0.6	5.2	1.4	11.2	9.9	1615	20.04
	May 23, 2014	143	3.1	-4.6	-1.5	0.7	5.9	2.0	12.3	10.4	1693	30.74
Deployment 5	June 13, 2014	164	2.6	-4.3	-1.7	0.6	5.7	2.8	11.6	8.8	1737	25.39
	June 14, 2014	165	3.5	-5.0	-1.6	0.7	5.8	2.3	12.7	10.3	1805	35.91
	June 15, 2014	166	2.8	-4.7	-1.9	0.6	5.4	1.7	12.6	10.8	1751	28.36
	June 16, 2014	167	3.3	-4.4	-1.1	0.7	6.0	0.5	13.2	12.7	1720	35.31
	June 17, 2014	168	3.0	-4.8	-1.8	0.6	5.6	0.5	12.3	11.8	1734	35.67
Deployment 6	July 8, 2014	189	2.3	-4.6	-2.4	0.5	4.2	0.8	9.3	8.5	1711	34.74
	July 9, 2014	190	2.5	-4.5	-2.0	0.6	4.8	2.2	10.1	7.9	1713	29.41
	July 10, 2014	191	2.3	-4.3	-1.9	0.5	4.8	2.1	10.0	7.9	1702	19.57

Atascadero Creek daily data (continued)

	Date	Day of Year	T1 logger Temperature				T2 logger Temperature				Toxy logger Temperature			
			Mean	Minimum	Maximum	Range	Mean	Minimum	Maximum	Range	Mean	Minimum	Maximum	Range
			°C	°C	°C	°C	°C	°C	°C	°C	°C	°C	°C	°C
Deployment 1	March 11, 2014	70	17.4	12.6	21.2	8.5	17.1	12.6	20.3	7.7	17.3	12.6	20.9	8.3
	March 12, 2014	71	15.6	12.0	19.8	7.8	14.8	12.5	16.9	4.4	15.5	12.0	19.5	7.5
	March 13, 2014	72	15.6	12.7	18.9	6.2	14.8	12.9	16.6	3.7	15.4	12.7	18.6	5.9
Deployment 2	April 3, 2014	93	14.7	11.3	18.2	7.0	13.5	11.0	15.8	4.8	14.5	11.0	18.3	7.3
	April 4, 2014	94	15.4	12.7	18.5	5.8	14.7	12.1	16.8	4.7	15.1	12.4	18.6	6.2
	April 5, 2014	95	15.4	12.5	18.9	6.5	14.3	12.1	16.5	4.4	15.2	12.2	19.3	7.1
Deployment 3	April 22, 2014	112	17.9	15.5	20.9	5.4	17.5	15.5	19.7	4.2	17.8	15.2	21.4	6.1
	April 23, 2014	113	17.1	14.5	20.1	5.6	16.6	14.2	18.6	4.4	17.1	14.1	20.5	6.4
	April 24, 2014	114	17.4	14.8	20.2	5.4	16.8	14.5	18.8	4.3	17.4	14.5	20.8	6.3
Deployment 4	May 20, 2014	140	19.6	17.3	22.5	5.2	19.5	17.2	22.2	4.9	19.4	17.1	22.6	5.6
	May 21, 2014	141	19.4	17.0	22.8	5.8	19.2	17.0	21.7	4.7	19.3	16.8	22.9	6.2
	May 22, 2014	142	19.1	17.2	21.7	4.5	19.5	17.3	21.3	4.0	18.9	16.9	21.5	4.6
	May 23, 2014	143	19.4	16.6	22.6	6.0	19.5	16.9	21.8	4.9	19.2	16.4	22.9	6.5
Deployment 5	June 13, 2014	164	18.9	17.0	22.1	5.2	--	--	--	--	18.8	16.8	21.8	5.1
	June 14, 2014	165	19.6	17.1	23.2	6.2	--	--	--	--	19.5	16.8	23.0	6.2
	June 15, 2014	166	20.1	18.4	23.4	5.0	--	--	--	--	20.1	18.3	23.3	5.0
	June 16, 2014	167	20.0	17.6	23.6	6.0	--	--	--	--	19.9	17.3	23.6	6.3
	June 17, 2014	168	20.0	17.6	23.3	5.7	--	--	--	--	19.9	17.1	23.5	6.4
Deployment 6	July 8, 2014	189	21.9	20.1	24.6	4.5	21.8	19.8	24.7	4.9	22.2	19.9	26.0	6.1
	July 9, 2014	190	22.0	20.4	24.4	4.0	21.9	20.2	24.5	4.3	22.0	20.1	25.2	5.2
	July 10, 2014	191	21.3	20.2	23.4	3.2	21.2	20.0	23.0	3.0	21.3	19.9	24.3	4.3

Appendix II: Daily metabolism data (continued)

Phelps Creek daily data

	Date	Day of year	Metabolism				Dissolved Oxygen				PAR	
			GPP	CR	NEP	P/R	Mean	Minimum	Maximum	Range	Peak	Total
			g O_2 m^{-2} d^{-1}	g O_2 m^{-2} d^{-1}	g O_2 m^{-2} d^{-1}	unitless	mg L^{-1}	mg L^{-1}	mg L^{-1}	mg L^{-1}	µmol photons s^{-1} m^{-2}	mol photons d^{-1} m^{-2}
Deployment 1	March 11, 2014	70	0.3	-2.6	-2.3	0.1	4.4	3.3	5.1	1.8	588	6.30
	March 12, 2014	71	0.6	-3.0	-2.4	0.2	4.6	3.4	5.5	2.2	711	5.87
	March 13, 2014	72	0.5	-2.8	-2.3	0.2	4.6	3.7	5.7	2.0	616	5.20
	March 14, 2014	73	0.6	-2.8	-2.2	0.2	4.8	3.7	6.0	2.3	512	5.89
	March 15, 2014	74	0.7	-3.4	-2.7	0.2	4.1	3.2	6.3	3.1	785	5.64
	March 16, 2014	75	0.7	-3.2	-2.5	0.2	3.9	3.0	6.7	3.7	549	5.49
Deployment 2	April 3, 2014	93	1.4	-3.8	-2.4	0.4	4.5	2.8	6.9	4.1	541	5.10
	April 4, 2014	94	1.4	-4.0	-2.5	0.4	4.3	2.6	7.1	4.5	791	5.51
	April 5, 2014	95	1.4	-4.4	-3.0	0.3	3.6	1.9	5.9	4.0	1116	6.47
Deployment 3	April 22, 2014	112	3.0	-5.7	-2.7	0.5	3.7	0.7	9.4	8.6	1235	6.68
	April 23, 2014	113	2.5	-5.1	-2.6	0.5	3.5	0.6	8.4	7.8	856	5.65
	April 24, 2014	114	3.0	-5.8	-2.8	0.5	3.5	0.6	8.3	7.7	844	5.82
	April 25, 2014	115	3.4	-5.6	-2.2	0.6	4.5	0.5	11.2	10.7	651	4.42
Deployment 4	May 20, 2014	140	1.8	-4.2	-2.4	0.4	3.7	0.8	7.1	6.2	1077	6.06
	May 21, 2014	141	2.8	-6.0	-3.2	0.5	2.9	0.6	6.8	6.2	691	4.10
	May 22, 2014	142	1.8	-5.2	-3.3	0.4	2.2	0.5	7.4	6.9	324	3.84
	May 23, 2014	143	2.1	-4.6	-2.5	0.5	3.6	0.8	8.7	7.9	1054	5.32
	May 24, 2014	144	2.4	-5.0	-2.6	0.5	3.7	0.5	8.6	8.1	258	3.49
	May 25, 2014	145	3.0	-5.0	-2.1	0.6	4.8	1.1	11.0	9.9	1290	6.26
	May 26, 2014	146	2.7	-4.9	-2.3	0.5	4.3	0.9	11.0	10.1	1102	4.94
	May 27, 2014	147	2.8	-5.3	-2.5	0.5	3.9	0.8	11.1	10.3	830	4.03
	May 28, 2014	148	2.6	-4.8	-2.3	0.5	4.3	1.0	11.7	10.7	464	3.57
	May 29, 2014	149	2.9	-4.7	-1.8	0.6	5.0	1.3	11.2	9.9	1238	5.92
Deployment 5	June 13, 2014	164	3.0	-3.9	-0.8	0.8	7.2	2.2	14.8	12.5	256	3.05
	June 14, 2014	165	4.9	-5.9	-1.0	0.8	7.5	3.0	14.9	12.0	1312	6.15
	June 15, 2014	166	3.1	-5.0	-1.9	0.6	5.3	1.3	11.2	9.9	550	3.18
	June 16, 2014	167	3.7	-5.2	-1.4	0.7	6.3	1.4	14.1	12.7	1489	6.60
	June 17, 2014	168	0.6	-3.3	-2.7	0.2	5.0	1.1	10.1	9.0	1581	6.79
	June 18, 2014	169	0.8	-2.8	-2.1	0.3	5.1	1.5	8.9	7.4	1527	6.64
Deployment 6	July 16, 2014	197	2.2	-5.2	-3.0	0.4	3.1	0.8	7.4	6.6	118	2.62
	July 17, 2014	198	2.7	-5.8	-3.0	0.5	3.0	0.4	7.4	7.0	1086	4.42
	July 18, 2014	199	1.8	-4.6	-2.8	0.4	2.7	0.0	7.2	7.2	1165	4.75
	July 19, 2014	200	2.4	-5.3	-2.9	0.5	2.9	0.0	9.3	9.3	1153	4.59
	July 20, 2014	201	1.9	-5.2	-3.3	0.4	2.2	0.0	7.3	7.3	1029	4.91
	July 21, 2014	202	2.8	-6.1	-3.3	0.5	2.2	0.0	6.4	6.4	926	3.94
	July 22, 2014	203	1.7	-4.7	-3.0	0.4	2.4	0.0	9.8	9.8	1168	4.08

Phelps Creek daily data (continued)

	Date	Day of Year	T1 logger Temperature				T2 logger Temperature				Toxy logger Temperature			
			Mean	Minimum	Maximum	Range	Mean	Minimum	Maximum	Range	Mean	Minimum	Maximum	Range
			°C	°C	°C	°C	°C	°C	°C	°C	°C	°C	°C	°C
Deployment 1	March 11, 2014	70	15.2	13.4	16.8	3.5	15.2	13.1	17.0	3.9	14.9	12.3	17.6	5.3
	March 12, 2014	71	15.0	12.9	17.0	4.1	15.0	12.6	17.4	4.8	14.6	11.8	17.7	5.9
	March 13, 2014	72	14.9	13.2	16.6	3.3	14.9	12.9	17.0	4.1	14.6	12.1	17.2	5.1
	March 14, 2014	73	15.0	12.7	16.9	4.3	15.0	12.3	17.4	5.1	14.8	11.5	18.0	6.5
	March 15, 2014	74	15.9	14.0	17.8	3.9	16.0	13.7	18.4	4.7	15.9	13.0	19.1	6.1
	March 16, 2014	75	15.9	13.7	18.0	4.3	15.9	13.3	18.5	5.2	15.8	12.5	19.1	6.6
Deployment 2	April 3, 2014	93	14.1	11.3	16.9	5.6	14.0	11.7	16.3	4.6	13.7	10.7	17.0	6.3
	April 4, 2014	94	14.5	12.2	16.8	4.6	14.4	12.5	16.4	3.9	14.2	11.6	16.8	5.2
	April 5, 2014	95	15.0	12.4	18.1	5.6	14.7	12.6	17.6	5.0	14.7	11.9	18.3	6.4
Deployment 3	April 22, 2014	112	17.2	14.8	20.3	5.5	16.9	14.8	20.2	5.4	17.0	14.5	20.4	6.0
	April 23, 2014	113	16.8	14.3	19.3	5.0	16.6	14.2	19.7	5.5	16.6	13.8	19.7	5.8
	April 24, 2014	114	16.8	13.8	19.6	5.8	16.3	13.6	19.3	5.7	16.6	13.2	19.8	6.5
	April 25, 2014	115	16.5	14.9	18.4	3.5	16.4	14.7	18.5	3.7	16.3	14.4	18.6	4.2
Deployment 4	May 20, 2014	140	17.9	15.6	21.1	5.6	17.7	15.6	20.9	5.3	17.0	14.7	18.9	4.2
	May 21, 2014	141	18.2	15.8	22.0	6.1	17.8	15.9	20.7	4.8	17.5	15.3	20.2	4.9
	May 22, 2014	142	17.8	15.9	19.6	3.7	17.6	15.7	19.7	4.1	17.3	15.1	19.5	4.5
	May 23, 2014	143	18.2	16.0	21.3	5.2	17.8	15.7	20.7	5.0	17.8	15.3	20.6	5.4
	May 24, 2014	144	17.9	17.0	19.1	2.1	17.9	16.8	19.4	2.6	17.7	16.5	19.2	2.8
	May 25, 2014	145	18.6	16.8	21.7	5.0	18.5	16.7	21.8	5.1	18.4	16.1	21.8	5.7
	May 26, 2014	146	18.8	17.5	20.8	3.3	18.7	17.6	21.0	3.4	18.5	17.1	21.3	4.2
	May 27, 2014	147	18.6	17.3	20.9	3.6	18.4	17.3	20.6	3.3	18.3	16.8	21.3	4.6
	May 28, 2014	148	18.9	17.6	21.3	3.7	18.8	17.5	21.2	3.6	18.7	17.0	21.7	4.6
	May 29, 2014	149	19.0	17.1	21.9	4.8	19.1	17.3	21.8	4.5	18.8	16.6	21.8	5.3
Deployment 5	June 13, 2014	164	17.4	16.1	19.5	3.5	17.5	16.4	19.0	2.5	17.3	15.8	19.6	3.8
	June 14, 2014	165	18.1	15.9	21.0	5.1	18.0	16.6	19.6	3.0	17.9	15.6	20.4	4.8
	June 15, 2014	166	18.6	17.1	21.3	4.3	18.2	17.2	19.8	2.6	18.3	16.9	20.4	3.5
	June 16, 2014	167	18.4	15.9	21.3	5.4	18.0	16.0	20.4	4.5	17.9	15.3	20.5	5.2
	June 17, 2014	168	18.5	15.8	22.5	6.7	18.0	15.9	20.6	4.7	17.8	15.4	19.8	4.4
	June 18, 2014	169	18.6	15.9	22.8	6.8	17.8	16.0	20.0	4.0	17.8	15.2	20.2	4.9
Deployment 6	July 16, 2014	197	20.3	19.5	21.3	1.8	20.2	19.6	21.1	1.5	20.0	19.2	21.0	1.9
	July 17, 2014	198	20.3	17.9	24.4	6.4	19.9	17.8	23.0	5.2	19.8	17.7	22.0	4.3
	July 18, 2014	199	20.3	18.0	24.0	5.9	19.8	18.1	22.0	3.9	19.9	17.6	22.0	4.4
	July 19, 2014	200	20.0	18.3	22.7	4.4	19.5	18.3	20.8	2.5	19.8	18.1	21.7	3.7
	July 20, 2014	201	20.8	18.9	24.3	5.3	20.2	19.0	22.2	3.2	20.4	18.8	22.6	3.8
	July 21, 2014	202	20.5	18.7	23.5	4.8	20.0	18.7	21.9	3.2	20.2	18.4	22.2	3.8
	July 22, 2014	203	20.8	18.3	24.8	6.6	20.1	18.4	22.2	3.8	20.5	18.2	22.7	4.5

Appendix II: Daily metabolism data (continued)

Arroyo Hondo Creek daily data

	Date	Day of year	Metabolism				Dissolved Oxygen				PAR	
			GPP	CR	NEP	P/R	Mean	Minimum	Maximum	Range	Peak	Total
			g O_2 m^{-2} d^{-1}	g O_2 m^{-2} d^{-1}	g O_2 m^{-2} d^{-1}	unitless	mg L^{-1}	mg L^{-1}	mg L^{-1}	mg L^{-1}	µmol photons m^{-2} s^{-1}	mol photons m^{-2} d^{-1}
Deployment 1	March 11, 2014	70	0.6	-6.0	-5.4	0.1	8.8	8.5	9.2	0.8	279	3.06
	March 12, 2014	71	0.5	-5.8	-5.3	0.1	8.9	8.6	9.2	0.6	386	2.97
	March 13, 2014	72	0.5	-5.5	-5.0	0.1	9.0	8.6	9.4	0.7	388	2.82
Deployment 2	April 2, 2014	92	0.4	-4.2	-3.7	0.1	8.7	7.8	9.2	1.5	384	3.03
	April 3, 2014	93	0.3	-3.6	-3.2	0.1	8.9	8.6	9.2	0.6	531	3.87
	April 4, 2014	94	0.4	-3.4	-3.0	0.1	9.0	8.6	9.4	0.8	356	3.29
Deployment 3	April 22, 2014	112	0.8	-5.9	-5.0	0.1	8.7	8.4	9.0	0.7	1265	4.60
	April 23, 2014	113	0.7	-6.0	-5.3	0.1	8.6	8.3	8.9	0.6	1155	4.61
	April 24, 2014	114	0.9	-6.4	-5.6	0.1	8.4	8.3	8.8	0.4	1445	4.77
Deployment 4	May 20, 2014	140	0.6	-4.1	-3.5	0.1	8.3	8.1	8.7	0.7	1542	6.85
	May 21, 2014	141	0.5	-3.8	-3.3	0.1	8.4	8.1	8.8	0.7	1580	7.36
	May 22, 2014	142	0.8	-4.3	-3.4	0.2	8.4	8.1	8.9	0.8	925	4.42
Deployment 5	June 13, 2014	164	0.5	-3.4	-2.9	0.1	8.3	7.9	8.8	0.9	688	4.48
	June 14, 2014	165	0.5	-3.4	-2.9	0.1	8.3	7.8	8.7	0.9	1226	5.34
	June 15, 2014	166	0.4	-3.4	-3.0	0.1	8.1	7.8	8.6	0.9	967	5.09
	June 16, 2014	167	0.4	-3.5	-3.0	0.1	8.2	7.8	8.5	0.7	997	5.59
	June 17, 2014	168	0.4	-3.3	-2.9	0.1	8.2	7.7	8.7	1.0	1389	5.69
	June 18, 2014	169	0.4	-3.1	-2.7	0.1	8.4	7.8	8.8	1.0	1424	5.57
Deployment 6	July 8, 2014	189	0.3	-2.1	-1.8	0.1	7.9	7.1	8.4	1.3	787	5.29
	July 9, 2014	190	0.2	-2.2	-2.0	0.1	7.8	7.4	8.2	0.8	994	5.88
	July 10, 2014	191	0.3	-2.2	-1.9	0.1	7.9	7.2	8.5	1.3	175	2.59

Arroyo Hondo Creek daily data (continued)

	Date	Day of Year	T1 logger Temperature				T2 logger Temperature				Toxy logger Temperature			
			Mean	Minimum	Maximum	Range	Mean	Minimum	Maximum	Range	Mean	Minimum	Maximum	Range
			°C	°C	°C	°C	°C	°C	°C	°C	°C	°C	°C	°C
Deployment 1	March 11, 2014	70	15.0	14.1	15.9	1.8	15.0	14.2	15.8	1.6	14.8	13.8	15.8	2.0
	March 12, 2014	71	14.7	13.8	15.9	2.2	14.7	13.9	15.8	1.9	14.5	13.5	16.0	2.5
	March 13, 2014	72	14.6	13.6	15.7	2.1	14.6	13.7	15.6	1.9	14.3	13.2	15.9	2.6
Deployment 2	April 2, 2014	92	13.8	13.1	14.9	1.8	13.9	13.3	14.6	1.4	13.4	12.6	14.6	2.0
	April 3, 2014	93	14.0	12.8	15.2	2.3	14.0	13.1	15.0	2.0	13.7	12.4	15.3	2.9
	April 4, 2014	94	14.1	13.4	15.3	1.9	14.2	13.6	15.2	1.6	13.8	13.0	15.2	2.2
Deployment 3	April 22, 2014	112	14.9	13.9	16.7	2.9	14.9	14.0	16.2	2.2	14.7	13.5	16.9	3.4
	April 23, 2014	113	14.8	13.7	16.6	2.9	14.8	13.9	16.1	2.2	14.5	13.2	16.8	3.6
	April 24, 2014	114	15.4	14.2	17.0	2.8	15.4	14.4	16.5	2.1	15.2	13.8	17.2	3.5
Deployment 4	May 20, 2014	140	15.8	14.9	17.8	2.9	15.9	15.2	17.2	2.0	15.4	14.4	17.7	3.3
	May 21, 2014	141	15.9	14.5	18.0	3.5	16.0	14.8	17.4	2.6	15.6	14.1	18.0	4.0
	May 22, 2014	142	15.9	14.6	17.2	2.6	16.0	15.0	17.1	2.1	15.6	14.1	16.9	2.8
Deployment 5	June 13, 2014	164	15.8	14.5	17.5	3.1	15.9	14.9	17.1	2.2	15.5	14.0	17.7	3.6
	June 14, 2014	165	16.0	14.3	17.9	3.6	16.1	14.7	17.4	2.6	15.6	13.7	18.0	4.2
	June 15, 2014	166	16.4	15.6	18.1	2.5	16.4	15.7	17.6	1.9	16.2	15.3	18.4	3.1
	June 16, 2014	167	16.2	14.9	18.3	3.4	16.3	15.2	17.7	2.6	15.9	14.5	18.5	4.0
	June 17, 2014	168	16.1	14.4	18.0	3.6	16.2	14.9	17.5	2.6	15.7	13.9	18.1	4.2
	June 18, 2014	169	16.0	14.1	18.1	4.0	16.1	14.6	17.5	2.9	15.6	13.6	18.0	4.5
Deployment 6	July 8, 2014	189	17.3	15.6	19.2	3.6	17.3	15.9	18.6	2.7	17.2	15.4	19.3	4.0
	July 9, 2014	190	17.5	16.0	19.5	3.5	17.4	16.2	18.8	2.5	17.4	15.8	19.5	3.7
	July 10, 2014	191	17.1	16.3	17.8	1.5	17.0	16.5	17.7	1.2	17.0	16.3	18.0	1.7

Rattlesnake Creek daily data

	Date	Day of year	Metabolism				Dissolved Oxygen				PAR	
			GPP	CR	NEP	P/R	Mean	Minimum	Maximum	Range	Peak	Total
			$g\ O_2\ m^{-2}\ d^{-1}$	$g\ O_2\ m^{-2}\ d^{-1}$	$g\ O_2\ m^{-2}\ d^{-1}$	unitless	$mg\ L^{-1}$	$mg\ L^{-1}$	$mg\ L^{-1}$	$mg\ L^{-1}$	$\mu mol\ photons\ m^{-2}\ s^{-1}$	$mol\ photons\ m^{-2}\ d^{-1}$
Deployment 1	March 25, 2014	84	0.3	-7.6	-7.2	0.0	8.8	8.6	9.0	0.4	221	4.30
	March 26, 2014	85	0.3	-7.8	-7.5	0.0	8.8	8.6	9.0	0.4	644	6.55
	March 27, 2014	86	0.3	-7.9	-7.6	0.0	8.8	8.5	9.1	0.6	780	6.04
Deployment 2	April 12, 2014	102	1.1	-15.9	-14.8	0.1	7.8	7.2	8.1	0.9	201	4.59
	April 13, 2014	103	1.0	-14.3	-13.3	0.1	8.1	7.8	8.5	0.7	638	6.31
	April 14, 2014	104	1.0	-13.6	-12.6	0.1	8.1	7.8	8.5	0.7	1604	10.96
Deployment 3	May 2, 2014	122	0.1	-2.0	-2.0	0.0	5.1	4.3	5.7	1.4	1394	12.56
	May 3, 2014	123	0.2	-2.3	-2.0	0.1	4.8	4.0	5.7	1.7	1207	11.42
	May 4, 2014	124	0.2	-2.1	-2.0	0.1	5.1	4.2	6.6	2.4	1393	12.80
	May 5, 2014	125	0.4	-2.2	-1.8	0.2	5.4	4.2	6.5	2.3	782	8.28

Rattlesnake Creek daily data (continued)

	Date	Day of Year	T1 logger Temperature				T2 logger Temperature				Toxy logger Temperature			
			Mean	Minimum	Maximum	Range	Mean	Minimum	Maximum	Range	Mean	Minimum	Maximum	Range
			°C	°C	°C	°C	°C	°C	°C	°C	°C	°C	°C	°C
Deployment 1	March 25, 2014	84	13.8	13.5	14.2	0.6	13.9	13.5	14.8	1.3	13.7	13.4	14.5	1.1
	March 26, 2014	85	13.6	13.1	14.0	0.9	13.7	13.0	15.0	2.0	13.5	12.8	14.6	1.8
	March 27, 2014	86	13.3	12.5	13.8	1.3	13.5	12.2	15.0	2.8	13.3	12.0	14.6	2.6
Deployment 2	April 12, 2014	102	--	--	--	--	13.8	13.2	14.5	1.2	13.6	13.1	14.2	1.2
	April 13, 2014	103	--	--	--	--	13.5	12.4	14.9	2.5	13.2	12.1	14.3	2.3
	April 14, 2014	104	--	--	--	--	14.1	12.6	16.2	3.6	13.8	12.3	15.6	3.4
Deployment 3	May 2, 2014	122	17.4	16.5	19.6	3.1	16.4	15.8	17.0	1.2	17.8	15.7	19.8	4.1
	May 3, 2014	123	16.7	16.2	17.8	1.6	16.9	16.4	17.1	0.7	18.1	16.7	20.2	3.5
	May 4, 2014	124	16.5	15.7	17.7	2.0	16.7	16.3	17.1	0.8	16.9	15.2	18.7	3.5
	May 5, 2014	125	16.1	15.4	17.1	1.8	16.3	16.0	16.6	0.6	16.0	14.7	17.7	3.0

Appendix II: Daily metabolism data (continued)

Sycamore Creek daily data

	Date	Day of year	Metabolism				Dissolved Oxygen				PAR	
			GPP	CR	NEP	P/R	Mean	Minimum	Maximum	Range	Peak	Total
			g O_2 m^{-2} d^{-1}	g O_2 m^{-2} d^{-1}	g O_2 m^{-2} d^{-1}	unitless	mg L^{-1}	mg L^{-1}	mg L^{-1}	mg L^{-1}	µmol photons m^{-2} s^{-1}	mol photons m^{-2} d^{-1}
Deployment 1	March 17, 2014	76	3.0	-7.9	-4.9	0.4	9.2	8.6	10.3	1.8	1114	2.61
	March 18, 2014	77	2.7	-7.9	-5.2	0.3	9.0	8.4	10.4	2.0	1309	2.79
	March 19, 2014	78	2.7	-7.5	-4.8	0.4	9.3	8.6	10.5	1.8	1381	3.29
Deployment 2	April 8, 2014	98	2.3	-8.9	-6.6	0.3	8.5	7.9	9.8	1.8	1485	6.38
	April 9, 2014	99	2.2	-9.1	-6.9	0.2	8.5	7.9	10.5	2.6	1545	6.30
	April 10, 2014	100	2.3	-8.4	-6.1	0.3	8.7	7.9	10.0	2.0	487	3.27
Deployment 3	April 29, 2014	119	1.2	-8.3	-7.1	0.1	7.3	7.1	8.3	1.2	1601	5.94
	April 30, 2014	120	1.3	-8.9	-7.6	0.1	7.1	6.5	8.3	1.8	1599	5.54
	May 1, 2014	121	1.6	-9.5	-7.9	0.2	7.1	6.5	8.5	2.1	1543	5.80
	May 2, 2014	122	1.4	-9.7	-8.3	0.1	6.8	6.0	8.5	2.5	1591	7.10
	May 3, 2014	123	2.0	-9.9	-7.9	0.2	7.0	6.2	8.9	2.6	1428	6.49
	May 4, 2014	124	1.7	-9.1	-7.4	0.2	7.2	6.1	9.0	2.9	1532	7.37
Deployment 4	May 30, 2014	150	2.5	-11.7	-9.2	0.2	6.3	5.0	8.1	3.1	1168	5.27
	May 31, 2014	151	3.0	-12.7	-9.7	0.2	6.1	4.3	8.2	3.9	1132	5.26
	June 1, 2014	152	2.5	-11.9	-9.4	0.2	6.2	5.1	8.2	3.1	1187	5.34
	June 2, 2014	153	2.7	-11.7	-9.0	0.2	6.3	5.1	8.4	3.4	1052	5.68
	June 3, 2014	154	3.0	-12.3	-9.3	0.2	6.3	4.7	8.5	3.8	1133	5.70
	June 4, 2014	155	2.5	-11.6	-9.1	0.2	6.3	5.0	8.4	3.4	1075	5.84
Deployment 5	June 21, 2014	172	2.2	-9.1	-6.9	0.2	6.1	4.7	8.4	3.6	1074	5.54
	June 22, 2014	173	2.1	-9.2	-7.1	0.2	6.0	4.5	8.2	3.7	1053	5.55
	June 23, 2014	174	2.2	-9.0	-6.8	0.2	6.2	4.7	8.5	3.8	1018	4.84
	June 24, 2014	175	2.0	-9.1	-7.1	0.2	6.1	4.6	8.2	3.6	965	5.36
	June 25, 2014	176	2.1	-9.1	-7.1	0.2	6.0	4.6	8.3	3.8	729	4.51
	June 26, 2014	177	1.5	-9.4	-7.9	0.2	5.6	4.3	7.6	3.4	1178	5.50
Deployment 6	July 16, 2014	197	0.4	-2.1	-1.7	0.2	5.4	4.5	6.8	2.2	109	1.81
	July 17, 2014	198	0.6	-2.2	-1.6	0.3	5.8	4.6	7.7	3.1	1449	5.89
	July 18, 2014	199	0.5	-2.5	-2.0	0.2	5.0	4.2	6.4	2.1	1332	5.80

Sycamore Creek daily data (continued)

	Date	Day of Year	T1 logger Temperature				T2 logger Temperature				Toxy logger Temperature			
			Mean	Minimum	Maximum	Range	Mean	Minimum	Maximum	Range	Mean	Minimum	Maximum	Range
			°C	°C	°C	°C	°C	°C	°C	°C	°C	°C	°C	°C
Deployment 1	March 17, 2014	76	15.3	13.5	17.4	3.9	15.2	13.5	17.4	3.9	15.2	13.5	17.3	3.8
	March 18, 2014	77	15.3	13.7	17.1	3.3	15.3	13.7	17.1	3.4	15.8	14.0	17.0	3.0
	March 19, 2014	78	14.5	12.6	16.3	3.8	14.5	12.6	16.4	3.8	14.5	12.6	16.2	3.6
Deployment 2	April 8, 2014	98	15.2	13.1	17.0	3.9	15.2	13.0	17.1	4.1	15.1	13.0	17.0	4.0
	April 9, 2014	99	15.0	13.5	16.3	2.7	15.1	13.4	16.8	3.3	15.1	13.5	16.8	3.3
	April 10, 2014	100	14.5	13.3	15.2	1.9	14.5	13.2	15.4	2.3	14.4	13.1	15.3	2.1
Deployment 3	April 29, 2014	119	16.2	14.6	17.7	3.0	16.7	14.5	19.1	4.6	16.5	14.5	18.8	4.3
	April 30, 2014	120	15.9	14.3	17.2	2.9	16.7	14.2	19.2	5.0	16.5	14.1	18.8	4.7
	May 1, 2014	121	15.8	14.6	16.7	2.1	16.8	14.4	19.4	5.0	16.6	14.4	19.0	4.6
	May 2, 2014	122	16.3	15.3	17.1	1.8	17.4	15.4	19.7	4.3	17.2	15.2	19.7	4.5
	May 3, 2014	123	16.4	15.4	17.2	1.8	17.1	15.4	19.3	3.9	17.0	15.3	19.3	4.1
	May 4, 2014	124	16.0	14.8	17.0	2.2	16.5	14.7	18.6	3.9	16.4	14.6	18.6	4.0
Deployment 4	May 30, 2014	150	16.5	15.3	17.4	2.1	17.3	15.3	19.8	4.4	17.3	15.5	19.9	4.4
	May 31, 2014	151	16.3	15.2	17.2	2.1	17.1	15.2	19.4	4.3	17.0	15.3	19.7	4.4
	June 1, 2014	152	16.2	15.0	17.1	2.1	17.0	15.0	19.3	4.3	16.9	15.1	19.5	4.4
	June 2, 2014	153	16.5	15.7	17.3	1.7	17.0	15.7	19.2	3.5	16.9	15.7	19.4	3.7
	June 3, 2014	154	15.8	14.5	16.8	2.3	16.6	14.5	19.2	4.6	16.5	14.7	19.3	4.6
	June 4, 2014	155	16.0	14.9	17.0	2.1	16.9	14.8	19.1	4.3	16.8	15.0	19.4	4.4
Deployment 5	June 21, 2014	172	16.8	15.9	17.8	1.9	17.7	15.9	20.1	4.2	17.7	16.1	20.2	4.1
	June 22, 2014	173	17.1	16.4	17.9	1.4	17.7	16.5	20.0	3.5	17.8	16.6	20.4	3.9
	June 23, 2014	174	16.3	15.3	17.2	2.0	17.1	15.3	19.2	3.9	17.1	15.5	19.5	3.9
	June 24, 2014	175	16.5	15.5	17.5	2.0	17.4	15.5	19.8	4.3	17.5	15.7	20.3	4.6
	June 25, 2014	176	16.9	16.0	17.7	1.7	17.7	16.0	19.6	3.5	17.7	16.1	19.9	3.8
	June 26, 2014	177	17.4	16.4	18.1	1.7	18.3	15.8	20.6	4.8	18.3	16.4	21.0	4.6
Deployment 6	July 16, 2014	197	19.2	19.0	19.5	0.5	19.3	19.0	19.8	0.8	19.1	18.9	19.7	0.8
	July 17, 2014	198	18.3	17.6	19.0	1.5	18.7	17.4	20.8	3.5	19.0	17.7	21.6	3.9
	July 18, 2014	199	18.2	17.4	18.8	1.5	18.6	17.0	20.8	3.9	19.0	17.1	22.1	5.0

Appendix III: Significant correlations between land use variables

	log(ws area)	log(ws urban area)	log(ws impervious area)	log(ws ceanothus area)	log(ws population)	log(ws golf parcel area)	log(ws septic parcels)	logit(ws %urban)	logit(ws %impervious)	logit(ws %ceanothus)	log(ws population density)	log(aoi area)	log(aoi urban area)	log(aoi impervious area)	log(aoi population)	log(aoi irrigated grass area)	log(aoi septic parcels)	logit(aoi %urban)	logit(aoi %impervious)	logit(aoi %irrigated grass area)	logit(aoi %channelized)	log(aoi population density)
log(ws area)																						
log(ws urban area)		0.98			0.90		0.91	0.92	0.93		0.94	0.85	0.89	0.99	0.99	0.98						0.93
log(ws impervious area)		0.98			0.95		0.97	0.83	0.92		0.93			0.97	0.98	0.99						0.93
log(ws ceanothus area)										0.93												
log(ws population)		0.90	0.95				0.99		0.93		0.93			0.91	0.92	0.94						0.94
log(ws golf parcel area)											1.00		0.85					0.83				
log(ws septic parcels)		0.91	0.97		0.99				0.93		0.93			0.91	0.91	0.95						0.94
logit(ws %urban)		0.92	0.83						0.92	-0.89	0.92		0.92	0.92	0.91	0.82		0.85	0.93		0.91	0.93
logit(ws %impervious)		0.93	0.92		0.93		0.93	0.92			1.00			0.92	0.92	0.90			1.00	0.92		1.00
logit(ws %ceanothus)				0.93				-0.89										-0.82			-0.95	
log(ws population density)		0.94	0.93		0.93		0.93	0.92	1.00					0.92	0.93	0.92			0.99	0.94		0.99
log(aoi area)		0.85											0.83	0.85	0.85	0.81						
log(aoi urban area)		0.89				0.85		0.92				0.83		0.91	0.91	0.83		0.84	0.82			0.82
log(aoi impervious area)		0.99	0.97		0.91		0.91	0.92	0.92		0.92	0.85	0.91		1.00	0.97			0.95	0.83		0.93
log(aoi population)		0.99	0.98		0.92		0.91	0.91	0.92		0.93	0.85	0.91	1.00		0.98			0.94	0.85		0.93
log(aoi irrigated grass area)		0.98	0.99		0.94		0.95	0.82	0.90		0.92	0.81	0.83	0.97	0.98				0.92	0.91		0.91
log(aoi septic parcels)						0.83		0.85		-0.82			0.84									
logit(aoi %urban)		0.95	0.94		0.93		0.94	0.93	1.00		0.99		0.82	0.95	0.94	0.92				0.90	0.82	1.00
logit(aoi %impervious)		0.86	0.91		0.95		0.97		0.92		0.94			0.83	0.85	0.91			0.90			0.91
logit(aoi %irrigated grass area)				-0.82				0.91		-0.95									0.82			
logit(aoi %channelized)		0.93	0.93		0.94		0.94	0.93	1.00		0.99		0.82	0.93	0.93	0.91			1.00	0.91		
log(aoi population density)																						

*Only significant correlations are shown ($p < 0.05$); ws = watershed; aoi = area of influence

Appendix IV: Ranking of seasonal temperatures, highest to lowest, across sites from 2002-2007

		Winter																							
		min						mean						max						range					
		2002	2003	2004	2005	2006	2007	2002	2003	2004	2005	2006	2007	2002	2003	2004	2005	2006	2007	2002	2003	2004	2005	2006	2007
		n = 14	n = 16	n = 16	n = 17	n = 14	n = 12	n = 14	n = 16	n = 16	n = 17	n = 14	n = 12	n = 14	n = 16	n = 16	n = 17	n = 14	n = 12	n = 14	n = 16	n = 16	n = 17	n = 14	n = 12
Site	AB00	8	11	12	10	10	6	10	11	11	12	12	9	10	11	11	14	11	10	6	7	7	13	6	10
	AB21	2	2	3	---	---	---	3	4	4	---	---	---	7	9	6	---	---	---	13	15	14	---	---	---
	AB25	10	8	---	---	---	---	7	7	---	---	---	---	2	3	---	---	---	---	2	2	---	---	---	---
	AT07	---	---	---	15	14	11	---	---	---	7	8	6	---	---	---	1	1	1	---	---	---	1	1	1
	BC02	---	---	---	9	12	10	---	---	---	13	14	11	---	---	---	15	14	11	---	---	---	14	12	7
	CP00	5	6	7	11	5	8	6	6	7	10	5	7	4	4	8	10	8	6	4	4	5	5	8	3
	DV01	---	---	4	5	4	7	---	---	3	5	3	8	---	---	4	8	4	9	---	---	11	12	3	6
	EL00	4	3	2	3	6	---	5	3	2	3	6	---	8	2	3	3	10	---	11	8	13	4	7	---
	FK00	6	5	8	2	---	---	2	2	5	2	---	---	1	1	1	2	---	---	1	1	1	3	---	---
	GB04	14	16	---	---	---	---	14	16	---	---	---	---	14	14	---	---	---	---	8	9	---	---	---	---
	GV01	9	9	9	7	8	4	9	9	10	8	9	5	5	8	9	9	9	7	3	5	4	8	4	5
	HO00	1	1	1	1	1	1	1	1	1	1	1	1	3	5	2	5	2	2	14	16	15	16	14	12
	MC00	3	4	5	6	3	3	4	5	6	6	4	3	6	7	7	7	6	4	10	11	8	9	10	8
	MC07	11	13	14	17	---	---	13	14	14	17	---	---	13	15	14	17	---	---	12	13	9	15	---	---
	ON02	---	---	---	4	2	2	---	---	---	4	2	2	---	---	---	6	3	3	---	---	---	10	13	11
	RG01	7	10	10	12	7	5	8	8	8	9	7	4	9	6	5	4	7	5	7	3	2	2	5	4
	RG09	---	7	6	---	---	---	---	10	9	---	---	---	---	12	12	---	---	---	---	14	16	---	---	---
	RN01	13	14	15	14	13	12	11	12	13	11	10	12	11	10	10	11	5	8	5	6	3	7	2	2
	RS02	12	12	13	8	11	9	12	13	15	16	13	10	12	13	15	16	13	12	9	12	10	17	9	9
	SR04	---	15	16	16	---	---	---	15	16	15	---	---	---	16	16	12	---	---	---	10	6	6	---	---
	TE03	---	---	11	13	9	---	---	---	12	14	11	---	---	---	13	13	12	---	---	---	12	11	11	---

		Spring																							
		min						mean						max						range					
		2002	2003	2004	2005	2006	2007	2002	2003	2004	2005	2006	2007	2002	2003	2004	2005	2006	2007	2002	2003	2004	2005	2006	2007
		n = 13	n = 16	n = 16	n = 17	n = 15	n = 13	n = 13	n = 16	n = 16	n = 17	n = 15	n = 13	n = 13	n = 16	n = 16	n = 17	n = 15	n = 13	n = 13	n = 16	n = 16	n = 17	n = 15	n = 13
Site	AB00	6	3	8	5	3	5	9	7	9	6	9	9	7	8	10	11	12	11	**7**	10	8	13	13	9
	AB21	2	2	3	---	---	---	3	3	5	---	---	---	8	10	9	---	---	---	12	14	15	---	---	---
	AB25	9	10	---	---	---	---	7	8	---	---	---	---	4	7	---	---	---	---	3	6	---	---	---	---
	AT07	---	---	---	6	5	11	---	---	---	3	2	3	---	---	---	1	2	2	---	---	---	1	2	2
	BC02	---	---	---	10	12	12	---	---	---	11	13	12	---	---	---	13	13	12	---	---	---	12	12	11
	CP00	4	7	6	13	8	7	6	4	7	9	6	7	5	4	7	5	6	6	6	4	7	3	5	5
	DV01	---	---	1	2	1	1	---	---	1	2	1	1	---	---	2	2	3	5	---	---	4	11	4	12
	EL00	---	6	10	12	14	---	---	9	12	12	12	---	---	9	12	10	11	---	---	8	14	7	10	---
	FK00	5	4	7	1	11	8	1	1	2	1	4	2	1	1	1	6	1	1	1	1	1	14	1	1
	GB04	13	16	---	---	---	---	10	13	---	---	---	---	10	12	---	---	---	---	4	9	---	---	---	---
	GV01	8	9	9	11	6	4	5	6	6	8	5	5	2	3	3	7	7	3	2	3	3	4	6	3
	HO00	1	5	5	8	10	2	4	11	11	15	14	6	9	13	14	15	14	10	13	15	16	16	15	13
	MC00	3	1	2	3	2	3	2	2	3	4	3	4	3	2	5	4	4	4	8	7	6	6	8	4
	MC07	10	13	14	15	---	---	12	14	14	16	---	---	13	14	13	16	---	---	11	13	11	15	---	---
	ON02	---	---	---	9	9	6	---	---	---	13	11	8	---	---	---	12	8	8	---	---	---	9	7	8
	RG01	7	8	12	7	7	9	8	5	8	7	10	10	6	5	4	8	9	7	5	5	2	5	9	6
	RG09	---	14	11	---	---	---	---	16	13	---	---	---	---	16	11	---	---	---	---	16	12	---	---	---
	RN01	12	11	13	16	13	10	11	10	10	10	8	11	11	6	8	3	5	9	9	2	5	2	3	7
	RS02	11	15	15	17	15	13	13	15	16	17	15	13	12	15	16	17	15	13	10	12	13	17	14	10
	SR04	---	12	16	14	---	---	---	12	15	14	---	---	---	11	15	14	---	---	---	11	9	8	---	---
	TE03	---	---	4	4	4	---	---	---	4	5	7	---	---	---	6	9	10	---	---	---	10	10	11	---

Appendix IV (continued): Ranking of seasonal temperatures, highest to lowest, across sites from 2002-2007.

		Summer																							
		min						mean						max						range					
		2002	2003	2004	2005	2006	2007	2002	2003	2004	2005	2006	2007	2002	2003	2004	2005	2006	2007	2002	2003	2004	2005	2006	2007
		n = 12	n = 15	n = 10	n = 17	n = 13	n = 10	n = 12	n = 15	n = 10	n = 17	n = 13	n = 10	n = 12	n = 15	n = 10	n = 17	n = 13	n = 10	n = 12	n = 15	n = 10	n = 17	n = 13	n = 10
Site	AB00	6	7	5	9	4	2	5	7	8	11	8	6	4	5	7	10	11	8	**5**	6	7	7	13	9
	AB21	1	1	---	---	---	---	4	3	---	---	---	---	7	6	---	---	---	---	11	14	---	---	---	---
	AB25	8	11	---	---	---	---	7	11	---	---	---	---	9	10	---	---	---	---	7	8	---	---	---	---
	AT07	---	---	---	8	5	4	---	---	---	1	2	1	---	---	---	1	1	1	---	---	---	1	1	1
	BC02	---	---	---	14	11	8	---	---	---	14	10	9	---	---	---	14	9	9	---	---	---	9	7	8
	CP00	4	4	6	7	7	6	6	6	7	7	6	7	8	7	9	4	6	6	8	7	9	4	4	6
	DV01	---	---	1	4	1	---	---	---	1	5	1	---	---	---	3	6	2	---	---	---	4	10	10	---
	EL00	---	10	---	13	12	---	---	12	---	13	11	---	---	12	---	13	10	---	---	11	---	8	8	---
	FK00	3	3	4	1	---	3	1	1	2	4	---	2	1	1	1	9	---	3	1	1	1	16	---	3
	GB04	---	15	---	---	---	---	---	15	---	---	---	---	---	14	---	---	---	---	---	13	---	---	---	---
	GV01	5	5	7	6	6	5	3	4	4	6	4	4	2	2	2	3	4	2	2	2	2	3	3	2
	HO00	7	13	8	15	13	10	12	14	10	16	13	10	12	15	10	17	13	10	12	15	10	17	12	10
	MC00	2	2	2	3	2	1	2	2	3	3	3	3	3	3	5	5	5	4	6	5	5	12	6	5
	MC07	11	9	---	17	---	---	10	9	---	17	---	---	6	9	---	16	---	---	4	9	---	13	---	---
	ON02	---	---	---	5	---	---	---	---	---	9	---	---	---	---	---	12	---	---	---	---	---	14	---	---
	RG01	12	6	10	10	8	9	9	5	6	10	9	5	5	4	4	8	7	5	3	3	3	5	5	4
	RG09	---	---	---	---	---	---	---	---	---	---	---	---	---	---	---	---	---	---	---	---	---	---	---	---
	RN01	9	12	9	12	10	7	8	8	9	8	7	8	10	8	8	2	3	7	9	4	6	2	2	7
	RS02	10	8	---	16	9	---	11	10	---	15	12	---	11	11	---	15	12	---	10	12	---	11	11	---
	SR04	---	14	---	11	---	---	---	13	---	12	---	---	---	13	---	11	---	---	---	10	---	6	---	---
	TE03	---	---	3	2	3	---	---	---	5	2	5	---	---	---	6	7	8	---	---	---	8	15	9	---

		Fall																							
		min						mean						max						range					
		2002	2003	2004	2005	2006	2007	2002	2003	2004	2005	2006	2007	2002	2003	2004	2005	2006	2007	2002	2003	2004	2005	2006	2007
		n = 13	n = 13	n = 14	n = 14	n = 14	n = 9	n = 13	n = 13	n = 14	n = 14	n = 14	n = 9	n = 13	n = 13	n = 14	n = 14	n = 14	n = 9	n = 13	n = 13	n = 14	n = 14	n = 14	n = 9
Site	AB00	9	1	7	13	13	7	9	3	9	13	14	9	10	5	11	13	14	9	**8**	8	8	7	13	9
	AB21	3	4	---	---	---	---	3	5	---	---	---	---	8	7	---	---	---	---	12	11	---	---	---	---
	AB25	7	---	---	---	---	---	8	---	---	---	---	---	6	---	---	---	---	---	6	---	---	---	---	---
	AT07	---	---	14	12	8	8	---	---	11	3	3	1	---	---	5	1	1	1	---	---	3	1	2	1
	BC02	---	---	13	11	10	5	---	---	14	14	12	8	---	---	14	14	13	8	---	---	12	11	9	8
	CP00	5	7	5	7	6	4	7	8	7	5	7	6	7	8	7	4	8	7	9	9	9	3	6	5
	DV01	---	8	3	4	14	---	---	7	3	6	13	---	---	6	6	7	12	---	---	4	6	9	7	---
	EL00	---	---	---	8	4	---	---	---	---	10	4	---	---	---	---	10	7	---	---	---	---	6	8	---
	FK00	1	6	4	---	11	---	1	2	1	---	8	---	1	2	1	---	2	---	1	1	2	---	1	---
	GB04	13	---	---	---	---	---	13	---	---	---	---	---	12	---	---	---	---	---	4	---	---	---	---	---
	GV01	6	9	8	9	5	3	5	6	6	8	6	3	3	4	3	6	3	2	3	3	4	4	5	3
	HO00	2	5	2	3	2	1	4	9	5	4	5	2	9	12	9	9	10	4	13	13	14	13	14	7
	MC00	4	2	1	2	1	2	2	4	2	2	1	4	4	3	4	5	4	6	10	6	7	10	10	6
	MC07	11	11	12	---	---	---	11	11	13	---	---	---	5	11	13	---	---	---	5	10	11	---	---	---
	ON02	---	---	---	1	3	---	---	---	---	1	2	---	---	---	---	3	9	---	---	---	---	14	12	---
	RG01	8	3	10	6	9	9	6	1	4	7	9	5	2	1	2	8	5	3	2	2	1	5	4	2
	RG09	---	12	---	---	---	---	---	13	---	---	---	---	---	13	---	---	---	---	---	12	---	---	---	---
	RN01	10	13	9	14	12	6	10	12	10	11	10	7	11	9	10	2	6	5	7	5	5	2	3	4
	RS02	12	10	11	10	7	---	12	10	12	12	11	---	13	10	12	12	11	---	11	7	13	8	11	---
	SR04	---	---	---	---	---	---	---	---	---	---	---	---	---	---	---	---	---	---	---	---	---	---	---	---
	TE03	---	---	6	5	---	---	---	---	8	9	---	---	---	---	8	11	---	---	---	---	10	12	---	---

Appendix V: Comparison of temperatures across land use categories: one-way ANOVA results

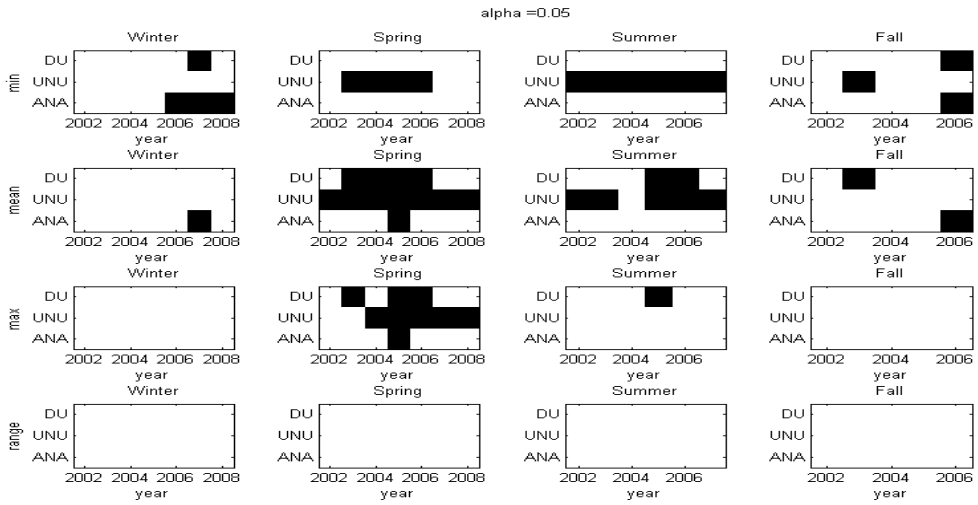

Figure A5.1: Significant differences between land use groups using seasonal data from all available sites. Group comparisons are noted as DU (Developed v. Undeveloped), UNU (Urban v. Non-urban), and ANA (Agricultural v. Non-agricultural). Years marked in black indicate significance at $\alpha = 0.05$.

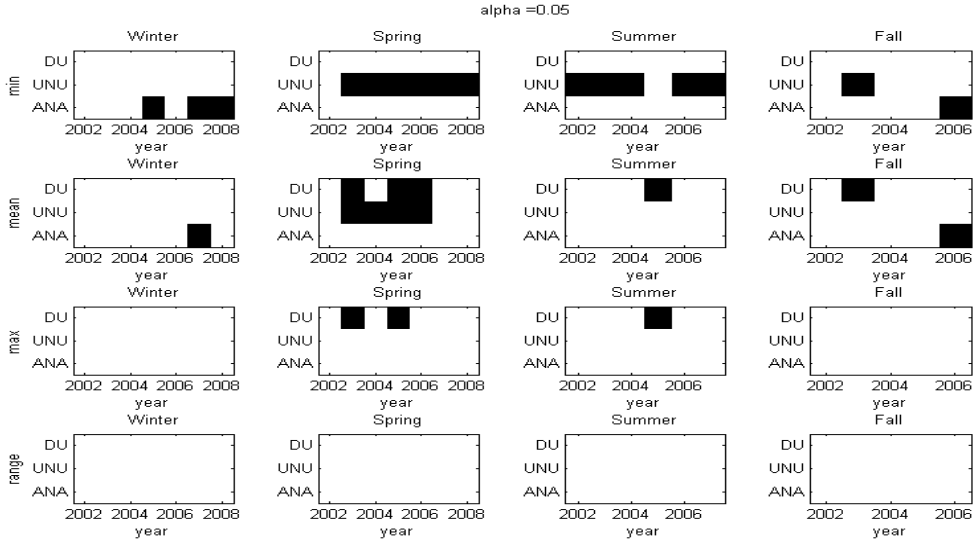

Figure A5.2: Significant differences between land use groups using seasonal data from all available sites except channelized sites (AT07 and FK00). Group comparisons are noted as DU (Developed v. Undeveloped), UNU (Urban v. Non-urban), and ANA (Agricultural v. Non-agricultural). Years marked in black indicate significance at $\alpha = 0.05$.

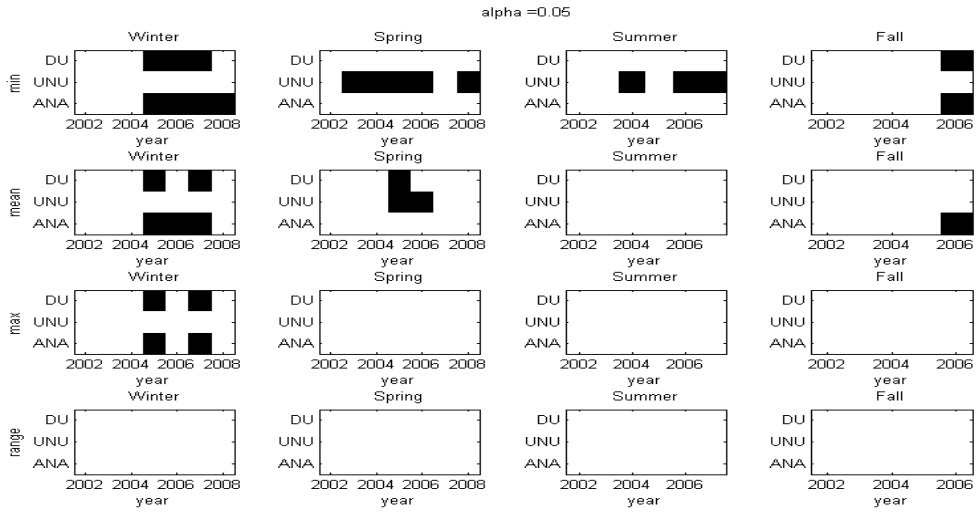

Figure A5.3: Significant differences between land use groups using seasonal data from all available sites except channelized sites (AT07 and FK00) and high elevation sites (MC07, RS02, SR04, RG09, and GB04). Group comparisons are noted as DU (Developed v. Undeveloped), UNU (Urban v. Non-urban), and ANA (Agricultural v. Non-agricultural). Years marked in black indicate significance at $\alpha = 0.05$.

Spring Min, Urb /Nurb

All Available Sites								Excluding AT07 and FK00								Excluding AT00, FK00, RS02, MC07, RG09, SR04, and GB04							
Year	N (Urb)	N (Nurb)	df (grp, err)	Mean (Urb, °C)	Mean (NUrb, °C)	F	p	Year	N (Urb)	N (Nurb)	df (grp, err)	Mean (Urb, °C)	Mean (NUrb, °C)	F	p	Year	N (Urb)	N (Nurb)	df (grp, err)	Mean (Urb, °C)	Mean (NUrb, °C)	F	p
2002	5	8	1, 11	13.3	12.2	2.38	0.15	2002	4	8	1, 10	13.5	12.2	2.62	0.14	2002	4	5	1, 7	13.5	12.7	0.67	0.44
2003	5	11	1, 14	13.9	12.5	14.32	**0.002**	2003	4	11	1, 13	14.1	12.5	14.34	**0.0023**	2003	4	6	1, 8	14.1	12.9	6.65	0.033
2004	5	11	1, 14	15.6	13.7	8.82	0.01	2004	4	11	1, 13	15.9	13.7	10.64	**0.0062**	2004	4	6	1, 9	15.9	14.2	6.14	0.035
2005	5	12	1, 15	15.0	13.1	22.82	**0.0002**	2005	3	12	1, 13	15.0	13.1	19.84	**0.0007**	2005	3	8	1, 10	15.0	13.3	16.37	**0.0023**
2006	5	10	1, 13	13.4	12.3	9.07	0.01	2006	3	10	1, 11	13.9	12.3	20.57	**0.0009**	2006	3	8	1, 10	13.9	12.5	33.08	**0.0002**
2007	5	8	1, 11	14.3	13.2	1.8	0.21	2007	3	8	1, 9	15.2	13.2	5.33	0.046	2007	3	7	1, 8	15.2	13.4	4.34	0.071
2008	4	7	1, 9	13.5	12.6	2.09	0.18	2008	2	7	1, 7	14.3	12.6	7.93	0.026	2008	2	6	1, 6	14.3	12.7	6.5	0.044

Summer Min, Urb/Nurb

2002	5	7	1, 10	17.5	15.9	7.34	0.022	2002	4	7	1, 9	17.6	15.9	6.37	0.033	2002	4	5	1, 7	17.6	16.1	3.74	0.095
2003	5	10	1, 13	18.1	16.4	8.27	0.013	2003	4	10	1, 12	18.2	16.4	6.96	0.022	2003	4	6	1, 8	18.2	16.7	3.44	0.1
2004	4	6	1, 8	18.3	16.7	5.57	0.046	2004	3	6	1, 7	18.6	16.7	6.96	0.034	2004	3	6	1, 7	18.6	16.7	6.96	0.034
2005	5	11	1, 15	18.4	16.8	7.43	0.016	2005	3	11	1, 13	18.3	16.8	4.57	0.052	2005	3	9	1, 10	18.3	17.2	2.99	0.11
2006	4	8	1, 11	19.6	17.3	12.49	**0.0047**	2006	3	8	1, 10	20.0	17.3	15.33	**0.0029**	2006	3	8	1, 9	20.0	17.3	13.17	**0.0055**
2007	4	6	1, 8	17.9	16.5	16.26	**0.0038**	2007	2	6	1, 6	18.5	16.5	32.12	**0.0013**	2007	2	6	1, 6	18.5	16.5	32.12	**0.0013**

Spring Mean, Urb/Nurb

2002	5	8	1, 11	15.6	14.2	5.61	0.037	2002	4	8	1, 10	15.3	14.2	3.29	0.1								
2003	5	11	1, 14	16.0	14.4	9.93	**0.0071**	2003	4	11	1, 13	15.8	14.4	6.31	0.026								
2004	5	11	1, 14	17.9	15.5	10.65	**0.0057**	2004	4	11	1, 13	17.7	15.5	7.43	0.017								
2005	5	12	1, 15	17.0	15.0	18.54	**0.0006**	2005	3	12	1, 13	16.8	15.0	8.57	0.012								
2006	5	10	1, 13	15.7	14.1	11.74	**0.0045**	2006	3	10	1, 11	15.7	14.1	6.93	0.023								
2007	5	8	1, 11	16.5	14.7	8.69	0.013	2007	3	8	1, 9	16.4	14.7	4.18	0.071								
2008	4	7	1, 9	16.5	14.9	5.67	0.041	2008	2	7	1, 7	16.0	14.9	1.3	0.29								

Spring Max, Urb/Nurb

2002	5	8	1, 11	19.4	17.0	3.18	0.1
2003	5	11	1, 14	19.3	16.8	4.42	0.054
2004	5	11	1, 14	21.5	18.0	5.74	0.031
2005	5	12	1, 15	19.8	17.6	5.68	0.031
2006	5	10	1, 13	19.1	16.2	9.88	0.0078
2007	5	8	1, 11	20.4	16.7	7.29	0.021
2008	4	7	1, 9	21.7	17.7	5.5	0.044

Summer Mean, Urb/Nurb

2002	5	7	1, 10	19.4	17.8	6.17	0.032
2003	5	10	1, 13	20.0	18.1	5.85	0.031
2004	4	6	1, 8	20.4	18.5	4.97	0.056
2005	5	11	1, 15	20.2	18.4	7.02	0.018
2006	4	8	1, 11	21.5	19.2	7.07	0.022
2007	4	6	1, 8	20.4	18.4	6.29	0.037

Figure A5.4: ANOVA results for spring and summer temperature comparisons. P values marked in bold are significant after Bonferroni correction for comparison-wise error.